Anastasiia Lopatina

FROM ALTERNATIVE SOURCES OF CELLULOSE TO ULTRAFILTRATION MEMBRANES

Anastasiia Lopatina

FROM ALTERNATIVE SOURCES OF CELLULOSE TO ULTRAFILTRATION MEMBRANES

Dissertation for the degree of Doctor of Science (Technology) to be presented with due permission for public examination and criticism in the Auditorium 1316 at Lappeenranta-Lahti University of Technology LUT, Lappeenranta, Finland on the 14th of December 2023, at noon.

Supervisors Professor Mari Kallioinen-Mänttäri
LUT School of Engineering Sciences
Lappeenranta-Lahti University of Technology LUT
Finland

Professor Mika Mänttäri
LUT School of Engineering Sciences
Lappeenranta-Lahti University of Technology LUT
Finland

Adjunct Professor Ikenna Anugwom
LUT School of Engineering Sciences
Lappeenranta-Lahti University of Technology LUT
Finland

Reviewers Professor Mathias Ulbricht
Membrane research and development functional polymer materials
Universität Duisburg-Essen
Germany

Professor Henrikki Liimatainen
Fiber and Particle Engineering Research Unit
University of Oulu
Finland

Opponent Professor Mathias Ulbricht
Membrane research and development functional polymer materials
Universität Duisburg-Essen
Germany

Abstract

Cellulose, the most abundant biopolymer on the planet, presents a renewable alternative to petroleum-based polymeric materials. One of its applications is the production of polymeric ultrafiltration membranes, which can be used for water treatment, protein separation, and many other processes. Cellulose is considered an attractive membrane material due to its' ability to form films, remarkable hydrophilicity and easily malleable charge on the surface, which can be helpful in the separation of charged compounds. Additionally, deriving cellulose from waste sources, such as agricultural and forest wastes and waste cotton textiles, adds additional advantages (e.g. reduced environmental impact and fuller utilisation of wastestreams and sidestreams). Moreover, if cellulose membranes are produced from alternative sources, such as wood chips or waste cotton textiles, their production can be understood as an upcycling procedure, contributing to a closed-loop economy. The utilisation of more sustainable solvents for cellulose membrane production is also required. The use of ionic liquids, which have high dissolution power over cellulose, and deep eutectic solvents, which demonstrate the ability to efficiently fractionate wood biomass in one step, is actively studied to develop and improve the process of cellulose membrane production.

This study was focused on the investigation of the use of wood biomass, in the form of wood chips, and waste cotton textiles as a source of cellulose for regenerated cellulose-based membrane production. Flat-sheet ultrafiltration membranes were prepared from wood biomass and cotton textile solutions in the 1-ethyl-3-methylimidazolium acetate −dimethyl sulfoxide mixture through a non-solvent-induced phase inversion technique. Variations in the casting procedure included tracing the effect of polymer composition, casting solution's concentration, casting thickness, coagulation bath composition and presence of lithium chloride additive on the performance of the prepared membranes. The membranes' performance and morphology were characterised using measurements of pure water permeance, retention of model compounds (polyethylene glycols of different molecular weight), contact angle and zeta potential, as well as Fourier-transform infrared and Raman spectroscopy. Additionally, the membranes were tested for the removal of phosphorus from the wastewater treatment plant's effluent and dye retention from the model solution representing the dye industry's wastewater.

The results revealed that membrane preparation was possible from both untreated wood biomass and cotton textiles. The applied wood delignifying treatments, such as treatment using deep eutectic solvent and bleaching chemicals, assisted the formation of membranes

with better retention properties, as the chemical composition of wood biomass became more homogeneous. An alkaline coagulation bath as a primary medium for coagulation was introduced in this study and turned out to be an efficient tool for controlling the membranes' permeance and surface charge. When lithium chloride was tested as an additive, an optimum concentration was found at which the solution's viscosity was the highest, resulting in the formation of a membrane with the densest structure, highest retention and lowest porosity. The prepared membranes demonstrated the ability to separate compounds whose size is considerably smaller than the membranes' molecular weight cut-off (e.g. residual phosphorus or dye molecules). Thus, this study identified two alternative sources of cellulose, reducing the dependence on commercially processed cellulose fibres in cellulose membrane production. Demonstrating interconnections between cellulose's purity and membrane performance, this study suggested more efficient utilisation of wood biomass to produce membranes. Conducting experiments using alkaline coagulation bath and adding lithium chloride to the casting solution provided additional theoretical knowledge on the cellulose and wood biomass dissolution-regeneration process. The measured ability of the prepared membranes to remove residual phosphorus and dye molecules demonstrated the potential of the prepared membranes to be used as a part of reagent-free water treatment processes.

Acknowledgements

Firstly, the gratitude is expressed to LUT University for being the place where my academic ambitions got to be realized. The funding ESAELY/774/2019 from Etelä-Karjalan Säästöpankki Säätiö and the Ministry of the Environment is deeply appreciated.

To my first supervisor, Prof. Mari Kallioinen-Mänttäri, for sharing her experience, both as academic peer and human being. For all the professional corrections and personal advice, I am grateful. To my second supervisor, Prof. Mika Mänttäri for representing the chaotic part in the birth of ideas, for being one of the most open people for discussions. For openness, readiness to talk through things, and upmost respect for knowledge regardless of rank. To my third supervisor, Adjunct Prof. Ikenna Anugwom, for jumping on this train of dissertation at the point where it was needed.

The gratitude is extended to my preliminary examiners, Prof. Mathias Ulbricht and Prof. Henrikki Liimatainen, for their thorough review and feedback on the dissertation text. I am also grateful to Prof. Mathias Ulbricht for agreeing to act as an opponent during the public examination.

To Amin for staying through these years a colleague and a friend. To Tiina for being an amazing example of a young woman in science, professional, smart, and diligent. To Liisa, Maaret, Mari, and Markku for all the practical help and putting up with all my questions. To Mikko for all the help, support, and laughter that he brought into my life. To Vadim for going all the way from stranger asking for advice to an amazing example of a young man. To Joona for bringing into my life all his intelligence, humour and straightforwardness. To Luis for getting stuck in Finland and becoming a friend. To Mehmet, Anastasia, Svetlana, Egor, Vitalii, Pavel, Iryna, Ekaterina, Soheil, Tobias, Alma, Evgeniya, Asiia, Niklas, Sabina, Christoph, Mikko-Jussi and Mariia for all the conversations, gossips, and posing many examples of how life can be. To Joshua for being an amazing listener and reminding me in a tough moment that I have a lot to share. To Aljona for entering my life as a perfect person to study Finnish with and becoming an uncompromisable friend. To people who organized Euromembrane conferences 2021-2022 and Summer School 2022 in Portugal, and to amazing people I met there.

To Vitalii, Daria, and Alina for being with me all these years. You monopolized my free time and gave me a lifelong share of memories and laughter.

To my mother, Natalia, for being with me every day, for raising me the person that I am, for all the love and acceptance and countless hours she spent listening me talking about my dissertation.

Anastasiia Lopatina
November 2023
Lappeenranta, Finland

I just made something unexpected
Something sharp
Something new
It's not symmetrical or perfect
But it's beautiful
And it's mine
What else can I do?

-- Isabela Madrigal

Et si on célébrait ceux qui ne célèbrent pas
Pour une fois, j'aimerais lever mon verre à ceux qui n'en
ont pas
À ceux qui n'en ont pas

-- Stromae | Santé

Contents

List of publications

This dissertation is based on publications I—IV. The rights have been granted by publishers to include the papers in the dissertation.

I.   Lopatina, A., Anugwom, I., Esmaeili, M., Puro, L., Virtanen, T., Mänttäri, M., Kallioinen, M. (2020). Preparation of cellulose-rich membranes from wood: effect of wood pretreatment process on membrane performance. *Cellulose* **27**, 9505–9523.

II. Lopatina, A., Anugwom, I., Blot, H., Sánchez Conde, Á., Mänttäri, M., Kallioinen, M. (2021). Re-use of waste cotton textile as an ultrafiltration membrane. *Journal of Environmental Chemical Engineering* **9**(4).

Lopatina, A., Anugwom, I., Blot, H., Sánchez Conde, Á., Mänttäri, M., Kallioinen-Mänttäri, M. (2023). Corrigendum to "Re-use of waste cotton textile as an ultrafiltration membrane" [J. Environ. Chem. Eng. 9 (2021) 105705]. *Journal of Environmental Chemical Engineering* **11**(2).

III. Lopatina, A., Liukkonen, A., Bec, S., Anugwom, I., Nieminen, J., Mänttäri, M., Kallioinen-Mänttäri, M. (2022). Wood-based cellulose-rich ultrafiltration membranes: alkaline coagulation bath introduction and investigation of its effect over membranes' performance. *Membranes* **12**, 581.

IV. Lopatina, A., Esmaeili, M., Anugwom, I., Mänttäri, M., Kallioinen-Mänttäri, M. (2023). Effect of low concentrations of lithium chloride additive on cellulose-rich ultrafiltration membrane performance. *Membranes* **13**(2):198.

Author contribution

Anastasiia Lopatina was the principal author and investigator in all publications. The author planned and conducted the experiments, interpreted the results and wrote the papers with the co-authors. Tiina Rissanen née Virtanen supervised the conduction of Raman experiments in Publication I. Liisa Puro performed GC experiments and supervised TG-MS experiments in Publication I. Hervé Blot and Ángela Sánchez Conde performed part of the membranes' characterisation and filtration experiments in Publication II. Alma Liukkonen performed part of the filtration experiments in Publication III, Joona Nieminen helped with the interpretation of the long-term filtration experiments and Sabina Bec assisted with the interpretation of the phosphorus removal results.

Besides the results published in the papers above, the dissertation contains work that has not yet been published.

Nomenclature

Symbols

A_f	the effective filtration area of the membrane sample	m^2
C_f	concentration in feed	mg/L
C_p	concentration in permeate	mg/L
C_r	concentration in retentate	mg/L
J	flux	$L/m^2 \cdot h$
pK_a	acid dissociation constant	
λ_{max}	wavelength at which a substance has its strongest photon absorption	nm
M_w	molecular weight	g/mol
p	the applied pressure in filtration process	bar
P	the membrane's permeance	$L/m^2 \cdot h \cdot bar$
R	retention	%
t	time interval for permeate collection	min
V_p	the collected permeate volume	L

Abbreviations

3D	three-dimensional
a.u.	absorbance units
AISL	acid insoluble lignin
ASL	acid soluble lignin
ATR	attenuated total reflection
CA	contact angle
CAS	chemical abstracts service (number)
CB	coagulation bath
CBT	coagulation bath temperature
CDW	construction and demolition wood
CHARMME	Harmonisation of characterisation procedures for porous membranes (project)
ChCl	choline chloride
DES	deep eutectic solvent
DI	deionised (water)
DP	degree of polymerisation
DMAc	dimethylacetamide
DMF	dimethylformamide
DMSO	dimethyl sulfoxide
EIPS	evaporation-induced phase separation
Emim	1-ethyl-3-methylimidazolium cation
FIR	far-infrared (spectroscopy)
FTIR	Fourier-transform infrared (spectroscopy)
HBA	hydrogen bond acceptor

HBD	hydrogen bond donor
H-bonds	hydrogen bonds
IEP	isoelectric point
IL	ionic liquid
kDa	kilodaltons
LAc	lactic acid
LCC	lignin carbohydrate complex
LIF	laser induced fluorescence
MF	microfiltration
MIR	mid-infrared (spectroscopy)
MWCO	molecular weight cut-off
NF	nanofiltration
NIPS	non-solvent-induced phase separation
NMMO	N-methylmorpholine N-oxide (more correctly 4-methylmorpholine 4-oxide)
NS	non-solvent
OAc	acetate anion
OH	hydroxyl (functional group)
P	polymer
PAN	polyacrylonitrile
PEG	polyethylene glycol
PES	polyethersulfone
PI	phase inversion
PS	phase separation
PVDF	polyvinylidene fluoride
RB2	reactive blue 2 (dye)
REACH	Registration, Evaluation, Authorisation and Restriction of Chemicals (legislation)
RO	reverse osmosis
rpm	revolutions per minute
S	solvent
SEM	scanning electron microscope
TG	thermogravimetry
TIPS	temperature-induced phase separation
UF	ultrafiltration
UV-Vis	ultraviolet/visible (spectrophotometry)
VIPS	vapor-induced phase separation
VRF	volume reduction factor
XRD	X-ray diffraction

1 Introduction

Science and technology development in the twenty-first century is focused on the utilisation of renewable materials and the improvement of existing technologies to sustain an environmentally safe approach to life and industry (Wang, Lu and Zhang, 2016; Sayyed, Deshmukh and Pinjari, 2019). Simultaneous depletion of oil, gas and coal, as well as the necessity to implement new discharge limits, motivates research and development of renewable technologies. When renewable materials are researched, the maximum attention is given to cellulose, which is the most abundant biopolymer on the planet, with annual natural production of over tens of billions of tons (Wang, Lu and Zhang, 2016; Sayyed, Deshmukh and Pinjari, 2019). Additionally, industrialisation and population growth from the second half of the twentieth century have introduced new challenges for the wastewater treatment industry. Along with municipal wastewater treatment, the urge to purify and recirculate wastewater of industrial origin has been increasing continuously. The classical approach to water treatment has been to combine the advantages of physical, biological and chemical treatment processes. However, efficient treatment has been followed by the creation of secondary waste, such as precipitate of the physical separation processes and the biological waste residuals, or the remaining residuals of the chemicals which are often toxic to the environment and living organisms (Bruggen *et al.*, 2003; Goh, Othman and Matsuura, 2021; Zou *et al.*, 2021). One separation method that can potentially be operated with little to no generation of secondary waste, as long as both the retentate and permeate produced in the process are utilised onwards, is membrane technology.

Membrane technology is based on the semi-permeability of films and three-dimensional (3D) structures, allowing the selective passage of some components while retaining others. Membrane technology is usually highlighted among other physical separation processes due to the combination of comparatively low energy requirements, low installation costs and several separation principles involved in a single-step separation (Mulder, 1996). Other advantages of membrane separation processes include the possibility of a continuous separation process, minimised need for additional chemicals and the general possibility of tailoring the membrane process to the needs of the media with an appropriate membrane choice. The driving forces involved in membrane separation processes include pressure gradient, charge difference, chemical nature of the constituents, concentration gradient and temperature difference (Bruggen *et al.*, 2003; Al Aani, Mustafa and Hilal, 2020).

The membrane market in Europe accounts for 25% of the global market and was estimated at €4.9 billion in 2020 (Novelli *et al.*, 2020). The specifics of membrane technology in the European market include dependence on few membrane manufacturers, as well as overall market consolidation resulting from membrane manufacturers being also the main users of membrane technology (Hamingerova, Borunsky and Beckmann, 2015). As a result, according to some authors, the industrial-level research in membrane technology is focused on the polishing and improvement of existing technologies, whereas more novel approaches are often overlooked due to their inability to be quickly

upscaled, which limits the development of the whole industry (Hamingerova, Borunsky and Beckmann, 2015).

Pressure-driven membrane processes are widely utilised for different industrial needs. These processes include microfiltration (MF), ultrafiltration (UF), nanofiltration (NF) and reverse osmosis (RO). MF and UF are additionally united as low-pressure membrane processes and began to be actively commercialised worldwide for water purification in the 1980 to the 1990s; thus, historically, UF is a rather young technology (Mulder, 1996; Kubota, Hashimoto and Mori, 2008; Mohanty and Purkait, 2011; Al Aani, Mustafa and Hilal, 2020). Initially launched as a separation technique in the 1950s for blood dialysis, low-pressure UF began to be actively used for the industrial needs of electrophoretic painting in the 1970s (Mulder, 1996; Kubota, Hashimoto and Mori, 2008; Mohanty and Purkait, 2011). Over the course of 50 years, UF membranes have been continuously improved and adapted to the needs of various separation processes, including wastewater treatment and water preparation, food processing, chemicals' recovery, oily wastewater applications, and medical use (Susanto and Ulbricht, 2005; Al Manasrah *et al.*, 2012; Al Aani, Mustafa and Hilal, 2020; Awad *et al.*, 2021). Nowadays, UF membranes are generally identified as those having a pore size of 0.001–0.1 µm and the capability to separate microorganisms, viruses and organic compounds of larger sizes while being operated typically at 1–10 bar pressure difference (Bruggen *et al.*, 2003; Hamingerova, Borunsky and Beckmann, 2015). Regardless of the process specifics, UF is universally recognised as a consistently low-energy process, resulting in at least 20% less energy consumption compared to NF and RO (Al Aani, Mustafa and Hilal, 2020; Awad *et al.*, 2021).

Though UF membranes are produced from various materials (e.g. metals, ceramics and polymers), their larger share is represented by petroleum-based polymeric membranes. Petroleum-based polymers [e.g. polyvinylidene fluoride (PVDF), polyethersulfone (PES) and polyacrylonitrile (PAN)] demonstrate attractive properties as a membrane material (e.g. well-controlled pore formation and sufficient chemical and mechanical resistance) (Bruggen *et al.*, 2003; Kubota, Hashimoto and Mori, 2008; Joshi *et al.*, 2023). However, these polymeric membranes hold disadvantages, including being produced from limited resources and often being prone to fouling due to hydrophobicity (Jönsson and Jönsson, 1995; Susanto and Ulbricht, 2005; Al Aani, Mustafa and Hilal, 2020). These disadvantages are continuously attempted to be mitigated to improve membranes' stability and increase their life-time. The current life-time of membrane modules' results in discarding more than 840 000 modules of only RO modules annually (Sérgio *et al.*, 2023). Continuous accumulation of non-recyclable petroleum-based products and development of pro-environmental regulations have resulted in environmental concerns and increased interest in biodegradable materials. The use of bio-based materials, which would combine the desired durability and stability with recyclability and sustainability, is also studied in the membrane technology field, with a large portion of attention being focused on cellulose-based membranes (Buschow *et al.*, 2001; Chen, 2021).

In addition to petroleum-based membranes, regenerated cellulose-based polymeric membranes also demonstrate attractive mechanical and chemical stability; however, they currently represent a much smaller share of UF membranes (Duolikun *et al.*, 2020; Awad *et al.*, 2021). Moreover, regenerated cellulose-based membranes are hydrophilic and potentially biodegradable once the polymeric support material can be effectively replaced with other bio-based polymers instead of petroleum-based ones (Susanto and Ulbricht, 2005; Nevstrueva *et al.*, 2018). There have been continuous attempts to study and fabricate regenerated cellulose-based membranes, but most of these studies have been focused on the use of commercially available cellulose fibres as a polymer source for membrane preparation. However, there is a considerable feedstock of cellulose from underutilised materials, such as wood chips remaining on the construction sites or wood preparation sites, and cotton textiles, which is generated as waste annually and can be used for cellulose-based membrane fabrication (Hummel *et al.*, 2016; Dahlbo *et al.*, 2017; Haslinger *et al.*, 2019; Navone *et al.*, 2020). Though extensive studies have reported the use of biomass as a polymer source, the described preparation of membranes is rarely organised without a complicated procedure of cellulose purification from biomass that has to be performed prior to membrane preparation (Chen, Wang and Liu, 2012; Figoli, Simone and Drioli, 2015; Esfahani *et al.*, 2020). The ones able to produce membranes directly from the source material rarely report examples of their implementation beyond the testing on the model solutions rather than the testing of the real or simulated wastewaters.

1.1   Objectives of this thesis

Hypothetically, there is a significant underutilised source of cellulose that can be efficiently used for cellulose-based membrane production. With the optimisation of the casting procedure parameters, the resulting membranes have a competitive potential with the existing commercial cellulose-based membranes, while simultaneously being more resource-efficient. This thesis is dedicated to considering the possibility of fabricating cellulose-based membranes from an unconventional resource (e.g. wood biomass) or waste resource (e.g. the used cotton textile). With the predetermined solvent choice, the experimental work was focused on searching optimal fabrication parameters and acquiring information on the interconnection among applied wood biomass treatments (DES treatment, bleaching and alkaline treatment, also known as α cellulose separation), fabrication conditions, and the resulting membranes' performance and characteristics.

The objectives of this thesis include the following:

- Presenting two alternative sources of cellulose for membrane production.

- Verifying the possibility of novel production of cellulose-based membranes directly from wood biomass and cotton textile without subjecting the source material to any chemical pretreatment.

- Evaluating the influence of the purity of the wood biomass-originated cellulose on the performance and characteristics of the produced membranes.

- Suggesting a reliable and reproducible upcycling-recycling procedure for waste cotton textile.

- Evaluating the effect of casting parameters (e.g. polymers' concentration, casting thickness, coagulation bath's composition and presence of the additive) on the prepared membranes' performance and characteristics.

- Evaluating membranes' performance and ability to provide removal of both suspended solids and dissolved molecules from model solutions and simulated wastewater.

1.2 Impacts of the research

By expanding the source pool of cellulose for producing membranes and identifying alternative sources, such as incompletely processed wood biomass and waste cotton fabric, this work enhances the sustainability and availability of regenerated cellulose-based membrane manufacturing. Resource efficiency is promoted by highlighting a more diversified supply of cellulose, thus reducing dependence on specific sources (e.g. commercially produced cellulose fibres). Eliminating the requirement for complete separation of cellulose from wood biomass, larger wood biomass volumes can be preserved, making the membrane fabrication more cost-efficient and promoting sustainable utilisation of forestry biomass (i.e. reducing waste matter and maximising resource use). Reduction of waste is also achieved through an upcycling-recycling procedure for waste cotton textile, which can be effectively transformed into a regenerated cellulose-based membrane, a value-added product, which in turn promotes circular economy principles in both the membrane and textile industries. The finding on the complex relationship of LiCl and wood biomass provides valuable theoretical knowledge for the future development of the cellulose and biomass dissolution-regeneration process and fine-tuned membrane fabrication. The evaluation of the prepared membranes' ability to remove residual phosphorus and dye molecules highlights the possibility of using them for water purification and pollutants' removal—which, in turn, contributes to the development of reagent-free water treatment practices.

In the future, the results of this study can be used as a basis for scaling up the membrane production and optimisation of the chosen casting parameters. The results can be used for comparison when other types of biomasses are tested for membrane fabrication. The knowledge produced in this study provides fundamental information on the effect of the chemical composition of the used carbohydrate fraction on membrane performance. The achieved results on real and simulated wastewater purification can be used in future pilot studies.

1.3 **Outline**

Consisting of four publications, this thesis summarises the research work focused on the fabrication and characterisation of cellulose-based membranes (Figure 1). The literature section discusses the place of cellulosic membranes in the current ultrafiltration membranes field, the choice of solvents for the biomass pretreatment facilitating membrane casting and casting solutions preparation, as well as the specifics of wood biomass and cotton textile as cellulose sources. The experimental part covers wood biomass treatment techniques, alteration of parameters in the membrane casting procedure, utilisation of additives and possible applications of ultrafiltration membranes in the purification of water-based wastestreams.

The objectives of this thesis | Corresponding Publications

| Alternative cellulose's source applicability | Waste cotton textile (2) Publication II | Debarked wood chips (1) Publication I |

| Wood biomass treatments and their effect on membrane performance | 1 → DES treatment (1.1) → bleaching (1.2) → alkaline treatment Publication I |

| Variations in casting procedure and their effect on membrane performance | 2 ✚ effect of casting solution concentration and casting thickness Publication II |
| | 1.1 ✚ alkaline coagulation bath (1.3) Publication III |

| Additive presence and its effect on membrane morphology and performance | 1.2 ✚ addition of LiCl (0 – 2 wt.%) Publication IV |

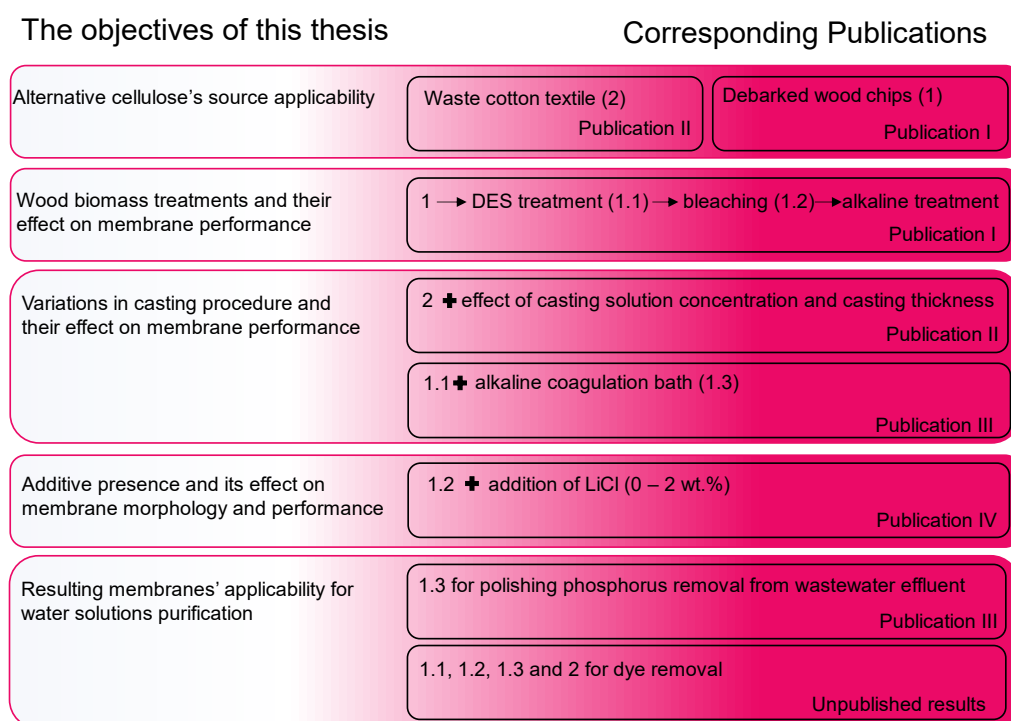| Resulting membranes' applicability for water solutions purification | 1.3 for polishing phosphorus removal from wastewater effluent Publication III |
| | 1.1, 1.2, 1.3 and 2 for dye removal Unpublished results |

Figure 1. Dissertation navigation scheme. To keep the scheme concise, numbers are used instead of full names of some biomass samples and corresponding membranes: 1 stands for untreated wood biomass, 1.1 the wood biomass after applied DES treatment, 1.3 for the wood biomass after consequent DES treatment and bleaching treatment, 2 stands for the waste cotton textile.

Publication I evaluates the possibility of cellulose membrane production directly from wood biomass, presents the sequence of treatment steps applied to wood biomass, intended to purify the cellulose share, and presents the fabrication of membranes from each biomass sample with further characterisation and analysis of cellulose purity's effect

on membranes' performance. Publication II introduces the second source material for membrane fabrication – cotton textile – and shows the influence of changes in casting conditions on membrane performance and characteristics. Publication III focuses on the possibility of improving membrane performance and proposes a dual-bath coagulation step, where an alkaline solution is used as a coagulation medium, taking advantage of biomass constituents' different solubilities in alkali solutions. Publication IV studies the effect of the inorganic salt lithium chloride used as an additive in the casting solution on the morphology and performance of the prepared membranes. In addition, the prepared membranes in Publications I–III were tested for purification of model dye solutions as mentioned in Figure 1.

2 Review of cellulose's chemistry and importance in membrane technology

2.1 Cellulose: chemistry and sources

From the moment of its discovery in 1838 by French chemist Anselme Payen, cellulose has not stopped seizing the attention of researchers due to its attractive properties (Chen, 2021). In its native form, cellulose is distributed all over Earth's surface, being represented by all kinds of grass, trees and other plant life. Cellulose is also the main biopolymer on the planet in terms of renewability, abundance and biodegradability (Isikgor and Becer, 2015; Giummarella, 2018; Aziz *et al.*, 2022). Cellulose is a linear biopolymer in which glucose is identified as a repeating unit of its structure, not cellobiose, as used to be referenced often (French, 2017). Glucose, or more correctly β-D-anhydroglucose, units are connected via β-1,4-glycosidic bonds (Figure 2.1). Each unit contains three reactive hydroxyl groups that are positioned in the plane of the ring and contribute to three kinds of H-bonds. The cellulose chains are reinforced by the intramolecular H-bonds (O2−H⋯O6 and O3−H⋯O5) and conjoined into cellulose sheets by intermolecular bonds (O6−H⋯O3). These sheets are further stacked by Van der Waals forces, resulting in the formation of semi-crystalline structures in a thin, long fibrillar shape, which is known as elementary fibril (Österberg, 2000; Alves, 2015; French, 2017; Wondraczek and Heinze, 2021). Due to the chemical nature of cellulose, it demonstrates an amphiphilic character. The highly developed network of hydrogen bonds regulates the chemical behaviour of cellulose and many of its properties. Moreover, the existence of Van der Waals interactions adds to the complexity of cellulose's chemistry (Rebière *et al.*, 2016). Thus, cellulose's semi-crystalline nature is accountable for its swelling, solubility and physical properties.

Yet, cellulose is often not the sole constituent of biomass; it is accompanied by two other main biopolymers: lignin and hemicellulose. Lignin is plants' second most abundant biopolymer, comprising repeated units of *p*-coumaryl, coniferyl and sinapyl alcohols interconnected by various carbon-carbon and ether bonds (Figure 2.1) (Giummarella, 2018; Melro *et al.*, 2018). Hemicellulose consists of pentose and hexose sugars arranged in different orders to form polymer chains with a degree of polymerisation (DP), usually up to 200 (Figure 2.1) (Shimizu *et al.*, 2020). Lignin and hemicellulose usually accompany cellulose, surrounding the latter in microfibrils, resulting in higher recalcitrance and rigidity in woods (Horvath, 2006; Isikgor and Becer, 2015; Giummarella, 2018). Although cellulosic materials can be used in their natural form, a more prospective approach would be their chemical processing—which allows the separation and recovery of cellulose in its purer form—and, if necessary, the introduction of chemical modifications, which makes the properties of cellulose more attractive. The commercialised cellulose production relies on the utilisation of highly pure sources of cellulose, such as cotton, or easily harvested ones, such as wood biomass. The Kraft

pulping process is currently used to produce a larger share of cellulose (Buschow *et al.*, 2001; Demesa, Laari and Sillanpää, 2020).
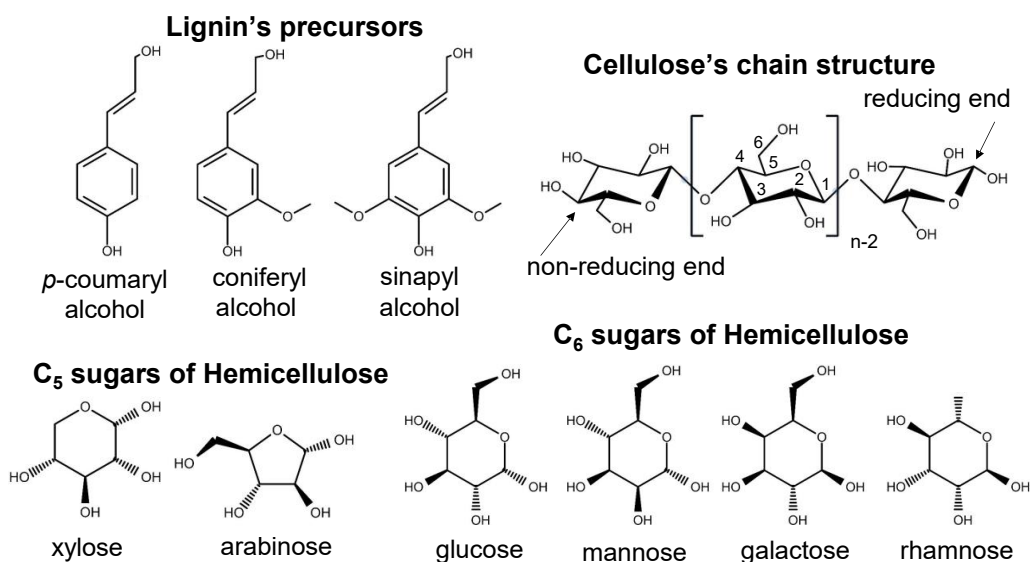
Lignin's precursors

p-coumaryl alcohol   coniferyl alcohol   sinapyl alcohol

Cellulose's chain structure

reducing end

non-reducing end

C$_5$ sugars of Hemicellulose

xylose   arabinose

C$_6$ sugars of Hemicellulose

glucose   mannose   galactose   rhamnose

Figure 2.1: Elementary chemical structures of cellulose, hemicellulose and lignin, adapted from (Isikgor and Becer, 2015).

2.1.1   Wood biomass as cellulose source

Wood biomass, in general, is an excellent source of cellulose, whose content in dry biomass weight can be up to 45% (Horvath, 2006; Giummarella, 2018; Demesa, Laari and Sillanpää, 2020). The recovery of cellulose from wood biomass is the most popular pathway in Europe, especially in Nordic countries, where the landscape primarily consists of forests (Nnberg, 2001). The share of wood biomass as a source of cellulose is also increasing annually, even in countries that traditionally relied on cotton linter (e.g. China) (Nnberg, 2001). This trend will lead to the creation of more forestry residues, which are currently either landfilled or incinerated, although they can be used as a cellulose-rich material without being heavily valorised (Loow *et al.*, 2017). In Europe alone (meaning EU-27 countries plus Norway, Switzerland and United Kingdom) annual wood consumption has been reported to reach 112.3 million tonnes in 2021 (CEPI (Confederation of European Paper Industries), 2021).According to a 2013 report (Searle and Malins, 2013), European countries produce approximately 80 million tons of forest residues annually, along with 350 million tons of agricultural crop residuals and 200 million tons of municipal lignocellulosic waste, including post-consumer furniture, paper and cardboard residuals, as well as food and garden wastes (Abushammala and Mao, 2020). Only one-third of the produced waste is accessible for utilisation other than incineration (Abushammala and Mao, 2020). The challenge regarding any processing and

valorisation of forestry waste biomass is related to its naturally complex chemical structure and recalcitrance. As a result, the utilisation of the forestry residue potential, using chemical processing, involves too many steps and uses chemicals (e.g., tetralin, acetone, methanol or ethanol) in large volumes to dissolve different wood compounds (Horvath, 2006).

The isolation of cellulose from wood biomass is one of the most important chemical processes (Buschow *et al.*, 2001; Isikgor and Becer, 2015). The conventional chemical approach to wood biomass valorisation aims to preserve the fibres, unlike mechanical, chemi-mechanical and semi-chemical approaches (Demesa, Laari and Sillanpää, 2020). The chemical approach is also focused on the preservation of cellulose, whereas lignin and hemicelluloses are mostly dissolved throughout the different stages of the process. In the most common Kraft sulphate pulping process the yield of production of pure cellulose remains at 43-45% and is associated with high energy consumption and large volume of chemicals. Combined with the necessity of sulphur compound utilisation and their occasional release into the atmosphere, the use of the chemical approach for cellulose production as a source material for membrane manufacturing is hardly sustainable (Buschow *et al.*, 2001; Isikgor and Becer, 2015; Loow *et al.*, 2017). All these existing challenges raise the importance of creating alternative effective wood biomass valorisation techniques, e.g., instead of focusing the attention on paper-grade cellulose production, more efficient utilisation of all wood biomass constituents should be considered.

2.1.2 Cotton textile as highly recyclable source of cellulose

As the textile market continues to grow alongside population growth and shortening of the fashion cycle, the recycling of waste textile has become more important than ever (Dahlbo *et al.*, 2017). Cotton textile is the second most mass-produced textile in the world, and its production is accompanied by water depletion (due to the required irrigation) and toxic pollution (due to the extensive use of pesticides) (Vats and Rissanen, 2016). Additionally, the production of cotton fibres is highly energy-intensive, requiring approximately 50 MJ of energy for the production of a single kilogram of cotton (Fletcher, 2014; Vats and Rissanen, 2016). Up to 95% of waste textile is not recycled but incinerated or landfilled, and the 5% that gets to be recycled is usually turned into products of lower quality (Dahlbo *et al.*, 2017; Sandin and Peters, 2018; Haslinger *et al.*, 2019; Navone *et al.*, 2020). Cotton textile, being produced from cotton plants, consists of pure cellulose, which makes the planning of the recycling strategy highly variable. The use of waste cotton textile as a part of reinforced composite production can be completed with only mechanical treatment of the waste cotton fabric. However, chemical recycling into new, value-added products and materials, as usual, is limited by the appropriate solvent choice. The production of cellulose membranes from waste cotton textile would fit into the definition of upcycling since the waste material is transformed into a value-added product (Leal Filho *et al.*, 2019).

2.2   Solvents for cellulose dissolution and processing

2.2.1   Cellulose dissolution, classic solvents and challenges

Due to the physical and chemical properties of cellulose, its processing is challenging (Figoli, Simone and Drioli, 2015; Rebière *et al.*, 2016; Loow *et al.*, 2017; Tang *et al.*, 2017). Unlike many petroleum-based polymers, most native forms of cellulose are not thermoplastic, which significantly limits the applicable technologies for its processing. Cellulose's degradation temperature is lower than its melting temperature and is highly dependent on the molecular structure. Studies have demonstrated how the degradation of cellulose is primarily influenced by its degree of crystallinity, since the degradation starts from the amorphous regions, meaning that the lower the crystallinity of initial cellulose, the more easily it will degrade under thermal processing (Figoli, Simone and Drioli, 2015). Thus, the processing of cellulose in its natural, unmodified form is limited. Among practical processing options are dissolution-regeneration of cellulose, as well as its disintegration to nanomaterials (Alves, 2015; Wang, Lu and Zhang, 2016; Sayyed, Deshmukh and Pinjari, 2019; Esfahani *et al.*, 2020).

Cellulose demonstrates extremely poor solubility in water and most common solvents due to a developed network of hydrogen bonds and Van der Waals interactions (Alves, 2015). As cellulose and biomass are recalcitrant to dissolution, displaying stability to a whole range of organic and inorganic solvents, many studies have been conducted throughout the last century to explain the issue related to cellulose's stability and how to overcome it (Alves, 2015). In the last decade, additional reasoning for cellulose's recalcitrance to dissolution has been brought up, resulting from its amphiphilic character and thus requiring amphiphilic solvent media for efficient dissolution (Alves, 2015). When wood biomass dissolution is in question, there is an added difficulty related to the simultaneous existence of hemicellulose and lignin within the microfibrils, limiting solvent penetration due to the complexity of intermolecular bonding (Jiang, Zhao and Hu, 2018).

The classical approach to cellulose separation and recovery from wood biomass includes a sequential treatment with acids and bases to dissolve hemicellulose and lignin and to isolate cellulose from the wood biomass. Separated cellulose's dissolution can be achieved by using rather specific solvent combinations, whose ability to weaken abundant hydrogen bonds consequently bring cellulose's molecules apart. Cellulose's dissolution is governed by either finding the solvent capable of direct cellulose dissolution (non-derivatising) or the ones that can form a soluble intermediate cellulose's modifications (derivatising) (Alves, 2015; Rebière *et al.*, 2016; Acharya *et al.*, 2021). Historically, derivatising solvents have been developed first and have achieved cellulose dissolution through introduction of changes in the chemical and physical structures of cellulose. Non-derivatising solvents can dissolve cellulose without inducing chemical modifications, only through physical intermolecular interactions (Wang, Lu and Zhang, 2016; Gubitosi *et al.*, 2017; Sayyed, Deshmukh and Pinjari, 2019; Aziz *et al.*, 2022). The most commonly studied derivatising processes include the viscose process, the cupro process and the

variations based on organic acids and N,N-dimethylformamide (DMF) (Alves, 2015). Non-derivatising dissolution processes are based on the use of copper salts and concentrated ammonia or concentrated chilled alkaline solutions. Despite the existing variety of suitable solvents, the dissolution process remains challenging due to the limited dissolution capacity of the solvents, their toxicity and strict operating conditions, all of which limit its industrial use (Alves, 2015).

The choice of solvent or solvent system is critical, as it has a direct effect on the properties of regenerated cellulose. During the dissolution of cellulose, its molecular structure is destroyed through the breakage of inter-chain hydrogen bonds or the rupture of its chains. After successful cellulose dissolution, it must be turned back to a solid state; that is, regenerated. The regeneration of cellulose is a process in which the cellulose solution is put in contact with a coagulation medium, which triggers dissolved cellulose to precipitate into a pre-shaped form (e.g. fibre or film) (Alves, 2015; Wang, Lu and Zhang, 2016; Acharya *et al.*, 2021). The regenerated cellulose materials usually demonstrate lower molecular weight compared to source cellulose, whereas other properties, such as morphology, crystallinity and strength, can be tuned through the accurate choice of experimental conditions (Alves, 2015).

2.2.2 Novel solvents for cellulose and wood biomass dissolution, valorisation and conversion: ionic liquids and deep eutectic solvents

Ionic liquids (ILs) belong to a non-derivatizing class of cellulose and biomass solvents, capable of dissolving polymers without intermediate derivatives through the destruction of the network of hydrogen bonds (Magalhães Da Silva *et al.*, 2013; Le, Rudaz and Budtova, 2014; Esfahani *et al.*, 2020; Acharya *et al.*, 2021). Along with ILs, this solvent class includes aqueous alkaline solutions, N-methylmorpholine N-oxide (NMMO) and dimethylacetamide (DMAc)/LiCl mixture. ILs are molten salts that remain in their liquid form below 100°C. Due to the strong ionic interaction between the ions, ILs have negligible vapour pressure, high thermal stability and usually non-flammability. Low-toxicity, non-corrosive ILs usually attract most research attention. Since 2009, when it was discovered that the complete dissolution of wood biomass could be reached in a single step using 1-ethyl-3-methylimidazolium acetate ([Emim][OAc]) as a solvent, the number of published research papers has been increasing annually, exploring the possibilities of IL utilisation in biomass processing and valorisation (Sun *et al.*, 2009; Magalhães Da Silva *et al.*, 2013).

[Emim][OAc] is an appropriate choice for wood biomass processing due to the properties of its ions (Sun *et al.*, 2009). The imidazolium cation 1-ethyl-3-methylimidazolium [Emim] is an efficient solvent for cellulose due to the higher hydrophilicity of the imidazolium ring introduced by the presence of an ethyl substituent, as opposed to other widespread substituents, namely allyl and benzyl. The acetate anion [Oac] can efficiently break hydrogen bonding due to its high basicity, which ultimately leads to better cellulose dissolution (Sun *et al.*, 2009; Abushammala and Mao, 2020; Aziz *et al.*, 2022). At the same time, [Emim][Oac] still has quite a high capability for the simultaneous dissolution

of lignin and hemicellulose due to its ability to cleave β-O-4 bonds through the attack of acetate ions on the hydrogen in the β carbon of lignin (Abushammala and Mao, 2020).

[Emim][Oac] is an IL with a lower corrosion ability compared to Ils based on halide anions (Isik, Sardon and Mecerreyes, 2014). It also demonstrates a relatively low viscosity of 162 mPa·s at 25°C, which makes its utilisation relatively easy (Gericke, Fardim and Heinze, 2012). These advantages result in high research interest toward [Emim][Oac]. For example, proionic GmbH produces this solvent between 1 and 10 tonnes per year (proionic GmbH, 2018). However, the price and a rapid increase in viscosity when cellulose or wood biomass solutions are formed usually require the addition of a co-solvent (Isik, Sardon and Mecerreyes, 2014; Livazovic *et al.*, 2015; Medronho and Lindman, 2015). The use of a co-solvent helps lower the overall viscosity of the solvent media, improves the dissolution kinetics, enhances the dissolution power over cellulose and decreases the price of the process as well as the potential toxicity of the solvent mixture (Le, Rudaz and Budtova, 2014; Radhi *et al.*, 2015). The addition of organic solvents, such as dimethyl sulfoxide (DMSO) (viscosity of 2 mPa·s at 25°C) or DMF, significantly reduces the viscosity without sacrificing the dissolution power of the IL towards cellulose or wood biomass (Esfahani *et al.*, 2020). The addition of DMSO to [Emim][Oac] can improve the dissociation of Ils and increase the total concentration of ions in the solution, which facilitates cellulose dissolution (Le, Rudaz and Budtova, 2014).

The history of deep eutectic solvents (DESs) is still relatively young, being the subject of active research from the beginning of the twenty-first century (Francisco, Van Den Bruinhorst and Kroon, 2012; Tang *et al.*, 2017). At first, DESs were understood as Ils, given that both solvent classes share properties such as a low melting point, negligible vapour pressure and stability over a wide range of temperatures. While DESs also have melting points below 100°C, their composition includes a hydrogen bond donor (HBD) and a hydrogen bond acceptor (HBA) instead of ions, as in Ils. The adopted definition of DESs is "DESs can be described as eutectic mixtures with an eutectic point temperature lower than their corresponding ideal liquid mixtures" (Martins, Pinho and Coutinho, 2019).The research on the applicability of DESs to biomass valorisation and modification has been intensive due to their ability to selectively dissolve individual components, allowing the organisation of the process with high solid/liquid ratios using environmentally friendly solvents, unlike the classical approach to biomass processing (Francisco, Van Den Bruinhorst and Kroon, 2012; Loow *et al.*, 2017; P. Li *et al.*, 2018). Biomass pretreatment with a mixture of choline chloride (ChCl) and lactic acid (LAc) has been reported on multiple occasions (Kumar, Parikh and Pravakar, 2016; Loow *et al.*, 2017; Melro *et al.*, 2018; Soto-Salcido *et al.*, 2020; Ippolitov *et al.*, 2022). The ChCl:LAc DES treatment showed efficiency in delignification under relatively mild treatment conditions, with applied temperatures below 100°C and treatment time of only several hours.

As research on the application of novel solvents progresses, the subject of their recyclability becomes more critical. The recycling of Ils is crucial to be conducted, as it

is the bottleneck of these solvents' large-scale utilisation due to their higher cost and toxicity potential (Kim and Nunes, 2021). The recyclability of DESs is less researched than that of Ils. However, due to cost-efficiency issues, DES recycling still has to be studied and developed to facilitate its large-scale applications (Loow *et al.*, 2017; Ippolitov *et al.*, 2022). According to the available literature, [Emim][Oac] up to 90–96% w/w can be recovered for up to five successive recycle cycles, depending on the temperature at which it was used (Gericke, Fardim and Heinze, 2012; Magalhães Da Silva *et al.*, 2013; Van Nguyen *et al.*, 2017). DESs can be purified using membrane filtration or vacuum rotary evaporation (Kumar, Parikh and Pravakar, 2016; Ippolitov *et al.*, 2022).

2.2.3 Dissolution-regeneration of cellulose in industrialized membrane production

Three main commercialised processing technologies have been used for the preparation of regenerated cellulose membranes: the lyocell, viscose and cupro processes (Wang, Lu and Zhang, 2016; Sayyed, Deshmukh and Pinjari, 2019; Chen, 2021). The viscose process was developed over a hundred years ago and still dominates the market for regenerated cellulose production and is expected to grow in the coming years (Wang, Lu and Zhang, 2016). The viscose process uses CS_2 to convert cellulose to cellulose xanthogenate, which is27olublee in aqueous NaOH solution and subsequently forms regenerated cellulose after acidic treatment. Although being effective and constantly improved, the process results in toxic emissions of H_2S and CS_2, which are harmful to the environment and extremely toxic to humans (Li, 2008; Wang, Lu and Zhang, 2016; Sayyed, Deshmukh and Pinjari, 2019). The cupro process was developed in the 1890s and was based on cuprammonium hydroxide as a derivatising cellulose solvent. Nowadays, the production of regenerated cellulose materials based on this process is limited due to the high toxicity and price of the chemicals involved (Chen, 2021).

Another industrialised process is the only one based on a non-derivatising solvent and uses a combination of NMMO/H_2O system for the dissolution of cellulose and further preparation of regenerated cellulose membranes (Wang, Lu and Zhang, 2016; Sayyed, Deshmukh and Pinjari, 2019). Different patent owners have reported different conditions, but the following common grounds can be highlighted: the NMMO:H_2O ratio is approximately 85:15, the concentration of cellulose is usually within 7–15% and the dissolution is achieved at 80–100°C in the presence of a pore-forming additive and antioxidant, such as n-propyl gallate. The source of cellulose has to be highly pure cellulose pulp with a degree of polymerization of 500–1200 and alpha-cellulose content above 98%, which incurs added costs (Chen, 2021). The applied aftertreatment solution is usually a glycerine–water mixture at a 10–50% mass concentration (Wang, Liu and Min, 2014). Another, more rarely reported, approach is to use cellulose acetate as a starting form of cellulose, where it is transformed into regenerated cellulose through the hydrolyzation of the prepared cellulose acetate film in 0.05 m/L sodium hydroxide solution at 50°C for 5 h (Zhong *et al.*, 2022).

However, as new regulations are developed, the chemical substances used in the processes gain importance. The introduction of the Registration, Evaluation, Authorisation and Restriction of Chemicals (REACH) legislation in 2006 did not exactly limit the existing production of regenerated cellulose membranes but lowered the threshold value for substances involved in membrane production (Lewis *et al.*, 2018). Since then, no new attempts to develop another commercialised process for preparing regenerated cellulose membranes have been reported, which has resulted in the poor representation of cellulose membranes in the market. Currently, regenerated cellulose membranes are mainly presented by Millipore, usually in pre-cut size for specific applications, or as single-pass modules, such as Cadence^{TM}.

2.3 Typical characteristics of cellulose-based membranes and examples of their applications

Using cellulose as a material for membrane manufacturing is attractive for several reasons. In addition to being available globally, thus enabling potential local harvesting instead of transporting the material, cellulose is also a renewable material (Isikgor and Becer, 2015). Cellulose films, as well as natural cellulose fibres, exhibit moderate chemical stability in most environments, likely due to the cellulose molecules' amphiphilic character (Mohamed *et al.*, 2019). From another viewpoint, cellulose's chemical structure results in a complex system of hydrogen bonds between molecular chains, making cellulose a good choice for applications where solvent resistance is required (Durmaz and Zeynep Çulfaz-Emecen, 2018). Solvent resistance is part of the membrane chemical stability, which also includes resistance to strong bases and acids (Mohamed *et al.*, 2019).

Cellulose is naturally hydrophilic in the equatorial direction of the glucopyranose ring, which makes cellulose membranes attractive for the purification of water-based media (Durmaz and Zeynep Çulfaz-Emecen, 2018; Mohamed *et al.*, 2019). Cellulose's hydrophilicity comes from many hydroxyl (−OH) functional groups (Figoli, Simone and Drioli, 2015). One of the usually highlighted properties of cellulose membranes is their elevated fouling resistance in aqueous media compared to most hydrophobic polymeric membranes (Figoli, Simone and Drioli, 2015). The definition of membrane fouling varies from researcher to researcher, as this phenomenon is complex. Generally, membrane fouling describes the undesirable deposition of retained particles, macromolecules, salts and colloid particles of different characteristics at the top of the membrane surface or inside its pores (Figoli, Simone and Drioli, 2015; Singh and Hankins, 2016; Al Aani, Mustafa and Hilal, 2020).

Due to cellulose's chemical stability, hydrophilicity and relatively high stability to fouling, compared to hydrophobic polymeric membranes, cellulose-based membranes are a good choice for the separation and purification of different water-based wastestreams, such as the recovery of compounds from pulp and paper and wood processing wastestreams. The chemical stability of cellulose membranes is also quite useful for the

membrane separation of proteins (Jönsson and Jönsson, 1995; Susanto and Ulbricht, 2005; Kallioinen *et al.*, 2010; Al Manasrah *et al.*, 2012; Naim *et al.*, 2015). Some examples of cellulose UF membranes used in separation processes are given in Table 2.1.

Table 2.1: Examples of the separation processes in which regenerated cellulose ultrafiltration membranes were tested.

Membrane	Example of an application	Lab scale vs industrial application	Which feature of RCM is the most contributing	Reference
C30FM (commercial), cut-off 30 kDa	Purification of pulp and paper ground wood mill circulation water; paper mill clear filtrate; spent sulphite liquor	lab-scale; pilot scale-up	lower fouling; hydrophilicity	(Kallioinen *et al.*, 2005, 2006, 2007)
UC030 (commercial), cut-off 10 kDa	Filtration of pulp mill process waters; recovery of galactoglucomannan from wood hydrolysate	lab-scale	hydrophilicity	(Puro *et al.*, 2011; Al Manasrah *et al.*, 2012)
RC70pp (commercial), cut-off 10 kDa	Treatment of spent DES; fractionation of phytosterols isolated from orange juice	lab-scale	chemical stability in organic solvents; hydrophilicity	(Abd-Razak, Chew and Bird, 2019; Ippolitov *et al.*, 2022)
XM50 (commercial), cut-off 64 kDa	Filtration of Ottawa River water (unpurified, highly coloured)	lab-scale	lower fouling	(Dang *et al.*, 2006)
CRC (commercial), cut-off 100 kDa	Separation of bovine serum albumin and lactoferrin mixtures	lab-scale	negatively charged surface	(Mehta, 2006; Valiño *et al.*, 2014)
(lab-made) deacetylated cellulose acetate membrane	Filtration of model yeast-based foulant mixture	lab-scale RO unit	hydrophilicity	(Naim *et al.*, 2015)
(lab-made) regenerated cellulose membrane	Filtration of model polymeric compounds	lab-scale	hydrophilicity	(Livazovic *et al.*, 2015; Durmaz and Zeynep Çulfaz-Emecen, 2018; Nevstrueva *et al.*, 2018; Tran and Ulbricht, 2023)
(lab-made) regenerated cellulose membrane	Recovery of protein-like compounds	lab-scale	hydrophilicity	(Zhang *et al.*, 2001; Chen, Wang and Liu, 2012)
(lab-made) regenerated cellulose membrane with modification	Oil/water emulsion separation; biotreated municipal wastewater purification	lab-scale	lower fouling; hydrophilicity	(Li *et al.*, 2021; Joshi *et al.*, 2023)

2.4 Phase inversion: main parameters and their effect on membrane formation

Phase inversion (PI) or phase separation (PS) is the most versatile and common method for polymeric membrane production. In this method, the initial homogeneous system (i.e. casting solution or dope solution) is placed under conditions that trigger its separation into two distinct phases. The solid phase consists of the polymer and becomes the

membrane matrix, whereas the liquid phase consists of the solvent and initiates pore formation within the membrane matrix. PS can be induced through different mechanisms: evaporation-induced (EIPS), vapor-induced (VIPS), temperature-induced (TIPS) and non-solvent-induced (NIPS). All phase separation, or precipitation, techniques are based on decreasing the polymer's solubility in the solvent, which induces the precipitation process and formation of two separate phases. Precipitation in TIPS is induced by lowering the system temperature, in NIPS with the introduction of the non-solvent into the system, and in VIPS via the entry of the non-solvent vapor phase into the system; in EIPS, the precipitation starts as the volatile solvent evaporates from the system. Although this is a common classification of PS techniques, some researchers have distinguished only temperature-and diffusion-induced precipitation, including EIPS, VIPS and NIPS, in the latter group (Mulder, 1996; Mohanty and Purkait, 2011; Figoli, Simone and Drioli, 2015). PI is rightfully considered an exceptionally versatile technique, allowing control over many casting parameters and resulting in an impressive variety of morphologies and properties of the resulting membranes.

The NIPS process starts from the preparation of a homogeneous solution of a polymer in the solvent of choice. The concentration of the casting solution should be determined correctly for the solution to have the right viscosity: high enough to hold the desired shape of the cast film and low enough to penetrate the carrier material and maintain the flow (El-Gendi, Abdalla and Ali, 2012). After the polymer is spread by a casting knife into a desired shape, the casting plate is transferred into a coagulation bath (CB) that is filled with the non-solvent. The changes occurring to the polymer/solvent/non-solvent (P/S/NS) system in the CB are best described with the use of ternary phase diagrams (Figure 2.2).
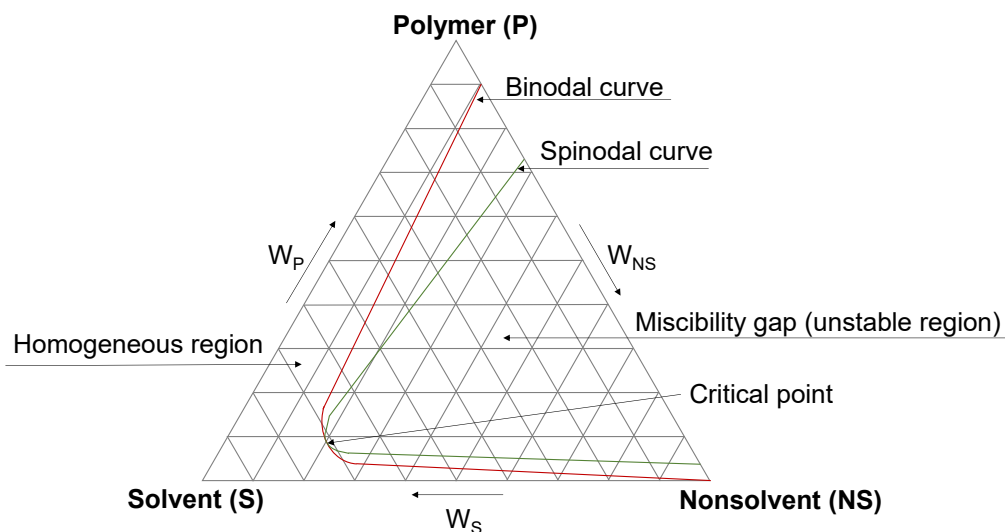

Figure 2.2: General example of a ternary phase diagram (mainly adapted from (El-Gendi, Abdalla and Ali, 2012))

The ternary phase diagram always refers to a certain temperature in a certain P/S/NS system and should be defined experimentally. The system must exhibit a miscibility gap or an unstable region, which is delimited by the spinodal curve. The metastable region is situated between the binodal and spinodal curves. The initial system composition point is in a random position in a homogeneous region, or stable region, where only the polymer and solvent are present. As the non-solvent enters the system, the system composition changes as the S-NS exchange starts occurring. Once the system goes beyond the miscibility gap, the formation of the membrane matrix is complete and polymer aggregates are formed. Many parameters can affect the pathway which the system will undergo as NS is added, which will impact the membrane's porosity, pores' interconnection and the performance (Table 2.2).

Table 2.2: Parameters affecting the outcome of NIPS (Lohokare, Bhole and Kharul, 2006; Figoli, Simone and Drioli, 2015; Nevstrueva *et al.*, 2018; Esfahani *et al.*, 2020).

Parameter	Effect on membrane's morphology and/or performance	Tested in this study
Polymer type	Defines hydrophilicity/hydrophobicity and fouling tendency, mechanical properties, chemical resistance and film-forming properties.	Yes
Polymer concentration	Low concentrations increase dope is instability and promote fast demixing, while high concentrations increase viscosity and lead to delayed demixing. Low concentrations result in the formation of macrovoids, uneven film formation and low mechanical stability. High concentrations result in the formation of a thicker active layer, which delays the coagulation of inner layers, lower overall porosity and increase in the hydrophilicity/surface charge due to a larger number of functional groups. Low concentrations – higher flux, worse retention; high concentrations – lower flux, better retention.	Yes
Solvent type/ non-solvent type	Solvent's polarity and miscibility with non-solvent affects the S/NS exchange rate, which in turn affects the membrane morphology.	Yes
Casting thickness	Decrease in thickness can reduce the efficiency of the filtration; the increase in thickness yields fewer defects in the film. The thicker the membrane, the larger is the hydraulic resistance of the membrane, which results in lower flux.	Yes
Viscosity	Higher viscosities control the kinetic factor of demixing, resulting in denser morphologies hindering the formation of macrovoids.	Yes
Temperature of solution	Affects casting solution viscosity, hence, the formation of a skin layer and the density and porosity of the membrane matrix.	Yes
Delay time	The interval between the moment of immersion in the coagulation bath and the start of liquid–liquid demixing process. If the delay time is increased, the system passes the metastable region of the diagram, and its morphology is defined by the formation and size of the formed nucleus.	No
CB temperature	Lower temperature supports delayed demixing, while higher temperatures trigger instantaneous demixing because, with the increase in temperature, the diffusion rate increases as well. Lower temperatures result in dense asymmetric morphologies, while higher temperatures are associated with the formation of finger-like macrovoids. Lower temperatures result in better retention and lower flux, whereas higher temperatures lead to better flux and worse retention.	Yes
Additives	Two types of additives—delaying and speeding the PS process—affect the thermodynamic/kinetic balance; modify hydrophilicity/ hydrophobicity, suppress the formation of macrovoids or promote pore formation.	Yes
Support material	Woven/non-woven structure, thickness, porosity, water-holding capacity of the support material affect mechanical stability, stretchability and pore formation of the membrane.	Yes

3 Materials and methods

3.1 Materials

Debarked birch wood chips (*Betula pendula*) with a nominal size of $5 \times 1 \times 0.1$ cm and a non-dyed bedsheet labelled 100% cotton were used as the cellulose sources. In addition, experiments were done using debarked pine wood chips (*Pinus Silvestris*) with a nominal size of $5 \times 1 \times 0.1$ cm and construction and demolition wood (CDW, grade A) with a size of particles approximately 1 mm. Wood biomass DES pretreatment was conducted using choline chloride (CAS # 67-48-1, Merck KGaA, Darmstadt, Germany), which was used as an HBA, and lactic acid (CAS # 79-33-4, Merck KgaA, Darmstadt, Germany), which was used as an HBD. Bleaching of the DES-treated biomass was organised with acetic acid (CAS # 64-19-7, Merck KgaA, Darmstadt, Germany) and sodium chlorite (CAS # 7758-19-2, Acros Organics, Geel, Belgium). The two-step alkaline treatment following DES treatment and bleaching was conducted using a NaOH solution which was prepared from sodium hydroxide (CAS # 1310-73-2, Merck KgaA, Darmstadt, Germany) in concentrations of 17.5% and 8.3% for treatment and washing, respectively.

A mixture of IL 1-ethyl-3-methylimidazolium acetate, 95% ([Emim][Oac], C_1C_2ImOAc, CAS # 143314-17-4, Iolitec Ionic Liquids Technologies GmbH) and DMSO (CAS # 67-68-5, Merck KgaA, Darmstadt, Germany) was used to prepare the casting solution for membrane preparation. The support material for membrane casting in Publications I and IV was mechanically cleaned non-woven polyester, which was obtained from used RO membranes. In Publications II and III, the Viledon® Novatexx 2484 carrier material was used as the support (Freudenberg, Germany; as reported by manufacturer, air permeability: 60 L/(s·m^2) at 200 Pa; weight per unit area: 85 g/m^2; maximum tensile force along/across: 300/200 N/5 cm; 25/30% elongation at maximum tensile force along/across and thickness: 0.12 mm). Additional experiments were performed using the Viledon® Novatexx 2482 carrier material (Freudenberg, Germany; as reported by manufacturer, air permeability: 8 L/(s·m^2) at 200 Pa; weight per unit area: 215 g/m^2; maximum tensile force along/across: 800/380 N/5 cm; 28/28% elongation at maximum tensile force along/across and thickness: 0.25 mm).

In the membrane rejection tests, poly(ethylene glycol) (CAS: 25322-68-3, Merck) in molar masses 1.5, 3, 8, 12 and 35 kDa was used for neutral compound representation. The discharge water of the Toikansuo wastewater treatment plant's secondary clarifier located in Lappeenranta, Finland, was used in the experiments as the purified wastewater. The Toikansuo plant's treatment capacity is approximately 20,000 m^3/day. The purified wastewater's parameters at the time of testing for Publication III were as follows: the total solids content: 12.1 mg/L, pH: 7.75, total carbon concentration: 5.92 mg/L, total nitrogen concentration: 9.4 mg/L and total phosphorous concentration: 0.35 mg/L. Reactive blue 2 dye (RB2, CAS #12236-82-7, M_w 774.16 g/mol, λ_{max} 607 nm, pK_a 5.5, number of ionizable groups 3, used for cellulose fibre, polyamide, wool, silk dyeing and printing) was used as a model dye contaminant.

3.2   Wood biomass treatments

3.2.1   Deep eutectic solvent treatment

The deep eutectic solvent was formed by combining 1 mole of ChCl with 9 moles of LAc, corresponding to a composition with high lignin dissolution power (A. L. Li *et al.*, 2018), and mixing chemicals together at 100°C until the formation of a clear homogeneous mixture. Birch wood chips were dried at 105°C overnight and taken at a 1:5 solid-to-liquid mass ratio and placed in DES for 18 h at 105°C. The treated pulp was washed with an ethanol–water mixture at a 9:1 volume ratio under vacuum filtration through filter paper. The pulp was dried at 50°C for 24 h.

3.2.2   Chlorite bleaching

After the pulp was dried after DES treatment, it was mixed with DI water, sodium chlorite and acetic acid. For each 2.5 g of pulp, 80 mL of DI water, 1 g of sodium chlorite and 0.5 mL of acetic acid were taken, and bleaching was carried out for 60 min at 70°C with repeated stirring every 5–7 min (Rowell, Pettersen and Tshabalala, 2012). As the pulp became almost white, the reaction was stopped, and the pulp was washed with water, ethanol and acetone to remove traces of bleaching chemicals. The pulp was dried at 50°C for 24 h.

3.2.3   Alpha cellulose separation

After consequent DES treatment and bleaching, the dried pulp was subjected to alkaline treatment, which is described in the literature as the separation of α-cellulose (Rowell, Pettersen and Tshabalala, 2012). According to the protocol, the pulp was treated in 17.5% NaOH solution to be further washed with 8.3% NaOH solution and DI water. After washing, the pulp was subjected to 10% acetic acid treatment and washed with DI water once again. The pulp was dried at 50°C for 24 h.

3.3   **Membrane preparation**

The membranes for all experimental studies were prepared using the NIPS technique with the Automatic Film Applicator L (BYK-Gardner, USA). The casting solutions were prepared by dissolving the measured amount of biomass or textile in the [Emim][OAc]–DMSO mixture. In Publication IV studies, LiCl was added to the [Emim][OAc]–DMSO mixture prior to the addition of bleached wood biomass. The casting solutions were heated at 70–120°C, depending on the composition, with constant stirring at 200 rpm until a homogeneous solution was formed. As the solution was ready, it was spread on top of the support material at defined casting thickness. After casting, the casting plate was transferred into the coagulation bath container, adding the second coagulation bath filled with alkali solution in Publication III, filled with an antisolvent to induce the precipitation

of the polymer. The membranes were kept in a coagulation bath for 24 h and rinsed with DI water to ensure thorough removal of the solvents from the membrane matrix.

3.4 Methods evaluating chemical composition of source materials and produced membranes

3.4.1 Fourier-transform infrared spectroscopy analysis

Due to the existence of several characteristic vibrational bands, Fourier-transform infrared (FTIR) spectroscopy can be adopted as a fast tool for comparing chemical changes in the membrane matrix. In all Publications I—IV, the infrared spectra of the membranes' top surfaces were recorded using a Frontier MIR/FIR Spectrometer (PerkinElmer Inc.). Equipped with a diamond crystal, the spectrometer recorded the spectral range in 400–4000 cm^{-1} interval, with a spectra resolution of 4 cm^{-1}. At least five random points were selected from each membrane for measurement, and the recorded spectra were averaged. The processing of all spectra included ATR correction, baseline correction and normalisation.

3.4.2 Raman spectroscopy analysis

Raman spectroscopy can be used to derive a quick conclusion about membrane chemistry, as it takes a short time and does not require additional processing of the raw data. Raman spectra of air-dried membranes were taken for Publication I. A Kaiser RXN1 spectrometer was used for the collection of the spectra with 785 nm laser excitation and maximum power of 200 mW. The spectra were recorded between 100 and 3425 cm^{-1} using a non-contact MR probe.

3.4.3 Thermogravimetric analysis

In Publication I, the membrane sample for thermogravimetric analysis was weighed to be approximately 10 ± 0.1 mg and heated from 25 to 900°C at 10°C/min rate under a constant flow rate of nitrogen at 40 mL/min. The evolved gas emission was analysed using a mass spectrophotometer coupled with thermogravimetry (TG) (MS 403C Aëolos Mass Spectrophotometer, NETZSCH-Gerätebau GmbH, Selb, Germany). The analysed mass range was 10–110 a.m.u. The results were interpreted with N-Proteus® software (NETZSCH-Gerätebau GmbH, Selb, Germany).

3.4.4 Carbohydrates analysis

To measure the hemicellulose and cellulose contents in the wood biomass samples for Publication I, analyses were run according to modified procedures (Holmbom and Örså, 1993; Sundberg *et al.*, 1996). The contents were measured using a gas chromatograph HP6890 + injector HP7683 (Agilent, USA). The column was a 25 m/0.20 mm internal

diameter. wide-bore capillary column with a non-polar phase (HP-1, Agilent Technologies) and a film thickness of 0.11 μm. To analyse hemicellulose's monosaccharides, acid methanolysis was applied to the samples. The GC results were calculated using relative response factors (*What is a Response Factor? Chromatography Today*, no date; Sundberg *et al.*, 1996; Anugwom *et al.*, 2012).

3.4.5   **Lignin analysis**

Lignin content was measured according to the procedure described in (Sluiter *et al.*, 2008). It was determined in two parts: acid soluble lignin (ASL) and acid insoluble lignin (AISL) or Klason lignin. ASL was measured from the liquid part of the samples using a UV-Vis spectrometer and calculated based on Beer-Lambert's law with absorptivity of $110 \text{ L g}^{-1} \text{ cm}^{-1}$ for 205 nm wavelength.

3.5   **Membrane performance evaluation**

The newly fabricated flat sheet membranes were tested on a small scale. Part of the filtration experiment was conducted in the Amicon dead-end filtration unit (Figure 3.1). The Amicon ultrafiltration cell (Millipore, Burlington, MA, USA, Cat No.: XFUF07611) contains a stirring device with a diameter of 60 mm.
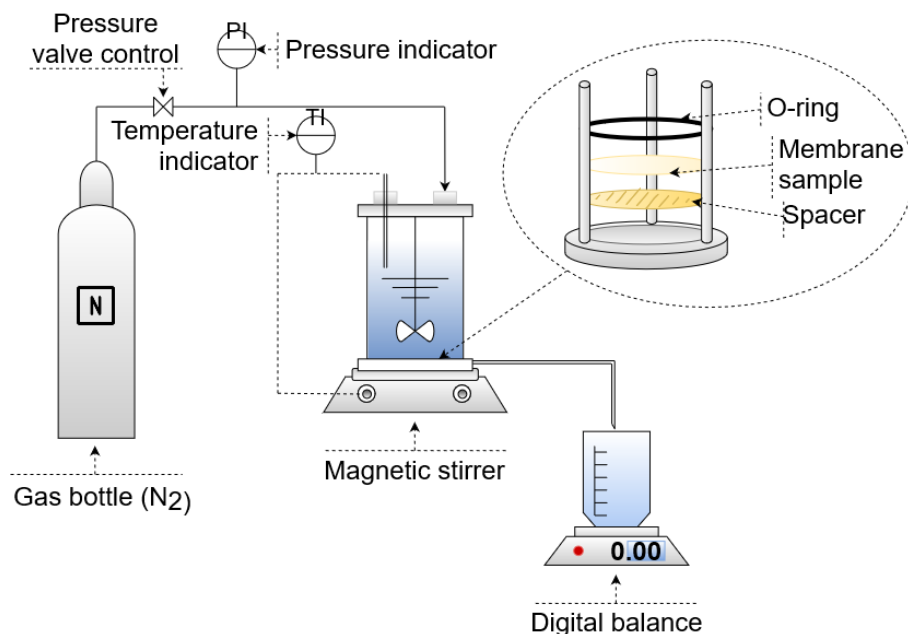
Figure 3.1: Schematic dead-end configuration of membrane filtration cell.

The other part of the filtration experiment was conducted using the cross-flow filtration module with four parallel cells (Figure 3.2). The cross-flow module also allows a

recirculation operational regime, making possible the organisation of 'more realistic' and economical filtration processes. The size of the membrane samples was 10.4 cm^2, and the experiments were performed at the crossflow velocity υ = 1.2 m/s, pressure of 1 bar and temperature of 20 ± 0.5°C.
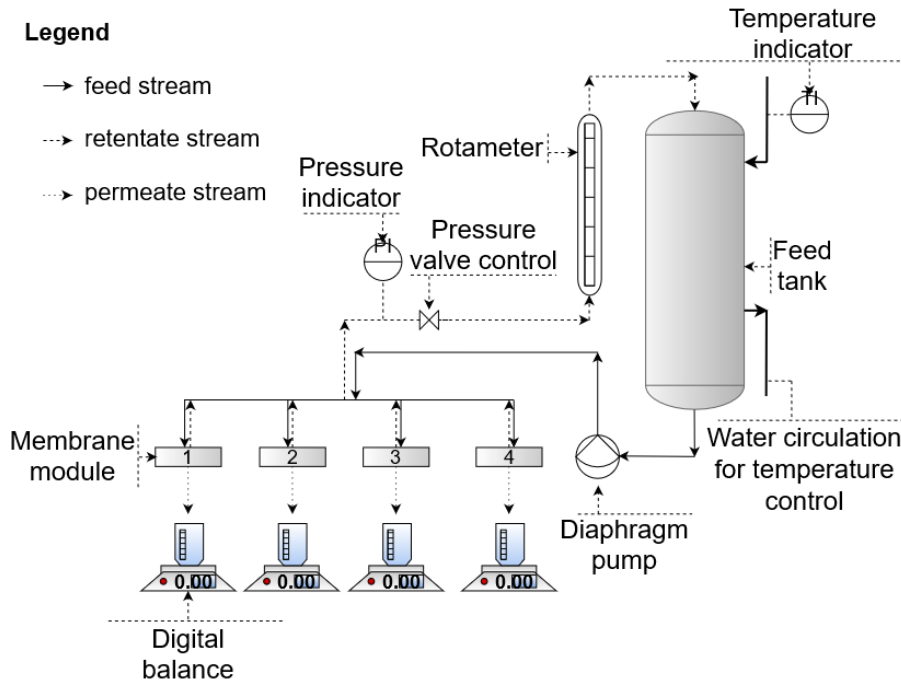

Figure 3.2: Schematic cross-flow configuration of membrane filtration cell.

Pure water permeance was calculated as a slope of parallel measurements of flux at 25 ± 0.5°C at 1, 2, 3 and 4 bars of pressure as follows:

$$P = \frac{\Delta V_p}{\Delta p \cdot A_f \cdot t_p}$$

(3.1)

where P is the tested membrane's permeance (L/(m^2·h·bar)), ΔV_P is the collected permeate volume (L), Δp is the applied pressure (bar), A_f is the effective filtration area of the membrane sample (m^2), and t_p is the time of collection of the permeate (h).

One of the most important characteristics of ultrafiltration membranes is the retention curve, which is measured with several model polymers with known molar mass. Whenever the polymers of a certain molar mass undergo 90% rejection, this is called a molecular mass cut-off (MWCO) of the membrane. Though variations are possible, ideally, the model solutions would be prepared from the polymers with a narrow molecular mass distribution, unaffected by pH, shear and ionic strength (Jonsson, 2001). The choice is usually narrowed down to proteins, dextrans and polyethylene glycols. The

current study used polyethylene glycols (PEGs) at 300 ppm concentration for plotting retention curves to ensure minimal solute–solute interactions. According to the CHARMME project, the optimal operating regime, which minimises fouling, was applicable at a constant permeate flux of 40 L h^{-1} m^{-2} (Jonsson, 2001).

In Publications I−IV, a model solution of PEG 35 (and PEG 20 in Publication II) was prepared with a concentration of 300 ppm and filtered through the membrane sample. The feed, retentate and permeate samples were collected and analysed for total organic carbon (TOC) content with a Shimadzu TOC analyser (TOC-L series, Japan). In yet unpublished experiments, the retention of the produced membranes was measured with a model solution of multiple PEGs (1.5, 3, 8, 12 and 35 kDa), each with a concentration of 300 ppm. The samples of the recirculated feed and permeate were collected and analysed using size-exclusion chromatography (SEC). In the SEC setup, a 300 mm × 7.8 mm PolySep-GFC-P 3000 column (Phenomenex) was connected to an Agilent Technologies 1260 Infinity HPLC system with a refractive index detector. Deionized water was used as the eluent.

The pressure was adjusted for each membrane individually to have approximately the same flux of 40 L/(m^2·h). Throughout the measurements, the temperature was maintained at 25 ± 0.5°C. When filtrations were performed in the Amicon stirring cell, the stirring speed was maintained at 300 rpm using a magnetic stirrer with an rpm indicator. The retention percentage measured from the samples was calculated as follows:

$$R = \left(1 - \frac{2 \cdot C_p}{C_f + C_r}\right) \tag{3.2}$$

where C_p, C_f and C_r are the TOC concentrations in the permeate, feed and retentate (mg/L), respectively.

3.6 Methods evaluating surface properties, morphology and crystallinity of membranes

3.6.1 X-ray diffraction analysis

Due to the semi-crystalline nature of cellulose, it is important to assess the resulting membrane's crystallinity, as it affects its morphology and performance (Rajesh *et al.*, 2011). A Bruker AXS D8 Advance X-ray diffractometer was used to record X-ray diffraction (XRD) patterns of biomass samples and membranes prepared in Publications I and III. Patterns were recorded using Cu Kα ($\lambda = 1.5418$ Å) at 40 kV and 40 mA in the range of $2\theta = 7$–$60°$.

3.6.2 Zeta potential (membrane charge)

Zeta potential describes the membrane's surface charge and is helpful in understanding the electrostatic interactions between the membrane's surface and the charged particles and developing strategies to improve membranes' performance (Ribitsch *et al.*, 2001; Fievet *et al.*, 2003; Yang *et al.*, 2021). The zeta potential of the solid surface is ascertained from the streaming current measurement, evaluating the electrical potential at the hydrodynamic plane of shear (Fievet *et al.*, 2003). The streaming current measurements were conducted using a SurPASS Electrokinetic analyzer (Anton Paar GmbH, Graz, Austria). The membrane samples were analysed using an adjustable gap cell method and a 0.001 M KCl solution as a background electrolyte. The zeta potential was measured in the 7.5–2.7 pH range. The starting value was adjusted with 0.1 M KOH solution and automatically titrated to more acidic values using 0.05 M HCl. During the measurement sequence, N_2 gas was bubbled to the electrolyte solution to avoid acidification caused by dissolved carbon dioxide. The zeta potential curves presented were calculated automatically using SurPASS software based on the Helmholtz-Smoluchowski equation.

3.6.3 Contact angle (hydrophilicity)

Contact angle (CA) measurement provides information about the membrane's surface energy, wettability and hydrophilicity. The membranes' contact angle values were measured using the captive bubble method (Zhang and Hallström, 1990). The measurements were performed using KSV CAM 101 equipment (KSV Instruments Ltd., Finland) connected to a CCD camera (DMK 21F04, Imaging Source Europe GmbH, Bremen, Germany). The membranes were attached to a piece of glass and submerged in water (top surface looking down). Contact angles were measured from 3–4 µL of air bubbles placed on the membrane surface by using a U-shaped needle. Six random points were measured from each membrane sample. Curve fitting analysis of the images was performed using CAM 2008 software.

3.6.4 Scanning electron microscopy imaging

The prepared membranes' morphology was examined with a scanning electron microscope (SEM) (Hitachi SU 3500, Japan) at an acceleration voltage of 1.5 kV under high vacuum conditions. Before the analysis, the membrane samples were dried in a manual freeze dryer ALPHA 2-4 LDplus (Martin Christ GmbH, Germany) to preserve the morphology from shrinking. The top surfaces of the membranes were analysed immediately after freeze-drying. For the cross-sectional images, narrow strips of the membranes were cut and split with two pairs of forceps under liquid nitrogen to obtain a clean cut.

4 Results and discussion

4.1 Preparation of membranes from wood biomass

4.1.1 Effect of purity of carbohydrate fraction recovered from wood biomass on the membrane properties

As shown in Publication I, the utilised mixture of [Emim][OAc]–DMSO could dissolve untreated milled wood biomass, which had the typical ratio of cellulose, hemicellulose and lignin within itself (Horvath, 2006), forming a 5 wt.% casting solution. Complete dissolution of wood biomass has been previously reported only in cases where pure [Emim][OAc] was used as a solvent (Kilpeläinen *et al.*, 2007; Sun *et al.*, 2009; Li *et al.*, 2010; Abushammala and Mao, 2020). However, the preparation of the solution from untreated wood biomass required a temperature of 120°C and up to 5 days to be completed. Although preparation of solutions using similar or same solvents' mixture required lower temperatures (80–90°C) and shorter time (up to 2 days), the cellulose sources used were commercially produced cellulose, not the wood biomass (Anokhina *et al.*, 2017; Durmaz and Zeynep Çulfaz-Emecen, 2018).

The applied DES treatment efficiently decreased the lignin and hemicellulose contents by 65% and 68%, respectively (Figure 4.1). Previous research findings support the achieved results, attributing the success of delignification treatment to the concentration of acid content in the DES mixture, showing the best results at a ChCl:LAc of 1:9 (Francisco, Van Den Bruinhorst and Kroon, 2012). Surprisingly, 28% of cellulose was also removed according to the GC results. Dubious dissolution of cellulose might be a result of thermal degradation at elevated temperatures (Kumar, Parikh and Pravakar, 2016; Loow *et al.*, 2017).

Further bleaching and alkaline treatment of biomass continuously lowered the proportions of lignin and hemicellulose by 94.5% and 83.5%, respectively, removing part of amorphous cellulose as well and resulting in an almost pure cellulose fraction. DES-treated wood biomass and the bleached wood biomass dissolution process required lower temperature (100°C) and shorter time compared to the dissolution of untreated wood biomass and alkali-treated wood biomass, both of which required a temperature of 120°C. Based on the literature, the presence of hemicellulose in wood biomass samples ensures its easier dissolution, owing to the presence of acetyl units that participate in the dissolution process, increasing the total polarity of the media and promoting the cleavage of hydrogen bonds (Li *et al.*, 2010; Triantafyllidis, Lappas and Stöcker, 2013). This explains why the almost pure cellulose fraction (alkali-treated birch; see Figure 4.1) took a longer time and required a higher temperature to be dissolved compared to the wood biomass samples with higher hemicellulose content.
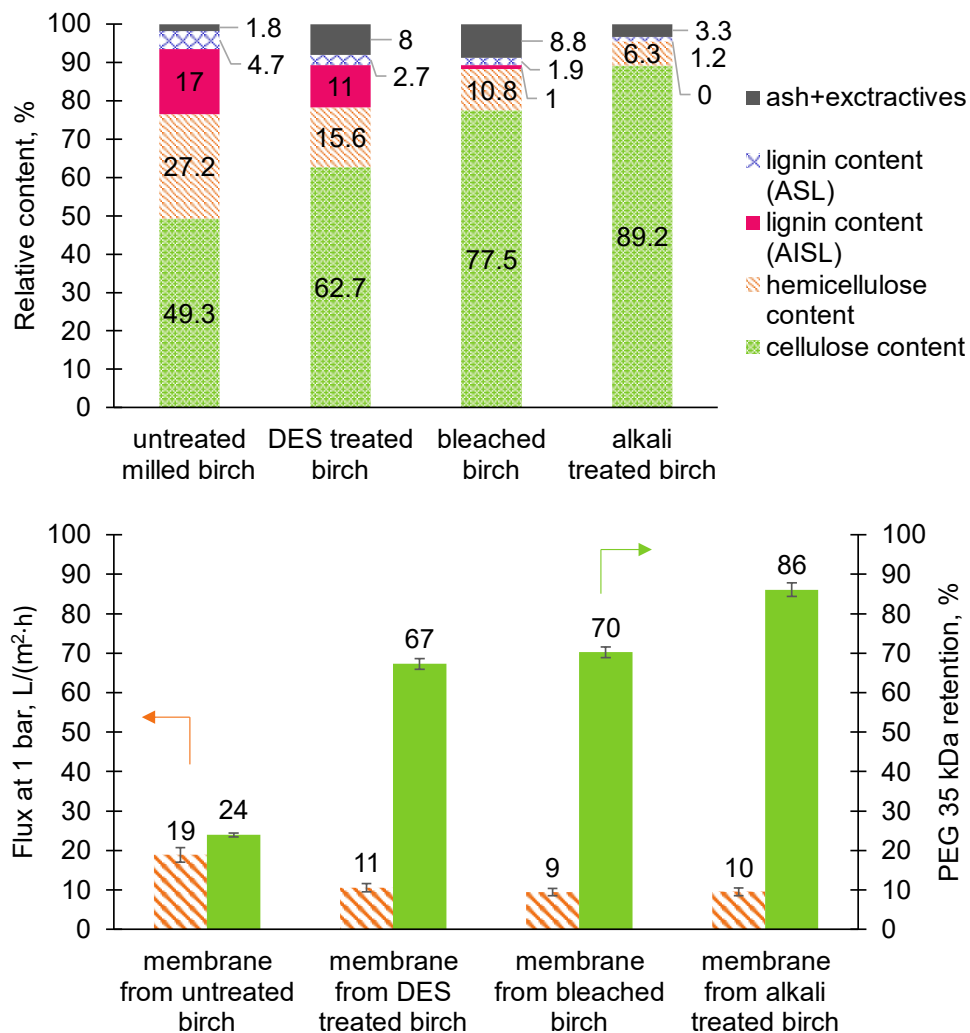
Figure 4.1: Chemical composition of wood pulp after consequently applied treatment steps (top) and pure water flux measured at 1 bar and retention of PEG 35 kDa (bottom) of membranes prepared from each pulp sample; all membranes were cast at 300 µm casting thickness and using old RO support as the carrier material. All measurements were conducted in the Amicon ultrafiltration cell at 25°C at a mixing rate of approximately 300 ppm; figures are adapted from Publication I.

The results depicted in Figure 4.1 emphasise the importance of cellulose fraction's high purity. The higher the share of cellulose present in the casting solution, the more uniform the top layer formed, and the better the retention. However, as lignin and hemicellulose contents in the wood biomass samples decreased simultaneously (see top part of Figure

4.1), it is challenging to distinguish among their individual effects on the final membrane's characteristics. Though the addition of lignin as a flux promoter has been studied previously (Esmaeili *et al.*, 2018), the direct transfer of lignin from wood biomass to the membrane matrix is aligned with not only increased flux but also decreased retention.

The process of dissolution and regeneration of biomass from an IL solution is sometimes classified as delignification, due to the noticeable difference in lignin content in the samples before dissolution and after regeneration (Sun *et al.*, 2009; Protz *et al.*, 2021). Loss of lignin in the dissolution–regeneration process resulted in the absence of lignin in the membranes prepared from bleached birch and alkali-treated birch. Hemicellulose was present in all prepared membranes, except for the one prepared from alkali-treated biomass. The reason for the absent or reduced amount of hemicellulose is the partial hemicellulose degradation in the IL and hence its easier washout during the solvent–non-solvent exchange (Li *et al.*, 2010).

From the IR spectra of the membranes reported in Publication I, the chemical changes in the membranes' matrix composition can be traced (Figure 4.2). Lignin characteristic peaks were located at 1592/1507 cm^{-1} (C=C stretching vibration), 1460 cm^{-1} (asymmetric bending in CH$_3$), 1420 cm^{-1} (C-H deformation), 1325 cm^{-1} (C-O vibration in the syringyl ring) and 1231 cm^{-1} (guaiacyl/syringyl ring and C-O stretching vibration) (Pandey and Pitman, 2003; Mohamed *et al.*, 2015). These peaks were the most prominent in the spectrum of membrane prepared directly from milled untreated wood biomass, which correlates with the highest lignin content in the membrane matrix. As treatment steps were applied, these peaks became less intense and/or turned into shoulder formation rather than distinct peaks, indicating a lower lignin content. The same applies to the peak at 1732 cm^{-1}, which was associated with carboxylic groups of lignin, hemicellulose and extractives in native wood; its intensity gradually reduced as more lignin and hemicellulose were removed. As this peak turned into a shoulder and moved to the left in the spectrum of the membrane prepared from alkali-treated wood biomass (green line), it presented as a sign of acetylation in the IL (Gericke, Fardim and Heinze, 2012). A common peak for all spectra at 1640 cm^{-1} was assigned to H-O-H bending vibration from residual water in the sample.
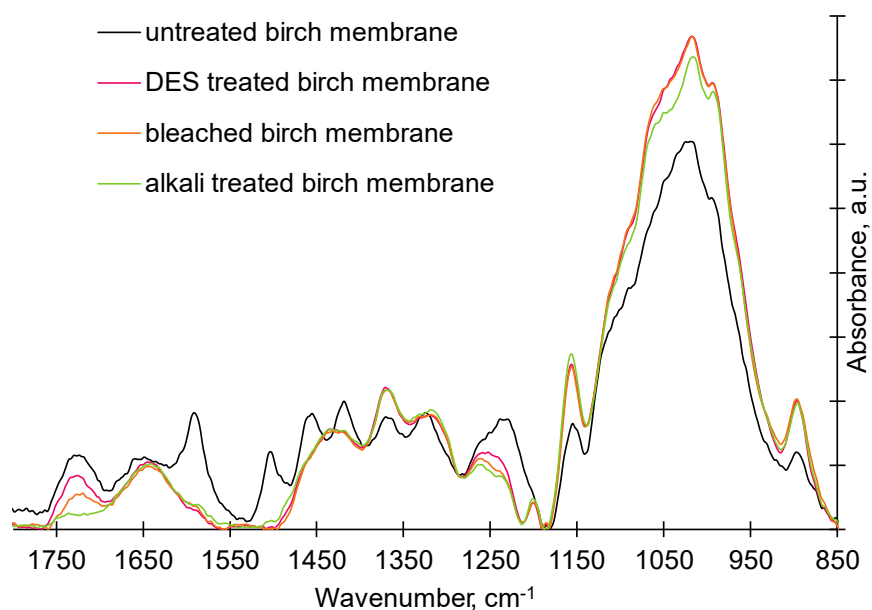
Figure 4.2: FTIR spectra of membrane samples were recorded using the Perkin Elmer Frontier spectrometer with a universal ATR module of diamond crystal at a resolution of 4 cm^{-1} in *absorbance* mode (adapted from Publication I).

Additionally, in Publication I, Raman spectroscopy was used to trace the purity of the carbohydrate fraction in the prepared membrane samples. Raman spectroscopy provides a semi-quantitative understanding of whether lignin and/or hemicellulose is present in the membrane matrix due to intense laser-induced fluorescence (LIF) caused by lignin's presence (Lähdetie, 2013), which can be seen as a background of high intensity in Figure 4.3. As the LIF faded away and the overall intensity of the spectrum lowered, the appearing peaks could be assigned to other biopolymers (e.g. a peak at 1840 cm^{-1}, characteristic for C=O bond, and 900, 1100, 1370 and 2900 cm^{-1} peaks, characteristic for cellulose) (Esfahani *et al.*, 2020).
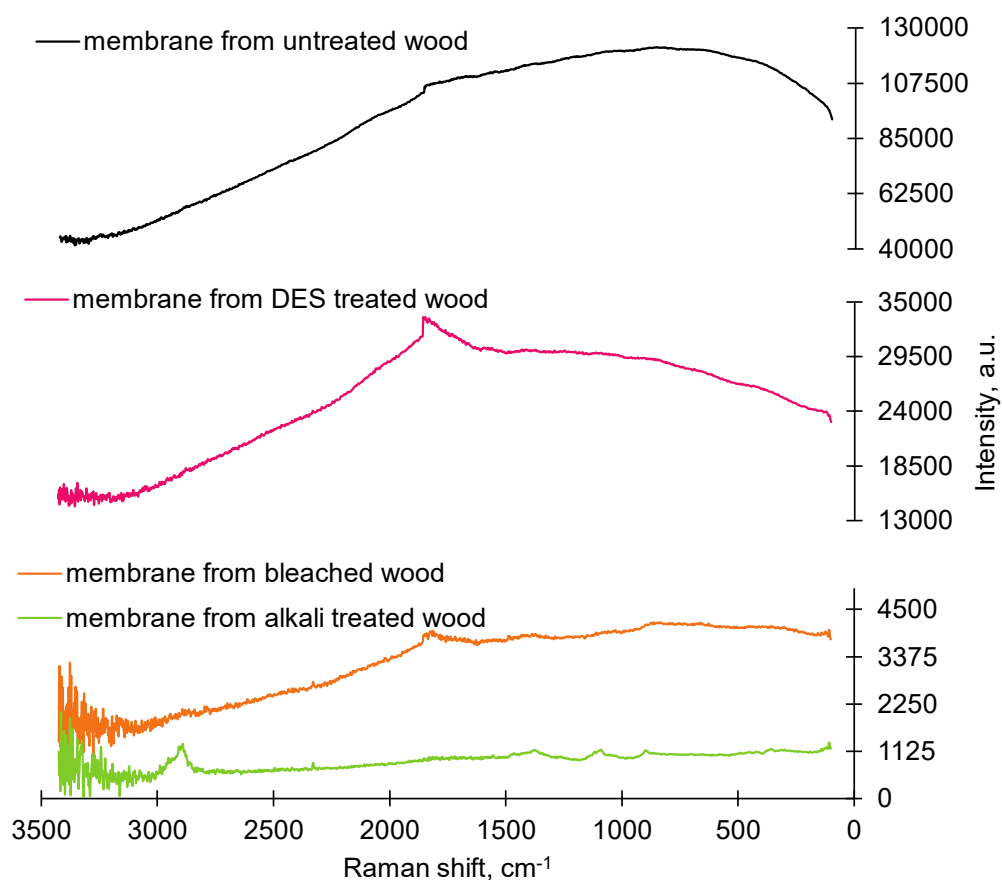
Figure 4.3: Raman spectra of membrane samples measured with Kaiser RXN1 spectrometer, 785 nm laser excitation and maximum power of 200 mW (adapted from Publication I).

4.1.2 Effect of wood raw material type on the membrane properties

While discussing the importance of the polymer type for the result of membrane production, the question of the suitability of different wood types was raised. Based on the results shown in Figure 4.4, the use of hardwood benefited the preparation of cellulose membranes due to its higher cellulose content (Rowell, Pettersen and Tshabalala, 2012), which had a direct effect on the membrane's separation performance. As discussed above, the presence of lignin's remnants mainly acted as a permeability promoter but also interfered with the formation of a uniform top layer. According to the FTIR spectra (Figure 4.2) shown in Publication I, both guaiacyl and syringyl units of hardwood lignin were present in the membrane matrix. According to the TG results (Supplementary material to Publication I), the transferred lignin was mainly guaiacyl units. The guaiacyl

units are typically assigned in the acid-insoluble lignin's part and show better stability to depolymerisation (Wikberg and Liisa Maunu, 2004; Anugwom *et al.*, 2022), which might be the reason for the presence of these units in the membrane matrix.
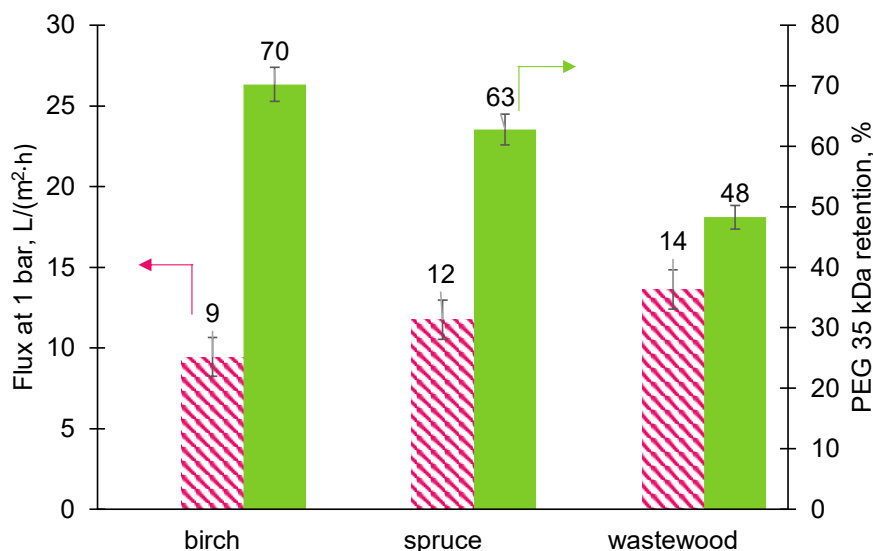
Figure 4.4: Pure water flux measured at 1 bar and the retentions of PEG 35 kDa values measured for membranes prepared from DES-treated and bleached samples of birch, spruce and construction-demolition wood samples. All membranes were cast at 300 µm casting thickness using old RO support as the carrier material. All measurements were performed in the Amicon ultrafiltration cell at 25°C at a mixing rate of approximately 300 ppm.

Softwood biomass contains a larger quantity of lignin, which is chemically different from the hardwood lignin, since syringyl units are absent (Rowell, Pettersen and Tshabalala, 2012). Biomass treatments have a similar effect on softwood biomass as on hardwood biomass (Figure 4.1). Bleaching, following DES treatment, led to the removal of almost the entire lignin from the hardwood, whereas a slightly larger amount remained in the softwood samples. Due to the higher initial amount of lignin in the softwood biomass samples, more lignin was transferred to the membrane matrix, which was observed from the membranes' flux and retention results. As more lignin, which was guaiacyl in this case, remained in a membrane, more hemicellulose would bond to it (Horvath, 2006; Giummarella, 2018; Anugwom *et al.*, 2022), which resulted in the formation of a more permeable membrane with more irregularities in the top layer, resulting in worse retention. The membranes prepared from construction and demolition wood(mainly softwood mixture) demonstrated the highest flux and lowest retention, probably due to the additional contamination of waste wood.

4.1.3   **Effect of casting conditions: casting solution concentration**

The choice to work with a 5 wt.% wood biomass casting solution was made based on the experimental results. Theoretically, the use of casting solutions with higher polymer concentrations should lead to the formation of membranes with thicker top layers, decreased porosity and overall improved separation properties (Kubota, Hashimoto and Mori, 2008). However, the experimental results showed only a small improvement of 5%−8% in separation efficiency, accompanied by a simultaneous decrease in permeance. More concentrated casting solutions (6–8 wt.%) demonstrated inevitably higher viscosity, which resulted in the need to use higher temperatures and a longer time during the dissolution. Furthermore, the literature review supported the experimental finding, as at higher concentrations, the wood dissolution would be significantly hindered (Sun *et al.*, 2009).

4.1.4   **Effect of casting conditions: coagulation bath chemistry and temperature**

According to the literature, the variations in the coagulation bath parameters considerably affect the resulting membranes' morphology (Table 2.2) (Zhang *et al.*, 2001; Mohamed *et al.*, 2015; Nevstrueva *et al.*, 2018). Based on lower miscibility between ILs and alcohols, some researchers have suggested the use of alcohols as a coagulation medium to slow down the demixing process and obtain a membrane with better separation properties (Tan *et al.*, 2019). However, the use of ethanol as a coagulation medium did not improve the separation performance of the membranes within this work; in contrast, such coagulation bath decreased both the permeability and retention efficiency of the resulting membranes by 10% and 14%, respectively. Furthermore, for practical reasons, the whole fabrication procedure should be maintained as simple and environmentally friendly as possible; hence, the use of organic antisolvents for cellulose precipitation (e.g. various alcohols) is undesirable.

The use of water as the coagulation medium is generally more attractive, as it allows the amount of chemicals used to be maintained low. The temperature of the coagulation bath medium affects the rate of the demixing process: a higher temperature generally results in instantaneous demixing, leading to the formation of a more permeable membrane with macrovoid formation in its morphology. A lower temperature leads to decreased solvent–non-solvent exchange rates and endorses the formation of a denser membrane structure (Nevstrueva *et al.*, 2018). In the current study, coagulation bath temperature (CBT) had the great effect on the membranes' separation performance, resulting in a retention decrease of 27% when CBT was increased from 0°C to 20°C and by 95% when increased to 50°C. Hence, the decision was made to continue with a 0°C temperature of coagulation bath to achieve better separation properties.

The use of acidic water-based solutions as coagulation media for cellulose solutions was reported to have a positive effect on the retention properties of the membranes (Mohamed *et al.*, 2015; Mazlan *et al.*, 2019; Taheri, Abdolmaleki and Fashandi, 2019). The usual explanation is based on the electrostatic effects: pK_a, which describes the acidity of a

particular molecule, of cellulose chains is approximately 13.5. Hence, using the coagulation media with higher acidity theoretically should lower the electrostatic repulsion between cellulose chains and allow closer packing, which should result in the formation of a tighter top layer of the membrane and consequently better separation properties (Mohamed *et al.*, 2015; Mazlan *et al.*, 2019; Taheri, Abdolmaleki and Fashandi, 2019). In contrast, the use of the alkaline solution as a coagulation medium for cellulose has not been studied as thoroughly. The use of alkaline solutions for hemicellulose and lignin extraction has long been known (Modenbach and Nokes, 2014; Alves *et al.*, 2016; Gubitosi *et al.*, 2017; Costa *et al.*, 2021); however, it has only been applied to solid biomass samples. Theoretically, based on the difference in biopolymers' solubility in alkali solutions and electrostatic effects, the precipitation process can be altered, which can loosen up the membrane morphology and result in higher flux rates. Thus, it was decided to implement the second coagulation bath, which would intervene with the precipitation process and alter the membrane matrix formation (Figure 4.5).
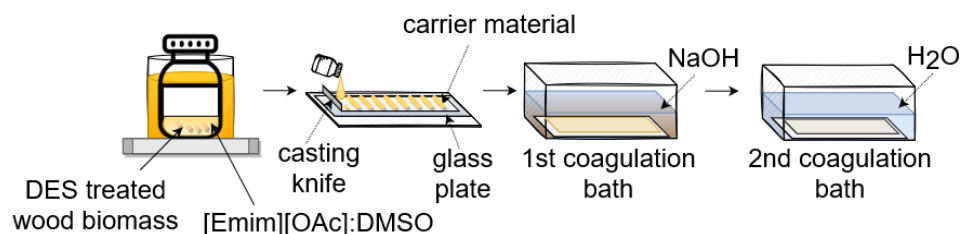
Figure 4.5: A schematic depiction of the two-step coagulation procedure developed in this study (adapted from Publication III).

Two different concentrations of NaOH solution were tested as coagulation media: 5 wt.% and 10 wt.%, both of which are sufficiently high for the dissolution of lignin and hemicellulose, whereas cellulose dissolution in the observed conditions is non-existent or negligible (Medronho and Lindman, 2014; Shi *et al.*, 2014; Melro *et al.*, 2018). The introduction of a NaOH coagulation bath resulted in additional lignin wash-out, which was observed as a change in the first coagulation bath colour from transparent to brownish. Alkali-based precipitation helped to significantly increase the water permeance of membranes (Figure 4.6). The 5/30 and 5/60 membranes' permeance was improved by approximately 36%, while as a 10% solution was used, the membranes' permeance could be improved by 200% and even more.

The experiments conducted in Publication III also demonstrated improvement in the retention of membranes that started the coagulation process in 10 wt.% NaOH solutions, but the difference between the parallel samples was quite high. The difficulty of the exact replication of the results can be explained by the metastability of the cold alkali solutions. Cold alkali solutions are metastable and thus reactive to the slightest changes in temperature and concentration (Le, Rudaz and Budtova, 2014; Medronho and Lindman, 2014; Alves *et al.*, 2016). Thus, without a completely controlled environment, namely temperature, humidity and the rate of temperature increase, the results will show quite a

bit of difference every time. Another reason for the observed differences in permeance and retention alterations could be the irregularity of the wood biomass itself (Horvath, 2006; Medronho and Lindman, 2014; Melro *et al.*, 2018; Costa *et al.*, 2021), resulting in different concentrations of lignin, hemicellulose and cellulose participating in the precipitation.
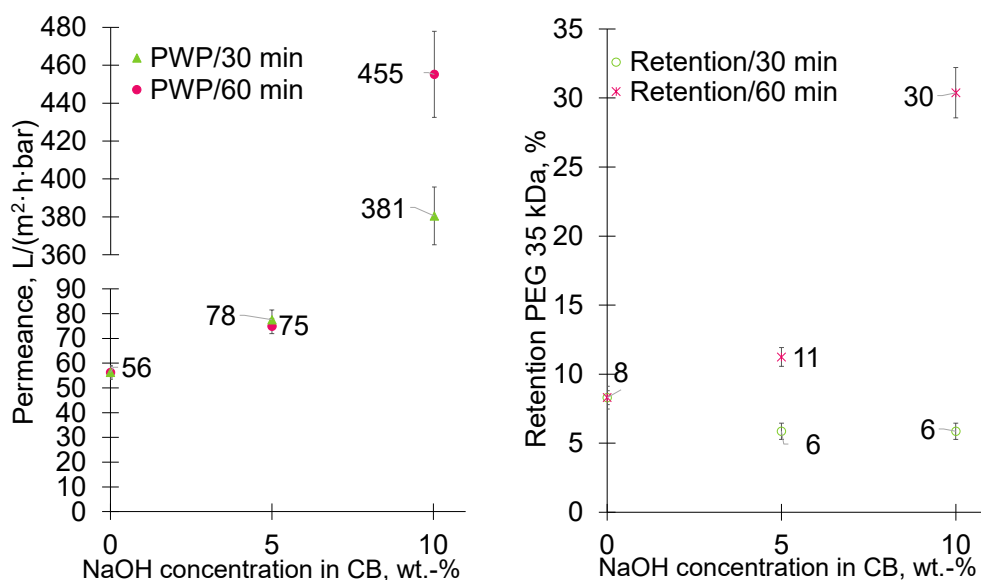

Figure 4.6: Pure water permeance and PEG 35 kDa retentions of the tested membranes, all measured in the Amicon ultrafiltration cell at 25°C and with a mixing rate of approximately 300 ppm (adapted from Publication III).

From Figure 4.7, several changes in the IR spectra of the membranes can be noticed when comparing the membrane that was coagulated only in water with those that started the coagulation process in the alkaline solution. Generally, membranes that have gone through an alkaline solution show less lignin content compared to those coagulated in water, which is observed from the decreased intensity of the characteristic lignin peaks of 1240 and 1507 cm^{-1} (Sescousse, Smacchia and Budtova, 2010; Gabov *et al.*, 2017; Wang *et al.*, 2018). IR spectra can also be used to gain additional information on cellulose's chemistry in the membrane matrix. The peak at 1429 cm^{-1} became weaker and existed as a shoulder peak, which indicates the destruction of cellulose I structure during dissolution. Based on the reported interactions during the cellulose dissolution process, the intramolecular hydrogen bond formed by O on C6 was broken, and the crystal structure of cellulose I was destroyed during the dissolution process (Wang, Lu and Zhang, 2016; Gubitosi *et al.*, 2017; Mazlan *et al.*, 2019). Similarly, the increased intensity of the peak at 897 cm^{-1} correlated with the increased share of amorphous cellulose in the membranes' matrix (Ciolacu, Ciolacu and and Popa, 2011; Li *et al.*, 2011). This peak is

characteristic of the β-glycosidic linkages deformation in the amorphous region in cellulose chains (Sun *et al.*, 2009; Nieminen *et al.*, 2022; Wei *et al.*, 2022).
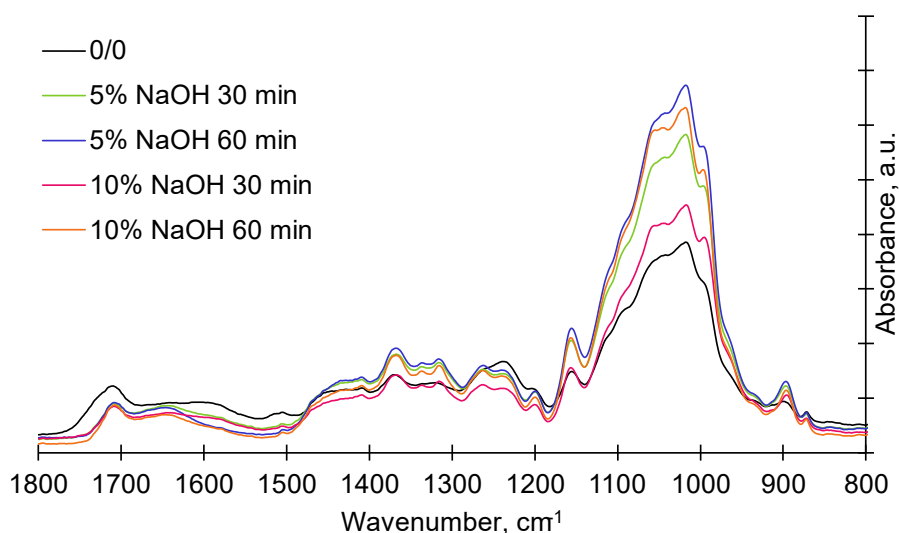

Figure 4.7: FTIR spectra of the membranes prepared using a NaOH coagulation bath, recorded using the Perkin Elmer Frontier spectrometer with a universal ATR module of diamond crystal at a resolution of 4 cm^{-1} in the *absorbance* mode (adapted from Publication III).

The regeneration conditions, namely time, temperature and chemistry of the anti-solvent, have a prominent effect on the structure and properties of the regenerated cellulose and regenerated polymers in general (Table 2.1) (Swatloski *et al.*, 2002; Alves, 2015; Gubitosi *et al.*, 2017; Lindman *et al.*, 2017). As shown in Figure 4.8, although membranes prepared in Publication I were quite different in their chemical compositions, their end crystallinities were approximately the same, showing the spectra of amorphous materials. Two membranes prepared in Publication III that went through dual coagulation bath casting showed a peak at 12.5°, which is a characteristic peak of cellulose II allomorph (Gubitosi *et al.*, 2017).

According to the findings of Publication I, more important factors are the casting parameters, rather than the type of treatment applied to solid biomass and its' chemical composition. Although some researchers have reported almost full transition of cellulose I to cellulose II after regeneration from IL-based solutions (Ling *et al.*, 2019; Taheri, Abdolmaleki and Fashandi, 2019), the membranes prepared within the scope of the current study showed a rather amorphous structure. The possible explanation comes from the fact that the membranes prepared were rarely pure cellulose and commonly the combination of cellulose, hemicellulose and lignin in different proportions. Due to the more amorphous nature of hemicellulose and lignin (Swatloski *et al.*, 2002; Gubitosi *et*

al., 2017; Taheri, Abdolmaleki and Fashandi, 2019), the resulting crystallinity of the membrane sample with a complex composition is typically lower than that of the pure cellulose sample. A commonly observed feature for cellulose dissolution-regeneration processes is that the crystallinity of the regenerated samples is lower than that of an undissolved material (Rebière *et al.*, 2016).
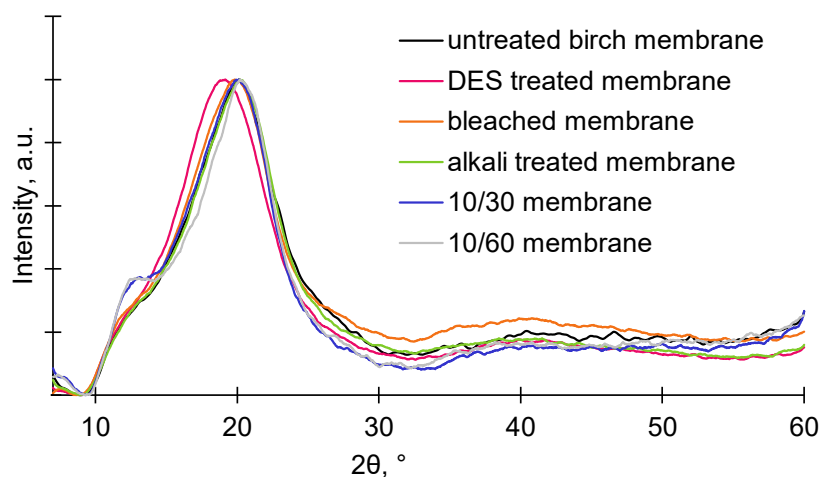

Figure 4.8: X-ray diffractograms of selected membranes from Publications I and III recorded with Bruker AXS D8 advance X-ray diffractometer.

Using alkaline solutions for membrane precipitation also opened up a tool for control over the charge available on the membrane surface. The slight negative charge of the cellulose membranes is often regarded as a positive feature of these membranes, as it enables charge repulsion to be an active participant in the removal of contaminants based on the repulsion of the same charges (Valiño *et al.*, 2014; Park, Kim and Kwak, 2016; Ji *et al.*, 2020; Nieminen *et al.*, 2022). As is evident from the zeta potential curves (Figure 4.9), further treatment applied to the membrane resulted in a more negatively charged surface, though not changing the acidic character of zeta potential curves (Gubitosi *et al.*, 2017). This can be understood as another implication of non-cellulosic compounds' removal, as cellulose surface groups become more accessible to electrokinetic measurements (Reischl, Stana-Kleinschek and Ribitsch, 2006). The second reason might lie within the increased share of amorphous material within cellulose chains, which possess a larger share of voids and flexible parts that are readily accessible for measurement and thus contribute to the total measurable charge (Reischl, Stana-Kleinschek and Ribitsch, 2006). Finally, the assumed increase in surface roughness, which might happen due to the disturbed precipitation process, results in an inevitable increase in the number of charged groups, adding to the net charge.
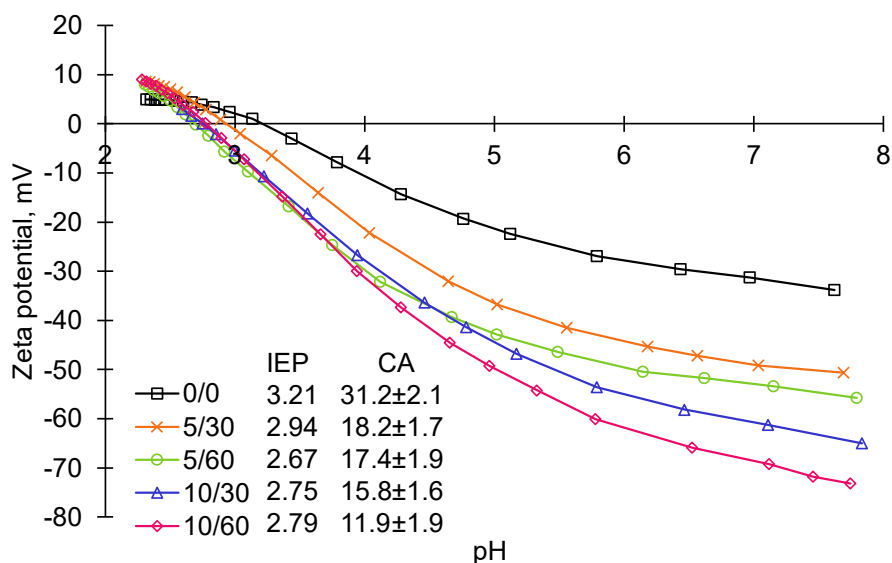
Figure 4.9: Zeta potential curves and isoelectric points (IEP) of the prepared membranes, recorded using a SurPASS electrokinetic analyser with the adjustable gap cell method and using 0.001 M KCl solution as an electrolyte; the contact angle (CA) values of the prepared membranes were recorded using the captive bubble method with KSV CAM 101 equipment connected to a CCD camera (adapted from Publication III).

4.1.5 Effect of casting conditions: influence of LiCl additive on wood-based cellulose membrane performance

The introduction of additives into membrane casting solutions is regarded as one of the most common methods to improve membrane performance (Table 2.1) (Awad *et al.*, 2021). High-molecular-weight additives (e.g. PEGs and polyvinylpyrrolidones PVPs) would not provide a desirable outcome in improved permeance due to their high molecular weight and thus delayed demixing rate (Bottino *et al.*, 1988; Li *et al.*, 2014; Esmaeili *et al.*, 2020; Awad *et al.*, 2021). Still, pore-forming additives with low molecular weight can be an appealing addition to the membrane fabrication process. The addition of LiCl is especially noteworthy given its ability to participate in the dissolution of cellulose. Inorganic additives based on lithium cations have already proven their effectiveness for the improvement in the performance of polymeric membranes, such as cellulose acetate, PES and PVDF, due to their small molecular weight and strong interaction behaviour. However, in these systems, LiCl has fewer interactions as opposed to the system in which cellulose is present, as LiCl is a dissolution-inducing agent in regard to cellulose (Medina-Gonzalez *et al.*, 2011; Lee *et al.*, 2015; Wang, Lu and Zhang, 2016; Sayyed, Deshmukh and Pinjari, 2019).

While LiCl has been reported to have a two-type effect on the casting solutions' viscosity (Bottino *et al.*, 1988; Lee *et al.*, 2002, 2015; Shi *et al.*, 2008; Li *et al.*, 2017), its effect in the current research was different. According to Publication IV, within the studied system, [Emim][OAc]-DMSO-bleached DES-treated wood biomass showed previously unreported effect on the casting solution's viscosity. The addition of up to 0.4 wt.% concentration LiCl, which most likely worked solely as an additive, made the solution more viscous. Starting from 0.5 wt.% concentration, LiCl acted more like a promoter of dissolution, resulting in a less viscous solution and membranes of higher porosity with macropores (Figure 4.10). This duality of LiCl effect can be explained through the possible existence of several complex interactions between Li^+ cations and hydroxyl groups in lignocellulose and intermolecular interactions of polymer chains with DMSO (Chen, Liang and Wang, 2005; Agarwal *et al.*, 2013; Lindman *et al.*, 2017).
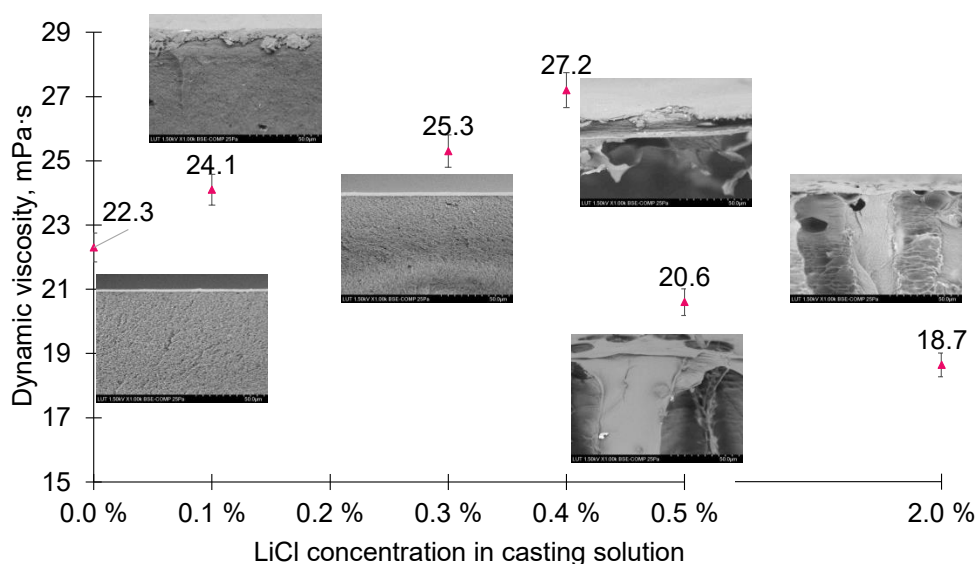
Figure 4.10: Dynamic viscosity values measured at 23°C and SEM images of membranes' cross-sections taken using an SEM (Hitachi SU 3500, Japan) at an acceleration voltage of 1.5 kV under high vacuum conditions as a function of LiCl concentration (adapted from Publication IV).

Changes in the viscosity of the casting solution had drastic effects on the membrane's morphology. An increase in viscosity in the 0–0.3 wt.% LiCl interval resulted in the formation of membranes with similar sponge-like morphology and a pronounced top layer (Figure 4.10). The thickness of the corresponding membranes continuously decreased within 0–0.4 wt.% LiCl addition interval, resulting in 75% thinner 0.4 wt.% LiCl membrane (30 µm thick) compared to the 0 wt.% LiCl membrane (122 µm thick). Similarly, the higher viscosity of the 0.4 wt.% LiCl casting solution resulted in a multilayered morphology of the corresponding membrane, as opposed to the membranes with lower concentrations of LiCl additive and sponge-like morphology. With increases

to 0.5 wt.% and higher in the LiCl concentration, the solutions' viscosity decreased sharply, which probably led to the accelerated demixing rate and the resulting membranes demonstrated finger-like pores and increased thickness (the 0.5 wt.% LiCl membrane was measured to be 200 µm thick and the 2 wt.% LiCl membrane was 240 µm thick).
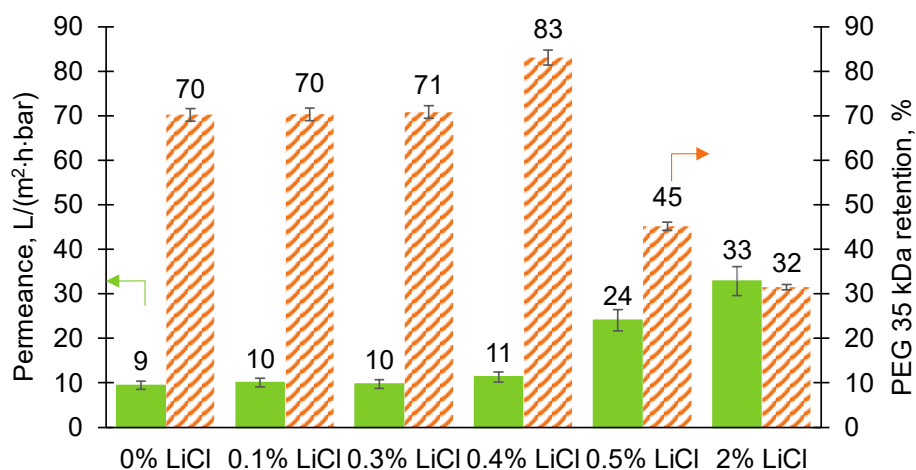

Figure 4.11: Pure water permeance and PEG 35 kDa retentions of the tested membranes, all measured in an Amicon ultrafiltration cell at 25°C and a mixing rate of approximately 300 ppm, adapted from Publication IV.

As expected, the addition of LiCl had a significant effect on the resulting membranes' performance (Figure 4.11). A small increase in the permeance of the 0.4 wt.% LiCl membrane is attributable to a reduced membrane thickness and, consequently, hydraulic resistance. As discussed above, a significant increase in the casting solution's viscosity affected the membrane formation, hindering the solvent/non-solvent exchange and causing the formation of a membrane with a denser structure. Slow demixing suppressed the macropore formation, resulting in 13% improvement in the retention efficiency of the 0.4 wt.% LiCl membrane without compromising its permeance. As for the 0.5 wt.% concentration of LiCl and higher, instantaneous demixing (i.e. enhanced exchange rate between the solvent and non-solvent) resulted in the formation of macrovoids in the corresponding membranes, improving their permeance at the cost of worsening the separation properties.

4.2 Preparation of membranes from cotton textile

4.2.1 Effect of casting conditions: casting solution concentration and casting thickness

While the preparation of membranes from wood biomass required several adjustments of the fabrication procedure (i.e. wood biomass treatments), the preparation of cellulose membranes from cotton textile can be genuinely viewed as a one-step process. As wood's cellulose has a hindered accessibility due to the presence of lignin-carbohydrate complexes (LCCs), the dissolution of cotton cellulose is easier than that of wood cellulose. The preparation of textile-based membranes showed more reproducible results due to the initial homogeneity of the polymer source, with cellulose's content as high as 99% (Gaur *et al.*, 2015). The only necessary action was a coarse shredding of the textile into smaller pieces to aid in the solvent's penetration.

The textile membranes were an easier object to study the effect of polymer concentration on membrane performance due to the lower difference between the casting solutions' viscosities. Attempts to increase wood biomass concentration, regardless of its chemical composition, led to a significantly longer time and higher temperature required for the dissolution. As the dissolution process depends on the ratio between the polymer and solvents' molecules (Le, Rudaz and Budtova, 2014), using the chosen solvent system would require staying in 5−8 wt.% wood biomass load for the dissolution process to be finished within 72 h. As for waste cotton textile's cellulose dissolution, the higher accessibility eased the dissolution to the point at which 9−12 wt.% solutions could be formed within 72 h. However, according to the results, it was not necessary to go for higher polymer concentrations, as the membranes showed retention values similar to those of the membranes prepared from 5–7 wt.% casting solution, at a detriment to the permeance.

According to Publication II, as the polymer concentration increased from 2 wt.% to 5 wt.% and above, permeance decreased drastically by 80%. However, the use of 2 wt.% casting solution was not practical due to the high difference in values measured from different samples and high errors resulting from uneven film formation and poor stability (Figure 4.12, top). The retention efficiency of the membranes prepared from 2 wt.% casting solution was low even for PEG 35 kDa model solutions (Figure 4.12, bottom), whereas the membranes prepared from 5−7 wt.% casting solutions demonstrated at least 78% removal efficiency of PEG 35 kDa for all tested samples.

Due to the stable and easily replicated results obtained from textile-based membranes, it was decided to briefly estimate the amount of the cellulose source's mass required for membrane production. According to the estimation, to prepare 1 m^2 of membrane, only 7 g of textile fabric is required. Consequently, from 1 m^2 of cotton fabric, approximately 20 m^2 of membrane can be produced, making the suggested recycling process of textile into membrane quite perspective.
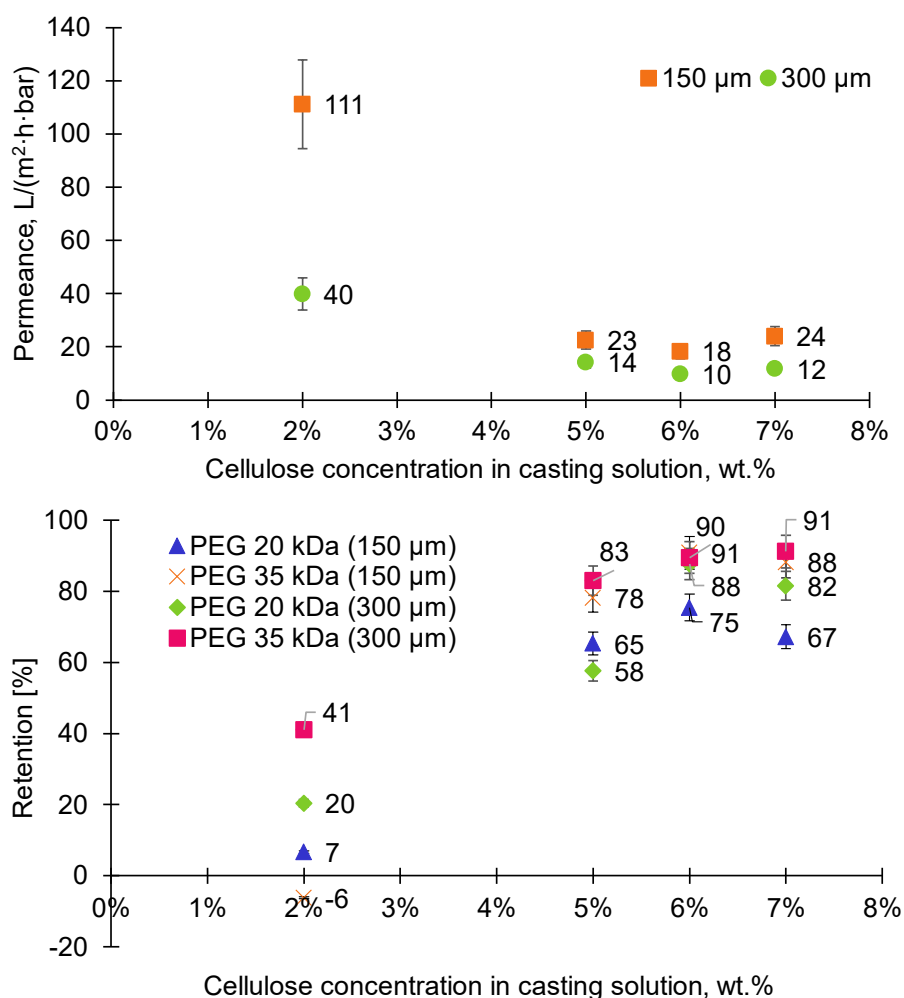
Figure 4.12: Pure water permeance and PEG retentions of the tested textile-based membranes, which were cast at either 150 or 300 µm casting thickness. All measurements were performed in the Amicon ultrafiltration cell at 25°C and with a mixing rate of approximately 300 ppm (adapted from Publication II).

4.2.2 **Effect of casting conditions: support material**

The importance of proper mechanical support cannot be overlooked, as clearly demonstrated in Figure 4.13. The properties of mechanical support are important both for membranes' permeance and retention. In the case of flat-sheet membrane preparation, the properties of the support used for additional mechanical stability also affect the formation

of the membrane matrix. It is important that the casting solution penetrates the support material for at least 10–30 µm to form an overlapping layer, ensuring the stability of the entire membrane (Lohokare, Bhole and Kharul, 2006). The use of non-woven support usually results in the formation of membranes with lower permeance but more stable performance in the range of pressures and better retention with fewer defects in the membrane matrix (Lohokare, Bhole and Kharul, 2006).

The casting solution with a 5 wt.% concentration was prepared from cotton textile and cast at the same thickness of 150 µm on three different support materials. Old support was made from mechanically cleaned old RO membranes, which probably had defects and unsuitable porosity, leading to the formation of membranes with lower permeance and worse retention properties. The Novatexx 2482 carrier material had low air permeability of only 8 L/(s·m^2) at 200 Pa and relatively high thickness of 0.25 mm, which resulted in the formation of a dense membrane with still low permeance and 37% improved retention properties, compared to membranes cast on the old RO membrane support. In contrast, the Novatexx 2484 carrier material with a higher air permeability of 60 L/(s·m^2) at 200 Pa and lower thickness of 0.12 mm allows the solution to partially penetrate it and thus form a stable membrane. The support's sufficient porosity promotes 64% higher permeance and formation of an even top layer, which provides more than two times better separation performance (Figure 4.13).
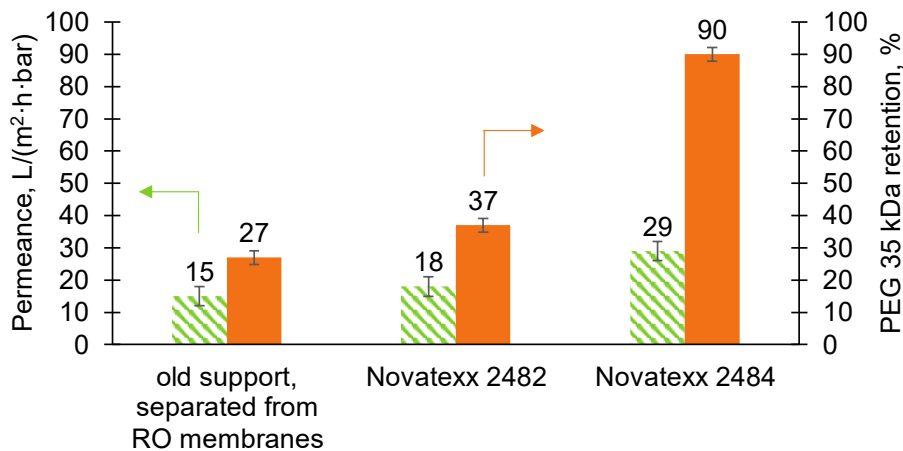

Figure 4.13: Visualisation of the importance of proper support material. Membrane casting thickness was kept at 150 µm, all measurements were conducted in the Amicon ultrafiltration cell at 25°C at a mixing rate of approximately 300 ppm.

4.3   Evaluation of the prepared membranes' usability

As shown in Table 2.1, ultrafiltration regenerated cellulose-based membranes can be used in various applications due to the attractive combination of properties, such as

pronounced hydrophilicity, slightly negatively charged membrane surface and lower fouling tendency, compared to hydrophobic petroleum-based membranes. These properties form the basis of cellulose-based membranes' compatibility with different separation and purification processes. Here, the characterisation results of the membranes selected from different publications are presented next to the description of their performance in the performed filtrations. The commercial cellulose-based membrane RC70pp was chosen as an industrial example of the desired characteristics and performance and for a general comparison with the lab-made membranes.

The measured contact angles of RC70pp and the membranes prepared in different Publications are shown in Figure 4.14. All membranes showed contact angles well below 40°, typical for hydrophilic materials (Livazovic *et al.*, 2015; Lindman *et al.*, 2017; Wang *et al.*, 2020). Though the measured contact angle indicates the general hydrophilicity of the material, the interpretation should be performed cautiously, as the measured value depends not only on the properties of the material itself but also the pore size and surface roughness (Jönsson and Jönsson, 1995; Rajesh *et al.*, 2011; Naim *et al.*, 2015; Esfahani *et al.*, 2020). Membranes with bigger surface pores show higher hydrophilicity due to a larger porosity. Though many researchers have attempted to correlate the contact angles of polymeric membranes with their stability to fouling, the data differ from one research to another (Jönsson and Jönsson, 1995). However, the regenerated cellulose membranes show good correlation between hydrophilicity and flux stability and recovery, though the data are often scattered.
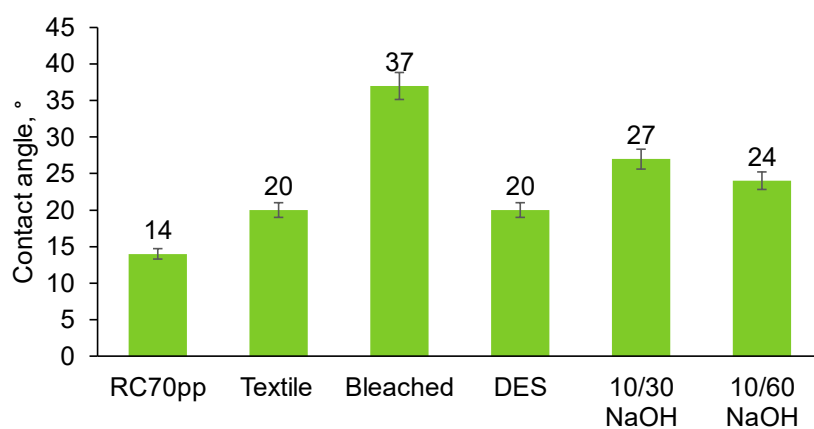

Figure 4.14: Static contact angles measured for membranes from different publications. Contact angle values were recorded using the captive bubble method with the KSV CAM 101 equipment connected to a CCD camera.

Cellulose-based membranes are slightly negatively charged (Medronho and Lindman, 2014, 2015; Nieminen *et al.*, 2022). Figure 4.15 demonstrates the zeta potential curves measured from membranes fabricated in different publications and compared with the zeta potential curve of the RC70pp membrane. All studied membranes presented

negatively charged surfaces over a wide pH range, with the textile-based membrane being the least charged in neutral conditions and the membrane prepared using 10 wt.% NaOH coagulation bath for 60 min being the most negatively charged. The measurement of zeta potential curves and, based on this, the interpretation of membranes' surface charge form an important characterisation step. When placed in contact with an aqueous solution, the membrane's surface and inner lining of the pores develop an electrical double layer, which is a special arrangement of ions and counterions, creating a concentration gradient of counterions and neutralising the membrane charge (Colburn *et al.*, 2019; Esfahani *et al.*, 2020; Nieminen *et al.*, 2022). Charged membranes can separate solutes of an even smaller size than the membrane pores when charge repulsion is involved in the separation mechanism (Butylina, 2007; Chen *et al.*, 2015; Ji *et al.*, 2020; Nieminen *et al.*, 2022).
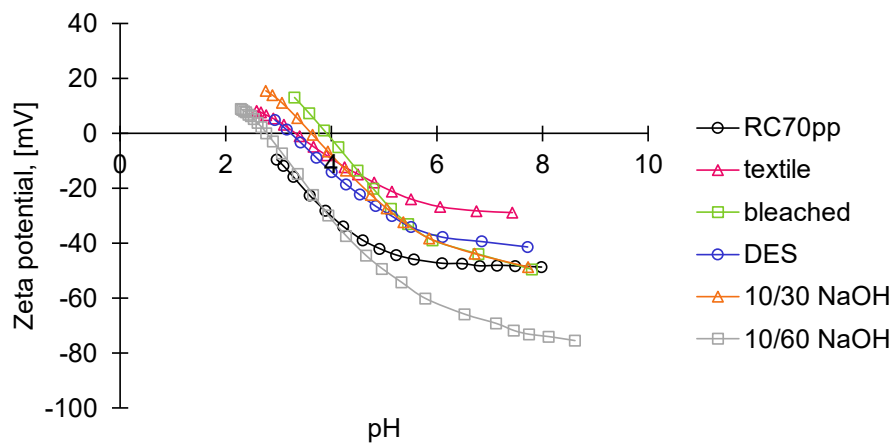
Figure 4.15: Zeta potential curves as a function of pH for membranes prepared in different publications. These curves were recorded with a SurPASS electrokinetic analyser using the adjustable gap cell method and 0.001 M KCl solution as an electrolyte.

In addition to the examples of applications listed in Table 2.1, cellulose-based UF membranes are important for typical contaminant removal in UF processes (e.g. microorganisms, suspended matter and the whole range of less conventional contaminants). UF membranes can be used for polishing purification of, for example, residual phosphorus if they are placed after a conventional physical treatment process, such as coagulation or flocculation (Kubota, Hashimoto and Mori, 2008; Mohanty and Purkait, 2011; Al Aani, Mustafa and Hilal, 2020). As observed in Publication III, three compared membranes, one of which was commercial RC70pp and two were prepared using an alkaline coagulation bath, showed similar removal of residual phosphorus from the effluent of a local Toikansuo municipal wastewater treatment plant (Table 4.1).

Table 4.1: Pure water fluxes before and after filtration of Toikansuo plant effluent, characteristics of used membranes and phosphorus removal efficiency (adapted from Publication III).

	10/60	10/30	RC70PP
Pure water flux before wastewater filtration at 2 bar, L/(m^2·h)	460	440	150
Wastewater flux at the beginning (8 min), L/(m^2·h)	106	105	64
Wastewater flux at VRF of ~3 (11 days), L/(m^2·h)	69	68	42
MWCO, kDa	NK	NK	3
Zeta potential in neutral pH, mV	-70	-60	-40
Phosphorous removal, %	67	69	68

NK – not known

The results presented in Table 4.1 demonstrate that lab-made 10/30 and 10/60 membranes showed similar retention of the residual phosphorus as did the commercial RC70pp membrane, however maintaining higher flux. Rather high removal efficiency can be related to the remains of the coagulants/flocculants used in the prior purification process. Larger flocs, or suspended matter in general, can be efficiently retained in membrane filtration, simultaneously improving the retention of dissolved compounds, such as residual phosphorus, whose size is smaller than the actual MWCO of the membrane (Kubota, Hashimoto and Mori, 2008; Mohanty and Purkait, 2011; Al Aani, Mustafa and Hilal, 2020). All membranes showed a significant pure water flux decrease; however, the flux loss of lab-made membranes was more significant. Fortunately, after rinsing with water, both 10/30 and 10/60 lab-made membranes demonstrated partial flux restoration of up to 60% and 95% of the initial pure water flux, respectively. This phenomenon is a known property of cellulose and is sometimes explained by the lower absorbance tendency of foulants on the surface of the cellulose-based membranes due to their hydrophilicity and negatively charged surface (Susanto and Ulbricht, 2005).

Despite rather similar characteristics (i.e. hydrophilic and negatively charged surfaces) (Figure 4.14 and Figure 4.15), all tested membranes had very different separation efficiencies (Figure 4.16, top). As expected, the commercial membrane RC70pp showed the tightest cut-off value, being able to separate PEG 3kDa molecules with more than 95% efficiency while having intermediate permeance of 50 L/m^2·h·bar. Produced within the current study, textile-based and bleached wood biomass-based membranes showed rather similar performance, both demonstrating 94% retention for PEG 35 kDa with approximately 35 L/m^2·h·bar permeance. The cut-off value for the membrane produced from DES-treated wood biomass was not defined, as the separation efficiency of PEG 35 kDa was only 67%. However, these membranes had higher permeance compared to the abovementioned membranes (i.e. 75 L/m^2·h·bar). Consequently, the 10/30 and 10/60 membranes fabricated using a dual coagulation bath (Section 4.1.4) showed the highest

permeance of 95 and 150 L/m^2·h·bar, respectively, while both had separation efficiency of less than 20% for PEG 35 kDa.
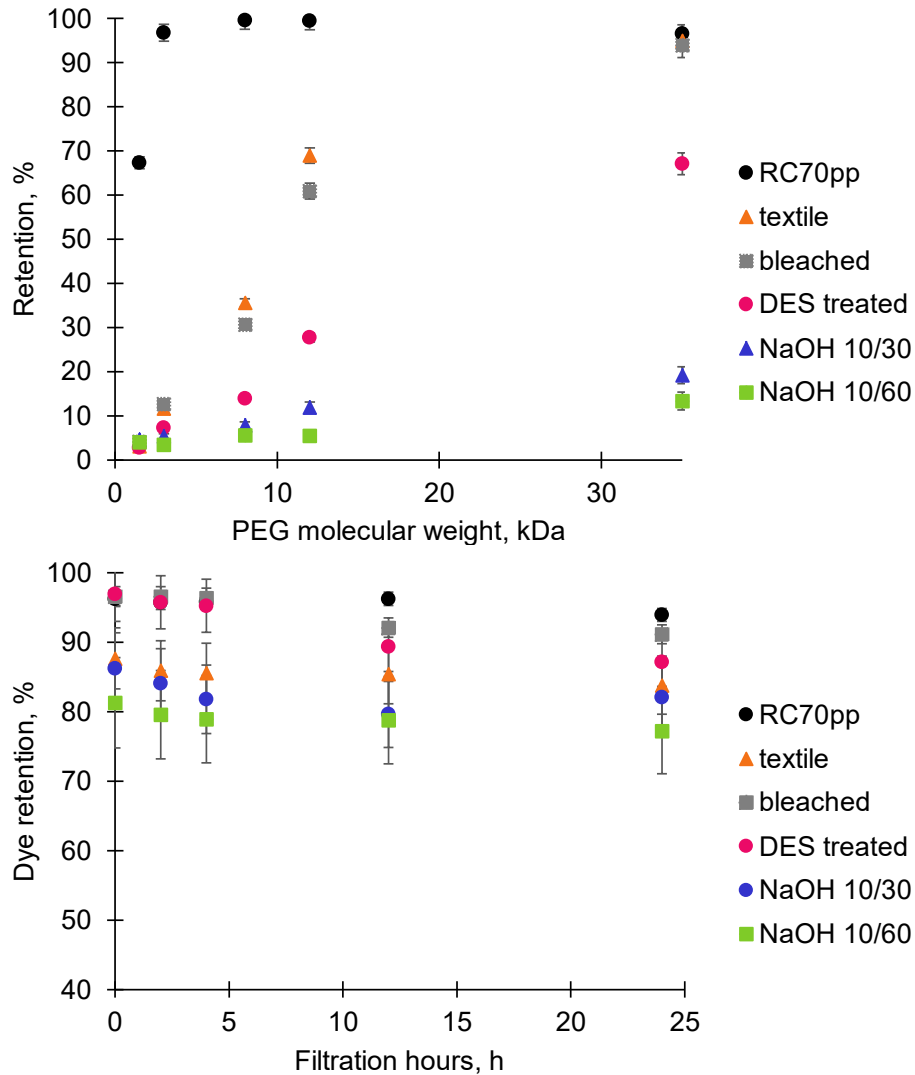

Figure 4.16: Molecular weight cut-off (MWCO) curves of tested membranes from different Publications and RC70pp as an example of commercial membrane (top) and dye retention efficiency from the model solution of 30 ppm of reactive blue 2 dye (bottom).

The possible removal of dyes with UF membranes is an attractive purification option. Dyes often have aromatic structures, and other elements, such as nitrogen and sulphur, in their composition, whose uncontrolled release in water bodies can negatively impact

aquatic and terrain organisms (Koumanova and Allen, 2005; Chen *et al.*, 2015; Kennedy, Maseka and Mbulo, 2018). Conventional methods for dye removal (e.g. adsorption, ion exchange, coagulation and flocculation) are usually flawed due to the addition of chemicals, high energy demand and generation of byproducts (Koumanova and Allen, 2005; Karthikeyan, Karthikeyan and Jothivenkatachalam, 2014; Chowdhury and Saha, 2016; Ćurić and Dolar, 2022). Among all used pigments, the reactive dyes are especially concerning. Their application is attractive due to the vibrant colours they bring to the textiles; however, the process of fixation of these dyes requires high salinity and strongly alkaline media (Karthikeyan, Karthikeyan and Jothivenkatachalam, 2014; Ahmed, Majewska-Nowak and Grzegorzek, 2021). Even in harsh conditions, their fixation of the fabric is limited; hence, up to 40% of dye load can end up in wastewater (Al-Degs *et al.*, 2008; Karthikeyan, Karthikeyan and Jothivenkatachalam, 2014; Chen *et al.*, 2015; Ahmed and Majewska-Nowak, 2020).

As indicated in Figure 4.16 (bottom), all membranes showed noticeable removal of the reactive blue 2 dye from the 30 ppm model solution. The dye retention efficiency remained stable for all tested membranes throughout the 24-h period. The lowest retention of approximately 80% was shown by alkali-treated 10/30 and 10/60 membranes, with the textile membrane's retention being closer to 90% and more stable than that for alkali-coagulated membranes. RC70pp and membranes prepared from DES-treated and bleached birch biomass showed similar dye retention behaviours. During the first 4 h, the retention of all three membranes remained approximately 95% and later decreased slightly to approximately 90% for the lab-made membranes. RC70pp showed the most stable performance, with the ending removal efficiency at the 24 h mark being 94%.

In summary, the fabrication of cellulose-based UF membranes from the tested alternative sources of cellulose is possible. The results clearly indicate the importance of cellulose fraction's purity for the formation of a uniform top layer of the membrane and thus better separation performance. Membranes prepared from waste cotton textile have better reproducibility due to the homogeneity of the cellulose's source, whereas wood biomass-based membranes' fabrication is more versatile. The modifications of casting parameters significantly affect the final membrane's performance. The addition of LiCl to the casting solutions and the use of alkali solution as a coagulation medium has provided valuable theoretical knowledge that can be used for the further development of cellulose-based membranes. The conducted filtration experiments with wastewater effluent and dye model solutions demonstrate the potential of the fabricated membranes to be use for water purification, polishing treatment and pollutant removal.

5 Conclusions and Future Perspectives

With membrane technology emerging as a sustainable and efficient treatment of water-based wastestreams, membrane development studies are attracting reasonable attention along with fouling mitigation. UF membranes can be implemented not only for a conventional separation of microorganisms and particles of larger size but also for the retention of smaller dissolved contaminants, if chosen correctly. Polymeric membranes produced from petrochemicals have proven efficiency and a wide range of applications; however, their usual hydrophobicity and problematic disposal call for environmentally friendly membrane materials. Cellulose-based membranes have natural hydrophilicity, show moderate chemical and mechanical stability and are prepared from renewable sources, unlike petrochemicals. However, their availability in the membrane market is scattered and represented mainly by pre-cut samples for particular applications. The development of new approaches to the fabrication of cellulose materials can help reintroduce them in the market.

The first part of this thesis, Publications I and II, explored new polymer sources for the preparation of cellulose membranes. Using the [Emim][OAc]–DMSO solvent system, the dissolution of unmodified cotton textile and wood was achieved and respective membranes were cast. The resulting textile-based membrane presents a fine cellulose layer on the mechanical support material and is ready to be used as such, showing 25–30 L/(m^2·h·bar) permeance and MWCO of 25–30 kDa. The dissolution of wood biomass occurred more slowly, requiring a longer time and higher temperature to overcome wood's natural recalcitrance. Although membrane fabrication directly from wood is possible, it became evident that to achieve better membrane performance, higher cellulose purity is required. All treatments except DES treatment used rather harsh chemicals, which can cause additional degradation of cellulose and require sufficient post-washing with large volumes of water.

Publications III and IV were about changes in the fabrication procedure of wood membranes and discussion of the changes caused by it. Publication III introduced the post-casting valorisation approach using the alkaline solution as a coagulation bath. The approach was born as an opposition to the classical use of acidic coagulation baths for improvement in the membranes' retention. Coagulation process in alkaline solutions was interrupted by different dissolution limits of wood biomass constituents, making cellulose precipitate, while lignin and hemicellulose remained dissolved. As a result, membranes with significantly higher permeance of up to 200 L/(m^2·h·bar) were prepared. Alkaline coagulation also introduced an additional negative charge on the membrane surface, making it possible to use ultrafiltration for the separation of charged dissolved molecules, which were much smaller than the membranes' MWCO. Publication IV explored the possibility of altering the casting solution's behaviour using LiCl additive. Though the initial intent was to significantly improve the membranes' performance, a rather unusual system behaviour was observed with significant differences in the viscosity of the casting solution, which affected the membranes' morphology and performance. The experiments

conducted on the removal of total phosphorus from the water treatment plant effluent with lab-made membranes in Publication III demonstrated the potential of prepared membranes to be used for polishing treatment of wastewater treatment plant effluents. The unpublished experiments on dye molecule retention demonstrate that the membranes prepared in the current study can be successfully used for the removal of dissolved molecules smaller than the membrane pores.

Altogether, this study identifies and suggests alternative sources of cellulose for membrane production. As both identified sources, namely unutilised wood biomass and waste cotton fabric, do not have to be heavily processed prior to casting solution preparation, the suggested approach improves the resource efficiency and sustainability of the fabrication process. Eliminating the need for complete cellulose purification from wood biomass, this study improves the cost efficiency of the membrane fabrication process and promotes efficient utilisation of wood biomass. The use of waste cotton fabric for membrane preparation promotes cotton textile recycling as a value-added product, thus contributing to the circular economy principles. The findings on the addition of LiCl and the use of alkali solutions as coagulation media provide valuable theoretical knowledge on the wood biomass and cellulose dissolution-regeneration processes. The demonstrated ability of the prepared membranes to remove residual phosphorus and dye molecules shows the membranes' potential to be used as part of reagent-free water treatment processes. The results can also be used as a comparison basis when other biomass types are tested for membrane preparation.

Based on the results of this research, the separation mechanisms involved in membrane filtration combine the sieving effect with charge repulsion. From the theoretical viewpoint, research on the optimal pore size–charge ratio is required to establish the actual separation capabilities of the UF membranes. From a practical viewpoint, the separation of other dissolved contaminants, such as pharmaceuticals, can be studied to determine if UF membranes are capable of removal of the emerging compounds.

Due to the chemistry of cellulose-based membranes (hydrophilicity and stability in most solvents), they can be tested for the separation of dual-phase media (e.g. the oil–water emulsions). Due to the existence of OH- groups, cellulose can be successfully modified chemically, which would allow potential tailoring of the membrane performance. If the aim is to prepare a pure cellulose membrane, one should think of using a cellulose source with initially high content of cellulose (e.g. grass cotton, bamboo and cotton textile). Preparation of membranes from wood biomass is more versatile, and although membranes consist of not only pure cellulose but also hemicelluloses and lignin remnants, it does not take away their advantage of being biodegradable and biobased.

Owing to cellulose's antifouling potential, filtration can be run without significant loss of permeance and shows quite stable retention values. Another advantage of cellulose-based membranes is their potential biodegradability. Regardless of the chosen polymer source, the prepared membranes consist of the mechanical support and cellulose or cellulose-rich layer on top of it. The danger of synthetic polymers is usually tied to their non-

degradability and emission of toxins (Mohamed *et al.*, 2015; Wang, Lu and Zhang, 2016; Duolikun *et al.*, 2020). Biopolymers demonstrate natural or bio-degradability, meaning that the deterioration of their chemical and physical properties (i.e. degradation) result in the formation of carbon dioxide, water and methane (Karthika *et al.*, 2019). Degradability can be achieved not only from biotic factors (e.g. microorganisms) but also abiotic factors (e.g. photodegradation, oxidation and hydrolysis). The maximalist approach would be to come up with a procedure for support material preparation, which would also consist solely of biomass or cellulose-based materials.

References

Al Aani, S., Mustafa, T. N. and Hilal, N. (2020) 'Ultrafiltration membranes for wastewater and water process engineering: A comprehensive statistical review over the past decade', *Journal of Water Process Engineering*, 35, pp. 1–36. doi: 10.1016/j.jwpe.2020.101241.

Abd-Razak, N. H., Chew, Y. M. J. and Bird, M. R. (2019) 'Membrane fouling during the fractionation of phytosterols isolated from orange juice', *Food and Bioproducts Processing*. Institution of Chemical Engineers, 113, pp. 10–21. doi: 10.1016/j.fbp.2018.09.005.

Abushammala, H. and Mao, J. (2020) 'A review on the partial and complete dissolution and fractionation of wood and lignocelluloses using imidazolium ionic liquids', *Polymers*, 12(1). doi: 10.3390/polym12010194.

Acharya, S. *et al.* (2021) 'Utilization of cellulose to its full potential: A review on cellulose dissolution, regeneration, and applications', *Polymers*, 13(24). doi: 10.3390/polym13244344.

Agarwal, S. *et al.* (2013) 'Imidazolium chloride-Licl melts as efficient solvents for cellulose', *Bulletin of the Korean Chemical Society*, 34(12), pp. 3771–3776. doi: 10.5012/bkcs.2013.34.12.3771.

Ahmed, A. E. and Majewska-Nowak, K. (2020) 'Removal of reactive dye from aqueous solutions using banana peel and sugarcane bagasse as biosorbents', *Environment Protection Engineering*, 46(3), pp. 121–135. doi: 10.37190/epe200308.

Ahmed, A. E., Majewska-Nowak, K. and Grzegorzek, M. (2021) 'Removal of Reactive Dyes From Aqueous Solutions Using Ultrafiltration Membranes', *Environment Protection Engineering*, 47(3), pp. 109–120. doi: 10.37190/epe210309.

Al-Degs, Y. S. *et al.* (2008) 'Effect of solution pH, ionic strength, and temperature on adsorption behavior of reactive dyes on activated carbon', *Dyes and Pigments*, 77(1), pp. 16–23. doi: 10.1016/j.dyepig.2007.03.001.

Alves, L. *et al.* (2016) 'Dissolution state of cellulose in aqueous systems. 1. Alkaline solvents', *Cellulose*, 23(1), pp. 247–258. doi: 10.1007/s10570-015-0809-6.

Alves, L. C. H. (2015) *Cellulose solutions: Dissolution, regeneration, solution structure and molecular interactions*. Universidade de Coimbra. Available at: https://estudogeral.sib.uc.pt/handle/10316/29319 (Accessed: 14 July 2020).

Anokhina, T. S. *et al.* (2017) 'Fabrication of composite nanofiltration membranes from cellulose solutions in an [Emim]OAc–DMSO mixture', *Petroleum Chemistry*. Maik Nauka-Interperiodica Publishing, 57(6), pp. 477–482. doi:

10.1134/S0965544117060020.

Anugwom, I. *et al.* (2012) 'Selective extraction of hemicelluloses from spruce using switchable ionic liquids', *Carbohydrate Polymers*, 87, pp. 2005–2011. doi: 10.1016/j.carbpol.2011.10.006.

Anugwom, I. *et al.* (2022) 'Esterified Lignin from Construction and Demolition Waste (CDW) as a Versatile Additive for Polylactic-Acid (PLA) Composites—The Effect of Artificial Weathering on its Performance', *Global Challenges*, 2100137. doi: 10.1002/gch2.202100137.

Awad, E. S. *et al.* (2021) 'A mini-review of enhancing ultrafiltration membranes (Uf) for wastewater treatment: Performance and stability', *ChemEngineering*, 5(3). doi: 10.3390/chemengineering5030034.

Aziz, T. *et al.* (2022) 'A Review on the Modification of Cellulose and Its Applications', *Polymers*, 14(15), pp. 1–36. doi: 10.3390/polym14153206.

Bottino, A. *et al.* (1988) 'High performance ultrafiltration membranes cast from LiCl doped solutions', *Desalination*, 68(2–3), pp. 167–177. doi: 10.1016/0011-9164(88)80052-3.

Bruggen, B. Van Der *et al.* (2003) 'Review of Pressure-Driven Membrane Processes', *Environmental Progress*, 22(1), pp. 46–56.

Buschow, K. H. J. *et al.* (2001) 'Cellulose: Chemistry and Technology', in *Encyclopedia of Materials - Science and Technology, Volumes 1-11*. Elsevier, pp. 1033–1050.

Butylina, S. (2007) *Effect Of Physico-Chemical Conditions And Operating Parameters On Flux And Retention Of Different Components In Ultrafiltration And Nanofiltration*. Acta Universitatis Lappeenrantaensis.

CEPI (Confederation of European Paper Industries) (2021) *Key Statistics 2021-22*. Brussels.

Chen, F. (2021) *Designing High Performance All-Cellulose Composites by Dissolution/Swelling of Macro- and Nano-scale Cellulose Fibers*. Aalto University. Available at: http://urn.fi/URN:ISBN:978-952-64-0236-9.

Chen, H., Liang, Y. and Wang, C. G. (2005) 'Solubility of highly isotactic polyacrylonitrile in dimethyl sulphoxide', *Journal of Polymer Research*, 12(4), pp. 325–329. doi: 10.1007/s10965-004-6387-1.

Chen, H. Z., Wang, N. and Liu, L. Y. (2012) 'Regenerated cellulose membrane prepared with ionic liquid 1-butyl-3-methylimidazolium chloride as solvent using wheat straw', *Journal of Chemical Technology and Biotechnology*, 87(12), pp. 1634–1640. doi:

10.1002/jctb.3802.

Chen, X. *et al.* (2015) 'Recovery of small dye molecules from aqueous solutions using charged ultrafiltration membranes', *Journal of Hazardous Materials*. Elsevier B.V., 284, pp. 58–64. doi: 10.1016/j.jhazmat.2014.10.031.

Chowdhury, S. and Saha, T. K. (2016) 'Adsorption of Reactive Blue 4 (RB4) onto Rice Husk in Aqueous Solution', *International Journal of Scientific & Engineering Research*, 7(3), pp. 7–12. Available at: http://www.ijser.org.

Ciolacu, D., Ciolacu, F. and and Popa, V. I. (2011) 'Amorphous Cellulose – Structure and Characterization', *Cellulose Chemistry and Technology*, 45, pp. 13–21.

Colburn, A. *et al.* (2019) 'Composite membranes derived from cellulose and lignin sulfonate for selective separations and antifouling aspects', *Nanomaterials*, 9(6). doi: 10.3390/nano9060867.

Costa, C. *et al.* (2021) 'Lignin enhances cellulose dissolution in cold alkali', *Carbohydrate Polymers*, 274(May). doi: 10.1016/j.carbpol.2021.118661.

Ćurić, I. and Dolar, D. (2022) 'Investigation of Pretreatment of Textile Wastewater for Membrane Processes and Reuse for Washing Dyeing Machines', *Membranes*. doi: 10.3390/membranes12050449.

Dahlbo, H. *et al.* (2017) 'Increasing textile circulation—Consequences and requirements', *Sustainable Production and Consumption*. Elsevier B.V., 9, pp. 44–57. doi: 10.1016/j.spc.2016.06.005.

Dang, H. T. *et al.* (2006) 'A comparison of commercial and experimental ultrafiltration membranes via surface property analysis and fouling tests', *Water Quality Research Journal of Canada*, 41(1), pp. 84–93. doi: 10.2166/wqrj.2006.009.

Demesa, A. G., Laari, A. and Sillanpää, M. (2020) *Value-added chemicals and materials from lignocellulosic biomass: Carboxylic acids and cellulose nanocrystals. Carboxylic acids and cellulose nanocrystals.*, *Advanced Water Treatment: Advanced Oxidation Processes*. doi: 10.1016/B978-0-12-819225-2.00006-5.

Duolikun, T. *et al.* (2020) 'Asymmetric cellulosic membranes: Current and future aspects', *Symmetry*, 12(7). doi: 10.3390/sym12071160.

Durmaz, E. N. and Zeynep Çulfaz-Emecen, P. (2018) 'Cellulose-based membranes via phase inversion using [EMIM]OAc-DMSO mixtures as solvent', *Chemical Engineering Science*. Elsevier Ltd, 178, pp. 93–103. doi: 10.1016/j.ces.2017.12.020.

El-Gendi, A., Abdalla, H. and Ali, S. (2012) 'Construction of ternary phase diagram and membrane morphology evaluation for polyamide/Formic acid/Water system', *Australian*

Journal of Basic and Applied Sciences, 6(5), pp. 62–68.

Esfahani, M. R. *et al.* (2020) 'Sustainable Novel Bamboo-Based Membranes for Water Treatment Fabricated by Regeneration of Bamboo Waste Fibers', *ACS Sustainable Chemistry and Engineering*, 8(10), pp. 4225–4235. doi: 10.1021/acssuschemeng.9b07438.

Esmaeili, M. *et al.* (2018) 'Utilization of DES-lignin as a bio-based hydrophilicity promoter in the fabrication of antioxidant polyethersulfone membranes', *Membranes*, 8(3), pp. 1–16. doi: 10.3390/membranes8030080.

Esmaeili, M. *et al.* (2020) 'The interplay role of vanillin, water, and coagulation bath temperature on formation of antifouling polyethersulfone (PES) membranes: Application in wood extract treatment', *Separation and Purification Technology*. Elsevier, 235(July 2019), p. 116225. doi: 10.1016/j.seppur.2019.116225.

Fievet, P. *et al.* (2003) 'Determining the ζ-potential of plane membranes from tangential streaming potential measurements: Effect of the membrane body conductance', *Journal of Membrane Science*, 226(1–2), pp. 227–236. doi: 10.1016/j.memsci.2003.09.007.

Figoli, A., Simone, S. and Drioli, E. (2015) *Membrane Fabrication*. Edited by N. Hilal, A. F. Ismail, and C. J. Wright. CRC Press Taylor & Francis Group. Available at: https://ebookcentral.proquest.com/lib/lut/reader.action?docID=1816357 (Accessed: 16 April 2023).

Fletcher, K. (2014) *Sustainable Fashion and Textiles*. Second Edi. London: Routledge.

Francisco, M., Van Den Bruinhorst, A. and Kroon, M. C. (2012) 'New natural and renewable low transition temperature mixtures (LTTMs): Screening as solvents for lignocellulosic biomass processing', *Green Chemistry*, 14(8), pp. 2153–2157. doi: 10.1039/c2gc35660k.

French, A. D. (2017) 'Glucose, not cellobiose, is the repeating unit of cellulose and why that is important', *Cellulose*. Springer Netherlands, 24(11), pp. 4605–4609. doi: 10.1007/s10570-017-1450-3.

Gabov, K. *et al.* (2017) 'Preparation, characterization and antimicrobial application of hybrid cellulose-lignin beads', *Cellulose*. Springer Netherlands, 24(2), pp. 641–658. doi: 10.1007/s10570-016-1172-y.

Gaur, R. *et al.* (2015) 'Evaluation of recalcitrant features impacting enzymatic saccharification of diverse agricultural residues treated by steam explosion and dilute acid', *RSC Advances*. Royal Society of Chemistry, 5(75), pp. 60754–60762. doi: 10.1039/c5ra12475a.

Gericke, M., Fardim, P. and Heinze, T. (2012) 'Ionic liquids - Promising but challenging

solvents for homogeneous derivatization of cellulose', *Molecules*, pp. 7458–7502. doi: 10.3390/molecules17067458.

Giummarella, N. (2018) *Fundamental Aspects of Lignin Carbohydrate Complexes (LCC) : Mechanisms, Recalcitrance and Material concepts*, *Trita-Cbh-Fou Nv - 2018:18*. KTH Royal Institute of Technology.

Goh, P. S., Othman, M. H. D. and Matsuura, T. (2021) 'Waste reutilization in polymeric membrane fabrication: A new direction in membranes for separation', *Membranes*, 11(10), pp. 1–31. doi: 10.3390/membranes11100782.

Gubitosi, M. *et al.* (2017) 'Stable, metastable and unstable cellulose solutions', *Royal Society Open Science*, 4(8). doi: 10.1098/rsos.170487.

Hamingerova, M., Borunsky, L. and Beckmann, M. (2015) *Membrane Technologies for Water and Wastewater Treatment on the European and Indian Market*, *Techview membrane*. Leipzig.

Haslinger, S. *et al.* (2019) 'Upcycling of cotton polyester blended textile waste to new man-made cellulose fibers', *Waste Management*. The Author(s), 97, pp. 88–96. doi: 10.1016/j.wasman.2019.07.040.

Holmbom, B. and Örså, F. (1993) 'Methods for analysis of dissolved and colloidal wood components in papermaking process waters and effluents', in *7th Int. Symp. Wood Pulping Chem.* Beijing.

Horvath, A. L. (2006) 'Solubility of structurally complicated materials: I. Wood', *Journal of Physical and Chemical Reference Data*, 35(1), pp. 77–92. doi: 10.1063/1.2035708.

Hummel, M. *et al.* (2016) 'Ionic Liquids for the Production of Man-Made Cellulosic Fibers: Opportunities and Challenges', in *Cellulose Chemistry and Properties: Fibers, Nanocelluloses and Advanced Materials*, pp. 133–168. doi: 10.1007/12_2015_307.

Ippolitov, V. *et al.* (2022) 'Cellulose Membranes in the Treatment of Spent Deep Eutectic Solvent Used in the Recovery of Lignin from Lignocellulosic Biomass', *Membranes*, 12(1). doi: 10.3390/membranes12010086.

Isik, M., Sardon, H. and Mecerreyes, D. (2014) 'Ionic liquids and cellulose: Dissolution, chemical modification and preparation of new cellulosic materials', *International Journal of Molecular Sciences*. MDPI AG, pp. 11922–11940. doi: 10.3390/ijms150711922.

Isikgor, F. H. and Becer, C. R. (2015) 'Lignocellulosic biomass: a sustainable platform for the production of bio-based chemicals and polymers', *Polymer Chemistry*. Royal Society of Chemistry, 6(25), pp. 4497–4559. doi: 10.1039/c5py00263j.

Ji, M. *et al.* (2020) 'Charge exclusion as a strategy to control retention of small proteins

in polyelectrolyte-modified ultrafiltration membranes', *Separation and Purification Technology*. Elsevier, 247(January), p. 116936. doi: 10.1016/j.seppur.2020.116936.

Jiang, Z., Zhao, P. and Hu, C. (2018) 'Controlling the cleavage of the inter- and intra-molecular linkages in lignocellulosic biomass for further biorefining: A review', *Bioresource Technology*. Elsevier, 256(January), pp. 466–477. doi: 10.1016/j.biortech.2018.02.061.

Jönsson, C. and Jönsson, A. S. (1995) 'Influence of the membrane material on the adsorptive fouling of ultrafiltration membranes', *Journal of Membrane Science*, 108(1–2), pp. 79–87. doi: 10.1016/0376-7388(95)00144-X.

Jonsson, G. (2001) 'Harmonisation of characterisation procedures for porous membranes, CHARMME Project, SMT4-CT98-7518'.

Joshi, R. *et al.* (2023) 'Low Fouling Nanostructured Cellulose Membranes for Ultrafiltration in Wastewater Treatment', *Membranes*, 13(2), p. 147. doi: 10.3390/membranes13020147.

Kallioinen, M. *et al.* (2005) 'Chemometrical approach in studies of membrane capacity in pulp and paper mill application', *Desalination*, 175(1 SPEC. ISS.), pp. 87–95. doi: 10.1016/j.desal.2004.11.004.

Kallioinen, M. *et al.* (2006) 'Examination of membrane performance with multivariate methods: A case study within a pulp and paper mill filtration application', *Chemometrics and Intelligent Laboratory Systems*, 84(1-2 SPEC. ISS.), pp. 98–105. doi: 10.1016/j.chemolab.2006.04.015.

Kallioinen, M. *et al.* (2007) 'Comparison of the performance of two different regenerated cellulose ultrafiltration membranes at high filtration pressure', *Journal of Membrane Science*, 294(1–2), pp. 93–102. doi: 10.1016/j.memsci.2007.02.016.

Kallioinen, M. *et al.* (2010) 'Membrane evaluation for the treatment of acidic clear filtrate', *Desalination*. Elsevier, 250(3), pp. 1002–1004. doi: 10.1016/j.desal.2009.09.090.

Karthika, M. *et al.* (2019) '7. Biodegradation of Green Polymeric Composites Materials', in Visakh, P. M.; Bayraktar, Oguz; Menon, G. (ed.) *Bio Monomers for Green Polymeric Composite Materials*. John Wiley & Sons, Ltd. doi: 10.1002/9781119301714.ch7.

Karthikeyan, K. T., Karthikeyan, S. and Jothivenkatachalam, K. (2014) 'Removal of reactive blue 2 dye from aqueous solution using turmeric industrial waste activated carbon', *Journal of Chemical and Pharmaceutical Sciences*, (4), pp. 52–54.

Kennedy, K. K., Maseka, K. J. and Mbulo, M. (2018) 'Selected Adsorbents for Removal of Contaminants from Wastewater: Towards Engineering Clay Minerals', *Open Journal*

of Applied Sciences, 08(08), pp. 355–369. doi: 10.4236/ojapps.2018.88027.

Kilpeläinen, I. *et al.* (2007) 'Dissolution of wood in ionic liquids', *Journal of Agricultural and Food Chemistry*, 55(22), pp. 9142–9148. doi: 10.1021/jf071692e.

Kim, D. and Nunes, S. P. (2021) 'Green solvents for membrane manufacture: Recent trends and perspectives', *Current Opinion in Green and Sustainable Chemistry*. Elsevier Ltd, 28, p. 100427. doi: 10.1016/j.cogsc.2020.100427.

Koumanova, B. and Allen, S. J. (2005) 'Decolourisation of Water / Wastewater Using Adsorption (Review)', *Journal of the University of Chemical Technology and Metallurgy*, 40(3), pp. 175–192.

Kubota, N., Hashimoto, T. and Mori, Y. (2008) 'Microfiltration and Ultrafiltration', in Li, N. N. et al. (eds) *Advanced Membrane Technology and Applications*. Shizuoka, Japan: John Wiley & Sons, Ltd. Available at: https://app-knovel-com.ezproxy.cc.lut.fi/web/view/khtml/show.v/rcid:kpAMTA000A/cid:kt00CR6Y12/viewerType:khtml/root_slug:advanced-membrane-technology/url_slug:microfiltration-ultrafiltration?&b-toc-cid=kpAMTA000A&b-toc-root-slug=advanced-membrane-technolo (Accessed: 16 April 2023).

Kumar, A. K., Parikh, B. S. and Pravakar, M. (2016) 'Natural deep eutectic solvent mediated pretreatment of rice straw: bioanalytical characterization of lignin extract and enzymatic hydrolysis of pretreated biomass residue', *Environmental Science and Pollution Research*, 23(10), pp. 9265–9275. doi: 10.1007/s11356-015-4780-4.

Lähdetie, A. (2013) *Wood biomass characterisation by Raman spectroscopy*. Aalto University. Available at: www.aalto.fi (Accessed: 29 April 2023).

Le, K. A., Rudaz, C. and Budtova, T. (2014) 'Phase diagram, solubility limit and hydrodynamic properties of cellulose in binary solvents with ionic liquid', *Carbohydrate Polymers*. Elsevier Ltd., 105(1), pp. 237–243. doi: 10.1016/j.carbpol.2014.01.085.

Leal Filho, W. *et al.* (2019) 'A review of the socio-economic advantages of textile recycling', *Journal of Cleaner Production*. Elsevier Ltd, pp. 10–20. doi: 10.1016/j.jclepro.2019.01.210.

Lee, H. J. *et al.* (2002) 'Solution properties of poly(amic acid)-NMP containing LiCl and their effects on membrane morphologies', *Journal of Membrane Science*, 196(2), pp. 267–277. doi: 10.1016/S0376-7388(01)00610-X.

Lee, J. *et al.* (2015) 'Effect of PVP, lithium chloride, and glycerol additives on PVDF dual-layer hollow fiber membranes fabricated using simultaneous spinning of TIPS and NIPS', *Macromolecular Research*, 23(3), pp. 291–299. doi: 10.1007/s13233-015-3037-x.

Lewis, E. *et al.* (2018) 'REACH Regulation', *Sustainaspeak*, pp. 219–219. doi: 10.4324/9781315270326-156.

Li, A. L. *et al.* (2018) 'Rice straw pretreatment using deep eutectic solvents with different constituents molar ratios: Biomass fractionation, polysaccharides enzymatic digestion and solvent reuse', *Journal of Bioscience and Bioengineering*. Elsevier Ltd, 126(3), pp. 346–354. doi: 10.1016/j.jbiosc.2018.03.011.

Li, B. *et al.* (2010) 'Factors affecting wood dissolution and regeneration of ionic liquids', *Industrial and Engineering Chemistry Research*, 49(5), pp. 2477–2484. doi: 10.1021/ie901560p.

Li, C. (李春涛) (2008) 'CN101274988A - Industrial method for preparing regenerated cellulose film'. Available at: https://patents.google.com/patent/CN101274988A/en?oq=CN101274988A (Accessed: 29 April 2023).

Li, H. Bin *et al.* (2014) 'Effects of additives on the morphology and performance of PPTA/PVDF in situ blend UF membrane', *Polymers*, 6(6), pp. 1846–1861. doi: 10.3390/polym6061846.

Li, P. *et al.* (2018) 'Recyclable deep eutectic solvent for the production of cationic nanocelluloses', *Carbohydrate Polymers*. Elsevier, 199(June), pp. 219–227. doi: 10.1016/j.carbpol.2018.07.024.

Li, X. *et al.* (2017) 'Fabrication of a robust high-performance FO membrane by optimizing substrate structure and incorporating aquaporin into selective layer', *Journal of Membrane Science*. Elsevier, 525(October 2016), pp. 257–268. doi: 10.1016/j.memsci.2016.10.051.

Li, X. L. *et al.* (2011) 'High-flux and anti-fouling cellulose nanofiltration membranes prepared via phase inversion with ionic liquid as solvent', *Separation and Purification Technology*. Elsevier B.V., 83(1), pp. 66–73. doi: 10.1016/j.seppur.2011.09.012.

Li, Z. *et al.* (2021) 'Eco-friendly self-crosslinking cellulose membrane with high mechanical properties from renewable resources for oil/water emulsion separation', *Journal of Environmental Chemical Engineering*. Elsevier Ltd, 9(5), p. 105857. doi: 10.1016/j.jece.2021.105857.

Lindman, B. *et al.* (2017) 'The relevance of structural features of cellulose and its interactions to dissolution, regeneration, gelation and plasticization phenomena', *Physical Chemistry Chemical Physics*, 19(35), pp. 23704–23718. doi: 10.1039/c7cp02409f.

Ling, Z. *et al.* (2019) 'Effects of ball milling on the structure of cotton cellulose', *Cellulose*. Springer Netherlands, 26(1), pp. 305–328. doi: 10.1007/s10570-018-02230-x.

Livazovic, S. *et al.* (2015) 'Cellulose multilayer membranes manufacture with ionic liquid', *Journal of Membrane Science*. Elsevier, 490, pp. 282–293. doi: 10.1016/j.memsci.2015.05.009.

Lohokare, H. R., Bhole, Y. S. and Kharul, U. K. (2006) 'Effect of support material on ultrafiltration membrane performance', *Journal of Applied Polymer Science*, 99(6), pp. 3389–3395. doi: 10.1002/app.23039.

Loow, Y. L. *et al.* (2017) 'Potential use of deep eutectic solvents to facilitate lignocellulosic biomass utilization and conversion', *Cellulose*. Springer Netherlands, 24(9), pp. 3591–3618. doi: 10.1007/s10570-017-1358-y.

Magalhães Da Silva, S. P. *et al.* (2013) 'Novel pre-treatment and fractionation method for lignocellulosic biomass using ionic liquids', *RSC Advances*, 3(36), pp. 16040–16050. doi: 10.1039/c3ra43091j.

Al Manasrah, M. *et al.* (2012) 'Recovery of galactoglucomannan from wood hydrolysate using regenerated cellulose ultrafiltration membranes', *Bioresource Technology*. Elsevier, 114, pp. 375–381. doi: 10.1016/j.biortech.2012.02.014.

Martins, M. A. R., Pinho, S. P. and Coutinho, J. A. P. (2019) 'Insights into the Nature of Eutectic and Deep Eutectic Mixtures', *Journal of Solution Chemistry*. Springer US, 48(7), pp. 962–982. doi: 10.1007/s10953-018-0793-1.

Mazlan, N. S. N. *et al.* (2019) 'Comparison of regenerated cellulose membrane coagulated in sulphate based coagulant', *Cerne*, 25(1), pp. 18–24. doi: 10.1590/01047760201925012586.

Medina-Gonzalez, Y. *et al.* (2011) 'Towards green membranes: Preparation of cellulose acetate ultrafiltration membranes using methyl lactate as a biosolvent', *International Journal of Sustainable Engineering*, 4(1), pp. 75–83. doi: 10.1080/19397038.2010.497230.

Medronho, B. and Lindman, B. (2014) 'Competing forces during cellulose dissolution: From solvents to mechanisms', *Current Opinion in Colloid and Interface Science*. Elsevier Ltd, 19(1), pp. 32–40. doi: 10.1016/j.cocis.2013.12.001.

Medronho, B. and Lindman, B. (2015) 'Brief overview on cellulose dissolution/regeneration interactions and mechanisms', *Advances in Colloid and Interface Science*. Elsevier B.V., 222, pp. 502–508. doi: 10.1016/j.cis.2014.05.004.

Mehta, A. (2006) *Performance Characteristics of Charged Ultrafiltration Membranes: Fundumental Studies and Applications*. The Pennsylvania State University.

Melro, E. *et al.* (2018) 'A brief overview on lignin dissolution', *Journal of Molecular Liquids*. Elsevier B.V, 265(2017), pp. 578–584. doi: 10.1016/j.molliq.2018.06.021.

Modenbach, A. A. and Nokes, S. E. (2014) 'Effects of sodium hydroxide pretreatment on structural components of biomass', *Transactions of the ASABE*, 57(4), pp. 1187–1198. doi: 10.13031/trans.56.10046.

Mohamed, M. A. *et al.* (2015) 'Feasibility of recycled newspaper as cellulose source for regenerated cellulose membrane fabrication', *Journal of Applied Polymer Science*, 132(43), pp. 1–10. doi: 10.1002/app.42684.

Mohamed, M. A. *et al.* (2019) 'Introduction to Green Polymeric Membranes', in Visakh, P. M.; Bayraktar, Oguz; Menon, G. (ed.) *Bio Monomers for Green Polymeric Composite Materials*. John Wiley & Sons, Ltd. Available at: https://app-knovel-com.ezproxy.cc.lut.fi/web/view/khtml/show.v/rcid:kpBMGPCM0U/cid:kt012ELMB1/viewerType:khtml/root_slug:bio-monomers-green-polymeric/url_slug:bio-monome-introduction-3?&b-toc-cid=kpBMGPCM0U&b-toc-title=Bio Monomers for Green Polymeric Com (Accessed: 23 December 2022).

Mohanty, K. and Purkait, M. K. (2011) *Membrane Technologies and Applications*. Taylor & Francis Group. Available at: https://ebookcentral.proquest.com/lib/lut/reader.action?docID=840382 (Accessed: 16 April 2023).

Mulder, M. (1996) *Basic Principles of Membrane Technology*. 2nd edn. Springer Dordrecht.

Naim, M. M. *et al.* (2015) 'Ultrafiltration by a super-hydrophilic regenerated cellulose membrane', *Water Practice and Technology*. IWA Publishing, 10(2), pp. 337–346. doi: 10.2166/wpt.2015.040.

Navone, L. *et al.* (2020) 'Closing the textile loop: Enzymatic fibre separation and recycling of wool/polyester fabric blends', *Waste Management*. Elsevier Ltd, 102, pp. 149–160. doi: 10.1016/j.wasman.2019.10.026.

Nevstrueva, D. *et al.* (2018) 'Effect of precipitation temperature on the properties of cellulose ultrafiltration membranes prepared via immersion precipitation with ionic liquid as solvent', *Membranes*. MDPI AG, 8(4). doi: 10.3390/membranes8040087.

Van Nguyen, Q. *et al.* (2017) 'Recyclable and scalable organocatalytic transesterification of polysaccharides in a mixed solvent of 1-ethyl-3-methylimidazolium acetate and dimethyl sulfoxide', *Polymer Journal*. Nature Publishing Group, 49(11), pp. 783–787. doi: 10.1038/pj.2017.49.

Nieminen, J. *et al.* (2022) 'TEMPO-mediated oxidation as surface modification for cellulosic ultrafiltration membranes: Enhancement of ion rejection and permeability', *Journal of Membrane Science*, 659(July), pp. 1–9. doi: 10.1016/j.memsci.2022.120786.

Nnberg, B. L. (2001) 'Industrial Cellulose', in Woodings, C. (ed.) *Regenerated Cellulose*.

Woodhead Publishing. Available at: https://app-knovel-com.ezproxy.cc.lut.fi/web/view/khtml/show.v/rcid:kpRCF00002/cid:kt003I56C1/viewerType:khtml/?view=collapsed&zoom=1&page=1 (Accessed: 16 April 2023).

Novelli, V. *et al.* (2020) *Open Innovation Test Bed for nano-enabled Membranes INNOMEM Preliminary Market Analysis (focus on demand)*. San Sebastián, Spain.

Österberg, M. (2000) *On the interactions in cellulose systems: Surface forces and adsorption*. KTH Royal Institute of Technology and Helsinki University of Technology. Available at: http://kth.diva-portal.org/smash/record.jsf?pid=diva2:8764.

Pandey, K. K. and Pitman, A. J. (2003) 'FTIR studies of the changes in wood chemistry following decay by brown-rot and white-rot fungi', *International Biodeterioration and Biodegradation*, 52(3), pp. 151–160. doi: 10.1016/S0964-8305(03)00052-0.

Park, S. Y., Kim, Y. J. and Kwak, S. Y. (2016) 'Versatile surface charge-mediated anti-fouling UF/MF membrane comprising charged hyperbranched polyglycerols (HPGs) and PVDF membranes', *RSC Advances*. Royal Society of Chemistry, 6(92), pp. 88959–88966. doi: 10.1039/c6ra19020k.

proionic GmbH (2018) *REACH registration for proionic's EMIM-OAc - the perfect ionic liquid for biomass applications*. Available at: https://proionic.com/downloads/files/proionic-downloads/newsletter-18092018.html.

Protz, R. *et al.* (2021) 'Solubility and spinnability of cellulose-lignin blends in specific ionic liquids', *Carbohydrate Polymer Technologies and Applications*. Elsevier Ltd, 2(December 2020), p. 100041. doi: 10.1016/j.carpta.2021.100041.

Puro, L. *et al.* (2011) 'Evaluation of behavior and fouling potential of wood extractives in ultrafiltration of pulp and paper mill process water', *Journal of Membrane Science*. Elsevier B.V., 368(1–2), pp. 150–158. doi: 10.1016/j.memsci.2010.11.032.

Radhi, A. *et al.* (2015) 'Macroscopic and microscopic study of 1-ethyl-3-methyl-imidazolium acetate-DMSO mixtures', *Journal of Physical Chemistry B.*, 119(4), pp. 1633–1640. doi: 10.1021/jp5112108.

Rajesh, S. *et al.* (2011) 'Preparation, morphology, performance, and hydrophilicity studies of poly(amide-imide) incorporated cellulose acetate ultrafiltration membranes', *Industrial and Engineering Chemistry Research*. American Chemical Society, 50(9), pp. 5550–5564. doi: 10.1021/ie1019613.

Rebière, J. *et al.* (2016) 'Structural modifications of cellulose samples after dissolution into various solvent systems', *Analytical and Bioanalytical Chemistry*. Springer, 408(29), pp. 8403–8414. doi: 10.1007/s00216-016-9958-1.

Reischl, M., Stana-Kleinschek, K. and Ribitsch, V. (2006) 'Electrokinetic Investigations

of Oriented Cellulose Polymers', *Macromolecular Symposia*. John Wiley & Sons, Ltd, 244(1), pp. 31–47. doi: 10.1002/masy.200651203.

Ribitsch, V. *et al.* (2001) 'The significance of surface charge and structure on the accessibility of cellulose fibres', *Macromolecular Materials and Engineering*, 286(10), pp. 648–654. doi: 10.1002/1439-2054(20011001)286:10<648::AID-MAME648>3.0.CO;2-6.

Rowell, R., Pettersen, R. and Tshabalala, M. (2012) *Cell Wall Chemistry*, *Handbook of Wood Chemistry and Wood Composites, Second Edition*. doi: 10.1201/b12487.

Sandin, G. and Peters, G. M. (2018) 'Environmental impact of textile reuse and recycling – A review', *Journal of Cleaner Production*. Elsevier Ltd, pp. 353–365. doi: 10.1016/j.jclepro.2018.02.266.

Sayyed, A. J., Deshmukh, N. A. and Pinjari, D. V. (2019) 'A critical review of manufacturing processes used in regenerated cellulosic fibres: viscose, cellulose acetate, cuprammonium, LiCl/DMAc, ionic liquids, and NMMO based lyocell', *Cellulose*. Springer Netherlands, 26(5), pp. 2913–2940. doi: 10.1007/s10570-019-02318-y.

Searle, S. and Malins, C. (2013) 'Availability of cellulosic residues and wastes in the EU - International Council on Clean Transportation.', *The International Council on Clean Transportation. White paper.*, (October). Available at: https://www.theicct.org/publications/availability-cellulosic-residues-and-wastes-eu.

Sérgio, M. *et al.* (2023) 'Recycling of Polymeric Membranes'.

Sescousse, R., Smacchia, A. and Budtova, T. (2010) 'Influence of lignin on cellulose-NaOH-water mixtures properties and on Aerocellulose morphology', *Cellulose*, 17(6), pp. 1137–1146. doi: 10.1007/s10570-010-9448-0.

Shi, L. *et al.* (2008) 'Effect of additives on the fabrication of poly(vinylidene fluoride-co-hexafluropropylene) (PVDF-HFP) asymmetric microporous hollow fiber membranes', *Journal of Membrane Science*, 315(1–2), pp. 195–204. doi: 10.1016/j.memsci.2008.02.035.

Shi, Z. *et al.* (2014) 'Effects of lignin and hemicellulose contents on dissolution of wood pulp in aqueous NaOH/urea solution', *Cellulose*, 21(3), pp. 1205–1215. doi: 10.1007/s10570-014-0226-2.

Shimizu, F. L. *et al.* (2020) 'Minimum Lignin and Xylan Removal to Improve Cellulose Accessibility', *Bioenergy Research*. Springer, pp. 1–11. doi: 10.1007/s12155-020-10120-z.

Singh, R. and Hankins, N. P. (2016) 'Introduction to Membrane Processes for Water Treatment', in *Emerging Membrane Technology for Sustainable Water Treatment*.

Elsevier B.V., pp. 15–52. doi: 10.1016/B978-0-444-63312-5.00002-4.

Sluiter, A. *et al.* (2008) 'Determination of Structural Carbohydrates and Lignin in Biomass: Laboratory Analytical Procedure (LAP) (Revised July 2011)'. Available at: http://www.nrel.gov/biomass/analytical_procedures.html (Accessed: 29 April 2023).

Soto-Salcido, L. A. *et al.* (2020) 'NADES-based fractionation of biomass to produce raw material for the preparation of cellulose acetates', *Cellulose*, 27(12), pp. 6831–6848. doi: 10.1007/s10570-020-03251-1.

Sun, N. *et al.* (2009) 'Complete dissolution and partial delignification of wood in the ionic liquid 1-ethyl-3-methylimidazolium acetate', *Green Chemistry*, 11(5), pp. 646–65. doi: 10.1039/b822702k.

Sundberg, A. *et al.* (1996) 'Determination of hemicelluloses and pectins in wood and pulp fibres by acid methanolysis and gas chromatography', *Nordic Pulp and Paper Research Journal*, 11(4), pp. 1–4. doi: 10.3183/npprj-1996-11-04-p216-219.

Susanto, H. and Ulbricht, M. (2005) 'Influence of ultrafiltration membrane characteristics on adsorptive fouling with dextrans', *Journal of Membrane Science*, 266(1–2), pp. 132–142. doi: 10.1016/j.memsci.2005.05.018.

Swatloski, R. P. *et al.* (2002) 'Dissolution of cellulose with ionic liquids', *Journal of the American Chemical Society*. American Chemical Society, 124(18), pp. 4974–4975. doi: 10.1021/ja025790m.

Taheri, N., Abdolmaleki, A. and Fashandi, H. (2019) 'Impact of non-solvent on regeneration of cellulose dissolved in 1-(carboxymethyl)pyridinium chloride ionic liquid', *Polymer International*. John Wiley & Sons, Ltd, 68(12), pp. 1945–1951. doi: 10.1002/PI.5903.

Tan, X. *et al.* (2019) 'Effect of anti-solvents on the characteristics of regenerated cellulose from 1-ethyl-3-methylimidazolium acetate ionic liquid', *International Journal of Biological Macromolecules*. Elsevier B.V., 124, pp. 314–320. doi: 10.1016/j.ijbiomac.2018.11.138.

Tang, X. *et al.* (2017) 'Green Processing of Lignocellulosic Biomass and Its Derivatives in Deep Eutectic Solvents', *ChemSusChem*, 10(13), pp. 2696–2706. doi: 10.1002/cssc.201700457.

Tran, D. H. and Ulbricht, M. (2023) 'Cellulose-cellulose composite membranes for ultrafiltration', *Journal of Membrane Science*. Elsevier B.V., 672(October 2022), p. 121426. doi: 10.1016/j.memsci.2023.121426.

Triantafyllidis, K. S., Lappas, A. A. and Stöcker, M. (2013) 'The role of catalysis for the sustainable production of bio-fuels and bio-chemicals'. Elsevier, p. 594.

Valiño, V. *et al.* (2014) 'Improved separation of bovine serum albumin and lactoferrin mixtures using charged ultrafiltration membranes', *Separation and Purification Technology*, 125, pp. 163–169. doi: 10.1016/j.seppur.2014.01.023.

Vats, S. and Rissanen, M. (2016) 'Parameters affecting the upcycling of waste cotton and PES/CO textiles', *Recycling*, 1(1), pp. 166–177. doi: 10.3390/recycling1010166.

Wang, D. *et al.* (2020) 'A cellulose-based nanofiltration membrane with a stable three-layer structure for the treatment of drinking water', *Cellulose*. Springer, 27(14), pp. 8237–8253. doi: 10.1007/s10570-020-03325-0.

Wang, Q. (汪前东), Liu, B. (刘必前) and Min, H. (何敏) (2014) 'CN103801202A - Regenerated cellulose ultrafiltration membrane and preparation method thereof'. China. Available at: https://patents.google.com/patent/CN103801202A/en?q=(regenerated+cellulose+ultrafil tration+membrane+preparation)&oq=regenerated+cellulose+ultrafiltration+membrane+ preparation (Accessed: 29 April 2023).

Wang, S., Lu, A. and Zhang, L. (2016) 'Recent advances in regenerated cellulose materials', *Progress in Polymer Science*. Elsevier Ltd, 53, pp. 169–206. doi: 10.1016/j.progpolymsci.2015.07.003.

Wang, Z. *et al.* (2018) 'Chemical and structural factors influencing enzymatic saccharification of wood from aspen, birch and spruce', *Biomass and Bioenergy*. Elsevier Ltd, 109(March 2017), pp. 125–134. doi: 10.1016/j.biombioe.2017.12.020.

Wei, J. *et al.* (2022) 'Research on the degradation behaviors of wood pulp cellulose in ionic liquids', *Journal of Molecular Liquids*. Elsevier B.V., 356, p. 119071. doi: 10.1016/j.molliq.2022.119071.

What is a Response Factor? Chromatography Today (no date). Available at: https://www.chromatographytoday.com/news/gc-mdgc/32/breaking-news/what-is-a-response-factor/31169 (Accessed: 29 April 2023).

Wikberg, H. and Liisa Maunu, S. (2004) 'Characterisation of thermally modified hard- and softwoods by 13 C CPMAS NMR'. doi: 10.1016/j.carbpol.2004.08.008.

Wondraczek, H. and Heinze, T. (2021) 'Cellulosic Biomaterials', in *Polysaccharides*. Jena, Germany. doi: 10.1007/978-3-319-03751-6.

Yang, M. *et al.* (2021) 'Antifouling nanocellulose membranes: How subtle adjustment of surface charge lead to self-cleaning property', *Journal of Membrane Science*. Elsevier B.V., 618(June 2020), p. 118739. doi: 10.1016/j.memsci.2020.118739.

Zhang, W. and Hallström, B. (1990) 'Membrane characterization using the contact angle technique I. methodology of the captive bubble technique', *Desalination*, 79(1), pp. 1–

12. doi: 10.1016/0011-9164(90)80067-L.

Zhang, Y. *et al.* (2001) 'Formation and Characterization of Cellulose Membranes from N-Methylmorpholine-N-oxide Solution', *Macromolecular Bioscience*, 1(4), pp. 141–148. doi: 10.1002/1616-5195(20010601).

Zhong, Q. (钟奇伟) *et al.* (2022) 'CN114653214A - Preparation method of regenerated cellulose ultrafiltration membrane with controllable product performance and product'. China. Available at: https://patents.google.com/patent/CN114653214A/en?q=(regenerated+cellulose+ultrafil tration+membrane+preparation)&oq=regenerated+cellulose+ultrafiltration+membrane+ preparation (Accessed: 29 April 2023).

Zou, D. *et al.* (2021) 'Recent advances in polymer membranes employing non-toxic solvents and materials', *Green Chemistry*. Royal Society of Chemistry, 23(24), pp. 9815–9843. doi: 10.1039/d1gc03318b.

Publication I

Lopatina, A., Anugwom, I., Esmaeili, M., Puro, L., Virtanen, T., Mänttäri, M., and
Kallioinen, M.

**Preparation of cellulose-rich membranes from wood: effect of wood pretreatment
process on membrane performance**

Preparation of cellulose-rich membranes from wood: effect of wood pretreatment process on membrane performance

Anastasiia Lopatina (iD) **· Ikenna Anugwom · Mohammadamin Esmaeili ·**
Liisa Puro · Tiina Virtanen · Mika Mänttäri · Mari Kallioinen

Abstract In this study cellulose-rich membranes were fabricated from untreated and treated hardwood biomass solutions in 1-ethyl-3-methylimidazolium acetate ([Emim][OAc])—dimetylsulfoxide (DMSO) system via wet phase separation. Wood treatment methods aimed to get purified cellulose fraction of wood. Treatment sequence was as followed: deep eutectic solvent pretreatment, sodium chlorite bleaching, and alkaline treatment. Resulted biomass after each treatment step was characterized by chemical composition and crystalline fraction content. Flatsheet membranes were produced from biomass samples after each treatment step. Characterization of membranes included measurements of pure water permeability and (poly)ethyleneglycol 35 kDa retention, Fourier-transform infrared and Raman spectroscopy, X-ray diffraction measurements and thermogravimetric analysis. The study revealed that it was possible to fabricate membrane from untreated wood as well as from wood biomass after each of treatment steps. The resulted membranes differed in chemical composition and filtration performance. Membrane prepared directly from untreated wood had the highest permeability, the lowest retention; and the most complex chemical composition among others. As treatment steps removed lignin and hemicelluloses from the wood biomass, the corresponding membranes became chemically more homogeneous and showed increased retention and decreased permeability values.

A. Lopatina (✉) · M. Esmaeili · L. Puro ·
T. Virtanen · M. Mänttäri · M. Kallioinen
Department of Separation Science, LUT School of
Engineering Science, LUT University, P.O. Box 20,
53851 Lappeenranta, Finland
e-mail: Anastasiia.Lopatina@lut.fi

M. Esmaeili
e-mail: Mohammadamin.Esmaeili@lut.fi

L. Puro
e-mail: Liisa.Puro@lut.fi

T. Virtanen
e-mail: Tiina.Virtanen@lut.fi

M. Mänttäri
e-mail: Mika.Manttari@lut.fi

M. Kallioinen
e-mail: Mari.Kallioinen@lut.fi

I. Anugwom
LUT Re-Source Research Platform, LUT University,
P.O. Box 20, 53851 Lappeenranta, Finland
e-mail: Ikenna.Anugwom@lut.fi

Introduction

Cellulose is considered an abundant renewable resource of great potential for bio-based materials and products. The attractive mechanical properties of this biopolymer enable production of a wide range of cellulose-based materials (Zhang et al. 2017; Khakalo et al. 2019). The presence of many hydroxyl groups, which gives cellulose its remarkably high hydrophilicity, and the extensive network of inter- and intramolecular hydrogen bonds, which provides relatively high chemical and thermal stability, make cellulose an attractive material for filtration membranes (Woodings 2001; Ślusarczyk and Fryczkowska 2019). The network of hydrogen bonds, however, causes difficulties in ensuring effective dissolution of cellulose, which is needed when membranes are produced via phase inversion methods. Solvents capable of cellulose dissolution can be divided into two groups: derivatizing solvents, which interact with hydroxyl groups and form a soluble intermediate that can be isolated later (e.g. conventional viscose and carbamate processes and solvent systems for cellulose such as DMF/N_2O_4 or DMSO/N_2O_4, CF_3COOH, $HCOOH/H_2SO_4$ and $Cl_2CHCOOH$) and non-derivatizing solvents, which do not alter the cellulose chemistry but break hydrogen bonds within the cellulose microfibrils during the dissolution process (e.g. cupro, NMMO·H_2O and lithium chloride/N,N-dimethylacetamide (LiCl/DMAc)) (Pinkert et al. 2009; Khakalo et al. 2019). Existing conventional cellulose dissolution and membrane fabrication (both derivatizing and non-derivatizing solvent-based processes) require expensive, hazardous chemicals and cause significant pollution, so there is a need for novel non-derivatizing solvents whose dissolution mechanism maintains the beneficial characteristics of cellulose as a membrane material (Zhang et al. 2017; Khakalo et al. 2019).

One type of novel non-derivatizing solvent, ionic liquids (ILs), is a mixture of solely ions with a melting point often below 100 °C (Parviainen et al. 2014). Due to their remarkably high stability up to 300-400°C, conductivity and wide liquid range, their use is advantageous in many applications, for example, in electrical devices as lubricants, for biomass pretreatment prior to preparation of composite materials, and for heat transfer (Saha et al. 2019). ILs are considered an attractive medium for the preparation of cellulose

and biomass casting solutions due to their high dissolution power and relatively mild dissolution conditions (Raut et al. 2015; Mohd and Draman 2017). The most suitable candidates for large-scale usage are halogen-free, non-corrosive, and reasonably low toxic ILs. An important practical challenge associated with utilization of ILs is their relatively high viscosities, which complicates the dissolution process and results in a need for high temperatures for process facilitation. High temperatures can lead to decomposition of ILs, which is an undesirable side reaction and should be avoided. To prevent decomposition of ILs, a co-solvent, e.g. DMSO, is usually added to the system, enhancing the solvent power of the IL by decreasing the time needed for dissolution even at lower temperatures (Isik et al. 2014). Of the many solvents available, 1-ethyl-3-methylimidazolium acetate ([Emim][OAc]) is considered an optimal choice as it has relatively low viscosity, high dissolution power for cellulose (up to 20–30 wt.% depending on the temperature of the dissolution) and even higher dissolution power for lignin and hemicelluloses, due to their non-crystalline structure, and it can thus be utilized in dissolution of untreated lignocellulosic materials (Beckwith et al. 2010; Mäki-Arvela et al. 2010; Li et al. 2011; Saha et al. 2017; Mohan et al. 2018).

Preparation of polymeric membranes using ILs as an effective and nonaggressive solvent for cellulose is the subject of intensive study. To cite several examples, Zhu et al. (2014) studied preparation of membranes from cellulose extracted from pineapple leaves with the ionic liquid [Bmim]Cl; Chen et al. (2012) investigated manufacturing of wheat straw regenerated cellulose membranes using the same IL; and Anokhina et al. (2017) researched manufacturing of composite NF membranes from cellulose solutions prepared with a [Emim][OAc]–DMSO mixture. Livazovic et al. (2015) studied preparation of multilayer NF and UF cellulose membranes from solutions made with [Emim][OAc]; Nevstrueva et al. (2018) studied the effect of precipitation temperature on properties of cellulose UF membranes prepared from purified cellulose via immersion precipitation with [Emim][OAc] as a solvent; Tran and Ulbricht (2019) produced UF composite cellulose-cellulose membranes from pure cellulose solutions in [Emim][OAc] and [Bmim][OAc], and studied effects of several parameters, including co-solvent (DMSO)

concentration, over the separation performance of manufactured membranes.

[Emim][OAc] has also been implemented for partial surface dissolution as a step in preparation of all-wood composites from delignified birch (Khakalo et al. 2019). However, a thorough literature search yielded that preparation of a membrane directly from wood, which is an abundant source of cellulose, has not been reported. The aim of this study is to investigate whether it is possible to fabricate a cellulose-rich polymeric membrane with UF membrane performance directly from untreated hardwood biomass. The term "cellulose-rich" is used as wood biomass contains lignin, hemicelluloses and extractives, in addition to cellulose, and they are present in the solution used for membrane manufacturing via directly dissolving the wood. The effect of the purification steps used in treatment of the wood biomass on the purity of the recovered cellulose-rich fraction and the properties of the produced membranes is examined to understand the influence of the cellulose purity of the fraction used to produce the cellulose-rich membranes.

A deep eutectic solvent (DES) consisting of choline chloride (ChCl) acting as a hydrogen bond acceptor (HBA) and lactic acid (LAc) as a hydrogen bond donor (HBD) was used to recover the cellulose-rich fraction from the wood. ChCl-LAc is attractive as regards wood fractionation and membrane preparation from lignocellulosic biomass as it possesses high and specific dissolution power for lignin and moderate dissolution power for hemicelluloses, leaving cellulose content almost unchanged (Mäki-Arvela et al. 2010; Alvarez-Vasco et al. 2016). In this study, the casting solutions were prepared by dissolving untreated birch, DES-treated birch, DES-treated and bleached birch, and DES-treated, bleached and alkali-extracted birch in a mixture of [Emim][OAc] and DMSO. The membranes were cast onto a non-woven polyester support and coagulated in ultra-pure deionized water. The membranes were tested for permeability and retention performance, and the chemical composition of the membranes and biomass samples was investigated to examine the influence of wood pretreatment on membrane manufacturing.

Experimental

Materials

Debarked birch wood (Betula pendula) chips with a nominal size of $5 \times 1 \times 0.1$ cm were used as a base material for all further operations.

For partial delignification of birch chips through DES treatment, choline chloride (ChCl) (CAS # 67–48-1, Merck KGaA, Darmstadt, Germany) was used as HBA and lactic acid (LAc) (CAS # 79–33-4, Merck KGaA, Darmstadt, Germany) as HBD. A mixture of ethanol and deionized water (DI, 15 MΩ, 0.5 – 1 μS/cm) at 9:1 volume ratio was used for filtration and washing of the partially delignified biomass. Subsequent bleaching of DES-treated biomass was done with acetic acid (CAS # 64–19-7, Merck KGaA, Darmstadt, Germany) and sodium chlorite (CAS # 7758–19-2, Acros Organics, Geel, Belgium).

For the two-step alkaline treatment, a NaOH solution was prepared from sodium hydroxide (CAS # 1310–73-2, Merck KGaA, Darmstadt, Germany) in concentrations of 17.5 and 8.3% for treatment and washing, respectively. Acetic acid (CAS # 64–19-7, Merck KGaA, Darmstadt, Germany) was used for washing of the treated cellulose.

In analysis of the biomass composition, DI water and 72% sulfuric acid (CAS # 7664–93-9, Merck KGaA, Darmstadt, Germany) were used in determination of the content of acid soluble and acid insoluble (Klason) lignin. Hydrochloric acid (HCl, CAS # 7647–01-0), anhydrous methanol (CAS # 67–56-1), resorcinol (CAS # 108–46-3, Merck KGaA, Darmstadt, Germany), pyridine (CAS # 110–86-1, Merck KGaA, Darmstadt, Germany), trimethylchlorosilane (TMCS, CAS # 75–77-4, Merck KGaA, Darmstadt, Germany) and N,O-bis-trimethylsilyl-trifluoroacetamide (BSTFA, CAS # 25,561–30-2, Merck KGaA, Darmstadt, Germany) were used in polysaccharide analysis.

A mixture of ionic liquid – 1-ethyl-3-methylimidazolium acetate, 95% ([Emim][OAc], C_1C_2ImOAc, CAS # 143,314–17-4, Iolitec Ionic Liquids Technologies GmbH) and DMSO (CAS # 67–68-5, Merck KGaA, Darmstadt, Germany) was utilized in preparation of the casting solution.

Non-woven polyester was taken from used RO membranes and cleaned mechanically for use as a

support material for the membrane preparation. Ultra-pure deionized water was produced by a CENTRA-R 60\120 system (Elga purification system, Veolia Water, UK) and used for washing and as a non-solvent and also in preparation of all solutions.

Polyethylene glycol (PEG, approx. M_w 35 000 g/mol, CAS # 25,322–68-3, Merck KGaA, Darmstadt, Germany) was used as a model compound for study of membrane retention.

Methods

The pretreatment steps described below are shown schematically in Fig. 1. Untreated birch chips were ground in a ball milling machine and sieved with a No. 120 mesh (nominal sieve opening, 0.125 mm) in order to ease the dissolution process and enable use of analytical methods (e.g. XRD, TG-MS).

DES treatment

For treatment of the birch wood chips, a DES was prepared from ChCl and LAc mixed at a 1:9 mole ratio respectively at 100°C until a homogeneous transparent mixture was formed. Birch chips and DES were taken at 1:5 mass ratio and placed into an oil bath, where the biomass load was cooked for 18 h at 105 °C. After the treatment was completed, the pulp was vacuum filtered through a filter paper and washed with a mixture of ethanol and DI water at 9:1 volume ratio until the treated pulp released no color. The filtrate was collected and the ethanol removed by evaporation. Recovered lignin was separated from the mixture of recovered DES by addition of water, which led to precipitation of the dissolved lignin. The DES-treated pulp was transferred to an oven and dried at 50 °C for 24 h.

Bleaching

The dried DES-treated pulp was bleached with sodium chlorite and acetic acid according to the "Preparation of Holocellulose" method described by Rowell (2013). At the end of the reaction, when the pulp was almost white-colored, the pulp was filtered and washed with DI water, ethanol and acetone. The pulp was then dried at 50 °C for 24 h.

Two-step alkaline treatment

DES-treated and bleached birch biomass was treated according to the "Preparation of α-cellulose" method by Rowell (2013), which can be described as a two-step alkaline treatment where the first step is treatment with 17.5% NaOH solution and the second step is washing of the treated biomass with 8.3% NaOH solution. The alkali-treated biomass was subsequently washed with DI water, subjected to 10% acetic acid treatment, and washed with DI water again. After the treatment was completed, the resultant pulp was dried at 50 °C for 24 h.

An overview of the analyses of the biomass pulps and membranes produced is presented in Table 1.

Lignin analysis

To estimate the amount of lignin in biomass samples B1–4 and the efficiency of its removal, determination of Klason or acid insoluble lignin (KL, AISL) and acid soluble lignin (ASL) was carried out according to the procedure described in NREL (2012). Acid soluble lignin concentrations were calculated from the obtained UV–Vis absorbance values based on Beer-Lambert's law with absorptivity of $110 \, \text{L} \, \text{g}^{-1} \, \text{cm}^{-1}$ for 205 nm wavelength.

Analysis of polysaccharides (Acid Methanolysis + GC)

To evaluate changes in hemicellulose content in pulp samples B1–4, analysis was done according to the modified procedure described by Holmbom and Örså (1993). Three parallel samples were measured for all biomass samples. The carbohydrates were analyzed according to Sundberg et al. (1996). The carbohydrate content was analyzed by gas chromatograph HP6890 + injector HP7683 (Agilent, USA). The column was a 25 m/0.20 mm i.d. wide-bore capillary column with a nonpolar phase (HP-1, Agilent Technologies) having a film thickness of 0.11 μm. Carbohydrates were analyzed as monosaccharides; thus, hemicelluloses were transformed to monosaccharides by acid methanolysis before analysis. Calculation of the GC results was done using Relative Response Factors (RRFs), which are described in detail elsewhere (Sundberg et al. 1996; Anugwom et al. 2012; Today 2019).
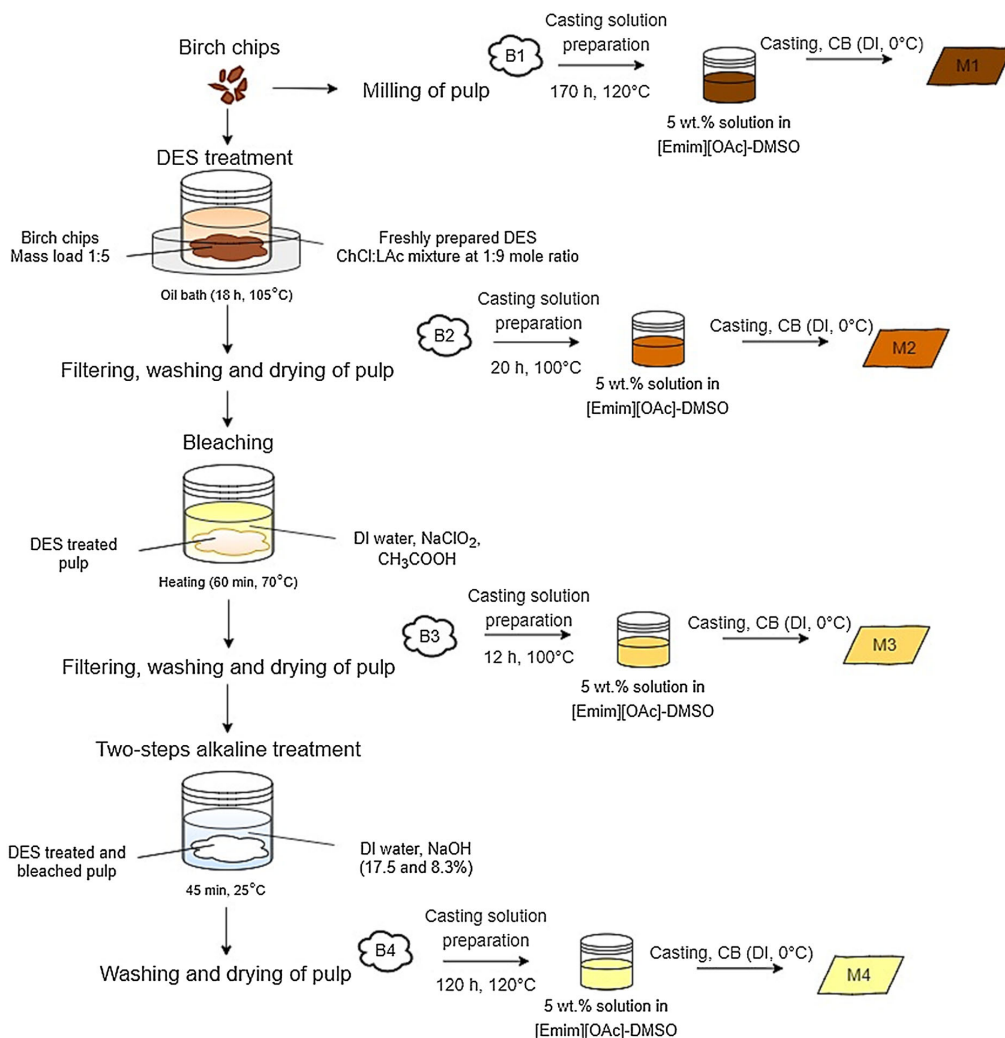
Fig. 1 Schematic overview of the pretreatment procedure; B1 stands for untreated birch, B2 for DES-treated birch, B3 for bleached DES-treated birch and B4 for alkali-treated bleached DES-treated birch; M1 – M4 stand for the membranes prepared from B1 – B4 respectively

Membrane preparation

As preparation as a casting solution, the biomass samples exposed to different pretreatments were dissolved in a mixture of [Emim][OAc] and DMSO at a mass ratio of 2:8 respectively. The temperature used depended on the pulp source, i.e. B2 and B3 dissolved at 100°C, while B1 and B4 dissolved at 120°C (Fig. 1). Flat sheet polymeric membranes were prepared by Automatic Film Applicator L (BYK-Gardner USA). In membrane casting, a prepared solution with 5 wt.-% concentration of polymer was poured onto a polyester support attached to the membrane casting plate, spread on the flat surface by

Table 1 Overview of analyses

	Lignin content	Acid methanolysis + GC	Permeability and retention	FTIR	TGA-MS	XRD	Raman
B1	✔	✔				✔	
B2	✔	✔				✔	
B3	✔	✔				✔	
B4	✔	✔				✔	
M1			✔	✔	✔	✔	✔
M2			✔	✔	✔	✔	✔
M3			✔	✔	✔	✔	✔
M4			✔	✔	✔	✔	✔

casting knife with casting thickness of 300 μm and speed 50 mm/s, and immediately after casting transferred into a coagulation bath filled with DI water at 0 °C, where the membrane was preserved for 24 h. All obtained membranes were washed under DI water and then cut into circular coupons with 0.0038 m^2 active area for further use. Membranes were stored in water until they were tested in the filtration experiments.

Membrane permeability and retention assessment

For the determination of permeability and separation capabilities of the prepared membranes, small-scale filtration experiments were conducted in an Amicon dead end stirring cell unit (Millipore, USA, Cat No.: XFUF07611, diameter of the stirring device 60 mm), which is presented schematically in Fig. 2.

Prior to determination of the membrane permeability, the membrane was compacted for 1 min at 1 bar, 2 min at 2 bars, 3 min at 3 bars, 4 min at 4 bars and 20 min at 5 bars to minimize errors from compaction of membrane in further measurements and to ensure that the solvents used in the biomass pretreatment and membrane manufacturing were completely rinsed from the membrane pores. The latter was checked by measurement of TOC content in a "leakage" sample (a sample of permeate that was taken while the membrane was compacted at maximum pressure of 5 bar). The permeability of the fabricated membranes was measured at four different pressures (1, 2, 3, and 4 bar) at 25 ± 0.5 °C. The permeability value was calculated with the following Eq. (1):

$$P = \frac{J/1000}{A \cdot \left(\frac{\tau}{60}\right) \cdot \Delta P} \tag{1}$$

where P – the permeability of the tested membrane (L/(m^{2}h bar)), J – the mass of pure water permeated through the membrane at 1 min (g/min), A – the area of membrane coupon (m^2), τ – the time of collection of the permeate (min), ΔP – the applied pressure (bar).

For the retention study, a solution of model compound PEG 35 kDa was prepared with concentration of 300 ppm and filtered through the membrane at a pressure that was set for each membrane individually in order to have approximately same PEG fluxes around 15 L/(m^2 h bar) at 25 °C and 300 rpm stirring speed. Samples of the feed, permeate and retentate were collected from each filtration and their total organic carbon concentration analyzed with a Shimadzu TOC analyzer (TOC-L series, Japan). Retention was calculated based on the concentrations of TOC content in the feed, permeate and retentate samples with the following Eq. (2):

$$R = \left(1 - \frac{2 \cdot C_p}{C_f + C_r}\right) \cdot 100 \tag{2}$$

where C_p, C_f and C_r are the total organic carbon concentrations in the permeate, feed and retentate (mg/L) respectively.

Optical spectroscopy analyses

The effect of different pretreatment steps on the chemical composition of membranes M1–4 was evaluated based on Fourier-transform infrared spectroscopy (FTIR) and Raman spectroscopy. The FTIR
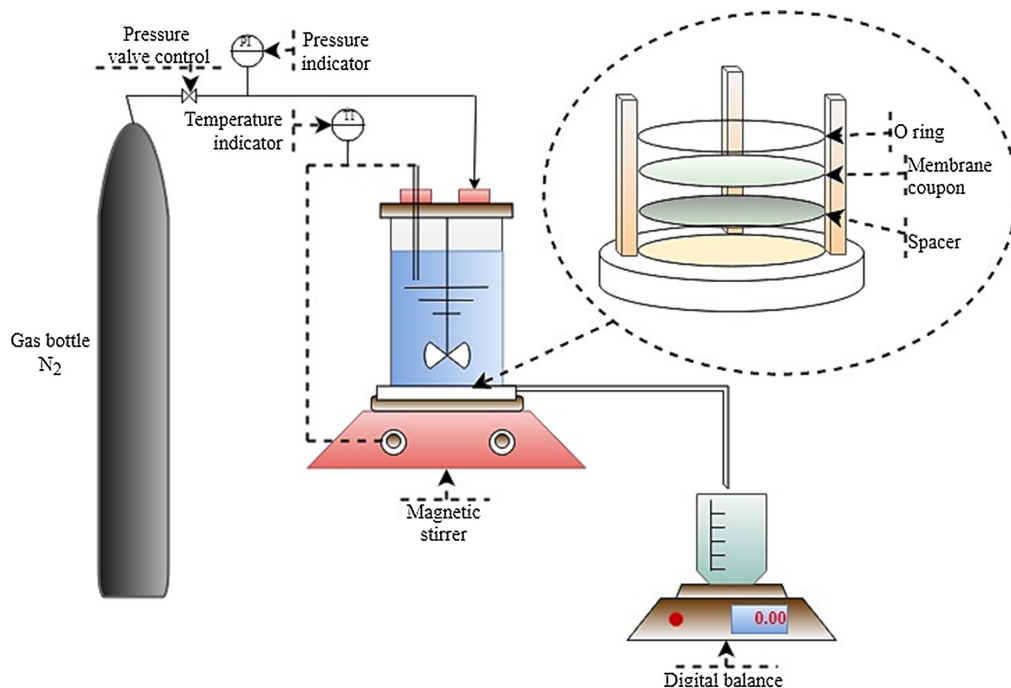
Fig. 2 Schematic configuration of Amicon dead-end filtration system

analysis was performed with a Frontier MIR/FIR spectrometer (PerkinElmer Inc.) with a universal diamond crystal ATR module in the range 400–4000 cm^{-1} with a resolution of 4 cm^{-1}. Membrane samples were air-dried and separated from the polyester support before analysis. Five points were measured for each membrane sample and measured values averaged. For further analysis, all the spectra were processed with ATR correction, baseline correction and normalization. Raman spectra of air-dried supportless membrane samples were collected using a Kaiser RXN1 spectrometer with 785 nm laser excitation and maximum power of 200 mW. Spectra were collected between 100–3425 cm^{-1} using a non-contact MR probe.

Thermogravimetric analysis

For thermogravimetric analysis, approx. 10 ± 0.1 mg of the specimen was heated from 25 to 900 °C at a rate of 10 °C/min under a nitrogen atmosphere of 40 mL/ min nitrogen at a constant flow rate. Evolved gas emission (EGA) during TGA was analyzed using a mass spectrophotometer (MS 403C Aëolos Mass Spectrophotometer, NETZSCH-Gerätebau GmbH, Selb, Germany) which was coupled with TGA. The analyzed mass range was 10–110 a.m.u. The results were interpreted with N-Proteus® software (NETZSCH-Gerätebau GmbH, Selb, Germany).

X-ray diffraction measurements

To reveal any changes in cellulose crystallinity, pulp B1–4 and membrane samples M1–4 were air-dried, separated from the support, and analyzed with an X-ray diffraction (XRD) device (Bruker AXS D8 Advance X-ray diffractometer). The X-ray diffraction patterns were obtained using Cu Kα ($\lambda = 1.5418$ Å) at 40 kV and 40 mA in the range of $2\theta = 7 – 60°$. To estimate the relative degree of crystallinity of the cellulose, a crystallinity index (CrI) was calculated

based on the XRD patterns using the relationship given by Segal et al. (1959) in the following Eq. (3):

$$CrI = \frac{I_{tot} - I_{am}}{I_{tot}} \times 100 \qquad (3)$$

where CrI – crystallinity index, I_{tot} – intensity at about $2\theta \approx 22°$ (represents the crystalline and amorphous material), I_{am} – intensity at the "valley" between the two main peaks at about $2\theta \approx 18°$ (represent the amorphous material).

Results and discussion

Chemical composition and crystallinity of the biomass samples after different pretreatment steps

To investigate the effect of different pretreatment steps on the birch biomass, total lignin and carbohydrates content was measured in oven-dried extractive-free samples of B1–4. Cellulose content in the biomass samples was calculated by subtraction of the other constituents. The results are presented in Table 2.

Based on the values presented in Table 2, DES treatment resulted in approximately 65% lignin extraction and approximately 68% and 28% decrease in hemicelluloses and cellulose content respectively. The surprisingly high removal of cellulose might result from thermal degradation of cellulose during the long reaction time at elevated temperatures. (Kumar et al. 2015; Li et al. 2017; Zdanowicz et al. 2018; Liu et al. 2019). It can also be seen from Table 2 that subsequent bleaching decreased total lignin and hemicelluloses content by approximately 94.5% and 83.5% respectively. This drop in the lignin and hemicelluloses content might be explained with the assumption made by Li et al. (2017) that DES treatment promotes partial cleavage of ether bonds between lignin and hemicelluloses, which then promotes further removal of these compounds during the bleaching step. Though relative content of cellulose increased after bleaching, its absolute content decreased slightly (from 35.3 to 32.4 g/100 g of biomass).

X-ray diffractograms of samples B1–4 are shown in Fig. 3a. It is important to note that the scattered intensity is presented in arbitrary units as the intensity was not normalized to the mass of the samples. Thus, ratios of peak heights rather than absolute intensities were used for comparison between different samples.

The three main peaks in the diffraction pattern are characteristic peaks for cellulose I. The main peak represents a direction perpendicular to the cellulose fiber axis ((200) plane of the I$_\beta$ crystal) (Cheng et al. 2011). The position of the peak varies depending on the pretreatment applied: 22.2° for untreated birch (B1), 22.7° for birch subjected to DES treatment (B2), and 22.8° for both bleached DES-treated birch (B3) and alkali-treated bleached DES-treated birch (B4). As this peak is indicative of the distance between the hydrogen-bonded sheets in cellulose I structure, its gradual shift to higher 2θ values shows that the interplanar spacing distance between cellulose sheets is decreasing as a consequence of the pretreatment steps applied. As amorphous lignin and hemicelluloses are removed, as well as part of amorphous cellulose, the remained crystalline regions show more regular and dense molecules arrangement, causing the main diffraction peak shift to higher 2θ values

Table 2 Chemical composition of wood pulps after different pretreatment (B1 stands for untreated birch, B2 for DES-treated birch, B3 for bleached DES-treated birch and B4 for alkali-treated bleached DES-treated birch)

Sample	Cellulose content		Hemicelluloses content		Lignin (Klason) content		Lignin (acid soluble) content	
	Absolute (g)	Relative* (%)	Absolute (g)	Relative* (%)	Absolute (g)	Relative* (%)	Absolute (g)	Relative* (%)
B1	49.3	49.3	27.2	27.2	17.0	17.0	4.7	4.7
B2	35.4	62.7	8.8	15.6	6.2	11.0	1.5	2.7
B3	32.4	77.5	4.5	10.8	0.4	1.0	0.8	1.9
B4	29.8	89.2	2.1	6.3	0.0	0.0	0.4	1.2

*Relative contents are calculated including the ash and extractives content, which are not presented in the table

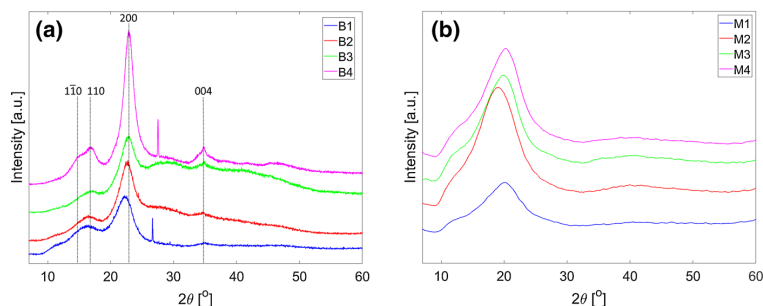**Fig. 3** X-ray diffraction (XRD) diffractograms of biomass samples B1–4 after different pretreatment (**a**), and M1–4 membrane samples prepared from biomass samples B1–4 respectively (**b**)

(Beckwith et al. 2010; Gunny, Arbain and Jamal 2017; Neto 2017).

The second characteristic peak at $\sim 16°$ is known to be a composite of the $(1\bar{1}0)$ and (110) planes of the I_β crystal (Cheng et al. 2011; French 2014). It is interesting to note that in samples B1–B3 these two peaks are presented as one composite peak, whereas in the diffractogram of sample B4 the peak shows two separate peaks at $16.7°$ and $14.9°$ (Wada, Kondo and Okano 2003; Neto 2017).

The third characteristic peak of cellulose I represents the direction parallel to the fiber axis ((004) plane). This peak is located at $\sim 34.5°$ (Thygesen et al. 2005; Cheng et al. 2011). The peak becomes increasingly distinctive after each pretreatment step applied, which suggests a relative increase in the crystalline phase due to the removal of amorphous compounds such as amorphous cellulose as well as lignin and hemicelluloses.

The CrI values of cellulose I of samples B1-B4 were calculated based on Eq. 3 and equals 54%, 59.9%, 46.4% and 57.8%, respectively, and is consistent with results obtained by Agarwal, Reiner and Ralph (2012). The results are in good accordance with theory as the relative crystalline content increases during DES treatment due to the partial removal of non-cellulosic amorphous compounds (lignin and hemicelluloses) (Beckwith et al. 2010). Although bleaching should have the same effect on sample crystallinity, because it continuously removes the non-cellulosic compounds, the decrease in crystallinity index found in this study might indicate that the bleaching conditions used were a bit too aggressive and led to partial decomposition of cellulose chains.

Strong alkaline treatment, as expected, removes mainly amorphous constituents, so relative content of the crystalline part increases again (Dinand et al. 2002; Lionetto et al. 2012).

XRD analysis of membrane samples

To show the type of cellulose present in membrane samples M1–M4, XRD patterns of air-dried membrane samples M1–M4 were measured and are plotted in Fig. 3b. For all samples, the main peak at $\sim 22.5°$ disappeared and a broad asymmetric peak appeared at $\sim 20°$ whose position varied as described above depending on the pretreatment: $20.1°$ for membrane prepared from untreated birch (M1), $19.2°$ for membrane prepared from DES-treated birch (M2), $19.8°$ for membrane prepared from bleached DES-treated birch (M3) and $20.1°$ for membrane prepared from biomass after the alkaline treatment step (M4). This position is typically assigned to the (110) plane of cellulose II crystals (Isogai et al. 1989; Cheng et al. 2011). Both the broad peak at $\sim 16°$ and the small peak at $\sim 34.5°$, which are characteristic for cellulose I, disappeared. The absence of these peaks is indicative of disruption of inter-chain hydrogen bonds and elimination of the alignment of the cellulose chains during the dissolution process, respectively (Pang et al. 2014). However, the only clear evidence of cellulose II is the appearance of a distinctive peak for $(1\bar{1}0)$ plane at $\sim 12.5°$, which is present only as a shoulder in the diffractograms of membrane samples M1–M4.

It is reported in literature that during dissolution (or partial dissolution) of cellulose in IL, the inter-chain hydrogen bonds are broken, or the cellulose chains

themselves are disrupted (Dinand et al. 2002; Cheng et al. 2011; Neto 2017). The regeneration process occurs upon precipitation in antisolvent, where new inter-sheet hydrogen bonds are established, however, the final regenerated cellulose crystallinity varies (from amorphous to crystalline) depending on the regeneration conditions (Zhu et al. 2006; Ling et al. 2017; Al Hakkaket al. 2019; Taheri, Abdolmaleki and Fashandi 2019). According to the latest findings, the diffractograms of membrane samples M1 – M4 should be recognized as amorphous patterns (Ling et al. 2019; French 2020). Recognition of these patterns as amorphous leads to a conclusion that the composition of dissolved biomass causes less effect on the crystallinity of regenerated cellulose-rich films than the regeneration conditions.

Performance and characteristics of the membranes prepared directly from untreated birch

The permeability and retention values of membranes M1—M4 are presented in Fig. 4. It can be seen that membrane M1 showed the highest permeability (18.9 L/(m^2 h bar)) and the lowest retention (24%) compared to the other membranes. As the retention of a membrane is mainly dependent on the properties of its top layer, it might be assumed that the formation of the top layer of membrane M1 prepared from B1 resulted in a loose or uneven structure. As seen in Table 2, the raw wood B1 consists of 21.7% lignin, 27.2% hemicelluloses and 49.3% cellulose. Dissolution of B1 was the most difficult of all the biomass samples and took 170 h at 120 °C. Though some authors, e.g.

Miao et al. (2017) and Mohan et al. (2018), state that [Emim][OAc] has high dissolution capacity over non-cellulosic compounds, it should be borne in mind that the studies were done with pure [Emim][OAc] whereas this work used a mixture of [Emim][OAc] and DMSO. Another possible reason for the complicated dissolution is the presence of lignin-carbohydrates complexes (Cheng et al. 2011). Thus, it may be inferred that the milder dissolution parameters used in our study (lower IL concentration, lower temperatures) and the complexity and heterogeneity of the biomass complicates the dissolution of untreated wood in [Emim][OAc]-DMSO and the resulting solution might be unable to form a uniform dense membrane top layer providing better separation performance. Another reason for the formation of an uneven membrane structure might be that the time and temperature (170 h, 120°C) for dissolution process in this study were sufficient to cause degradation of the cellulose (Kumar et al. 2015; Li et al. 2017; Zdanowicz et al. 2018).

To reveal the chemical composition of the membranes, FTIR spectra of air-dried membranes M1 – M4 were taken and are shown in Fig. 5. It can be seen that clearly visible peaks are located in the fingerprint region (1750 – 1100 cm^{-1}). The assigned wavelengths are given in Table 3. The spectrum for membrane M1 shows peaks at 1592, 1507, 1460, 1325 and 1120 cm^{-1}, which might be related to aromatic skeletal vibrations, CH$_2$- and OCH$_3$- groups, and deformation vibrations of C–H bonds in syringyl rings, and can be considered characteristic peaks of lignin according to Bykov (2008). Consequently, it
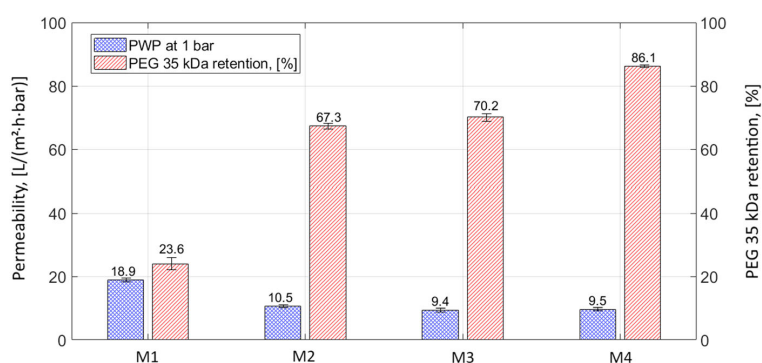
Fig. 4 Permeability of pure water measured at 1 bar and retention of PEG 35 kDa values for M1–4 membrane samples prepared from biomass samples B1–4 respectively

might be concluded that some amount of lignin has been dissolved and later participated in the formation of the matrix of M1. A peak at 1732 cm^{-1} is also present and, as reported by Weng et al. (2017), might be related to unconjugated C=O groups in lignin, carboxylic ester hemicellulose structures and some hardwood extractives as they have not been specifically removed (Routa et al. 2017). A small shoulder peak appears at ∼ 1250 cm^{-1}, which might result from C–O bonds in xylan and vibrations of syringyl rings in lignin structures (Pandey and Pitman 2003).

To test our hypothesis about the presence of lignin in the membrane matrix of membrane M1, the membrane sample was analyzed using Raman spectroscopy to compare the presence and intensity of the background fluorescence seen in the presence of lignin. The emitted laser induced fluorescence (LIF) caused by lignin is usually regarded as a major drawback of Raman spectroscopy (Lähdetie 2013). However, within the framework of this study, lignin-caused fluorescence emission is useful as an elegant tool for qualitative determination of the presence of lignin in the membrane matrix. The Raman spectrum of the air-dried membrane M1 is given in Fig. 6 together with spectra of other membrane samples. It can be seen that the fluorescence background is the strongest for membrane M1, indicating a greater lignin content in the membrane. Though the spectrum does

not give any certain peak due to the strong background fluorescence, a small "wave" can be noticed at 1840 cm^{-1} which can be assigned to the C=O bond (Lähdetie 2013).

Both FTIR and Raman spectroscopy support the conclusion that lignin was present in the membrane matrix of M1. However, the absence of characteristic peaks in FTIR and strong fluorescence in the Raman spectra mean that the presence of hemicelluloses remains unclear. To ascertain the presence of hemicelluloses and study thermal degradation of the membranes, TG-MS analysis was performed on the freeze-dried support-free membrane samples. The TG and DTG curves of samples M1–4 are presented in Figs. 7 and 8 respectively. It can be seen from Fig. 7 that the studied membranes decomposed over a large temperature range following the four-stage pyrolysis process described for lignocellulosic biomass by Sanchez-Silva et al. (2012). The moisture evolution and loss of volatiles happened at approximately 75—120 °C. Biomass decomposition slowly started at approx. 170 °C, indicating the presence of hemicelluloses in the membrane matrix of M1, as both lignin and cellulose decomposition start at higher temperatures (above 310 °C) (Sanchez-Silva et al. 2012; López-González et al. 2013).

It can be seen in Fig. 8 that the DTG curve of membrane M1 has a broad shoulder at 230–295 °C,
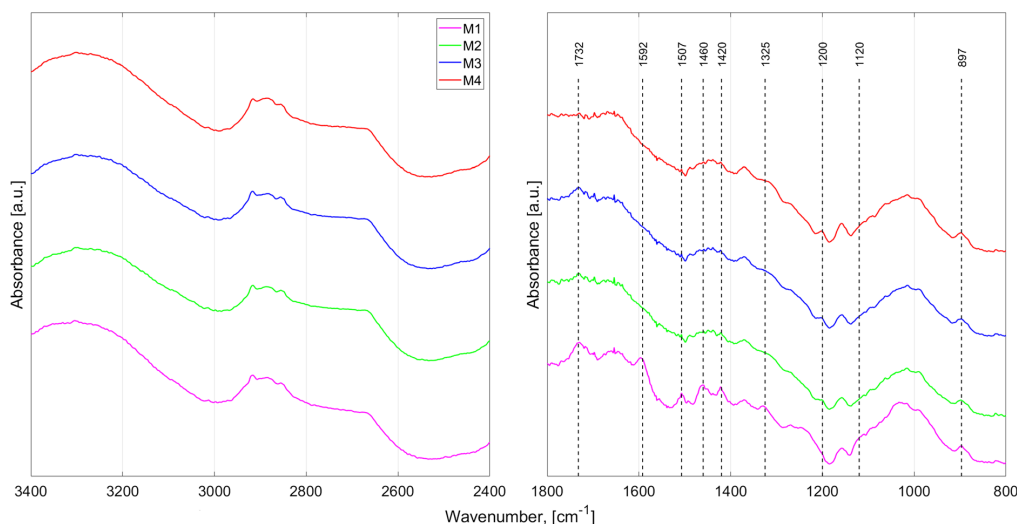
Fig. 5 FTIR spectra of M1–4 membrane samples prepared from biomass samples B1–4 respectively

Table 3 Allocation of characteristic absorption IR bands of M1-4 samples in the fingerprint region (L – lignin, H – hemicelluloses, C – cellulose)

Wavenumber (cm^{-1})	Functional group	Assignment	Reference
1732	C=O stretching in unconjugated ketones aldehydes and carbonyl	H, L	Weng et al. (2017)
1507, 1592	C=C stretching of the aromatic ring	L	Bykov (2008)
1460	CH$_2$- groups deformation vibration	L, H	
1325	Vibrations of syringyl rings and stretching vibrations of C–O bonds	L	
1200	C–O stretching vibrations	C, H	Pandey and Pitman (2003)
1120	Deformation vibrations of C–H bonds in syringyl rings	L	Bykov (2008)
897	C–O stretching vibration in the amorphous region	C$_{amorphous}$	Li et al. (2011)

Fig. 6 Raman spectra of membrane samples M1–M4 (Kaiser RXN1, 785 nm laser excitation, maximum power 200 mW)
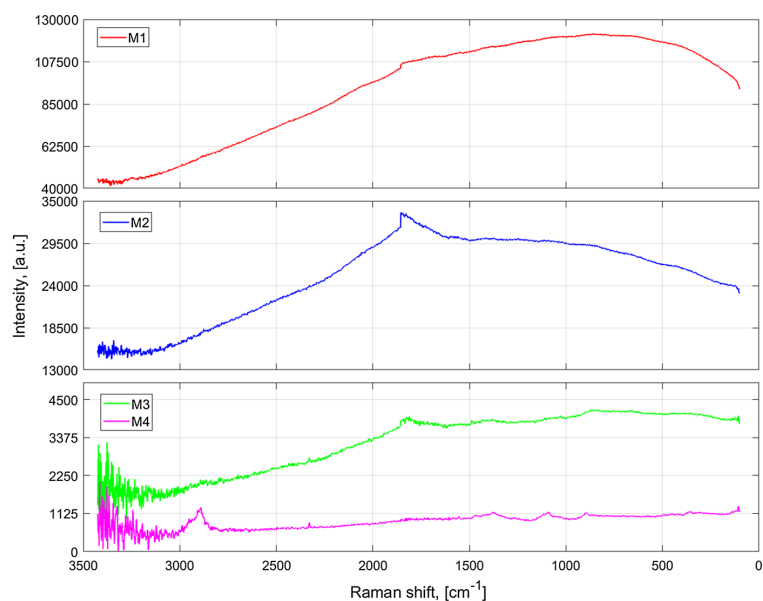
which is a clear evidence of hemicelluloses presence, and the main peak shifts to 350 °C, which also points to the presence of lignin structures with higher thermal stability than those of hemicelluloses and cellulose.

As wood biomass consists mainly of different polymeric compounds, its thermal degradation is a complex process that produces a wide range of low-molecular weight compounds (Lv and Wu 2012). MS fragments that have relatively high intensity were selected from pyrolysis of sample M1 and their evolution profiles with pyrolysis temperature were plotted and are shown in Online Resource Figs. S1 – 3. The release of major compounds from membrane M1 has broad peaks due to the presence of components with different thermal stability whose decomposition starts and finishes at different temperatures. The important releasing profile of m/z 109 (guaiacol) is present in Fig. S3. This MS curve was the only characteristic curve for the evolution of products of lignin pyrolysis and its presence in sample M1 is in

Fig. 7 TG curves of membrane samples M1 – 4 prepared from biomass samples B1–4 respectively
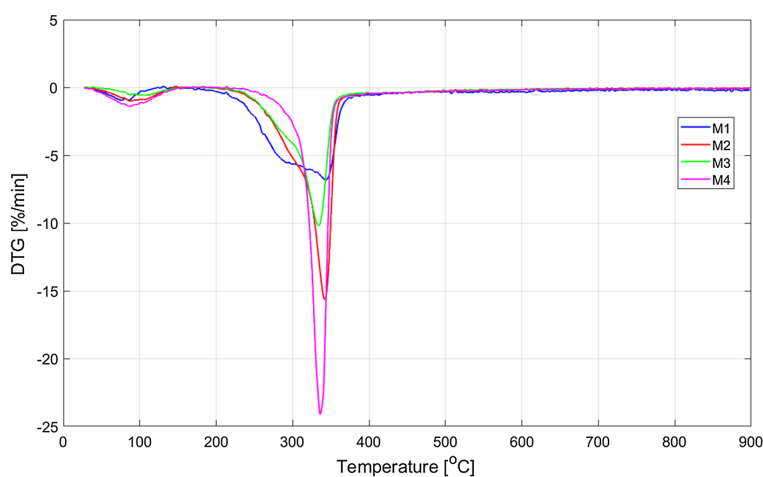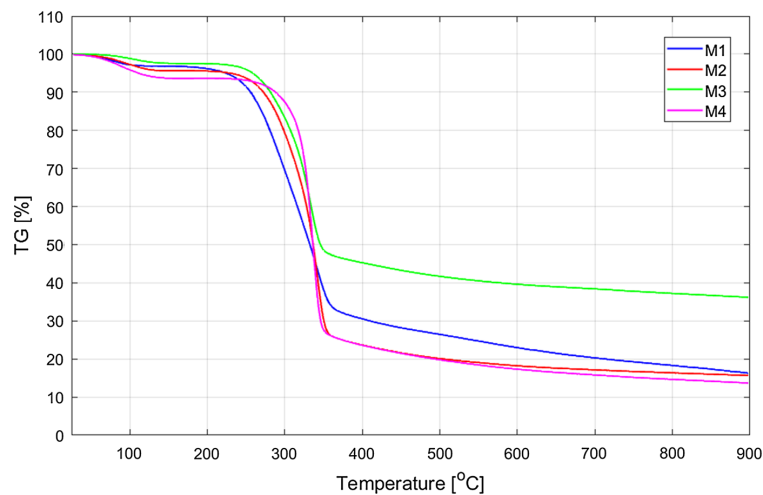
Fig. 8 DTG curves of membrane samples M1 – 4 prepared from biomass samples B1–4 respectively

agreement with results from FTIR and Raman spectroscopy, confirming the presence of lignin in the membrane matrix (Brebuet al. 2013).

Performance and chemical content of the membranes prepared from DES-treated birch

Membrane M2 was prepared from B2 following the same procedure as described above. Dissolution of the DES-treated birch biomass (B2) was much easier than that of the raw wood (B1) and took approximately 20 h at 100 °C. Permeability and retention values measured with this membrane are shown in Fig. 4. Membrane M2 shows lower permeability than M1 (10.5 to 18.9 L/(m^2 h bar)) and significantly higher retention of PEG 35 kDa (67.3 to 24%). From Table 2, it can be seen that the DES treatment removed approximately 65% of lignin and 68% of hemicelluloses, which might ease the dissolution of the pulp and

promote the formation of a homogeneous solution, which thus resulted in a more uniform and denser top layer giving better retention values.

FTIR, Raman spectroscopy and TG-MS analyses were performed to compare the chemical composition of membranes M2 and M1, and the results are presented in Figs. 5, 6, 7, 8, and S1-3 respectively. In Fig. 5, the FTIR spectrum of M2 is significantly different from that of M1, where no characteristic peaks for lignin are found. The peak at 1732 cm^{-1} has slightly lower intensity and, as discussed above, cannot be exclusively attributed to lignin, hemicelluloses or extractives. The peak at 1200 cm^{-1} might result from C–O stretching vibrations formed from xylan degradation (Pandey and Pitman 2003), which is in good agreement with results in Table 2 and shows that the decrease in hemicelluloses content might result from degradation of xylan during the DES treatment or more complete dissolution of xylan due to its initially lower content in sample B2. The absence of characteristic peaks and quite low penetration of FTIR spectra (approx. 10 μm) means that it cannot be guaranteed that no lignin was present in membrane M2.

It can be seen from Fig. 6 that the Raman spectrum of membrane M2 shows significantly lower background fluorescence than M1, suggesting that some amount of lignin might still be present in the matrix of M2, but lignin content is lower than in sample M1. Though the spectrum does not exhibit any certain peak, due to strong background fluorescence, a peak can nevertheless be seen at 1840 cm^{-1} that might be assigned to the C=O bond (Lähdetie 2013).

Figures 7 and 8 give TG and DTG curves for membrane M2. The degradation curves follow the same pattern as those of M1, decomposing across a large temperature range with humidity elimination below 120 °C and aromatic condensation above 400 °C, resulting in slow loss of mass at high temperatures. In Fig. 7, however, it can be seen that the slope of the curve becomes sharper, indicating a more homogeneous chemical composition for M2 than M1. In Fig. 8, the shoulder at 240–305 °C becomes smaller, indicating that the hemicelluloses (which have lower degradation temperature) are still present but their content has decreased.

The profiles of the main degradation products in Figs. S1-3 mostly follow the same trend: peaks become sharper and narrower, and they shift to higher temperatures, indicating, as discussed above, that the composition of membrane M2 became more uniform as lignin and hemicelluloses are partially removed. It is important to note that the guaiacol releasing profile (m/z 109) is still present for membrane M2, demonstrating that some amount of lignin remained in the membrane matrix even though its initial concentration in the pulp of B2 was significantly lower than in pulp B1.

Performance and chemical composition of the membranes prepared from bleached DES treated birch

Membrane M3 from bleached DES-treated birch biomass (B3) was prepared the same way as membrane M2. Dissolution was done at the same temperature and took shorter time (12 h). Permeability and retention values measured with this membrane are shown in Fig. 4. It can be seen that although the lignin and hemicelluloses content of the biomass is noticeably lower than that of B2, no significant changes were observed for permeability (9.4 to 10.5 L/(m^2 h bar)) nor retention (70.2 to 67.3%). The result might suggest that lignin and hemicelluloses content have an impact on membrane permeability and retention only above a certain threshold concentration, but this hypothesis needs further investigation.

In Fig. 5, the same FTIR peaks are found in the spectrum of membrane M3 as membrane M2. However, the Raman spectrum of M3, presented in Fig. 6, is clearly different from the spectra of membrane M1 and M2. Comparing the intensities of background fluorescence, it can be seen that intensity decreases in the following order: M1 > M2 > M3, indicating a decrease in lignin content in the membrane matrix. The peak at 1840 cm^{-1} is still present in the spectrum of membrane M3, which might be interpreted as a sign of the presence of hemicelluloses as there is no peak at this wavenumber in the spectrum of membrane M4 (Lähdetie 2013). Furthermore, the presence of hemicelluloses is in agreement with the results presented in Table 2.

The TG and DTG curves of M3 can be seen in Figs. 7, 8. The M3 degradation curves follow the same pattern as those for membranes M1 and M2, decomposing in a large temperature range with humidity elimination below 120 °C and aromatic condensation above 400 °C, followed by slow loss of mass at high

temperatures. However, the curve slope in Fig. 7 is sharper, indicating even more homogeneous chemical composition in M3 than M1 and M2. The TG curve of membrane M3 shows that it has three times higher residue than the other samples. A possible explanation might be traces of the bleaching chemical (i.e. sodium chlorite) in the biomass. Inorganic salts are well-known to cause increased char formation (due to increase in the dielectric constant of the carbohydrates melt in the presence of salt). It is also possible that salt catalyzed a branch of the reaction network that forms more char (Varhegyi et al. 1988).

The shoulder at 240–305 °C in Fig. 8 is smaller than for M1 and M2, showing that the hemicelluloses (which have lower degradation temperature) content has decreased. Interestingly, M3 has lower DTG_{max} (10 vs 15%/min) than M2, which can also be attributed to char formation reactions due to the presence of alkaline ions.

The same trend can be seen in the releasing profiles of the main degradation products in Figs. S1-3, i.e. peaks become sharper and narrower, and they shift to higher temperatures, indicating, as discussed above, that the composition of membrane M3 became more uniform as lignin and hemicelluloses content continued to decrease. Another important result is that the guaiacol releasing profile (m/z 109) disappeared, showing that no lignin remained in the membrane matrix, even though a small amount was present in B3 (Table 2). It might be concluded that acid soluble lignin (as the only fraction present in the composition of biomass B3) tends to be removed from the membrane matrix during precipitation in a coagulation bath.

Performance and chemical composition of the membranes prepared from DES-treated, bleached alkali-extracted birch

Clear trends can be observed in the permeability and retention results presented in Fig. 4. The pure water permeability of the membranes decreases with each pretreatment step, showing the highest value for membrane M1 (18.9 L/(m²h bar)) and the lowest for membranes M3 (9.4 L/(m²h bar)) and M4 (9.5 L/(m²h bar)). Conversely, the retention of PEG 35 kDa increased with each pretreatment step applied, showing the lowest value for membrane M1 (24%) and the highest for membrane M4 (86%). The permeabilities of membranes M2–4 are in the same range and differ from that of membrane M1.

Membrane M4 prepared from alkali-treated bleached DES-treated birch biomass (B4) was prepared in the same way as membrane M1: the dissolution was done at the same temperature (120 °C) but took longer (120 h) than preparation of casting solutions from biomass B2 and B3. The longer time and higher temperatures of B4 dissolution might be explained with reference to the chemical composition of the biomass, which becomes more homogeneous with each pretreatment step applied. The overall decrease in lignin and hemicelluloses content after the final pretreatment step equals 98% and 92% respectively. The relative content of cellulose in biomass sample B4 is 89.2% (Table 2). The presence of hemicelluloses in the biomass has been reported to ease the dissolution process, due to the release of acetic acid from the acetyl units of hemicelluloses, which increases the overall polarity and thus promotes further dissolution (Triantafyllidis et al. 2013). Thus, it might be the case that removal of hemicelluloses after some point hampers the dissolution process as acetyl units no longer contribute to the polarity.

From another point of view, it seems that even small concentrations of hemicelluloses can affect the formation of the top layer, since, as can be seen in Table 2, there is no large difference in hemicelluloses content between biomass B3 (10.8%) and B4 (6.3%) but the retention values of membranes M3 and M4 are significantly different (70.2 vs 86.1%). Moreover, it has been suggested that lignin can act like a pore-former agent due to the accelerated diffusional rate between solvent and non-solvent caused by the presence of lignin in the casting solution, which might also contribute to the formation of a looser membrane structure when lignin is present in the biomass (Vilakati et al. 2015; Esmaeili et al. 2018). The FTIR spectrum of M4, shown in Fig. 5, differs from that of the others as it does not have a peak at 1732 cm⁻¹, which might mean that there are no hemicelluloses, lignin or extractives in the membrane matrix. From Fig. 6, it can be seen that the Raman spectrum of membrane M4 has common features with spectra presented elsewhere (Beckers 2015; Lähdetie 2013), showing peaks at 900, 1100, 1370 and 2900 cm⁻¹, which might be attributed to amorphous cellulose, C–C and C–O stretch, HCC, HCO and HOC bending and C–H stretch sp³ respectively.

Membrane M4 has the highest degradation rate (DTG$_{max}$ 24%/min) and the steepest slope on the TG graph (Figs. 7 and 8), showing that the chemical composition is as homogeneous as possible and membrane M4 consists mainly of cellulose. The absence of a shoulder and only one main peak in Fig. 8 indicates that no hemicelluloses remained in the membrane matrix of M4. The evolution of the main m/z signals in Figs. S1-3 confirms the trend discussed above that as the composition of the pulps becomes more homogeneous, so too does the composition of the derived membrane. Broad mass peaks become narrower as they no longer derive from different sources but only from cellulose, which exhibits a sharp devolatilization process (Lv and Wu 2012).

Conclusions

Fabrication of polymeric cellulose-rich membranes from hardwood (birch) biomass subjected to different pretreatments and dissolved in a mixture of [Emim][OAc]-DMSO via phase inversion method was performed. Characterization of the membranes was done by measuring pure water permeability and PEG retention, and carrying out ATR-FTIR, Raman spectroscopy, XRD and TG-MS measurements. Wood biomass was subjected to sequential pretreatment steps: partial removal of lignin and carbohydrates during DES extraction (ChCl-Lac, 1:9 mol ratio), NaClO$_2$ bleaching, and two-step (17.5 and 8.3%) alkaline treatment, described in literature for the preparation of α-cellulose. The resultant chemical composition was characterized by XRD, total lignin, hemicelluloses and cellulose content.

The results showed that it is possible to fabricate a membrane from each type of the utilized biomass, even by dissolving milled hardwood directly without any pretreatment. However, the biomass pretreatments significantly affected the dissolution of biomass in the mixture of [Emim][OAc]-DMSO and the properties of the prepared membranes.

Chemical characterization of the prepared membranes showed that all membranes but one had complex chemical composition. The exception was the membrane prepared from biomass after alkaline extraction, which consisted of pure cellulose. This difference in chemical composition was clearly observed in thermogravimetric analysis, FTIR and Raman spectroscopy analysis. Measurement of background fluorescence in Raman spectroscopy showed that there was lignin in the membrane matrix of the first two membranes. Hemicelluloses were present in all the membranes bar the membrane prepared from biomass, which was also alkali-extracted. As lignin and hemicelluloses were present in all biomass samples and were found in some but not all membranes, two findings should be noted. First, the [Emim][OAc]-DMSO mixture is capable of dissolving some amount of lignin and hemicelluloses, and second, below a certain concentration these compounds do not remain in the membrane matrix and may be removed during either precipitation or washing of the membrane. The membrane fabricated from untreated birch showed the highest permeability and the lowest retention. This result might be attributed to the complexity and recalcitrance of the chemical composition of the untreated wood, which makes the dissolution harder and prevents formation of dense top-layer, as well as to the pore-forming properties of lignin and overall complexity of the membrane formed. The retention of cellulose-rich membrane was found to depend on the purity of cellulose in its matrix, because with each pretreatment step applied to the biomass, the resulting membrane became chemically more homogenous, tighter, and showed better retention. The results also demonstrated that although it is possible to prepare ultrafiltration type membranes directly from wood, the novel pretreatments prior to dissolution applied in this study lead to better membrane properties.

Compliance with ethical standards

References

Agarwal U, Reiner R, Ralph S (2012) Estimation of cellulose crystallinity of lignocelluloses using near-IR FT-Raman spectroscopy and comparison of the raman and segal-WAXS methods. J Agric Food Chem 61(1):103–113. https://doi.org/10.1021/jf304465k

Al Hakkak J, Grigsby W, Kathirgamanathan K, Edmonds N (2019) Generation of spherical cellulose nanoparticles from ionic liquid processing via novel nonsolvent addition and drying. Adv Mater Sci Eng. https://doi.org/10.1155/2019/2081027

Alvarez-Vasco C, Ma R, Quintero M, Guo M, Geleynse S, Ramasamy K, Wolcott M, Zhang X (2016) Unique low-molecular-weight lignin with high purity extracted from wood by deep eutectic solvents (DES): a source of lignin for valorization. Green Chem 18(19):5133–5141. https://doi.org/10.1039/c6gc01007e

Anokhina T, Pleshivtseva T, Ignatenko V, Antonov S, Volkov A (2017) Fabrication of composite nanofiltration membranes from cellulose solutions in an [Emim]OAc–DMSO mixture. Pet Chem 57(6):477–482. https://doi.org/10.1134/S096554411706002

Anugwom I, Mäki-Arvela P, Virtanen P, Willför S, Sjöholm R, Mikkola J (2012) Selective extraction of hemicelluloses from spruce using switchable ionic liquids. Carbohydr Polym 87(3):2005–2011.

Beckers M (2015) Analysing lignin and wheat straw pre-treated by novel solvents. Master thesis. Eindhoven University of Technology.

Beckwith SW, Albers RG, Hubert P (2010) SAMPE 2010 - New materials and processes for a new economy, Seattle WA, May 17–20, 2010 - 66.3.2 Crystal Structure. Society for the Advancement of Material and Process Engineering (SAMPE)

Brebu M, Tamminen T, Spiridon I (2013) Thermal degradation of various lignins by TG-MS/FTIR and Py-GC-MS. J Anal Appl Pyrolysis 104:531–539. https://doi.org/10.1016/j.jaap.2013.05.016

Bykov I (2008) Characterization of natural and technical lignins using FTIR spectroscopy. Master thesis. Luleå University of Technology.

Chen H, Wang N, Liu L (2012) Regenerated cellulose membrane prepared with ionic liquid 1-butyl-3-methylimidazolium chloride as solvent using wheat straw. J Chem Technol Biotechnol 87(12):1634–1640. https://doi.org/10.1002/jctb.3802

Cheng G, Varanasi P, Li C, Liu H, Melnichenko Y, Simmons B, Kent M, Singh S (2011) Transition of cellulose crystalline structure and surface morphology of biomass as a function of ionic liquid pretreatment and its relation to enzymatic hydrolysis. Biomacromol 12(4):933–941. https://doi.org/10.1021/bm101240z

Dinand E, Vignon M, Chanzy H and Heux L (2002) Mercerization of primary wall cellulose and its implication for the conversion of cellulose I→cellulose II. Cellulose, 9, 7–18. doi.org:10.1023/A:1015877021688

Esmaeili M, Anugwom I, Mänttäri M, Kallioinen M (2018) Utilization of DES-lignin as a bio-based hydrophilicity promoter in the fabrication of antioxidant polyethersulfone membranes. Membranes 8(3):80. https://doi.org/10.3390/membranes8030080

French AD (2014) Idealized powder diffraction patterns for cellulose polymorphs. Cellulose 21:885–896. https://doi.org/10.1007/s10570-013-0030-4

French AD (2020) Increment in evolution of cellulose crystallinity analysis. Cellulose 27:5445–5448. https://doi.org/10.1007/s10570-020-03172-z

Gunny A, Arbain D, Jamal P (2017) Effect of structural changes of lignocelluloses material upon pre-treatment using green solvents. https://doi.org/10.1063/1.4981844

Holmbom B, and Örså F (1993) Methods for analysis of dissolved and colloidal wood components in papermaking process waters and effluents. In: Proceedings of the 7th International Symposium, Wood Pulping Chem. Beijing, vol 2, pp 810–817

Isik M, Sardon H, Mecerreyes D (2014) Ionic liquids and cellulose: dissolution, chemical modification and preparation of new cellulosic materials. Int J Mol Sci 15(7):11922–11940. https://doi.org/10.3390/ijms150711922

Isogai A, Usuda M, Kato T, Uryu T, Atalla R (1989) Solid-state CP/MAS carbon-13 NMR study of cellulose polymorphs. Macromolecules 22(7):3168–3172. https://doi.org/10.1021/ma00197a045

Khakalo A, Tanaka A, Korpela A, Hauru L, Orelma H (2019) All-wood composite material by partial fiber surface dissolution with an ionic liquid. ACS Sustain Chem Eng 7(3):3195–3202. https://doi.org/10.1021/acssuschemeng.8b05059

Kumar A, Parikh B, Pravakar M (2015) Natural deep eutectic solvent mediated pretreatment of rice straw: bioanalytical characterization of lignin extract and enzymatic hydrolysis of pretreated biomass residue. Environ Sci Pollut Res 23(10):9265–9275. https://doi.org/10.1007/s11356-015-4780-4

Lähdetie A (2013) Wood biomass characterization by Raman spectroscopy. Doctoral dissertation. Aalto University.

Li T, Lyu G, Liu Y, Lou R, Lucia L, Yang G, Chen J, Saeed H (2017) Deep eutectic solvents (DESs) for the isolation of willow lignin (Salix matsudana cv Zhuliu). Int J Mol Sci 18(11):22–66. https://doi.org/10.3390/ijms18112266

Li X, Zhu L, Zhu B, Xu Y (2011) High-flux and anti-fouling cellulose nanofiltration membranes prepared via phase inversion with ionic liquid as solvent. Sep Purif Technol 83:66–73. https://doi.org/10.1016/j.seppur.2011.09.012

Ling Z, Chen S, Zhang X, Takabe K, Xu F (2017) Unraveling variations of crystalline cellulose induced by ionic liquid and their effects on enzymatic hydrolysis. Sci Rep. https://doi.org/10.1038/s41598-017-09885-9

Ling Z, Wang T, Makarem M, Santiago Cintrón M, Cheng HN, Kang X, Bacher M, Potthast A, Rosenau T, King H, Delhom CD, Nam S, Edwards JV, Kim SH, Xu F, French AD (2019) Effects of ball milling on the structure of cotton cellulose. Cellulose 21:885–896. https://doi.org/10.1007/s10570-018-02230-x

Lionetto F, Del Sole R, Cannoletta D, Vasapollo G, Maffezzoli A (2012) Monitoring wood degradation during weathering by cellulose crystallinity. Materials 5(10):1910–1922. https://doi.org/10.3390/ma5101910

Liu Q, Yuan T, Fu Q, Bai Y, Peng F, Yao C (2019) Choline chloride-lactic acid deep eutectic solvent for delignification and nanocellulose production of moso bamboo. Cellulose 26(18):9447–9462. https://doi.org/10.1007/s10570-019-02726-0

Livazovic S, Li Z, Behzad A, Peinemann K, Nunes S (2015) Cellulose multilayer membranes manufacture with ionic liquid. J Membr Sci 490:282–293. https://doi.org/10.1016/j.memsci.2015.05.009

López-González D, Fernandez-Lopez M, Valverde J, Sanchez-Silva L (2013) Thermogravimetric-mass spectrometric analysis on combustion of lignocellulosic biomass. Bioresour Technol 143:562–574. https://doi.org/10.1016/j.biortech.2013.06.052

Lv G, Wu S (2012) Analytical pyrolysis studies of corn stalk and its three main components by TG-MS and Py-GC/MS. J Anal Appl Pyrolysis 97:11–18. https://doi.org/10.1016/j.jaap.2012.04.010

Mäki-Arvela P, Anugwom I, Virtanen P, Sjöholm R, Mikkola J (2010) Dissolution of lignocellulosic materials and its constituents using ionic liquids—A review. Ind Crops Prod 32(3):175–201. https://doi.org/10.1016/j.indcrop.2010.04.005

Miao J, Yu Y, Jiang Z, Tang L, Zhang L (2017) Partial delignification of wood and membrane preparation using a quaternary ammonium ionic liquid. Sci Rep. https://doi.org/10.1038/srep42472

Mohan M, Deshavath N, Banerjee T, Goud V, Dasu V (2018) Ionic liquid and sulfuric acid-based pretreatment of bamboo: biomass delignification and enzymatic hydrolysis for the production of reducing sugars. Ind Eng Chem Res 57(31):10105–10117. https://doi.org/10.1021/acs.iecr.8b00914

Mohd N, Draman S, SallehYusof MN (2017) Dissolution of cellulose in ionic liquid: a review. AIP Conf Proc 1809:020035. https://doi.org/10.1063/1.4975450

National Renewable Energy Laboratory, NREL (2012) Determination of structural carbohydrates and lignin in biomass. TP-510–42618.

Neto W (2017) Morphological investigation of cellulose nanocrystals and nanocomposite applications. Ph.D. Université Grenoble Alpes; Universidade Federal de Uberlândia, 2.

Nevstrueva D, Pihlajamäki A, Nikkola J, Mänttäri M (2018) Effect of precipitation temperature on the properties of cellulose ultrafiltration membranes prepared via immersion precipitation with ionic liquid as solvent. Membranes 8(4):87. https://doi.org/10.3390/membranes8040087

Pandey K, Pitman A (2003) FTIR studies of the changes in wood chemistry following decay by brown-rot and white-rot fungi. Int Biodeterior Biodegradation 52(3):151–160. https://doi.org/10.1016/S0964-8305(03)00052-0

Pang J, Liu X, Wu M, Wu Y, Zhang X, Sun R (2014) Fabrication and characterization of regenerated cellulose films using different ionic liquids. J Spectrosc (Hindawi) 2014:1–8. https://doi.org/10.1155/2014/214057

Parviainen H, Parviainen A, Virtanen T, Kilpeläinen I, Ahvenainen P, Serimaa R, Grönqvist S, Maloney T, Maunu S (2014) Dissolution enthalpies of cellulose in ionic liquids. Carbohydr Polym 113:67–76. https://doi.org/10.1016/j.carbpol.2014.07.001

Pinkert A, Marsh K, Pang S, Staiger M (2009) Ionic liquids and their interaction with cellulose. Chem Rev 109(12):6712–6728. https://doi.org/10.1021/cr9001947

Raut D, Sundman O, Su W, Virtanen P, Sugano Y, Kordas K, Mikkola J (2015) A morpholinium ionic liquid for cellulose dissolution. Carbohydr Polym 130:18–25. https://doi.org/10.1016/j.carbpol.2015.04.032

Routa J, Brännström H, Anttila P, Mäkinen M, Jänis J and Asikainen A (2017) Wood extractives of Finnish pine, spruce and birch – availability and optimal sources of compounds : A literature review. Natural resources and bioeconomy studies 73/2017. Natural Resources Institute Finland, Helsinki. 55 p.

Rowell R (2013) Handbook of wood chemistry and wood composites. Taylor & Francis, Boca Raton

Saha K, Dasgupta J, Chakraborty S, Antunes FAF, Sikder J, Curcio S, Santos JC, Arafat HA, Silva SS (2017) Optimization of lignin recovery from sugarcane bagasse using ionic liquid aided pretreatment. Cellulose 24:3191–3207. https://doi.org/10.1007/s10570-017-1330-x

Saha K, Verma P, Sikder J, Chakraborty S, Curcio S (2019) Synthesis of chitosan-cellulase nanohybrid and immobilization on alginate beads for hydrolysis of ionic liquid pretreated sugarcane bagasse. Renew Energ 133:66–76. https://doi.org/10.1016/j.renene.2018.10.014

Sanchez-Silva L, López-González D, Villaseñor J, Sánchez P, Valverde J (2012) Thermogravimetric–mass spectrometric analysis of lignocellulosic and marine biomass pyrolysis. Bioresour Technol 109:163–172. https://doi.org/10.1016/j.biortech.2012.01.001

Segal L, Creely J, Martin A, Conrad C (1959) An empirical method for estimating the degree of crystallinity of native cellulose using the X-Ray diffractometer. Text Res J 29(10):786–794. https://doi.org/10.1177/004051755902901003

Ślusarczyk C, Fryczkowska B (2019) Structure-property relationships of pure cellulose and GO/CEL membranes regenerated from ionic liquid solutions. Polymers 11(7):1178. https://doi.org/10.3390/polym11071178

Sundberg A, Sundberg K, Lillandt C, Holmbom B (1996) Determination of hemicelluloses and pectins in wood and pulp fibers by acid methanolysis and gas chromatography.

Nord Pulp Pap Res J 4:216–226. https://doi.org/10.3183/NPPRJ-1996-11-04-p216-219

Taheri N, Abdolmaleki A, Fashandi H (2019) Impact of non-solvent on regeneration of cellulose dissolved in 1-(carboxymethyl)pyridinium chloride ionic liquid. Polym Int 68(12):1945–1951. https://doi.org/10.1002/pi.5903

Thygesen A, Oddershede J, Lilholt H, Thomsen AB, Ståhl K (2005) On the determination of crystallinity and cellulose content in plant fibres. Cellulose 12:563. https://doi.org/10.1007/s10570-005-9001-8

Today C (2019) What is a response factor? Chromatography today. https://www.chromatographytoday.com/news/gc-mdgc/32/breaking-news/what-is-a-response-factor/31169. Accessed 10 Jun. 2019

Tran D, Ulbricht M (2019) Herstellung von Ultrafiltrations-Membranen aus Lösungen von Cellulose in ionischen Flüssigkeiten. Chem Ing Tech 91(8):1123–1128. https://doi.org/10.1002/cite.201900044

Triantafyllidis KS, Lappas AA, Stöcker M (2013) Role of catalysis for the sustainable production of bio-fuels and bio-chemicals - 7.8 ionic liquids. Elsevier, Amsterdam

Varhegyi G, Antal M, Szekely T, Till F, Jakab E (1988) Simultaneous thermogravimetric-mass spectrometric studies of the thermal decomposition of biopolymers. 1. Avicel cellulose in the presence and absence of catalysts. Energy Fuels 2(3):267–272. https://doi.org/10.1021/ef00009a007

Vilakati GD, Hoek E, Mamba BB (2015) Investigating the usability of alkali lignin as an additive in polysulfone ultrafiltration membranes. BioResources 10:3079–3096. https://doi.org/10.15376/biores.10.2.3056-3069

Wada M, Kondo T, Okano T (2003) Thermally induced crystal transformation from cellulose Iα to Iβ. Polym J 35(2):155–159. https://doi.org/10.1295/polymj.35.155

Weng R, Chen L, Xiao H, Huang F, Lin S, Cao S, Huang L (2017) Preparation and characterization of cellulose nanofiltration membrane through hydrolysis followed by carboxymethylation. Fibers Polym 18(7):1235–1242. https://doi.org/10.1007/s12221-017-7200-1

Woodings C (2001) Regenerated cellulose fibres - 5.4 Products and Application. Woodhead Publishing, Amsterdam

Zdanowicz M, Wilpiszewska K, Spychaj T (2018) Deep eutectic solvents for polysaccharides processing A review. Carbohydr Polym 200:361–380. https://doi.org/10.1016/j.carbpol.2018.07.078

Zhang J, Wu J, Yu J, Zhang X, He J, Zhang J (2017) Application of ionic liquids for dissolving cellulose and fabricating cellulose-based materials: state of the art and future trends. Mater Chem Front 1(7):1273–1290. https://doi.org/10.1039/C6QM00348F

Zhu S, Wu Y, Chen Q, Yu Z, Wang C, Jin S, Ding Y, Wu G (2006) Dissolution of cellulose with ionic liquids and its application: a mini-review. Green Chem 8(4):325. https://doi.org/10.1039/b601395c

Zhu X, Wang Y, Wei X, Li J, Wang F (2014) Preparation of pineapple leaf cellulose membrane. Adv Mat Res 1046:13–17. https://doi.org/10.4028/www.scientific.net/AMR.1046.13

Publisher's Note Springer Nature remains neutral with regard to jurisdictional claims in published maps and institutional affiliations.

Preparation of cellulose-rich membranes from wood: Effect of wood pretreatment process on membrane performance

Anastasiia Lopatina[1], Ikenna Anugwom[2], Mohammadamin Esmaeili[1], Liisa Puro[1], Tiina Virtanen[1], Mika Mänttäri[1], Mari Kallioinen[1]

[1] *Department of Separation Science, LUT School of Engineering Science, LUT University, P.O. Box 20, FI-53851 Lappeenranta, Finland;*

[2] *LUT Re-Source Research Platform, LUT University, P.O. Box 20, FI-53851 Lappeenranta, Finland.*

Corresponding author: Anastasiia Lopatina (Anastasiia.Lopatina@lut.fi)
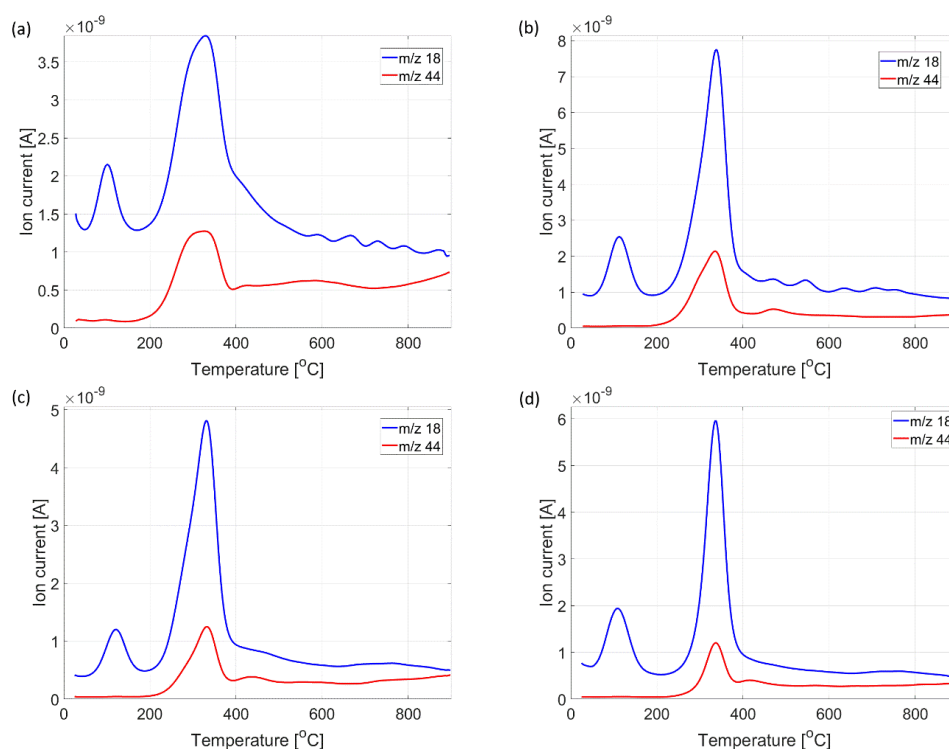
Fig S1 Evolution of H_2O (m/z 18) and CO_2 (m/z 44) for membrane samples prepared from untreated birch (a), DES treated birch (b), DES treated and bleached birch (c), and alkaline-treated bleached DES-treated birch (d)
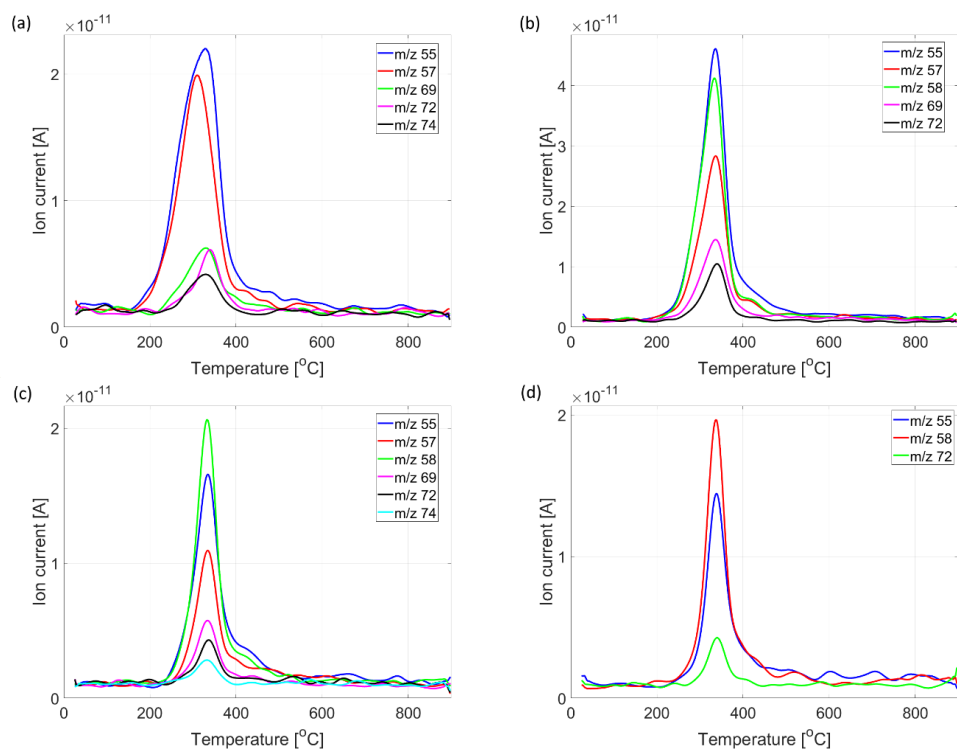
Fig S2 Selected MS ion intensity curves of membrane samples prepared from untreated birch (a), DES treated birch (b), DES treated and bleached birch (c), and alkaline-treated bleached DES-treated birch (d)
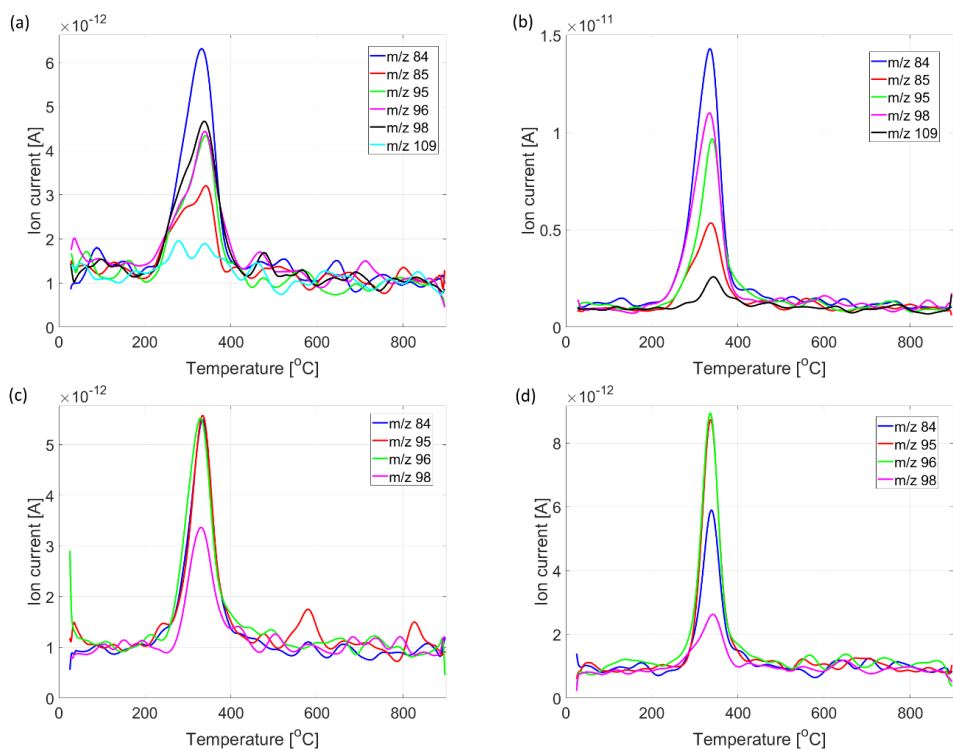
Fig S3 Selected MS ion intensity curves of membrane samples prepared from untreated birch (a), DES treated birch (b), DES treated and bleached birch (c), and alkaline-treated bleached DES-treated birch (d)

Publication II

Lopatina, A., Anugwom, I., Blot, H., Sánchez Conde, Á., Mänttäri, M., and Kallioinen, M.

Re-use of waste cotton textile as an ultrafiltration membrane

and

Lopatina, A., Anugwom, I., Blot, H., Sánchez Conde, Á., Mänttäri, M., and Kallioinen-Mänttäri, M.

Corrigendum to "Re-use of waste cotton textile as an ultrafiltration membrane" [J. Environ. Chem. Eng. 9 (2021) 105705]

Re-use of waste cotton textile as an ultrafiltration membrane

Anastasiia Lopatina [a,*], Ikenna Anugwom [b], Hervé Blot [c], Ángela Sánchez Conde [d],
Mika Mänttäri [a], Mari Kallioinen [a]

[a] *Department of Separation Science, LUT School of Engineering Science, LUT University, P.O. Box 20, FI-53851 Lappeenranta, Finland*
[b] *LUT Re-Source Research Platform, LUT University, P.O. Box 20, FI-53851 Lappeenranta, Finland*
[c] *Génie chimique, Génie des Procédés, Paul Sabatier University, Toulouse 3, IUT A, 115C route de Narbonne, 31077 Toulouse Cedex-4, France*
[d] *Department of Chemical and Nuclear Engineering. Higher Technical School of Industrial Engineering, Universidad Politècnica of Valencia, 46022 Valencia, Spain*

ARTICLE INFO	ABSTRACT
Editor: V. Victor *Keywords:* Membranes Cellulose Cotton recycling Textile EmimOAc	Textile industry produces millions of tons of waste annually, which is predominantly incinerated or landfilled. Cotton textile comprises a quarter of total textile production, and although being renewable, its production is highly chemical- and water-intensive, rising the need for effective waste cotton textile recycling. This study presents an investigation whether it is possible to utilize waste cotton textile as a cellulose source for the fabrication of cellulose membranes. The effect of casting thickness and cellulose concentration on the prepared membranes' performance was studied. Membranes cast from 2 wt% casting solutions exhibited the highest permeabilities of 1.11 and 3.09 $m^3/(m^2 \cdot s \cdot Pa)$ for 300 and 150 μm casting thickness, respectively, but poor adhesion stability and low retention. Membranes cast from solutions of higher concentrations (5, 6, and 7 wt%) resulted in membranes with more stable performance. The permeability values for 300 μm membranes were in the range of 0.27 – 0.39 $m^3/(m^2 \cdot s \cdot Pa)$ and for 150 μm 0.51 – 0.67 $m^3/(m^2 \cdot s \cdot Pa)$. The retention values of these six membranes were relatively close to each other, showing 80 – 92% retention of polyethylene glycol (PEG) 35 kDa. Three most promising membranes (5, 6, and 7 wt% cast at 150μm) were additionally characterized, showing negative zeta potential within −23 – −35 mV range at pH 7 and contact angles of very hydrophilic material (14 – 16°). Overall, the results showed that very hydrophilic ultrafiltration membranes having attractive permeability and retention properties can be made from textile waste. 1 m^2 of cotton bed linen is enough to produce approximately 20 m^2 of cellulose membrane.

1. Introduction

The continuous and steady growth of the textile market can be attributed to several reasons. The main reason behind is the growth of population itself [1]. Another reason is shortening of the fashion cycle. The textiles are also becoming cheaper than before compared to the other consumer goods. According to [2], the clothing purchase in EU-28 has increased by 40% in less than twenty years. Even in Finland, where the clothing consumption is smaller compared to other European countries, the number of owned goods has doubled since the 1990 s [2]. Among with the growth of the textile industry, the challenges attributed to handling the environmental, energy, and resource related issues arise.

Textile market is currently dominated (63%) by synthetic fibers, which are mainly produced from petrochemicals, generating significant carbon dioxide (CO_2) emissions. The next widespread is cotton, of which production is associated with water depletion and toxic pollution, due to extensive use of pesticides [2–4]. According to the estimations, the global consumption of cellulosic fibers is going to reach 5.4 kg per capita level by 2030, whereas the forecasted availability is going to comprise only 3.1 kg of cotton per capita [1].

Textile industry is known to be chemical-, water-, and energy-intensive. The global impact of the textile industry was reported by the Ellen MacArthur Foundation in 2017 [5]. According to the forecasts, textile industry will continue to grow, raising the urgent need for

efficient recycling as one of the key directions towards sustainable development [1,6]. Currently, 95% of the wasted post-consumer textile is not recycled but either incinerated or landfilled, which causes additional environmental problems. The recycled part is mainly going through down-cycling routines, resulting in product with lower quality, which limits its further utilization [3,4,7].

Due to its' properties, cotton textile is the most prospective material for efficient recycling, as it consists solely of cellulose which can be utilized variously, from reinforced composites to completely different products [8]. Because of cellulose's attractive properties, recycling of waste cotton, which can no longer serve any purpose, into various value-added products with adjustable features and sustainable utilization potential can be considered upcycling [9,10]. One of the possible yet not researched options is production of cellulose membranes which is possible once appropriate solvent medium is found. Dissolution of cellulose in ionic liquids (IL) and IL-cosolvent systems is widely discussed nowadays [11–13]. A favorable choice is the use of 1-ethyl-3-methylimidazole acetate ([Emim][OAc]), the low-corrosive and -toxic IL, mixed with dimethylsulfoxide (DMSO), giving the middle-viscous and -cheap system for preparation of membrane casting solutions [12,14,15]. As resulted membranes consist of cellulose, they can be useful in many applications due to cellulose's hydrophilicity, biocompatibility and relatively good stability. The hydrophilicity makes the cellulose membrane to be a feasible option for instance for treatment of different water streams in the pulp and paper industry and biorefinery streams [16–19].

Literature research showed that so far there is only one study existing, which reports the preparation of membranes from waste textile resources. In that study the IL-extracted keratin from wool was used in the fabrication of blended nanofiltration membranes [20]. However, to the best of our knowledge there seems to be no papers reporting a preparation of membranes directly from the cotton textile. Thus, in this study the aim was to investigate the possibility to make a filtration membrane from wasted cotton textile. The flat sheet membranes were prepared via wet phase inversion method from 100% cotton bed linen dissolved in the mixture of [Emim][OAc]-DMSO using the procedure developed and presented in our previously reported study [15]. The usability of the produced membranes was tested by measuring the water permeability and retention of polyethylene glycols (PEGs). In addition, hydrophilicity, zeta potential, membrane porosity, and chemical structure of the fabricated membranes were characterized.

2. Materials and methods

2.1. Materials

The non-dyed bed sheet labeled as 100% cotton was purchased from a local supermarket and used for preparation of casting solution and membrane fabrication. It was preliminary cut in approximately to 1.5×1.5 cm pieces and used directly without any pretreatment. Membrane casting solutions were prepared using the mixture of ionic liquid – 1-ethyl-3-methylimidazolium acetate, 95% ([Emim][OAc], CAS # 143314–17–4, Iolitec Ionic Liquids Technologies GmbH) and DMSO (CAS # 67–68–5, Merck KGaA, Darmstadt, Germany). Flat-sheet membranes were cast on nonwoven polypropylene/polyethylene carrier material Viledon® Novatexx 2484 (60 L/(s·m^2) air permeability, 85 g/m^2 weight per unit area, 300/200 N/5 cm maximum tensile force along/across, 25/30% elongation at maximum tensile force along/across, and 0.12 mm thickness, Freudenberg, Germany).

Ultra-pure deionized (DI, 15 MΩ, 0.5 – 1 μS/cm) water was produced by CENTRA-R 60\120 system (Elga purification system, Veolia Water, UK). DI water was used in washing of the membranes, in measuring the membrane permeability, and as a non-solvent in membrane manufacturing as well as in preparation of all solutions.

In the measurement of the retention of the manufactured membranes, polyethylene glycol (PEG) of two different molecular weights were used as a model compound. The PEGs (PEG 20, approximate M_w

20,000 g/mol and PEG 35, approximate M_w 35,000 g/mol) were purchased from Merck KGaA (Darmstadt, Germany; CAS # 25322–68–3).

2.2. Methods

2.2.1. Membrane preparation

Homogeneous solutions of cellulose in [Emim][OAc]-DMSO were prepared with different concentrations of 2, 5, 6, and 7 wt% by stirring cotton textile shreds overnight at constant heating in oil bath at 70 °C. As a result of dissolution, visually transparent homogeneous solutions were formed as shown in Fig. S1.

The prepared solutions were cast at room temperature on the carrier material placed on a glass plate, by spreading an appropriate amount with Automatic Film Applicator L (BYK-Gardner USA) with casting knife (with casting thickness 150 or 300 μm) at 50 mm/s speed. Eight different types of membranes were cast, as two parameters, casting solution concentration and casting thickness, varied. For future convenience, Table 1 summarizes the casting parameters variations and gives codes for the membrane types produced.

Without a preceding dry phase inversion in the air, the films were immediately immersed in the coagulation bath of DI water at 0 °C temperature. In order to guarantee a complete phase separation, the membranes were kept in the coagulation bath overnight. After that, they were washed with water and used for analyses without drying if not stated otherwise.

2.2.2. Membrane permeability and retention measurements

Permeability and retention of the prepared membranes were measured with the Amicon dead-end stirring cell equipment (Millipore, USA, Cat No.: XFUF07611, diameter of the stirring device 60 mm). The circular membrane sample with effective filtration area of 0.0040 m^2 was cut and placed in the Amicon filtration cell (Fig. 1.).

Prior to the filtration experiments, each membrane was compacted for 60 s at 100 kPa, 120 s at 200 kPa, 180 s at 300 kPa, 240 s at 400 kPa, and 1200 s at 500 kPa. This also ensured that the solvents used in the membrane manufacturing were completely rinsed from the membrane pores. Solvents' removal was checked through the measurement of total organic carbon (TOC) content in a permeate sample collected during the

Table 1
Casting parameters combinations and assigned membrane codes.

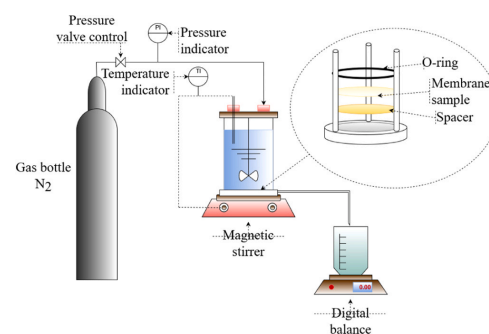| Casting thickness, μm	Cellulose concentration in casting solution, wt.-%			
	2	5	6	7
150	2/150	5/150	6/150	7/150
300	2/300	5/300	6/300	7/300

Fig. 1. Schematic configuration of Amicon dead-end filtration system.

membrane compaction at maximum pressure of 500 kPa.

Pure water permeability of the membranes was measured at $25 \pm 0.5\,°C$ and determined as a slope of plotted four flux values, measured at 100, 200, 300, and 400 kPa pressure and calculated using the Eq. (1):

$$J = \frac{Q_P/1000}{A \cdot \tau}$$

where J – tested membrane's flux ($m^3/m^2\cdot s$), Q_P – the gravimetric flow of water permeate through the membrane (g/s), A – the area of membrane sample (m^2), τ – the time of collection of the permeate (s).

To demonstrate the differences between the different membrane samples also membrane hydraulic resistance values (R_m) were calculated at different transmembrane pressures from the slope of pure water flux versus transmembrane pressure difference Eq. (2):

$$R_m = \frac{\Delta P_T}{J \cdot \mu}$$

where R_m – the hydraulic resistance of the membrane sample (1/m), ΔP_T – the transmembrane pressure (Pa), J – the pure water flux ($m^3/m^2\cdot s$), and μ is the dynamic viscosity of water at $25\,°C$ ($8.90 \cdot 10^{-4}$ Pa·s) [21].

For the retention study two model solutions of PEG 20 and PEG 35 were prepared with concentration of 300 ppm and filtered through the membrane at a pressure that was set for each membrane individually in order to have approximately same model solutions' flux around 0.83 $m^3/$ (m^2·s)). Throughout all the measurements, the stirring speed was maintained at 300 rpm using the magnetic stirrer with a rpm indicator and the temperature was kept at $25 \pm 0.5\,°C$. The samples of feed, retentate, and permeate were collected and analyzed for TOC content with a Shimadzu TOC analyzer (TOC-L series, Japan). Membrane retentions were calculated out of measured TOC content in the samples with the Eq. (3):

$$R = (1 - \frac{2 \cdot C_p}{C_f + C_r}) \cdot 100$$

where C_p, C_f and C_r are the total organic carbon concentrations in the permeate, feed and retentate (mg/L) respectively.

2.2.3. Examination of hydrophilicity of the membranes

For the assessment of membranes hydrophilicity static contact angle (CA) of selected membranes was measured based on the captive bubble method. Nearly 3–4 μL of air bubble volume was placed by the means of U-shaped needle on the surface of the tested membrane attached to a piece of glass with double sided tape and submerged into DI water at the room temperature. For each membrane sample six independent measurements of CA were made at different points with the average value of recorded data taken as final CA. The CA was measured with KSV CAM 101 equipment (KSV Instruments Ltd., Finland) connected to a CCD camera (DMK 21F04, The Imaging Source Europe GmbH, Bremen, Germany). To determine the CA, the obtained images were treated by curve fitting analysis with CAM 2008 software.

2.2.4. Examination of the zeta potential of the membranes

The streaming potential which characterizes the charge of the membrane surface was measured with the SurPASS Electrokinetic Analyzer (Anton Paar GmbH, Graz, Austria) with an adjustable gap cell method and using 0.001 M KCl solution as a background electrolyte. The membranes were preliminary stored at approximately $5\,°C$ for 24 h in a fridge. Before the start of the experiment the solution pH was shifted to 7.5 by addition of 0.1 M KOH solution and then automatically titrated to 2.7 with use of 0.05 M HCl solution as the analysis was carried on. The final value of the zeta potential was calculated automatically by Sur-PASS software based on the Helmholtz-Smoluchowski equation.

2.2.5. Examination of chemical structure of the membranes

To identify the functional groups presented and assess changes in crystallinity, which occurred through solution preparation and

membrane formation, the FTIR analysis was performed with the Frontier MIR/FIR Spectrometer (PerkinElmer Inc.) with the universal diamond crystal ATR module in the range $400 – 4000$ cm^{-1} of wave number with the spectra resolution of 4 cm^{-1}. Air-dried samples of selected membranes were recorded in pentaplicate and averaged. For the graphical representation all the spectra were processed with ATR correction, baseline correction and normalization. The ratio of the not-normalized absorption bands A_{1428}/A_{897} was used to calculate Lateral Order Index (LOI), as was proposed by Nelson and O'Connor [22,23].

2.2.6. Estimation of membrane porosity

Membrane porosity (ε) was determined via gravimetric method with following Eq. (4):

$$\varepsilon = \frac{\frac{(w_w - w_d)}{\rho_H}}{\frac{(w_w - w_d)}{\rho_H} + \frac{w_d}{\rho_c}} \cdot 100$$

where ε - the membrane porosity (%), w_w and w_d – the weight of wet and dry membrane, respectively (g), ρ_H – the density of water at $25\,°C$ (0.997 g/cm^3), ρ_c – the density of cellulose (1.5 g/cm^3) [24].

3. Results and discussion

3.1. Membranes performance

The casting result differed depending on the chosen parameters. Casting solutions with cellulose concentrations of 5, 6, and 7 wt% resulted in formation of uniform film, showing even adhesion to carrier material, whereas 2 wt% membranes showed poor adhesion probably related to the use of too low concentration of casting solutions. However, it was still possible to perform filtration experiments with the membranes cast from 2 wt% solutions. For filtration experiments three samples of each membrane were used, and the results presented in Fig. 2 are the averaged values of pure water permeabilities from individual experiments.

It can be seen that all the membranes cast at 150 and 300 μm show the same trend of permeabilities. With increase of concentration of cellulose in the membrane matrix, the permeability decreases, and the highest values are obtained with the 2/300 and 2/150 membranes. The hydraulic resistances of the membranes cast with a lower cellulose concentration were also clearly lower compared to the membrane cast from the solutions containing higher amounts of cellulose (Fig. 3.). As the cellulose concentration increases in the solvent, the polymer concentration at the nonsolvent interface is higher during precipitation. Consequently, a membrane with lower porosity is obtained [25]. From the values in Table 3 it can be seen that experimental results are in good
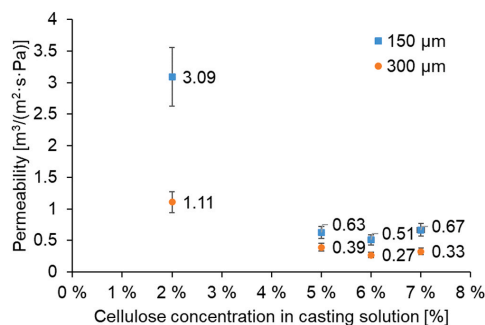

Fig. 2. Pure water permeabilities of the tested membranes all measured in the Amicon ultrafiltration cell at $25\,°C$ and mixing rate approximately 300 rpm.
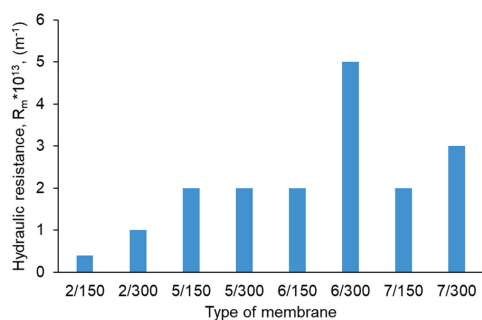
Fig. 3. Membrane hydraulic resistance calculated for each type of membrane tested in the Amicon ultrafiltration cell at 25 °C and mixing rate approximately 300 rpm.

agreement with theoretical assumptions. However, when these values are considered, it has to be taken into account that the method used here to estimate the membrane porosity does not show the porosity given by the pores, which really lead through the membrane. The results also reveal that the membranes cast at 150 μm show noticeably higher permeabilities than the membranes of the same concentrations but cast at 300 μm. This difference can be seen also from the hydraulic resistances of the membranes. The reasons for this might be in the physical structure of the membranes originating both from the different thicknesses of the layers and the possible differences in the macrovoids structures [26].

The retention values measured with PEG 20 and PEG 50 model solutions for all the manufactured membranes are presented in Fig. 4, a and b respectively. The lowest retentions were obtained with the 2/150 and 2/300 membranes. Membranes with the 5, 6, and 7 wt% cellulose concentration showed small difference between values measured for 150- and 300-μm casting thicknesses.

In order to evaluate whether the membranes prepared in this study are competitive compared to the commercial membranes and also

regenerated cellulose membranes prepared by other research groups, their performance was compared to results published by other research groups and to the RC70pp (Alfa Laval) membrane (Fig. 5.). The membranes prepared by other researchers were picked for comparison based on the existence of common parameters with current study, i.e. the same cellulose concentration in casting solution or similar composition of solvent mixture. It is vital to mention that presented comparison serves only as nominal, since the presented combination of cellulose source, solvent system, casting parameters, and performance measurement parameters differs from one study to another, almost never coincides, and can be found in details in the original articles [12,27]. Information about performance of RC70pp membrane was taken from the works that reported it earlier [28,29].

It can be seen from Fig. 5 that the membranes prepared within this study from the waste cotton show performance that is close to both lab-made membranes. Membrane performance depends mostly on the membrane morphology, which is in turn dependent on the polymer concentration, casting thickness, etc. [13]. The "Durmaz" membrane in Fig. 5 was formed from casting solution with 8 wt% cellulose in the mixture of [Emim][OAc]-DMSO and it had significantly lower pure water permeability and higher retention compared to the membranes prepared within current study [27]. The "Durmaz" membrane retention was evaluated with Blue Dextran (20 kDa). The "Livazovic" membrane was prepared from 5 wt% cellulose (Avicel pH101 microcrystalline cellulose) solution in pure [Emim][OAc] which had the same pure water permeability as the membranes prepared in this study (6/300 and 7/300 in Fig. 5) but the retention was lower based on the evaluation with PEG molecules [12]. The commercial RC70pp membrane demonstrates more or less the same permeation rate as the membranes prepared within this research, however, the 90% retention was achieved with significantly smaller molecules [28,29].

The comparison presented above proves the suitability of waste cotton textile as a material for membrane preparation as it shows competitive performance to referenced laboratory-made membranes prepared from commercially available cellulose feedstock, like cotton linter from fibers and microcrystalline cellulose [12,27]. Based on the square masses of the used substrate and the final membrane product (7/150), 7 g of cellulose is needed to produce 1 m² of membrane. Thus,

Table 3
Membranes and cotton textile characterization.

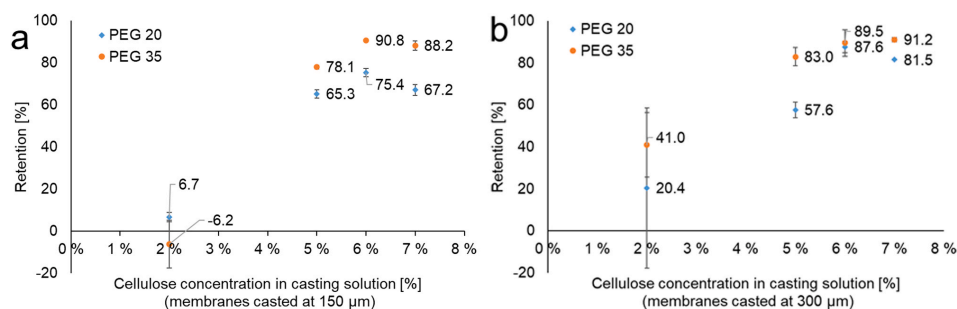| Sample	PWP, m³/ (m²·s·Pa)	$R_m·10^{13}$, 1/m	PEG 35 kDa retention, %	Porosity, %	Contact angle, °	Zeta potential at pH 7, mV	LOI A_{1428}/A_{897}
Textile	nd	nd	nd	nd	nd	nd	0.86
5/150	0.63	2	78.1	59.2	15.6 ± 2.8	-25	0.60
6/150	0.51	2	90.8	56.3	16.3 ± 5.7	-23	0.47
7/150	0.67	2	88.2	49.6	14.0 ± 5.6	-35	0.50

nd – no data

Fig. 4. Retention measurements of membranes cast at 150 μm (a) and 300 μm (b) all measured in the Amicon ultrafiltration cell at 25 °C and mixing rate approximately 300 rpm.
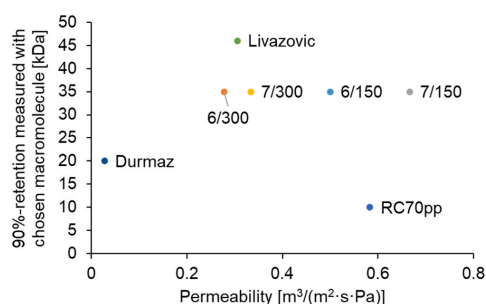
Fig. 5. Permeability and the retention values of the membranes prepared within current research and membranes which were chosen for comparison; membranes chosen for comparison are named after first authors Durmaz [27] and Livazovic [12], information about RC70pp was taken from [28,29]; membranes prepared in this research are signed as cellulose wt% concentration in casting solution/casting thickness in μm.

it can be evaluated that 1 m^2 of bed linen is enough for production of approximately 20 m^2 of membrane.

3.2. Membrane characterization results

Aiming to assess the changes occurred in the chemical composition and crystallinity of cellulose, as cotton textile was dissolved and the membrane was prepared, FTIR spectra of non-woven carrier material, untreated cotton textile, and two selected membranes prepared in this study are presented in Fig. 6. The spectra were recorded from all the membrane samples, and all of them can be divided into two groups: showing similar peaks as either 5/150 membrane or 2/150 membrane (Fig. 6.). The difference seen between the spectra of the membranes made from 2 wt% and 5 wt% cellulose solutions was that in the spectrum of the 2/150 membrane small peaks at 1710, 1570, 870, and 720 cm^{-1} were present. These peaks do not belong to cellulose and are distinctively present in the spectrum of the carrier material. Same peaks were found in all the 300 μm membranes, which shrank during the drying and from which the cellulose skin layer was partly separated from the carrier material. In the spectra of 5/150, 6/150, and 7/150 membranes (represented as 5/150 membrane spectrum in Fig. 6) the peak at 1734 cm^{-1} can be seen. This might be interpreted as a sign of

Table 2
General interpretation of FTIR spectra, [35–37].

Wavenumber (cm^{-1})	Assignments
3600–3000	OH stretching broad peak
2896	CH symmetric stretching
1734	CO stretching
1645	OH bending/adsorbed H$_2$O
1428, 1367	CH bendings
1314	CH$_2$ wagging
1278[a]	CH deformation
1158, 1107[a], 1054, 1029[a],	asymmetric CO stretchings in C-O-C and C-O-H
983	fragments
660–500	OH out-of-plane bending

[a] peaks are distinctive only in untreated cotton textile.

derivatization side-reaction happening during cellulose dissolution, which is already discussed in a number of works [30–32]. Increased intensity of peak at 897 cm^{-1}, which is assigned to the amorphous region in cellulose, is in the agreement with the earlier reported changes in cellulose structure due to dissolution and regeneration processes [33, 34]. Assignments of the cellulose-belonging peaks from the untreated textile and membranes with spectrum as of the 5/150 membrane are described in Table 2.

Considering the membrane performance described earlier, it seems reasonable to pay more attention to membranes cast at 150 μm, as they are offering higher permeability and almost the same retention, than the membranes of the same concentration but cast at 300 μm. Membranes cast from the 2 wt% casting solutions showed high permeability but poor retention, so it was decided to characterize the hydrophilicity and surface zeta potential of the membranes formed from solutions with higher concentrations. Thus, the characterization was done for the membranes cast from the solutions with 5, 6, and 7 wt% concentrations of cellulose at 150 μm. Contact angle and surface zeta potential measurements were performed on undried membranes, whereas for FTIR measurements the membranes were air-dried overnight. LOI was calculated from ATR- and baseline-corrected spectra without normalization.

As has been mentioned earlier, the commercial regenerated cellulose membrane RC70pp (Alfa Laval) was chosen for comparison with the membranes prepared in this study, and its' characteristics were found in other reported works [28,29]. The following values are combined for the RC70pp membrane from these two works: membrane showed −30 mV zeta potential at pH 7, 0.58 m^3/(m^2·s·Pa) permeability at 1 bar, molecular weight cut-off (MWCO) of 10 kDa, as announced by Alfa Laval,
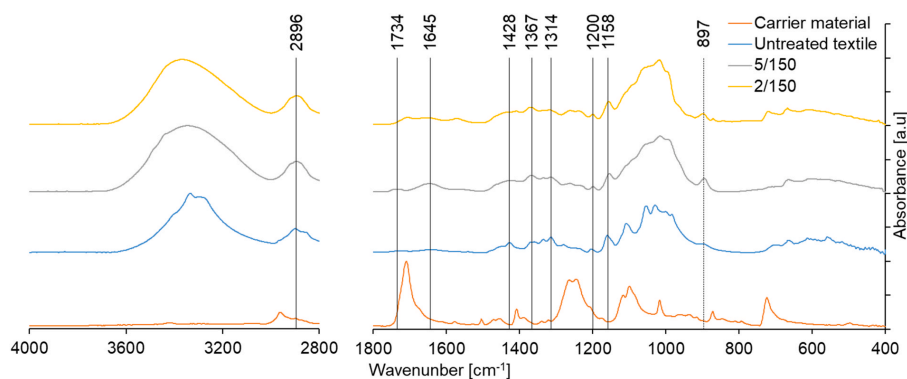

Fig. 6. FTIR spectra of nonwoven support material, untreated cotton textile, and representative membranes recorded via using the Perkin Elmer Frontier spectrometer with universal ATR module of diamond crystal at a resolution of 4 cm^{-1} in the absorbance mode.

membrane hydraulic resistance $0.25 \cdot 10^{13}$ m^{-1}, and contact angle 11°. From the values presented in Table 3, it can be seen, that membranes, prepared within the scope of this study, show lower retention and higher hydraulic resistance than the commercial membrane.

As it was briefly discussed in 3.1 subsection, the increase in cellulose concentration in theory should lead to the formation of membrane with lower porosity. From the values in Table 3 it can be seen that experimental results are in good agreement with theoretical assumptions.

Membrane hydrophilicity affects permeability, retention, and fouling behavior of membranes [38]. The contact angles of membranes cast from 5, 6, and 7 wt% casting solutions are presented in Table 3 and are quite close to each other, demonstrating that all the membranes can be classified as very hydrophilic. Therefore, the hydrophilicity of membranes might not account for any differences in water permeability or retention observed here, and differences exist more likely due to structural changes.

From Table 3 it can be seen that all the tested membranes are negatively charged at pH 7. Based on the FTIR spectra, the reason for this is at least partly the acetylation of hydroxyl groups during the membrane manufacturing process. The C˜O stretch can be seen at 1734 cm^{-1} (Fig. 6). As TOC results showed no traces of solvents in permeate collected during the membrane compaction step, we might assume that C˜O stretch comes from acetylated fragments of cellulose, as was reported previously, and not from the traces of solvents used in the process [31,32].

Permeability of ultrafiltration membranes is dependent on their microcrystalline structure, and highly crystalline membranes usually show lower permeabilities than more amorphous ones [39]. Thus, it is important to understand membrane's crystallinity, and the easiest way of assessment is to calculate the crystallinity index. First suggested by Nelson and O'Connor [22,23], the LOI is still widely used for the assessment of crystalline fraction of cellulose. The LOI is revealed from the ratio at 1428 cm^{-1} in-plane symmetric bending, characteristic for cellulose I$_\beta$ crystal, and C-H deformation in β-glycosidic linkages at 897 cm^{-1}, specific for amorphous cellulose regions (A_{1428}/A_{897}) [33,40]. From the values presented in Table 3, it can be seen that LOI values for prepared membranes are relatively close to each other. There is no correlation found between LOI and permeability values, however, it seems that LOI values are inversely proportional to retention values showed by these membranes with PEG 35 kDa measurements (i.e., the lower the LOI value, the higher the retention was). As LOI is correlated to the overall degree of order in cellulose, it can be concluded that there is less crystalline fraction in the membrane matrix than in original cotton textile. This is in the agreement with previous studies of cellulose crystallinity changes after dissolution in ILs and subsequent regeneration [34,41].

4. Conclusions

This study aimed to test the usability of waste cotton textile for the fabrication of cellulose membranes. Waste cotton textile was dissolved in the mixture of [Emim][OAc] – DMSO. Two parameters, casting thickness and cellulose concentration in casting solution, were varied during the membrane fabrication process. Characterization of the prepared membranes was done by measuring water permeability, PEG retentions, and carrying out ATR-FTIR, hydrophilicity, and zeta-potential measurements. Additionally, membrane hydraulic resistance and porosity were calculated. The results showed that it is possible to prepare an ultrafiltration membrane from waste cotton textile without any pretreatment. However, use of too low concentration of cellulose seems unreasonable, as membranes prepared from the solution with 2 wt% cellulose concentration showed poor adhesion stability and uneven performance. More stable membranes were achieved from the solutions with 5, 6, and 7 wt% cellulose concentration. Membranes cast at 150 μm thickness showed higher permeabilities and approximately same retentions as membranes cast at 300 μm. Membranes with 5%, 6%, and

7% concentration of cellulose cast at 150 μm showed water permeabilities in the range of $0.51 - 0.67$ m^3/(m^2·s·Pa) and their retention of PEG 35 kDa is close to 90%. All the prepared membranes prepared were very hydrophilic and had negative surface charge based on the streaming potential measurements. Based on our results and preliminary calculations, 1 m^2 of cotton bed linen should be enough for production of approximately 20 m^2 of cellulose membrane. This study demonstrates well that membrane manufacturing from waste textile is a potential process for upcycling of waste materials.

CRediT authorship contribution statement

Anastasiia Lopatina: Conceptualization, Methodology, Investigation, Writing - original draft, Writing - review & editing. **Ikenna Anugwom:** Conceptualization, Investigation, Writing - review & editing. **Hervé Blot:** Investigation, Methodology. **Ángela Sánchez Conde:** Investigation. **Mika Mänttäri:** Conceptualization, Methodology, Resources, Writing - review & editing, Supervision, Project administration. **Mari Kallioinen:** Conceptualization, Methodology, Resources, Writing - review & editing, Supervision, Project administration, Funding acquisition.

Declaration of Competing Interest

The authors declare that they have no known competing financial interests or personal relationships that could have appeared to influence the work reported in this paper.

Appendix A. Supporting information

Supplementary data associated with this article can be found in the online version at doi:10.1016/j.jece.2021.105705.

References

[1] M. Hummel, A. Michud, M. Tanttu, S. Asaadi, Y. Ma, L.K.J. Hauru, A. Parviainen, A.W.T. King, I. Kilpeläinen, H. Sixta, Ionic liquids for the production of man-made cellulosic fibers: opportunities and challenges. Cellulose Chemistry and Properties: Fibers, Nanocelluloses and Advanced Materials, Springer, 2016, pp. 133–168, https://doi.org/10.1007/12_2015_307.

[2] H. Dahlbo, K. Aalto, H. Eskelinen, H. Salmenperä, Increasing textile circulation—consequences and requirements, Sustain. Prod. Consum. 9 (2017) 44–57, https://doi.org/10.1016/j.spc.2016.06.005.

[3] G. Sandin, G.M. Peters, Environmental impact of textile reuse and recycling – a review, J. Clean. Prod. 184 (2018) 353–365, https://doi.org/10.1016/j.jclepro.2018.02.266.

[4] L. Navone, K. Moffitt, K.A. Hansen, J. Blinco, A. Payne, R. Speight, Closing the textile loop: enzymatic fibre separation and recycling of wool/polyester fabric blends, Waste Manag 102 (2020) 149–160, https://doi.org/10.1016/j.wasman.2019.10.026.

[5] Circular Fashion - A New Textiles Economy: Redesigning fashion's future, (n.d.). https://www.ellenmacarthurfoundation.org/publications/a-new-textiles-economy-redesigning-fashions-future (Accessed 14 July 2020).

[6] W. Leal Filho, D. Ellams, S. Han, D. Tyler, V.J. Boiten, A. Paco, H. Moora, A. L. Balogun, A review of the socio-economic advantages of textile recycling, J. Clean. Prod. 218 (2019) 10–20, https://doi.org/10.1016/j.jclepro.2019.01.210.

[7] W. Liu, S. Liu, T. Liu, T. Liu, J. Zhang, H. Liu, Eco-friendly post-consumer cotton waste recycling for regenerated cellulose fibers, Carbohydr. Polym. 206 (2019) 141–148, https://doi.org/10.1016/j.carbpol.2018.10.046.

[8] N. Pensupa, S.Y. Leu, Y. Hu, C. Du, H. Liu, H. Jing, H. Wang, C.S.K. Lin, Recent trends in sustainable textile waste recycling methods: current situation and future prospects, Top. Curr. Chem. 375 (2017) 76, https://doi.org/10.1007/s41061-017-0165-0.

[9] S. Vats, M. Rissanen, Parameters affecting the upcycling of waste cotton and PES/CO textiles, Recycling 1 (2016) 166–177, https://doi.org/10.3390/recycling1010166.

[10] Ś. Czesław, F. Beata, Structure – property relationships of pure cellulose and GO / CEL membranes regenerated from ionic, in: Polymers, 11, 2019, p. 1178.

[11] T.S. Anokhina, T.S. Pleshivtseva, V.Y. Ignatenko, S.V. Antonov, A.V. Volkov, Fabrication of composite nanofiltration membranes from cellulose solutions in an [Emim]OAc–DMSO mixture, Pet. Chem. 57 (2017) 477–482, https://doi.org/10.1134/S0965544117060020.

[12] S. Livazovic, Z. Li, A.R. Behzad, K.V. Peinemann, S.P. Nunes, Cellulose multilayer membranes manufacture with ionic liquid, J. Memb. Sci. 490 (2015) 282–293, https://doi.org/10.1016/j.memsci.2015.05.009.

[13] D. Nevstrueva, A. Pihlajamäki, J. Nikkola, M. Mänttäri, Effect of precipitation temperature on the properties of cellulose ultrafiltration membranes prepared via immersion precipitation with ionic liquid as solvent, Membranes (2018), https://doi.org/10.3390/membranes8040087.

[14] M. Isik, H. Sardon, D. Mecerreyes, Ionic liquids and cellulose: dissolution, chemical modification and preparation of new cellulosic materials, Int. J. Mol. Sci. 15 (2014) 11922–11940, https://doi.org/10.3390/ijms150711922.

[15] A. Lopatina, I. Anugwom, M. Esmaeili, L. Puro, T. Virtanen, M. Mänttäri, M. Kallioinen, Preparation of cellulose-rich membranes from wood: effect of wood pretreatment process on membrane performance, Cellulose 0 (2020), https://doi.org/10.1007/s10570-020-03430-0.

[16] M. Al Manasrah, M. Kallioinen, H. Ilvesniemi, M. Mänttäri, Recovery of galactoglucomannan from wood hydrolysate using regenerated cellulose ultrafiltration membranes, Bioresour. Technol. 114 (2012) 375–381, https://doi.org/10.1016/j.biortech.2012.02.014.

[17] M. Kallioinen, M. Mänttäri, M. Nyström, J. Nuortila-Jokinen, P. Nurminen, T. Sutela, Membrane evaluation for the treatment of acidic clear filtrate, Desalination 250 (2010) 1002–1004, https://doi.org/10.1016/j.desal.2009.09.090.

[18] M.M. Naim, A.A. El-Shafei, A.A. Moneer, M.M. Elewa, Ultrafiltration by a super-hydrophilic regenerated cellulose membrane, Water Pract. Technol. 10 (2015) 337–346, https://doi.org/10.2166/wpt.2015.040.

[19] L. Bai, N. Bossa, F. Qu, J. Winglee, G. Li, K. Sun, H. Liang, M.R. Wiesner, Comparison of hydrophilicity and mechanical properties of nanocomposite membranes with cellulose nanocrystals and carbon nanotubes, Environ. Sci. Technol. 51 (2017) 253–262, https://doi.org/10.1021/acs.est.6b04280.

[20] X. Zhong, R. Li, Z. Wang, W. Wang, D. Yu, Eco-fabrication of antibacterial nanofibrous membrane with high moisture permeability from wasted wool fabrics, Waste Manag. 102 (2020) 404–411, https://doi.org/10.1016/j.wasman.2019.11.005.

[21] H.T. Dang, R.M. Narbaitz, T. Matsuura, K.C. Khulbe, A comparison of commercial and experimental ultrafiltration membranes via surface property analysis and fouling tests, Water Qual. Res. J. Can. 41 (2006) 84–93, https://doi.org/10.2166/wqrj.2006.009.

[22] M.L. Nelson, R.T. O'Connor, Relation of certain infrared bands to cellulose crystallinity and crystal lattice type. Part II. A new infrared ratio for estimation of crystallinity in celluloses I and II, J. Appl. Polym. Sci. 8 (1964) 1325–1341, https://doi.org/10.1002/app.1964.070080323.

[23] M.L. Nelson, R.T. O'Connor, Relation of certain infrared bands to cellulose crystallinity and crystal latticed type. Part I. Spectra of lattice types I, II, III and of amorphous cellulose, J. Appl. Polym. Sci. 8 (1964) 1311–1324, https://doi.org/10.1002/app.1964.070080322.

[24] M.A. Mohamed, W.N.W. Salleh, J. Jaafar, A.F. Ismail, M. Abd. Mutalib, S.M. Jamil, Feasibility of recycled newspaper as cellulose source for regenerated cellulose membrane fabrication, J. Appl. Polym. Sci. 132 (2015) 1–10, https://doi.org/10.1002/app.42684.

[25] G.R. Guillen, Y. Pan, M. Li, E.M.V. Hoek, Preparation and characterization of membranes formed by nonsolvent induced phase separation: A review, Ind. Eng. Chem. Res. 50 (2011) 3798–3817, https://doi.org/10.1021/ie101928r.

[26] G. Arthanareeswaran, S.A. Kumar, Effect of additives concentration on performance of cellulose acetate and polyethersulfone blend membranes, J. Porous Mater. 17 (2010) 515–522, https://doi.org/10.1007/s10934-009-9319-y.

[27] E.N. Durmaz, P. Zeynep Çulfaz-Emecen, Cellulose-based membranes via phase inversion using [EMIM]OAc-DMSO mixtures as solvent, Chem. Eng. Sci. 178 (2018) 93–103, https://doi.org/10.1016/j.ces.2017.12.020.

[28] C.H. Obi, Use Of Nanofibrillated Cellulose In The Modification of Ultrafiltration Membranes, LUT University, 2019. https://lutpub.lut.fi/bitstream/handle/10024/160346/Mastersthesis_Obi_Chike.pdf?sequence=1.

[29] N.H. Abd-Razak, Y.M.J. Chew, M.R. Bird, Membrane fouling during the fractionation of phytosterols isolated from orange juice, Food Bioprod. Process. 113 (2019) 10–21, https://doi.org/10.1016/j.fbp.2018.09.005.

[30] M. Gericke, P. Fardim, T. Heinze, Ionic liquids - promising but challenging solvents for homogeneous derivatization of cellulose, Molecules 17 (2012) 7458–7502, https://doi.org/10.3390/molecules17067458.

[31] T. Zweckmair, H. Hettegger, H. Abushammala, M. Bacher, A. Potthast, M. P. Laborie, T. Rosenau, On the mechanism of the unwanted acetylation of polysaccharides by 1,3-dialkylimidazolium acetate ionic liquids: part 1—analysis, acetylating agent, influence of water, and mechanistic considerations, Cellulose 22 (2015) 3583–3596, https://doi.org/10.1007/s10570-015-0756-2.

[32] S.K. Karatzos, L.A. Edye, R.M. Wellard, The undesirable acetylation of cellulose by the acetate ion of 1-ethyl-3-methylimidazolium acetate, Cellulose 19 (2012) 307–312, https://doi.org/10.1007/s10570-011-9621-0.

[33] A. Kljun, T.A.S. Benians, F. Goubet, F. Meulewaeter, J.P. Knox, R.S. Blackburn, Comparative analysis of crystallinity changes in cellulose i polymers using ATR-FTIR, X-ray diffraction, and carbohydrate-binding module probes, Biomacromolecules 12 (2011) 4121–4126, https://doi.org/10.1021/bm201176m.

[34] L.C.H. Alves, Cellulose solutions: Dissolution, regeneration, solution structure and molecular interactions, 2015. https://estudogeral.sib.uc.pt/handle/10316/29319 (Accessed 14 July 2020).

[35] C. Chung, M. Lee, E.K. Choe, Characterization of cotton fabric scouring by FT-IR ATR spectroscopy, Carbohydr. Polym. 58 (2004) 417–420, https://doi.org/10.1016/j.carbpol.2004.08.005.

[36] J. Široký, R.S. Blackburn, T. Bechtold, J. Taylor, P. White, Attenuated total reflectance Fourier-transform Infrared spectroscopy analysis of crystallinity changes in lyocell following continuous treatment with sodium hydroxide, Cellulose 17 (2010) 103–115, https://doi.org/10.1007/s10570-009-9378-x.

[37] P. Peets, I. Leito, J. Pelt, S. Vahur, Identification and classification of textile fibres using ATR-FT-IR spectroscopy with chemometric methods, Spectrochim. Acta - Part A Mol. Biomol. Spectrosc. 173 (2017) 175–181, https://doi.org/10.1016/j.saa.2016.09.007.

[38] S.Y. Park, Y.J. Kim, S.Y. Kwak, Versatile surface charge-mediated anti-fouling UF/MF membrane comprising charged hyperbranched polyglycerols (HPGs) and PVDF membranes, RSC Adv. 6 (2016) 88959–88966, https://doi.org/10.1039/c6ra19020k.

[39] S. Rajesh, K.H. Shobana, S. Anitharaj, D.R. Mohan, Preparation, morphology, performance, and hydrophilicity studies of poly(amide-imide) incorporated cellulose acetate ultrafiltration membranes, Ind. Eng. Chem. Res. 50 (2011) 5550–5564, https://doi.org/10.1021/ie1019613.

[40] B. Poyraz, A. Tozluoğlu, Z. Candan, A. Demir, M. Yavuz, Ü. Büyuksarı, H.İ. Ünal, H. Fidan, R.C. Saka, TEMPO-treated CNF composites: pulp and matrix effect, Fibers Polym. 19 (2018) 195–204, https://doi.org/10.1007/s12221-018-7673-y.

[41] J. Rebière, M. Heuls, P. Castignolles, M. Gaborieau, A. Rouilly, F. Violleau, V. Durrieu, Structural modifications of cellulose samples after dissolution into various solvent systems, Anal. Bioanal. Chem. 408 (2016) 8403–8414, https://doi.org/10.1007/s00216-016-9958-1.

Corrigendum

Corrigendum to "Re-use of waste cotton textile as an ultrafiltration membrane" [J. Environ. Chem. Eng. 9 (2021) 105705]

Anastasiia Lopatina [a,*], Ikenna Anugwom [b], Hervé Blot [c], Ángela Sánchez Conde [d], Mika Mänttäri [a], Mari Kallioinen-Mänttäri [a]

[a] *Department of Separation Science, LUT School of Engineering Science, LUT University, P.O. Box 20, FI-53851 Lappeenranta, Finland*
[b] *LUT Re-Source Research Platform, LUT University, P.O. Box 20, FI-53851 Lappeenranta, Finland*
[c] *Génie chimique, Génie des Procédés, Paul Sabatier University, Toulouse 3, IUT A, 115C route de Narbonne, 31077 Toulouse Cedex-4, France*
[d] *Department of Chemical and Nuclear Engineering. Higher Technical School of Industrial Engineering, Universidad Politècnica of Valencia, 46022 Valencia, Spain*

The authors regret the existence of an error on the pure water permeability results reported in the original and published manuscript. The error has been identified and corrected as follows:

- In Abstract, the lines "permeabilities of 1.11 and 3.09 m^3/(m^2·s·Pa) for 300 and 150 μm casting thickness, respectively, but poor adhesion stability and low retention. Membranes cast from solutions of higher concentrations (5, 6, and 7 wt%) resulted in membranes with more stable performance. The permeability values for 300 μm membranes were in the range of 0.27 – 0.39 m^3/(m^2·s·Pa) and for 150 μm 0.51 – 0.67 m^3/(m^2·s·Pa)." should be read as "permeabilities of 1.11·10^{-10} and 3.09·10^{-10} m^3/(m^2·s·Pa) for 300 and 150 μm casting thickness, respectively, but poor adhesion stability and low retention. Membranes cast from solutions of higher concentrations (5, 6, and 7 wt%) resulted in membranes with more stable performance. The permeability values for 300 μm membranes were in the range of 0.27·10^{-10} – 0.39·10^{-10} m^3/(m^2·s·Pa) and for 150 μm 0.51·10^{-10} – 0.67·10^{-10} m^3/(m^2·s·Pa)."
- In Subsection 2.2.2, the Equation 1 "$J = Q_p/1000/A\cdot\tau$" should be read as "$J = Q_p/A\cdot\tau$".
- In Subsection 2.2.2, the lines "approximately same model solutions' flux around 0.83 m^3/(m^2·s))." should be read as "approximately same model solutions' flux around 0.83·10^{-10} m^3/(m^2·s))."
- In Subsection 3.2, the lines "RC70pp membrane from these two works: membrane showed – 30 mV zeta potential at pH 7, 0.58 m^3/(m^2·s·Pa) permeability at 1 bar" should be read as "RC70pp membrane from these two works: membrane showed – 30 mV zeta potential at pH 7, 0.58·10^{-10} m^3/(m^2·s·Pa) permeability at 1 bar".
- In Section 4., the lines "Membranes with 5%, 6%, and 7% concentration of cellulose cast at 150 μm showed water permeabilities in the range of 0.51 – 0.67 m^3/(m^2·s·Pa)" should be read as "Membranes with 5%, 6%, and 7% concentration of cellulose cast at 150 μm

showed water permeabilities in the range of 0.51·10^{-10} – 0.67·10^{-10} m^3/(m^2·s·Pa)".
- In Subsection 3.1., Fig.2. Pure water permeabilities of the tested membranes all measured in the Amicon ultrafiltration cell at 25 °C and mixing rate approximately 300 rpm.; corrections made to y-axis title.
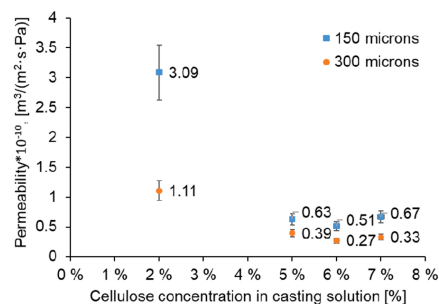
- In Subsection 3.1., Fig. 5. Permeability and the retention values of the membranes prepared within current research and membranes which were chosen for comparison; membranes chosen for comparison are named after first authors Durmaz [27] and Livazovic [12], information about RC70pp was taken from [28,29]; membranes prepared in this research are signed as cellulose wt% concentration in casting solution/casting thickness in μm.; corrections made to x-axis title.
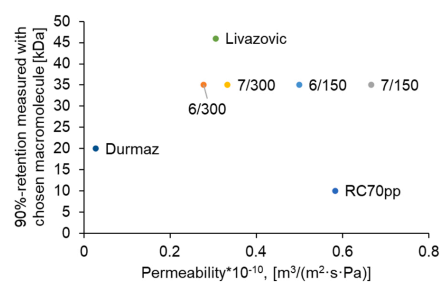

Sample	PWP·10⁻¹⁰, m³/(m²·s·Pa)	R_m·10¹³, 1/m	PEG 35 kDa retention, %	Porosity, %	Contact angle, °	Zeta potential at pH 7, mV	LOI A_{1428}/A_{897}
Textile	nd	nd	nd	nd	nd	nd	0.86
5/150	0.63	2	78.1	59.2	15.6 ± 2.8	-25	0.60
6/150	0.51	2	90.8	56.3	16.3 ± 5.7	-23	0.47
7/150	0.67	2	88.2	49.6	14.0 ± 5.6	-35	0.50

The authors would like to apologise for any inconvenience caused. All authors agree with this decision of corrigendum.

- In Subsection 3.2., Table 3 Membranes and cotton textile characterization., the column title "PWP, m³/(m²·s·Pa)" should be read as "PWP·10⁻¹⁰, m³/(m²·s·Pa)".

Publication III

Lopatina, A., Liukkonen, A., Bec, S., Anugwom, I., Nieminen, J., Mänttäri, M., and Kallioinen-Mänttäri, M.

Wood-Based Cellulose-Rich Ultrafiltration Membranes: Alkaline Coagulation Bath Introduction and Investigation of Its Effect over Membranes' Performance

Article

Wood-Based Cellulose-Rich Ultrafiltration Membranes: Alkaline Coagulation Bath Introduction and Investigation of Its Effect over Membranes' Performance

Anastasiia Lopatina * , **Alma Liukkonen, Sabina Bec, Ikenna Anugwom, Joona Nieminen, Mika Mänttäri** and **Mari Kallioinen-Mänttäri**

Department of Separation Science, LUT School of Engineering Science, LUT University, P.O. Box 20,
FI-53851 Lappeenranta, Finland; alma.liukkonen@student.lut.fi (A.L.); sabina.bec@lut.fi (S.B.);
ikenna.anugwom@lut.fi (I.A.); joona.nieminen@lut.fi (J.N.); mika.manttari@lut.fi (M.M.);
mari.kallioinen-manttari@lut.fi (M.K.-M.)
* Correspondence: anastasiia.lopatina@lut.fi

Abstract: In this study, wood-based cellulose-rich membranes were produced with a novel approach to casting procedure. Flat-sheet membranes were prepared from birch biomass pretreated with deep eutectic solvent and dissolved in ionic liquid-dimethylsulfoxide system via phase inversion method. Alkaline coagulation bath filled with sodium hydroxide solution was added to the process before a water coagulation bath and aimed to improve membranes' performance. The effect of NaOH coagulation bath on the membrane was studied based on two NaOH concentrations and two different treatment times. The characterisation methods included measuring pure water permeabilities, polyethylene glycol 35 kDa model solution retentions, hydrophilicity, zeta potential, and chemical structure. Additionally, suitability of the membranes for removing residual phosphorous from a municipal wastewater treatment plant's effluent was studied. The study revealed that introduction of the alkaline coagulation bath led to additional removal of lignin from membrane matrix and increase in the filtration capacity up to eight times. The resulting membranes can be characterised as very hydrophilic, with contact angle values 11.9–18.2°, negatively charged over a wide pH range. The membranes with the highest permeability, 380–450 L/m^2·h·bar, showed approximately 70% phosphorus removal from purified wastewater, good removal of suspended solids, and low irreversible fouling tendency.

Keywords: membrane fabrication; cellulose; wood; ultrafiltration; wastewater treatment; phosphorus removal; alkaline treatment; 1-ethyl-3-methylimidazolium acetate; choline chloride; lactic acid

1. Introduction

The significance of cellulose-based pressure-driven membrane filtration has been extensively described in literature [1–5]. Despite the chosen method of describing cellulose as a polymer—regardless of whether it is recognised as hydrophilic or an amphiphilic one [5–9]—the regenerated cellulose membranes are universally acknowledged as very hydrophilic, having higher biocompatibility and lower fouling tendency when compared with petroleum-based polymers due to cellulose being a biopolymer [10–13]. The existing research focusing on the manufacturing of cellulose membranes is highly variable regarding whether research groups prefer to use commercially produced cellulose [14–16] or bio-based cellulose sources [2,17,18], using various solvents with high capacity for cellulose dissolution [3,4,19]. The steady interest towards ionic liquids (ILs) as cellulose and biomass solvent media is supported with such characteristics as their potential recyclability, low vapour pressure, and good chemical and thermal stability [20–23]. The challenges regarding ILs' high price and high viscosity can be mitigated successfully by the addition of a co-solvent [13,16,21,24–27].

In a previous study [18] we showed that it is possible to produce membranes from carbohydrates originating from birch. However, the membrane retention and filtration capacity that were achieved in that process were not at the level required for a good, commercially feasible membrane. It is known that changing the fabrication procedure conditions enables controlling the membrane morphology and surface properties, which then significantly influences membrane performance [28]. Thus, the possibilities to improve the performance of the birch-based cellulose-rich membranes were studied from the related literature. The use of dilute acidic solutions as the coagulation bath media is well studied [29]; however, the use of alkaline solutions for the coagulation purposes seemed to be lacking attention. Cellulose behaviour in alkali systems is well studied for the case when alkaline solutions are used for the dissolution or extraction of cellulose [30,31]. However, this information can only be partly applied to the needs of membrane manufacturing, considering the backwards direction of the process. Thus, we chose to focus on the possibility to improve the performance of the birch-based cellulose-rich membrane via the use of an additional coagulation bath filled with alkaline solution.

Although there are countless combinations of alkali with additive systems (e.g., NaOH and urea, NaOH and PEG, KOH as a NaOH substitute, etc.), when pure NaOH is used for the cellulose dissolution, the range of applicable concentrations is very specific (7–10 wt.% below $-5\,^{\circ}$C) [6]. There are studies reporting the dissolution of cellulose in an NaOH solution of lower concentrations; however, the cellulose described there is usually amorphous and has a degree of polymerisation (DP) ≤ 200. It is also important to remember that the presence of lignin affects the dissolution process of cellulose in alkaline solutions, usually making it easier [9]. Lignin dissolution by itself requires a significantly lower NaOH concentration, starting from an approximately 1 wt.% solution [32–34]. Hemicelluloses usually require slightly higher NaOH concentrations (starting at 4 wt.%) but still lower ones than needed for the cellulose dissolution [35]. Thus, the concentrations of interest were picked in order to have: (1) a lower concentration (5 wt.%) of NaOH at which the dissolution of lignin and hemicelluloses should happen but at which cellulose is left intact; and (2) a higher concentration (10 wt.%) of NaOH at which there might be observable changes to cellulose structure [36,37].

The wood-based cellulose-rich membranes were prepared via a non-solvent induced phase inversion method from birch biomass purified from lignin with deep eutectic solvent (DES), consisting of choline chloride (ChCl) acting as a hydrogen bond acceptor (HBA) and lactic acid (LAc) acting as a hydrogen bond donor (HBD). The treated biomass was dissolved in a 1-ethyl-3-methylimidazolium (Emim) acetate (OAc) dimetylsulphoxide (DMSO) system; the detailed procedure can be found in our previous publication [18]. The casting procedure was improved with the addition of a second coagulation bath, filled with sodium hydroxide solution, that aimed to improve the performance of the membranes. The membranes' permeability was measured in both dead-end and cross-flow membrane modules. Membranes' retention properties were characterised with both the filtration of model solutions (polyethylene glycol (PEG), CaCO$_3$) and the filtration of purified municipal wastewater to remove phosphorous. Additionally, the hydrophilicity, zeta potential, and chemical structure of the membranes were characterised in order to examine the influence of the alkaline coagulation bath.

2. Materials and Methods

2.1. Materials

Debarked birch (*Betula pendula*) woodchips with a nominal size of $5 \times 1 \times 0.1$ cm were used as a base material for all further operations. Partial delignification of the birch chips was done via DES treatment, where choline chloride (CAS # 67-48-1, Merck KGaA, Darmstadt, Germany) was used as an HBA, and lactic acid (CAS # 79-33-4, Merck KGaA, Darmstadt, Germany) was used as an HBD. A mixture of ethanol and deionised (DI) water (15 MΩ, 0.5–1 μS/cm) at a 9:1 volume ratio was used for washing out the residual DES from the partially delignified biomass. A mixture of ionic liquid–1-ethyl-3-methylimidazolium

acetate, 95% (C_1C_2ImOAc, CAS # 143314-17-4, Iolitec Ionic Liquids Technologies GmbH) and dimethylsulphoxide (CAS # 67-68-5, Merck KGaA, Darmstadt, Germany) was used for preparation of the casting solution. Sodium hydroxide pellets (>99%, CAS # 1310-73-2, Merck KGaA, Darmstadt, Germany) were used for membrane precipitation in the preparation of alkaline solutions.

Flat-sheet membranes were cast on nonwoven polypropylene/polyethylene carrier material (Viledon® Novatexx 2484, Freudenberg, Germany; air permeability: 60 L/(s·m^2); weight per unit area: 85 g/m^2; maximum tensile force along/across: 300/200 N/5 cm; 25/30% elongation at maximum tensile force along/across; and thickness: 0.12 mm). Ultra-pure DI water (15 MΩ, 0.5–1 μS/cm) was produced by a CENTRA-R 60/120 system (Elga purification system, Veolia Water, London, UK) and used for washing, as a non-solvent, and in the preparation of all solutions.

Polyethylene glycol (approximately Mw 35,000 g/mol, CAS # 25322-68-3, Merck KGaA, Darmstadt, Germany) was used as a model compound for the study of membrane retention. Calcium carbonate (powder, ≤50 μm particle size, >98%, CAS # 471-34-1) was used as a model compound in the experiments showing the removal of suspended solids with the produced membranes. The purified wastewater used in the experiments was the discharge water of the Toikansuo wastewater treatment plant's secondary clarifier, located in Lappeenranta, Finland. The Toikansuo plant's treatment capacity is approximately 20,000 m^3/day. The purified wastewater's pH was 7.75, its total carbon concentration was 5.92 mg/L, its total nitrogen concentration was 9.4 mg/L, and its total phosphorous concentration was 0.35 mg/L. The performance of the birch-based membranes produced in this study was compared with the performance of the commercial membrane RC70PP (Alfa Laval; support material: polypropylene; membrane matrix: regenerated cellulose acetate; molecular weight cut-off (MWCO) 10,000 kDa).

2.2. Methods

2.2.1. DES Treatment

For treatment of the birch woodchips, DES was prepared from ChCl and LAc mixed at a 1:9 mole ratio, respectively, at 100 °C until a homogeneous transparent mixture formed. The birch chips and DES were taken at a 1:5 mass ratio and placed into an oil bath, wherein the biomass load was cooked for 18 h at 105 °C. After the treatment was completed, the pulp was vacuum filtered through filter paper and washed with a mixture of ethanol and DI water at a 9:1 volume ratio until the treated pulp released no colour. The DES-treated pulp was transferred to an oven and dried at 50 °C for 24 h.

2.2.2. Membrane Preparation

Homogeneous solutions of the DES-treated biomass samples were prepared in a mixture of Emim OAc and DMSO with 5 wt.% concentration by constant stirring overnight under constant heating in an oil bath at 90 °C. The prepared solutions were cooled down to room temperature and cast on the carrier material placed on a glass plate by spreading an appropriate amount with Automatic Film Applicator L (BYK-Gardner, Pompano Beach, FL, USA) with a 150 μm casting knife at a speed of 50 mm/s. Immediately after casting, the membrane was transferred into the first coagulation bath filled with NaOH solution and, after that, it was moved into the second coagulation bath filled with DI water at 0 °C, where the membrane was preserved for 24 h to guarantee a complete phase separation (see Figure 1).

In addition to the alkaline solutions strength justification discussed in the Introduction, it is vital to mention that cellulose solutions in cold alkali are recognised as metastable (i.e., sensitive to the slightest pH or temperature changes and aging, all of which can trigger the gelation-regeneration process) [6,8,24]. Naturally, when cellulose behaviour in alkali was studied, the conditions were maintained as stable as possible; however, when the current case of a coagulation bath is discussed, there is no need to stabilise the cellulose's state in the alkaline solution, thus only the starting temperature of the alkaline solution was

adjusted to 0 °C. During the precipitation process, the temperature was allowed to rise in a natural way. The obvious assumption here would be that cellulose precipitation should be described as delayed (both due to the low temperature and the alkaline conditions) but nonetheless surely existing in the alkaline solution [6,38].
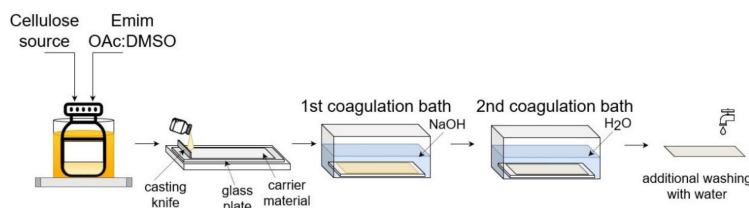

Figure 1. A schematic of the casting procedure.

Regarding the residence time in the coagulation bath, it was chosen based on the reported cellulose gelation rates. Although various researchers stated different gelation rates for the solutions of biomass, it is generally acknowledged that, within the range of concentrations and time intervals chosen for the experiments, the gelation is supposed to happen within 30–40 min, depending on the temperature [38]. Thus, two time intervals were tested: (1) a shorter one (30 min), the alleged minimum time required for gelation process; and (2) a longer one (60 min), when gelation surely happened. Taking into consideration that the temperature of the alkaline solutions was allowed to rise naturally, it can be safely assumed that cellulose precipitation should be finished by the time the coagulation bath is changed in both time cases. Table 1 summarises the casting parameters' variations and gives codes for the membrane types produced.

Table 1. The casting parameters' combinations and assigned membrane codes (0/0 for the membrane only coagulated in water).

NaOH Concentration, wt.%	Time Spent in NaOH Coagulation Bath, Min		
	0	**30**	**60**
0	0/0	-	-
5	-	5/30	5/60
10	-	10/30	10/60

All the obtained membranes were washed under DI water and then stored in water and used for analyses without drying if not stated otherwise. An overview of the analyses of the prepared membranes is presented in Table 2.

Table 2. An overview of the analyses.

	FTIR	Zeta Potential	Amicon (Dead-End)				Cross-Flow		Contact Angle	P Tubes
			PWP	PEG Retention	CaCO₃	WW Flux	PWP	WW Flux		
0/0	✔	✔	✔	✔					✔	
5/30	✔	✔	✔	✔					✔	
5/60	✔	✔	✔	✔					✔	
10/30	✔	✔	✔	✔		✔	✔	✔	✔	✔
10/60	✔	✔	✔	✔	✔	✔	✔	✔	✔	✔

2.2.3. Membrane Permeability and Retention Measurements

The permeability and retention of the prepared membranes were measured with Amicon dead-end stirring cell equipment (Millipore, Burlington, MA, USA, Cat No.: XFUF07611;

diameter of the stirring device: 60 mm) (see Figure 2). Before the filtration experiments, each membrane was compacted for 1 min at 1 bar, 2 min at 2 bars, 3 min at 3 bars, 4 min at 4 bars, and 20 min at 5 bars. This also ensured that the solvents used in the membrane manufacturing were completely rinsed from the membrane pores. This was also checked through the measurement of total organic carbon (TOC) content in a permeate sample collected during the membrane compaction at 5 bars.
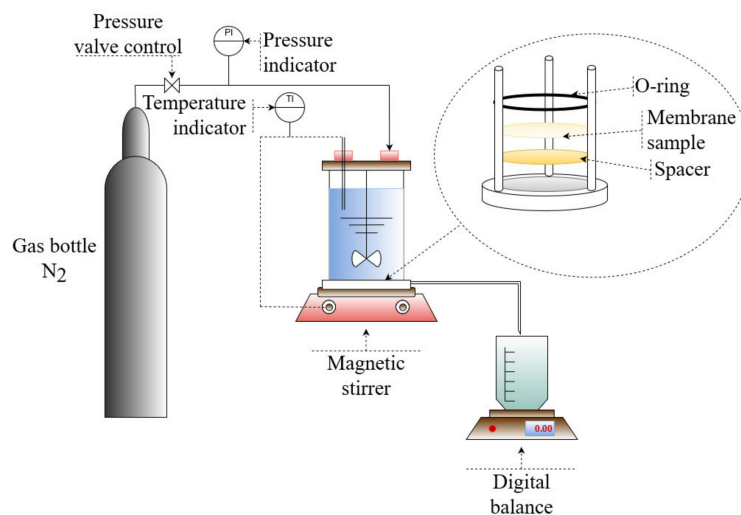

Figure 2. Schematic configuration of Amicon dead-end filtration system.

The pure water permeability of the membranes was determined as a slope of four plotted flux values, measured at 1, 2, 3, and 4 bars of pressure at $25 \pm 0.5\ °C$ and calculated using Equation (1):

$$J = \frac{Q_P/1000}{A \cdot \frac{\tau}{60}},\tag{1}$$

where J is the tested membrane's flux (L/(m^2·h)), Q_P is the gravimetric flow of water permeating through the membrane (g/min), A is the area of the membrane sample (m^2), and τ is the time of collection of the permeate (min).

Using the 10/30 and 10/60 membranes, the permeate flux of the purified wastewater was followed as a function of time. The total filtration experiment took place for 11 days with a volume reduction factor (VRF; the volume ratio between the permeate and the initial feed) of about 3. Additionally, the pure water permeabilities were determined before and after the long wastewater filtration. The filtration experiments with wastewater were performed in a cross-flow filtration module, with the size of a single membrane coupon of 10.4 cm^2 (see Figure 3). The cross-flow velocity used in the wastewater experiments was $v = 1.2$ m/s, measured at 1 bar pressure and $20 \pm 0.5\ °C$.

For studying the retention of the produced membranes, a model solution of PEG 35 was prepared with a concentration of 300 ppm and filtered through the membrane at a pressure that was set for each membrane individually in order to have approximately the same flux. Throughout all the measurements, the stirring speed was maintained at 300 rpm using the magnetic stirrer with an rpm indicator. The temperature was kept at $25 \pm 0.5\ °C$. The samples of the feed, retentate, and permeate were collected and analysed for total organic carbon (TOC) content with a Shimadzu TOC analyser (TOC-L series, Kyoto, Japan).

Membrane retentions were calculated out of the measured TOC content in the samples using Equation (2):

$$R = \left(1 - \frac{2 \cdot C_p}{C_f + C_r} \right) \cdot 100, \tag{2}$$

where C_p, C_f, and C_r are the TOC concentrations in the permeate, feed, and retentate (mg/L), respectively.
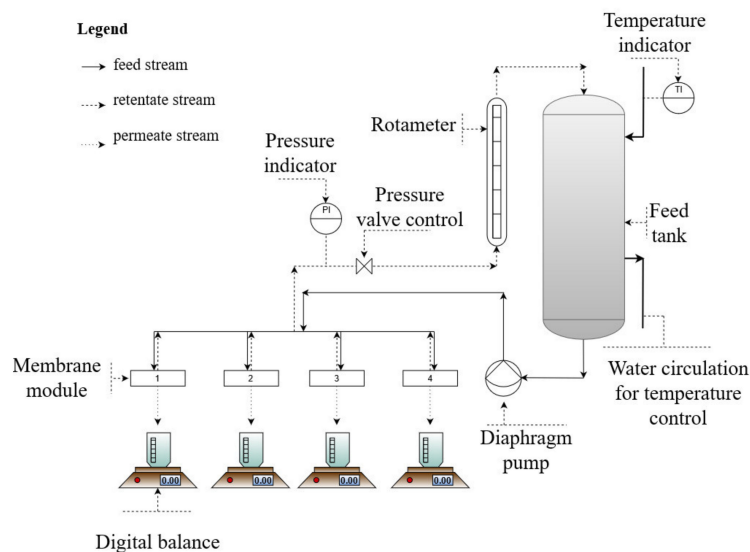

Figure 3. A schematic of the configuration of the cross-flow filtration system.

To measure the removal of suspended solids, filtration experiments with $CaCO_3$ (1000 ppm) solution were conducted. The turbidity of the samples was measured with the Hach Model DR/2010 Spectrophotometer by means of the preinstalled programme #750. The removal efficiency was calculated using Equation (2).

The purified wastewater from the Toikansuo wastewater treatment plant's secondary clarifier was used for the assessment of total phosphorus removal with the manufactured membranes. The samples were analysed with the Spectroquant® tubes kit (o-phosphate and total phosphorous), using the photometric method: PMB 0.05–5.00 mg/L, PO_4- P 0.2–15.3 mg/L, PO_4^{3-} 0.11–11.46 mg/L P_2O_5. The photometer used was a NOVA 60 A Spectroquant®. The removal efficiency was calculated using Equation (2).

2.2.4. Membrane Characterisation
Examination of the Zeta Potential of the Membranes

The zeta potential was measured with a SurPASS electrokinetic analyser (Anton Paar GmbH, Graz, Austria) with an adjustable gap cell method and using 0.001 M KCl solution as a background electrolyte. The membranes were preliminary stored at approximately 5 °C for 24 h in a fridge. Before the start of the experiment, the electrolyte solution's pH was shifted to 7.6 by the addition of 0.1 M KOH solution and then automatically titrated to 2.4 with use of a 0.05 M HCl solution as the analysis carried on. The final value of the zeta potential was calculated automatically by SurPASS software, based on the Helmholtz–Smoluchowski equation. In addition to zeta potential values, the isoelectric point (IEP), the pH value where the zeta potential equals 0 mV, was identified.

Examination of the Chemical Structure of the Membranes

The Fourier-transform infrared spectroscopy (FTIR) spectra of membrane samples were measured with a Frontier MIR/FIR spectrometer (PerkinElmer Inc., Waltham, MA, USA) with the universal diamond crystal attenuated total reflectance (ATR) module in the range of wave numbers 400–4000 cm^{-1}, with the spectra resolution of 4 cm^{-1}. Air-dried samples of the selected membranes were recorded in pentaplicate and averaged. For the graphical representation, all the spectra were processed with ATR correction, baseline correction, and normalisation. The ratio of the not-normalised absorption bands A_{1428}/A_{899} was used to calculate a lateral order index (LOI), as was proposed by Nelson and O'Connor [39,40].

Examination of the Hydrophilicity of the Membranes

The membranes' hydrophilicity was measured with a static contact angle (CA) procedure based on the captive bubble method [41]. The U-shaped needle placed nearly 3–4 µL of air bubble volume on the surface of the tested membrane, attached to a piece of glass with double-sided tape and submerged into DI water at room temperature. For each membrane sample, six independent measurements of the CA were made at different points with the average value of recorded data taken as the final CA. The CA was measured with KSV CAM 101 equipment (KSV Instruments Ltd., Espoo, Finland) connected to a charged-coupled device (CCD) camera (DMK 21F04, Imaging Source Europe GmbH, Bremen, Germany). To determine the CA, the obtained images were treated by curve-fitting analysis with CAM 2008 software.

3. Results and Discussion

3.1. Changes in Membrane Characteristics Due to the Alkaline Treatment

When the alkaline bath was introduced into the membrane manufacturing process, a common observation with all the condition and concentration combinations used in the experiments was the change of the first (alkaline) coagulation bath's colour from transparent to brownish. This is a clear indication of partial lignin washing out from the membrane matrix into the coagulation bath [32]. Based on the FTIR spectra measured in this study, the changes happening to the cellulose surface, or biomass surface for that matter, in the used conditions were not significant (see Figure 4), which was reported earlier for similar treatment conditions [36].

Comparing the reference spectrum (0/0) with the membranes prepared with the alkaline bath in the production line, small changes in the 900–1100 cm^{-1} region and consistent changes of the wave numbers in the 1200–1700 cm^{-1} region can be seen. The presence of the peak at 1710 cm^{-1} in all the spectra is indicative of the introduction of C=O groups as a result of the cellulose's partial acetylation during the dissolution process in IL, which has been previously reported and attributed to either overall biomass complexity or the presence of water residuals [37,42]. Comparison of the 0/0 membrane with the other membranes that started the coagulation process in the alkaline bath shows an increase of the peak at 899 cm^{-1} due to alkaline treatment, which is a characteristic peak of C–O stretching vibration in the amorphous region of cellulose, implying an increase in the total amount of amorphous cellulose in the membrane matrix [43,44]. The easiest way to reaffirm crystallinity assessment is the calculation of either the crystallinity index or the LOI, as was suggested by Nelson and O'Connor [39,40]. The LOI is revealed from the ratio at 1428 cm^{-1} in-plane symmetric bending, characteristic for cellulose I$_\beta$ crystal, and C–H deformation in β-glycosidic linkages at 899 cm^{-1}, specific for amorphous cellulose regions (A_{1428}/A_{899}) [45,46]. The calculation showed the distinct difference between membranes coagulated using the alkaline coagulation bath and the 0/0 membrane: the membrane coagulated in water shows a LOI value of 0.82 whereas all the other membranes show a LOI value within 0.62–0.65, definitely showing a smaller content of crystalline cellulose and thus a larger share of amorphous region. According to results previously reported by other researchers, the decrease in the crystallinity of the membrane would lead to a

decrease in the membranes' tensile properties and a simultaneous increase in the elongation break values [12,47]. These changes might have an impact on the usability of a membrane; however, no noticeable difference was observed in the scope of this study. The small decrease, which can be observed at wave numbers 1240 and 1507 cm^{-1}, can be assigned to the different units of lignin, which suggests additional removal of lignin in the alkaline coagulation bath [32,48–50].
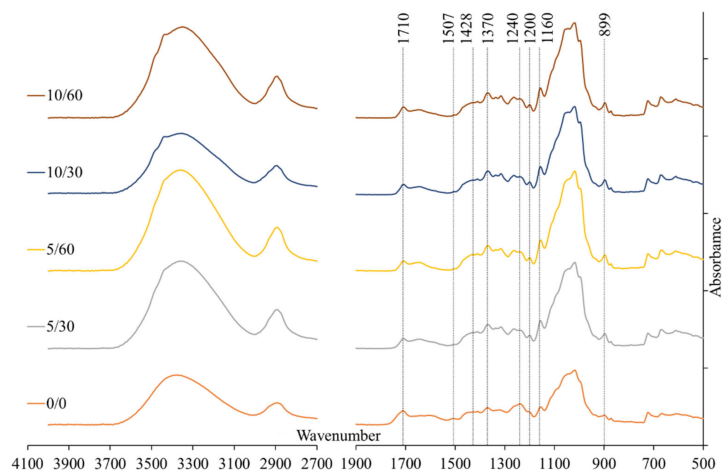

Figure 4. The FTIR spectra of the prepared membranes, recorded using the Perkin Elmer Frontier spectrometer with a universal ATR module of diamond crystal at a resolution of 4 cm^{-1} in the *absorbance* mode.

The CA measurements show that all the membranes can be characterised as hydrophilic (0/0) membranes or super-hydrophilic membranes (5/30, 5/60, 10/30, 10/60 membranes) (see Figure 5). This was expected due to the fact that hydrophilicity is common for cellulose membranes as regenerated cellulose films are known to be amongst the most hydrophilic polymers [38]. Generally, the CAs of alkali-treated membranes are noticeably smaller than those coagulated in DI water, which correlates well with FTIR measurements, suggesting that similar changes are happening within the membrane matrix from the chemical point of view (i.e., there is additional removal of lignin within the matrix). The zeta potential results demonstrate that all the membranes are negatively charged over a wide range of pH (see Figure 5). The membranes demonstrate stronger negative zeta potential at a neutral pH as a stronger NaOH concentration and longer time were applied in the first (alkaline) coagulation bath.

The more negative zeta potential values might be the result of the removal of non-cellulosic compounds, which makes the cellulose's surface groups more accessible for detection. It can also be speculated that the charge and hydrophilicity become stronger as the cellulose crystallinity reduces, leading to the increased amount of voids and flexible parts within the cellulose fibres and, thus, the better accessibility of the surface groups [36].
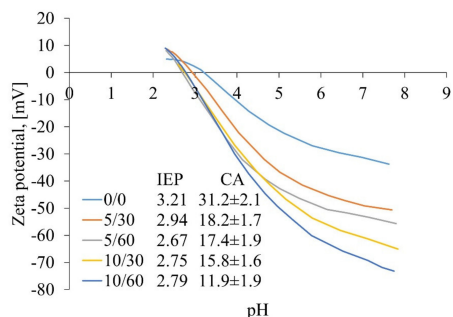
Figure 5. The zeta potential curves and isoelectric points (IEPs) of prepared membranes, recorded using a SurPASS electrokinetic analyser with the adjustable gap cell method and using 0.001 M KCl solution as an electrolyte; the contact angle values of the prepared membranes were recorded using the captive bubble method with KSV CAM 101 equipment connected to a CCD camera.

3.2. Membrane Performance

The results revealed that introducing the alkaline bath in the membrane manufacturing process improves the filtration capacity of the prepared cellulose membranes (see Figure 6a). The filtration capacities of the prepared membranes were actually increasing so much that the capability of the membranes to retain suspended solids was tested with a $CaCO_3$ suspension. It was found that the 10/60 membranes retained more than 97% of the suspended $CaCO_3$ particles. Although the filtration capacity change was significant, the retention of PEG molecules was at the same level for the reference membrane (0/0), for the membranes prepared with the 30-min alkaline bath treatment (5 and 10%), and for the membrane prepared with the longer alkaline treatment in the 5% alkaline bath (see Figure 6b).
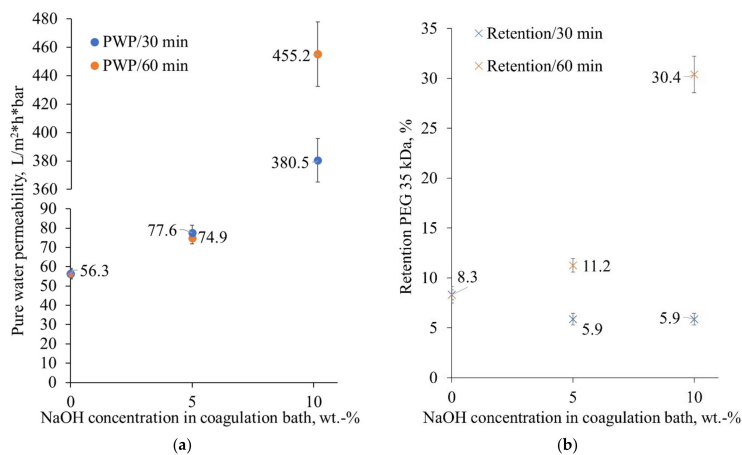
Figure 6. The pure water permeabilities (PWP) (**a**) and PEG 35 kDa retentions (**b**) of the tested membranes, all measured in the Amicon ultrafiltration cell at 25 °C and with a mixing rate of approximately 300 rpm.

As the permeability of ultrafiltration membranes prepared from semicrystalline polymers is highly dependent on the ratio between crystalline and amorphous parts, it is generally acknowledged that higher amorphous content results in better permeability [51]. This correlates well with the zeta potential measurements, where the strength of the charge on the membrane surface at neutral pH was directly proportional to the strength of the alkaline bath used.

Based on the high permeabilities, and thus the potential to be scaled up, the 10/30 and 10/60 membranes were taken onto further tests with the cross-flow module and their performance is compared with the commercially available RC70PP membrane (Alfa Laval). The results showed that the removal efficiency for the residual phosphorous from the effluent of the municipal wastewater treatment plant were at the same level with all membranes (see Table 3). The sufficient removal of phosphorus from anthropogenic wastewaters should be met by any treatment plant effluent before being discharged to the surface water. According to the present regulations, the maximum allowable amount of phosphorus in the purified wastewater effluent in Lappeenranta is 0.5 mg P/L [52,53]. However, future regulations will limit the total phosphorus concentration to below 0.1 mg P/L [54]. The effluent used in the filtrations contained phosphorous levels of about 0.25 mg/L. The phosphorous concentration in the permeate of the studied membranes was around 0.09 mg/L and, thus, below the future regulation. Current removal techniques demand a large footprint and the use of additional chemicals to achieve appropriate removal efficiency. Based on the results shown here, one solution could be the introduction of the membrane filtration step at the end of the treatment line.

Table 3. Pure water fluxes before and after effluent filtration, and permeate fluxes at the beginning and the end of the concentration filtration.

	10/60	10/30	RC70PP
Pure water flux before wastewater filtration at 2 bar, L/(m²h)	460	440	150
Wastewater flux at the beginning (8 min), L/(m²h)	106	105	64
Wastewater flux at VRF ~3 (11 days), L/(m²h)	69	68	42
Phosphorous removal, %	67	69	68

The filtration was made at a constant 1 bar pressure, which means that the measured initial fluxes of the 10/30 and 10/60 membranes were about two times higher (pure water fluxes: about three times higher) compared with the flux of the RC70PP membrane. This also means that concentration polarisation was stronger with the 10/30 and 10/60 membranes, leading to a significant decrease in flux. However, the permeate fluxes were still a bit higher with the 10/30 and 10/60 membranes at the end of the filtration than with the reference RC70PP membrane. The measurements of pure water fluxes before and after the filtration of the effluent showed that the pure water fluxes decreased more with laboratory-made membranes when compared with the RC70PP membrane. In addition, it was observed that the fluxes of the 10/30 and 10/60 membranes increased during water flux measurement.

A similar phenomenon was observed when the same membranes were used for wastewater filtration in the Amicon dead-end filtration module. The wastewater permeate flux declined by approximately 45% and 38% for the 10/30 and 10/60 membranes, respectively, when compared with the initial pure water permeability (PWP) value of those membranes. When the same membrane samples were simply rinsed with clean water, the permeability was restored to up to 60% and 95% of the initial PWP for the 10/30 and 10/60 membranes, respectively. This means that irreversible fouling of the membranes was low. Partial restoration of permeability is a known phenomenon of cellulose behaviour and sometimes linked to a negatively charged surface [55,56]. Since such membranes show

the ability for partial permeability restoration, it means that not only the membrane has some intrinsic stability against fouling but also that cleaning procedures potentially do not require harsh chemicals, and it is possible to just clean them with water, thus reducing stress of the environment and the membrane over its life cycle.

The 10/30 and 10/60 membranes also showed similar removal of total phosphorous, 72% and 75%, respectively. The reason behind such good phosphorus removal with such open membranes might be that the residual phosphorus in the purified wastewater is due to the use of precipitation chemicals in the water treatment process in the form of very fine precipitates.

4. Conclusions

The fabrication of wood-based cellulose-rich membranes from DES-treated biomass solutions in a mixture of Emim OAc and DMSO, and using the phase inversion method was performed using a procedure involving two subsequent coagulation baths. The introduction of the additional coagulation bath filled with NaOH solution was done to improve the membranes' performance. Two NaOH concentrations (5 and 10 wt.%) and two residence times (30 and 60 min) were studied. Characterisation of the prepared membranes was done by measuring pure water permeability in both dead-end and cross-flow modules, as well as by measuring PEG 35 kDa retention, $CaCO_3$ suspension separation, and the removal of total phosphorus from purified wastewater from a local treatment plant. Additionally, ATR-FTIR, static CA, and zeta potential measurements were carried out in order to study any changes occurring.

According to the results, the introduction of the alkaline coagulation bath into the casting procedure promotes the additional removal of lignin in the coagulation bath, while cellulose already starts the precipitation process. All the membranes prepared with the use of the NaOH bath showed higher hydrophilicity compared with the reference membrane (only precipitated in water) and a tendency to have a more negatively charged surface as stronger alkaline treatment was applied. The utilisation of the additional coagulation bath filled with NaOH solution proved to have a positive effect on the performance of the cellulose-rich wood-based membranes: they showed a significant increase of their filtration capacity alongside almost unchanged retention characteristics. Based on the $CaCO_3$ retention (97%) and total phosphorus removal from purified wastewater (approximately 70%), these membranes might be an attractive alternative for use in the removal of residual phosphorous as a tertiary treatment at wastewater treatment plants due to the possibility to achieve a relatively good removal efficiency with a low pressure difference.

Author Contributions: Conceptualisation: A.L. (Anastasiia Lopatina), M.M. and M.K.-M.; methodology, A.L. (Anastasiia Lopatina), M.M. and M.K.-M.; formal analysis: A.L. (Anastasiia Lopatina) and J.N.; investigation, A.L. (Anastasiia Lopatina), A.L. (Alma Liukkonen), S.B. and J.N.; resources: M.M. and M.K.-M.; writing—original draft preparation: A.L. (Anastasiia Lopatina); writing—review and editing: A.L. (Anastasiia Lopatina), A.L. (Alma Liukkonen), S.B., I.A., J.N., M.M. and M.K.-M.; visualisation: A.L. (Anastasiia Lopatina); supervision: M.M. and M.K.-M.; project administration: M.M. and M.K.-M.; and funding acquisition: M.K.-M. All authors have read and agreed to the published version of the manuscript.

Institutional Review Board Statement: Not applicable.

Informed Consent Statement: Not applicable.

Data Availability Statement: The data presented in this study are available upon request from the corresponding author.

Conflicts of Interest: The authors declare no conflict of interest.

References

1. Dang, H.T.; Narbaitz, R.M.; Matsuura, T.; Khulbe, K.C. A Comparison of Commercial and Experimental Ultrafiltration Membranes via Surface Property Analysis and Fouling Tests. *Water Qual. Res. J.* **2006**, *41*, 84–93. [CrossRef]
2. Mohamed, M.A.; Salleh, W.N.W.; Jaafar, J.; Ismail, A.F.; Abd. Mutalib, M.; Jamil, S.M. Feasibility of Recycled Newspaper as Cellulose Source for Regenerated Cellulose Membrane Fabrication. *J. Appl. Polym. Sci.* **2015**, *132*, 1–10. [CrossRef]
3. Gopakumar, D.A.; Arumughan, V.; Pasquini, D.; Leu, S.Y.; Abdul Khalil, H.P.S.; Thomas, S. Nanocellulose-Based Membranes for Water Purification. In *Nanoscale Materials in Water Purification*; Thomas, S., Pasquini, D., Leu, S.-Y., Gopakumar, D.A., Eds.; Elsevier: Amsterdam, The Netherlands, 2018; pp. 59–85. ISBN 978-0-12-813926-4.
4. Nancy, L.; Jackie, Z.; Hadi, P.; Yang, M.; Huang, X.; Ma, H.; Walke, H.W.; Hsiao, B.S. Synthesis and Characterization of a High Flux Nanocellulose–Cellulose Acetate Nanocomposite Membrane. *Membranes* **2019**, *9*, 70. [CrossRef]
5. Acharya, S.; Liyanage, S.; Abidi, N.; Parajuli, P.; Rumi, S.S.; Shamshina, J.L. Utilization of Cellulose to Its Full Potential: A Review on Cellulose Dissolution, Regeneration, and Applications. *Polymers* **2021**, *13*, 4344. [CrossRef] [PubMed]
6. Medronho, B.; Lindman, B. Competing Forces during Cellulose Dissolution: From Solvents to Mechanisms. *Curr. Opin. Colloid Interface Sci.* **2014**, *19*, 32–40. [CrossRef]
7. Alves, L.C.H. Cellulose Solutions: Dissolution, Regeneration, Solution Structure and Molecular Interactions. Ph.D. Thesis, Universidade de Coimbra, Coimbra, Portugal, 2015.
8. Alves, L.; Medronho, B.; Antunes, F.E.; Topgaard, D.; Lindman, B. Dissolution State of Cellulose in Aqueous Systems. 1. Alkaline Solvents. *Cellulose* **2016**, *23*, 247–258. [CrossRef]
9. Costa, C.; Medronho, B.; Eivazi, A.; Svanedal, I. Lignin Enhances Cellulose Dissolution in Cold Alkali. *Carbohydr. Polym.* **2021**, *274*, 118661. [CrossRef]
10. Kallioinen, M.; Mänttäri, M.; Nyström, M.; Nuortila-Jokinen, J.; Nurminen, P.; Sutela, T. Membrane Evaluation for the Treatment of Acidic Clear Filtrate. *Desalination* **2010**, *250*, 1002–1004. [CrossRef]
11. Abd-Razak, N.H.; Chew, Y.M.J.; Bird, M.R. Membrane Fouling during the Fractionation of Phytosterols Isolated from Orange Juice. *Food Bioprod. Process.* **2019**, *113*, 10–21. [CrossRef]
12. Mazlan, N.S.N.; Zakaria, S.; Gan, S.; Hua, C.C.; Baharin, K.W. Comparison of Regenerated Cellulose Membrane Coagulated in Sulphate Based Coagulant. *Cerne* **2019**, *25*, 18–24. [CrossRef]
13. Zou, D.; Nunes, S.P.; Vankelecom, I.F.J.; Figoli, A.; Lee, Y.M. Recent Advances in Polymer Membranes Employing Non-Toxic Solvents and Materials. *Green Chem.* **2021**, *23*, 9815–9843. [CrossRef]
14. Livazovic, S.; Li, Z.; Behzad, A.R.; Peinemann, K.V.; Nunes, S.P. Cellulose Multilayer Membranes Manufacture with Ionic Liquid. *J. Membr. Sci.* **2015**, *490*, 282–293. [CrossRef]
15. Anokhina, T.S.; Pleshivtseva, T.S.; Ignatenko, V.Y.; Antonov, S.V.; Volkov, A.V. Fabrication of Composite Nanofiltration Membranes from Cellulose Solutions in an [Emim]OAc–DMSO Mixture. *Pet. Chem.* **2017**, *57*, 477–482. [CrossRef]
16. Durmaz, E.N.; Çulfaz-Emecen, P.Z. Cellulose-Based Membranes via Phase Inversion Using [EMIM]OAc-DMSO Mixtures as Solvent. *Chem. Eng. Sci.* **2018**, *178*, 93–103. [CrossRef]
17. Da Silva Meireles, C.; Filho, G.R.; Fernandes Ferreira, M.; Cerqueira, D.A.; Assunção, R.M.N.; Ribeiro, E.A.M.; Poletto, P.; Zeni, M. Characterization of Asymmetric Membranes of Cellulose Acetate from Biomass: Newspaper and Mango Seed. *Carbohydr. Polym.* **2010**, *80*, 954–961. [CrossRef]
18. Lopatina, A.; Anugwom, I.; Esmaeili, M.; Puro, L.; Virtanen, T.; Mänttäri, M.; Kallioinen, M. Preparation of Cellulose-Rich Membranes from Wood: Effect of Wood Pretreatment Process on Membrane Performance. *Cellulose* **2020**, *27*, 9505–9523. [CrossRef]
19. Zhang, S.; Kai, C.; Liu, B.; Zhang, S.; Wei, W.; Xu, X.; Zhou, Z. Facile Fabrication of Cellulose Membrane Containing Polyiodides and Its Antibacterial Properties. *Appl. Surf. Sci.* **2020**, *500*, 144046. [CrossRef]
20. Swatloski, R.P.; Spear, S.K.; Holbrey, J.D.; Rogers, R.D. Dissolution of Cellulose with Ionic Liquids. *J. Am. Chem. Soc.* **2002**, *124*, 4974–4975. [CrossRef]
21. Radhi, A.; Le, K.A.; Ries, M.E.; Budtova, T. Macroscopic and Microscopic Study of 1-Ethyl-3-Methyl-Imidazolium Acetate-DMSO Mixtures. *J. Phys. Chem. B* **2015**, *119*, 1633–1640. [CrossRef]
22. Zhong, X.; Li, R.; Wang, Z.; Wang, W.; Yu, D. Eco-Fabrication of Antibacterial Nanofibrous Membrane with High Moisture Permeability from Wasted Wool Fabrics. *Waste Manag.* **2020**, *102*, 404–411. [CrossRef]
23. Xia, Z.; Li, J.; Zhang, J.; Zhang, X.; Zheng, X.; Zhang, J. Processing and Valorization of Cellulose, Lignin and Lignocellulose Using Ionic Liquids. *J. Bioresour. Bioprod.* **2020**, *5*, 79–95. [CrossRef]
24. Le, K.A.; Rudaz, C.; Budtova, T. Phase Diagram, Solubility Limit and Hydrodynamic Properties of Cellulose in Binary Solvents with Ionic Liquid. *Carbohydr. Polym.* **2014**, *105*, 237–243. [CrossRef] [PubMed]
25. Saba, H.; Yumei, Z.; Huaping, W. Physical Properties and Solubility Parameters of 1-Ethyl-3-Methylimidazolium Based Ionic Liquids/DMSO Mixtures at 298.15 K. *Russ. J. Phys. Chem.* **2015**, *89*, 2381–2387. [CrossRef]
26. Wittmar, A.S.M.; Koch, D.; Prymak, O.; Ulbricht, M. Factors Affecting the Nonsolvent-Induced Phase Separation of Cellulose from Ionic Liquid-Based Solutions. *ACS Omega* **2020**, *5*, 27314–27322. [CrossRef] [PubMed]
27. Kim, D.; Nunes, S.P. Green Solvents for Membrane Manufacture: Recent Trends and Perspectives. *Curr. Opin. Green Sustain. Chem.* **2021**, *28*, 100427. [CrossRef]
28. Nevstrueva, D.; Pihlajamäki, A.; Nikkola, J.; Mänttäri, M. Effect of Precipitation Temperature on the Properties of Cellulose Ultrafiltration Membranes Prepared via Immersion Precipitation with Ionic Liquid as Solvent. *Membranes* **2018**, *8*, 87. [CrossRef]

29. Zhang, Y.; Shao, H.; Wu, C.; Hu, X. Formation and Characterization of Cellulose Membranes from N-Methylmorpholine-N-Oxide Solution. *Macromol. Biosci.* **2001**, *1*, 141–148. [CrossRef]
30. Duolikun, T.; Ghazali, N.; Leo, B.F.; Lee, H.V.; Lai, C.W.; Bin Johan, M.R. Asymmetric Cellulosic Membranes: Current and Future Aspects. *Symmetry* **2020**, *12*, 1160. [CrossRef]
31. Frollini, E.; Ass, B.A.P. Linters Cellulose: Characterization and Acetylation in N, n-Dimethylacetamide/Lithium Chloride. In Proceedings of the 5th International Symposium on Natural Polymers and Composites, 8th Brazilian Symposium on the Chemistry of Lignins and Other Wood Component. pp. 25–28. Available online: https://www.eucalyptus.com.br/artigos/2004 _Eigth+Symposium+Lignins+Wood+Components_Arquivo+78.pdf (accessed on 27 April 2022).
32. Sescousse, R.; Smacchia, A.; Budtova, T. Influence of Lignin on Cellulose-NaOH-Water Mixtures Properties and on Aerocellulose Morphology. *Cellulose* **2010**, *17*, 1137–1146. [CrossRef]
33. Melro, E.; Alves, L.; Antunes, F.E.; Medronho, B. A Brief Overview on Lignin Dissolution. *J. Mol. Liq.* **2018**, *265*, 578–584. [CrossRef]
34. Swensson, B.; Larsson, A.; Hasani, M. Dissolution of Cellulose Using a Combination of Hydroxide Bases in Aqueous Solution. *Cellulose* **2020**, *27*, 101–112. [CrossRef]
35. Shi, Z.; Yang, Q.; Cai, J.; Kuga, S.; Matsumoto, Y. Effects of Lignin and Hemicellulose Contents on Dissolution of Wood Pulp in Aqueous NaOH/Urea Solution. *Cellulose* **2014**, *21*, 1205–1215. [CrossRef]
36. Ribitsch, V.; Stana-Kleinschek, K.; Kreze, T.; Strnad, S. The Significance of Surface Charge and Structure on the Accessibility of Cellulose Fibres. *Macromol. Mater. Eng.* **2001**, *286*, 648–654. [CrossRef]
37. Ciacco, G.T.; Morgado, D.L.; Frollini, E.; Possidonio, S.; El Seoud, O.A. Some Aspects of Acetylation of Untreated and Mercerized Sisal Cellulose. *J. Braz. Chem. Soc.* **2010**, *21*, 71–77. [CrossRef]
38. Lindman, B.; Medronho, B.; Alves, L.; Costa, C.; Edlund, H.; Norgren, M. The Relevance of Structural Features of Cellulose and Its Interactions to Dissolution, Regeneration, Gelation and Plasticization Phenomena. *Phys. Chem. Chem. Phys.* **2017**, *19*, 23704–23718. [CrossRef]
39. Nelson, M.L.; O'Connor, R.T. Relation of Certain Infrared Bands to Cellulose Crystallinity and Crystal Lattice Type. Part II. A New Infrared Ratio for Estimation of Crystallinity in Celluloses I and II. *J. Appl. Polym. Sci.* **1964**, *8*, 1325–1341. [CrossRef]
40. Nelson, M.L.; O'Connor, R.T. Relation of Certain Infrared Bands to Cellulose Crystallinity and Crystal Latticed Type. Part I. Spectra of Lattice Types I, II, III and of Amorphous Cellulose. *J. Appl. Polym. Sci.* **1964**, *8*, 1311–1324. [CrossRef]
41. Zhang, W.; Hallström, B. Membrane Characterization Using the Contact Angle Technique I. Methodology of the Captive Bubble Technique. *Desalination* **1990**, *79*, 1–12. [CrossRef]
42. Karatzos, S.K.; Edye, L.A.; Wellard, R.M. The Undesirable Acetylation of Cellulose by the Acetate Ion of 1-Ethyl-3-Methylimidazolium Acetate. *Cellulose* **2012**, *19*, 307–312. [CrossRef]
43. Ciolacu, D.; Ciolacu, F.; Popa, V.I. Amorphous Cellulose—Structure and Characterization. *Cellul. Chem. Technol.* **2011**, *45*, 13–21.
44. Li, X.L.; Zhu, L.P.; Zhu, B.K.; Xu, Y.Y. High-Flux and Anti-Fouling Cellulose Nanofiltration Membranes Prepared via Phase Inversion with Ionic Liquid as Solvent. *Sep. Purif. Technol.* **2011**, *83*, 66–73. [CrossRef]
45. Kljun, A.; Benians, T.A.S.; Goubet, F.; Meulewaeter, F.; Knox, J.P.; Blackburn, R.S. Comparative Analysis of Crystallinity Changes in Cellulose i Polymers Using ATR-FTIR, X-Ray Diffraction, and Carbohydrate-Binding Module Probes. *Biomacromolecules* **2011**, *12*, 4121–4126. [CrossRef] [PubMed]
46. Poyraz, B.; Tozluoğlu, A.; Candan, Z.; Demir, A.; Yavuz, M.; Büyuksarı, Ü.; Ünal, H.İ.; Fidan, H.; Saka, R.C. TEMPO-Treated CNF Composites: Pulp and Matrix Effect. *Fibers Polym.* **2018**, *19*, 195–204. [CrossRef]
47. Ma, B.; Qiao, X.; Hou, X.; He, C. Fabrication of Cellulose Membrane with "Imprinted Morphology" and Low Crystallinity from Spherulitic [Bmim]Cl. *J. Appl. Polym. Sci.* **2016**, *133*, 1–7. [CrossRef]
48. Liu, Y. Recent Progress in Fourier Transform Infrared (FTIR) Spectroscopy Study of Compositional, Structural and Physical Attributes of Developmental Cotton Fibers. *Materials* **2013**, *6*, 299–313. [CrossRef]
49. Gabov, K.; Oja, T.; Deguchi, T.; Fallarero, A.; Fardim, P. Preparation, Characterization and Antimicrobial Application of Hybrid Cellulose-Lignin Beads. *Cellulose* **2017**, *24*, 641–658. [CrossRef]
50. Wang, Z.; Winestrand, S.; Gillgren, T.; Jönsson, L.J. Chemical and Structural Factors Influencing Enzymatic Saccharification of Wood from Aspen, Birch and Spruce. *Biomass Bioenergy* **2018**, *109*, 125–134. [CrossRef]
51. Rajesh, S.; Shobana, K.H.; Anitharaj, S.; Mohan, D.R. Preparation, Morphology, Performance, and Hydrophilicity Studies of Poly(Amide-Imide) Incorporated Cellulose Acetate Ultrafiltration Membranes. *Ind. Eng. Chem. Res.* **2011**, *50*, 5550–5564. [CrossRef]
52. Zheng, X.; Plume, S.; Ernst, M.; Croué, J.P.; Jekel, M. In-Line Coagulation Prior to UF of Treated Domestic Wastewater—Foulants Removal, Fouling Control and Phosphorus Removal. *J. Membr. Sci.* **2012**, *403–404*, 129–139. [CrossRef]
53. Koh, K.Y.; Zhang, S.; Chen, J.P. Improvement of Ultrafiltration for Treatment of Phosphorus-Containing Water by a Lanthanum-Modified Aminated Polyacrylonitrile Membrane. *ACS Omega* **2020**, *5*, 7170–7181. [CrossRef]
54. Hyvän Pilotointi on Meneillään Toikansuolla Lappeenrannan Energia. Available online: https://www.lappeenrannanenergia.fi/hyva-blogi/hyvan-pilotointi-meneillaan-toikansuolla (accessed on 27 April 2022).
55. Warsinger, D.M.; Chakraborty, S.; Tow, E.W.; Plumlee, M.H.; Bellona, C.; Loutatidou, S.; Karimi, L.; Mikelonis, A.M.; Achilli, A.; Ghassemi, A.; et al. A Review of Polymeric Membranes and Processes for Potable Water Reuse. *Prog. Polym. Sci.* **2018**, *81*, 209–237. [CrossRef] [PubMed]
56. Yang, M.; Hadi, P.; Yin, X.; Yu, J.; Huang, X.; Ma, H.; Walker, H.; Hsiao, B.S. Antifouling Nanocellulose Membranes: How Subtle Adjustment of Surface Charge Lead to Self-Cleaning Property. *J. Membr. Sci.* **2021**, *618*, 118739. [CrossRef]

Publication IV

Lopatina, A., Esmaeili, M., Anugwom, I., Mänttäri, M., and Kallioinen-Mänttäri, M.

Effect of Low Concentrations of Lithium Chloride Additive on Cellulose-Rich Ultrafiltration Membrane Performance

Article

Effect of Low Concentrations of Lithium Chloride Additive on Cellulose-Rich Ultrafiltration Membrane Performance

Anastasiia Lopatina *[ID]**, Mohammadamin Esmaeili** [ID]**, Ikenna Anugwom, Mika Mänttäri** [ID]
and Mari Kallioinen-Mänttäri [ID]

Department of Separation Science, LUT School of Engineering Science, LUT University, P.O. Box 20,
FI-53851 Lappeenranta, Finland
* Correspondence: anastasiia.lopatina@lut.fi

Abstract: Various water treatment processes make extensive use of porous polymeric membranes. A key objective in membrane fabrication is to improve membrane selectivity without sacrificing other properties such as permeability. Herein, LiCl (0–2 wt.%) was utilised as a preforming agent in fabricating biomass-derived cellulosic membranes. The fabricated membranes were characterised by dope solution viscosity, surface and cross-sectional morphology, pure water flux, relative molecular mass cut-off (MWCO, 35 kDa), membrane chemistry, and hydrophilicity. The results demonstrated that at the optimum LiCl concentration (0.4 wt.%), there is an interplay of thermodynamic instability and kinetic effects during membrane formation, wherein the membrane morphology and hydrophilicity can be preferably altered and thus lead to the formation of the membrane with better rejection at no detriment to its permeability.

Keywords: lithium chloride; wood; membrane fabrication; ultrafiltration; 1-ethyl-3-methylimidazolium acetate; choline chloride; lactic acid

1. Introduction

Pressure-driven membrane filtration is universally utilised to treat wastewater in different fields. A wide selection of polymeric membranes allows precise tailoring of the treatment process, using particular advantages of a membrane's characteristics to the process's benefit [1–3]. Cellulose-based membranes are usually defined to be hydrophilic, biodegradable, and low-fouling, thus having an advantage over most petroleum-based polymeric membranes [4,5]. The use and fabrication of cellulose-based pressure-driven membranes represent the development of more environmentally intelligent technologies as it both meets the demand for renewable materials and provides reliable and highly efficient treatment of waste streams without secondary pollution [1,3,6]. The general challenge, however, in manufacturing cellulose membranes is finding the appropriate solvent system for cellulose dissolution and regeneration. Recently, the research has been focused on using ionic liquids (ILs), the class of solvents consisting of a mixture of solely ions with a melting point usually below 100 °C, and their different combinations with co-solvents [7–10]. The utilisation of ILs for cellulose and biomass dissolution and treatment has been consecutively studied over the last two decades [11–14]. Various ILs have been successfully utilised for biomass and cellulose dissolution, preparation of composite materials, and fabrication of cellulose-based membranes [4,15–20]. However, the performance of lab-made cellulose-based membranes is usually less effective compared to both lab-made petroleum-based polymeric membranes and commercial membranes [21]. Different strategies are utilised to improve the performance of lab-made cellulose-based membranes, including the variations in the used coagulation bath conditions, the choice of cellulose solvents, and the utilisation of additives [4,22,23].

Lithium chloride (LiCl) is a well-known pore-forming additive and has been abundantly tested for the production of polymeric membranes with higher permeance rates [22,24–28]. One of the reasons why lithium chloride is principally appealing as an inorganic salt additive for membrane casting solutions is that LiCl interacts strongly to form complexes with solvents frequently used for membrane preparation [27]. However, the reported concentrations of both the polymer and the additive were usually higher than 5 wt.%, thus raising concerns about the sustainability of LiCl utilisation, keeping in mind the scarcity of lithium resources [27,29,30].

LiCl has already contributed to the development of cellulose dissolution studies, being part of the LiCl/ dimethylacetamide (DMac) solvent system [31–33]. Some of the studies also report the positive effect of the addition of LiCl to ILs and dimethylsulfoxide (DMSO) on the dissolution of cellulose and biomass in general [14,34,35]. Though studies are reporting the effect of LiCl addition on the properties of cellulose acetate membranes, to the current knowledge, there is no study reporting the influence of LiCl over the performance of cellulose-based membranes, especially the ones that are made from partially purified biomass source [36].

The present study aims to investigate the effect of LiCl salt on the rheology of dope solutions containing 1-ethyl-3-methylimidazolium acetate ([Emim][OAc])–DMSO–biomass-derived cellulose and further its role on the morphology and performance of fabricated biomass-derived cellulosic membranes. The cellulose-rich membranes were prepared using the wet-phase inversion technique. The casting solution was prepared from birch biomass pretreated with deep eutectic solvent (DES) for partial delignification and consequently bleached for further purification of the cellulose fraction; the detailed procedure and its effect on the biomass composition can be found in the previous publication [37]. The treated biomass was dissolved in the [Emim][OAc]–DMSO–LiCl system. The LiCl concentration was kept below 2 wt.% to take advantage of LiCl being a suitable pore former and additive and study its effect on the membranes' morphology and performance while bearing in mind the scarcity of LiCl.

2. Materials and Methods

2.1. Materials

Debarked birch chips (*Betula pendula*) with an average size of $5 \times 1 \times 0.1$ cm were used as source material for all described operations. DES treatment was applied for partial delignification of the biomass. Utilised DES consisted of choline chloride (ChCl, CAS # 67-48-1, Merck KGaA, Darmstadt, Germany), acting as a hydrogen bond acceptor (HBA), and lactic acid (LAc, CAS # 79-33-4, Merck KGaA, Darmstadt, Germany), acting as hydrogen bond donor (HBD). Deionised (DI) water mixed with ethanol at a 1:9 ratio was used for washing residual DES from treated biomass. Consequent bleaching of biomass was completed using acetic acid (CAS # 64-19-7, Merck KGaA, Darmstadt, Germany) and sodium chlorite (CAS # 7758-19-2, Acros Organics, Geel, Belgium). Ionic liquid (95% 1-ethyl-3-methylimidazolium acetate; C_1C_2ImOAc, CAS # 143314-17-4, Iolitec Ionic Liquids Technologies GmbH, Heilbronn, Germany) mixed with dimethylsulphoxide (CAS # 67-68-5, Merck KGaA, Darmstadt, Germany) at a 2:8 mass ratio was used for the preparation of the casting solution.

Non-woven polyester was used as a support material for the membrane preparation and was taken from used reverse osmosis (RO) membranes and cleaned mechanically and chemically. CENTRA-R 60\120 system (Elga purification system, Veolia Water, Lane End, UK) was used to produce ultra-pure DI water (15 MΩ, 0.5–1 μS/cm), which was used for the washing process, preparation of water-based solutions, and as a non-solvent in the coagulation bath. Anhydrous LiCl (CAS # 7447-41-8, Merck KGaA, Darmstadt, Germany) was used as an additive. Polyethylene glycol (PEG, approx. M_w 35 000 g/mol, CAS # 25322-68-3, Merck KGaA, Darmstadt, Germany) was used to prepare a model solution for the membrane retention study.

2.2. Methods

2.2.1. DES Treatment

For the partial delignification of the birch woodchips, ChCl and LAc were taken at a 1:9 mole ratio, respectively, and mixed at 100 °C until a clear homogeneous mixture formed. The DES treatment was performed at a 1:5 solid-to-liquid mass ratio for 18 h at constant heating at 105 °C. The treated pulp was filtered through a filter paper under vacuum and washed with an ethanol/water mixture at a 9:1 volume ratio. The DES-treated pulp was moved to an oven and dried at 50 °C for 24 h.

2.2.2. Bleaching

The bleaching of dried pulp was performed with DI water, sodium chlorite and acetic acid taken at an 80 mL:1 g:0.5 mL ratio to each 2.5 g of biomass. Bleaching was performed at constant heating at 70 °C for 60 min with repeated stirring every 5–7 min to ensure even treatment of the pulp load. At the end of the reaction (when the pulp was almost white-coloured), the pulp was separated from the liquid and subsequently washed with water, ethanol, and acetone. Then the pulp was dried in the oven at 50 °C until the measured weight difference was less than 1%.

2.2.3. Membrane Preparation

For the preparation of the casting solution, LiCl in various concentrations was dissolved in the mixture of [Emim][OAc] and DMSO. After the dissolution of the additive was completed, the DES-treated and bleached pulp was added to the solution in small portions up to 5 wt.-% concentration. The solution was continuously heated at 100 °C (Heidolph Instruments GmbH & CO., Schwabach, Germany) under a constant stirring rate of 200 rpm until the pulp dissolved.

Automatic Film Applicator L (BYK-Gardner, Geretsried, Germany) was used for membrane casting: a prepared solution was cooled down to room temperature, poured on a casting plate with attached polyester support, and spread on a flat surface by casting knife with 300 μm casting thickness and 50 mm/s speed. Immediately after casting, the casting plate was transferred into a water coagulation bath (0 °C), where it was kept for 24 h. After the coagulation bath, membranes were washed under the DI water current to guarantee the complete removal of the solvents from the membrane structure. Circular coupons of 0.0038 m^2 area were cut for further use.

2.2.4. Casting Solutions Viscosity Measurements

The viscosity of the casting solutions cooled down to room temperature was measured based on Stokes' law using the falling sphere method performed in the vertical glass cylinder. The measurement of each solution was repeated five times, and the presented results are averaged values.

2.2.5. Membrane Permeability and Retention Measurements

Amicon dead-end stirring cell equipment (Millipore, Temecula, CA, USA, Cat No.: XFUF07611; diameter of the stirring device: 60 mm) was used to measure the permeability and retention of the prepared membranes (see Figure 1). Prior to the filtration experiments, each membrane was compacted for 1 min at 1 bar, 2 min at 2 bars, 3 min at 3 bars, 4 min at 4 bars, and 20 min at 5 bars. The compaction process guaranteed the complete removal of the solvents used in the membrane manufacturing from the membrane pores. A permeate sample collected during the membrane compaction at 5 bars was analysed for total organic carbon (TOC) content to prove the absence of solvents' remains.
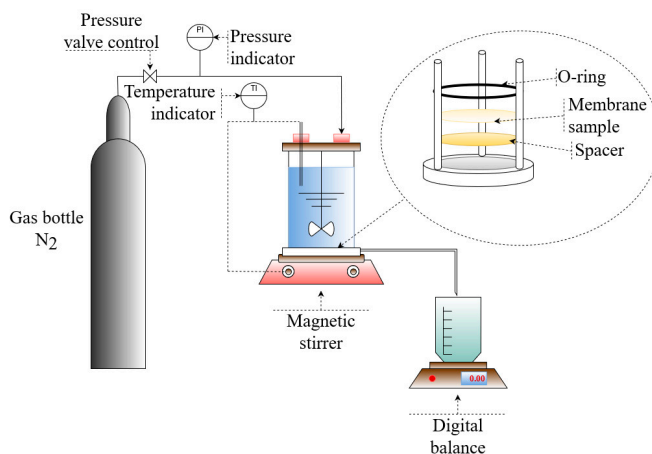
Figure 1. Amicon dead-end filtration system's schematic configuration [38].

For the determination of pure water permeability, membranes' water flux was measured at 25 ± 0.5 °C at 1, 2, 3, and 4 bars of pressure, calculated using Equation (1), and plotted as a function of pressure:

$$J = \frac{Q_p/100}{A \cdot \frac{t}{60}},$$ (1)

where J is the tested membrane's flux (L/(m^2·h)), Q_P is the gravimetric flow of water permeating through the membrane (g/min), A is the area of the membrane sample (m^2), and t is the time of collection of the permeate (min).

The retention of the produced membranes was studied with a model solution of PEG 35 kDa at a concentration of 300 ppm, which was filtered through the membrane samples at comparable flux values. All measurements were performed at 300 rpm stirring speed and 25 ± 0.5 °C. The feed, retentate, and permeate samples were collected and analysed for TOC content with a Shimadzu TOC analyser (TOC-L series, Japan). Equation (2) was used to calculate the retention values:

$$R = \left(1 - \frac{2 \cdot C_p}{C_f + C_r}\right) \times 100,$$ (2)

where C_p, C_f, and C_r are the TOC concentrations in the permeate, feed, and retentate (mg/L), respectively.

2.2.6. SEM Analysis

The morphology of the prepared membranes was studied with the scanning electron microscope (Hitachi SU 3500, Tokyo, Japan) at an acceleration voltage of 1.5 kV in high vacuum conditions. For the analysis, the membrane samples were dried in Manual Freeze Dryer ALPHA 2-4 LDplus (Martin Christ GmbH, Osterode am Harz, Germany). The top surfaces of the membranes were analysed straight after freeze-drying. For the cross-sectional images, the narrow strips of membranes were cut and broken with two pairs of forceps under the liquid nitrogen to obtain a clean cut.

2.2.7. Examination of the Chemical Structure of the Membranes

Frontier MIR/FIR Spectrometer (PerkinElmer Inc., Rodgau Germany) equipped with a diamond crystal was used to analyse the chemical structure of the membrane samples. The spectral range was 400–4000 cm^{-1}, with a spectra resolution of 4 cm^{-1}. Five points were measured from each membrane and averaged. All the spectra were processed for the graphical representation with ATR correction, baseline correction, and normalisation. The ratio of the non-normalised absorption bands A_{1430}/A_{899} was used to calculate a lateral order index (LOI), as was proposed by Nelson and O'Connor [39,40].

2.2.8. Contact Angle Measurements

The captive bubble method was applied for the evaluation of membrane hydrophilicity by a measure of static contact angle [41]. KSV CAM 101 equipment (KSV Instruments Ltd., Espoo, Finland) connected to a CCD camera (DMK 21F04, The Imaging Source Europe GmbH, Bremen, Germany) was used to measure contact angles. Each tested membrane was attached to a piece of glass with double-sided tape and submerged in DI water at room temperature. A U-shaped needle placed approximately 3–4 μL of air bubble volume on the membrane surface. Six points were measured from each membrane and averaged. The taken images were treated by curve fitting analysis with CAM 2008 software (Sydney Australia).

2.2.9. Contact Angle Measurements

The water uptake capacity of the membrane samples was used to determine the membranes' porosity. After being soaked in DI water for 24 h and carefully mopped with filter paper to remove the excess water, the wet membrane sample was weighed. Afterwards, the wet sample was dried in an oven at 60 °C for 24 h. The dry weight of the membrane sample was then measured until the sample weight became constant. The membrane porosity of the sample was subsequently calculated using Equation (3):

$$\varepsilon = \frac{w_w - w_d}{\rho_w A l},\tag{3}$$

where ε is the membrane's porosity, w_w and w_d are the weights of the wet and dry membrane samples (g), respectively, ρ_w is the density of water at the temperature recorded during the measurement (23 °C) (0.997538 g/cm^3), A is the area of the membrane samples (cm^2), and l is the thickness of the membrane sample (cm), measured from the SEM images. The reported measurements are the averaged results from at least two membrane samples.

2.2.10. Membrane Zeta Potential Measurement

The SurPASS electrokinetic Analyzer (Anton Paar GmbH, Graz, Austria) was used to measure the zeta potential of the membranes' samples with an adjustable gap cell method and using 0.001 M KCl solution as a background electrolyte. Before the measurement, the membranes were kept in a fridge at approximately 4 °C for 24 h. The measurement started from pH 7.5, to which it was shifted by the addition of 0.1 M KOH solution and then automatically titrated to 2.7 using 0.05 M HCl solution as the analysis was carried on. The final value of the zeta potential was calculated automatically by SurPASS software (Anton Paar GmbH, Graz, Austria) based on the Helmholtz–Smoluchowski equation.

3. Results and Discussion

3.1. The Effect of LiCl Content on the Viscosity of Polymer Solution

Viscosity possesses a crucial role in controlling the formation kinetics of the membrane on both the skin layer and the sublayer level, which ultimately defines the performance of the fabricated membranes [42]. Figure 2 shows the effect of LiCl dosage on the viscosity of the casting solutions. Herein, the obtained viscosities align with the cellulose's solution viscosities measured and reported in previous studies [43,44]. Although the role of LiCl in the changes happening to the casting solution viscosity has been highlighted in several studies, its effect on the viscosity of a complex interacting polymer solution mixture con-

taining ionic liquid, DMSO, cellulose, and lignocellulose material has not been investigated to date [25,27,45,46]. As seen in Figure 2, the viscosity is sensitive to the amount of LiCl, and two distinct viscosity trends can be distinguished concerning the amount of added LiCl. A linear increase in viscosity with a successive increase in LiCl content up to 0.4 wt.% can be observed, after which it decreases by about 33% when the LiCl concentration reaches 2 wt.%.
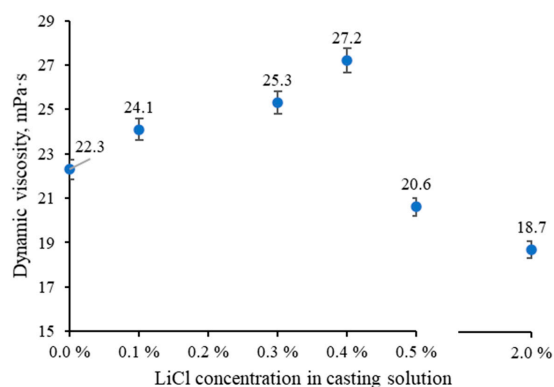

Figure 2. Dynamic viscosity values were measured with the falling sphere method at 23 °C.

The initial increase in viscosity can be attributed to the strong interactions between Li^+ cation and electron donor groups within the solvent mixture [Emim][OAc]–DMSO, resulting in the reduced overall solvating power which in turn causes the formation of more prominent clusters of the polymer chains and thus increasing the viscosity [47–50]. It is worth mentioning that there is another possible interaction between the Li^+ cation and hydroxyl groups in lignocellulose, which can aid swelling and dissolution of ligno-cellulose, especially hemicellulose and lignin when added to the ILs and DMSO solutions [14,34,35,51,52]. The decrease in dope solution viscosity at LiCl concentration above 0.4 wt.% could be related to the change of its interaction nature. It is known that alkali salts greatly influence intermolecular interactions when dissolved in DMSO solvent, destroying entanglement networks within molecular chains and, consequently, reducing viscosity [53].

3.2. The Effect of LiCl Content on the Morphology of the Membranes

3.2.1. Physical Structure of the Membranes

Figures 3–5 show that the top layer morphologies and the cross-sections of membranes cast from LiCl-doped solutions are compared with the membrane cast from the unmodified solution. As can be seen (Figure 3), LiCl positively affects the dissolution process, resulting in a smaller number of visible fibrils and a smoother top layer. A positive effect of the presence of LiCl on the dissolution process in IL media has been reported for different kinds of polymers [14,34,51]. Up to 0.4% LiCl addition, membranes demonstrate smoothing of the top surface, which correlates well with the increase in the viscosity of the casting solutions and, thus, higher resistance of mass transfer during the phase inversion process and, eventually, delayed demixing and denser morphology (Figure 2). The 0.5 and 2 wt.% LiCl membranes show openings in the top layer, which agrees well with the lower viscosity of the respective casting solutions and the theory behind precipitation phenomena, where lower viscosity of the casting solution leads to quicker solvent-nonsolvent exchange process and thus more open membrane morphology [54].
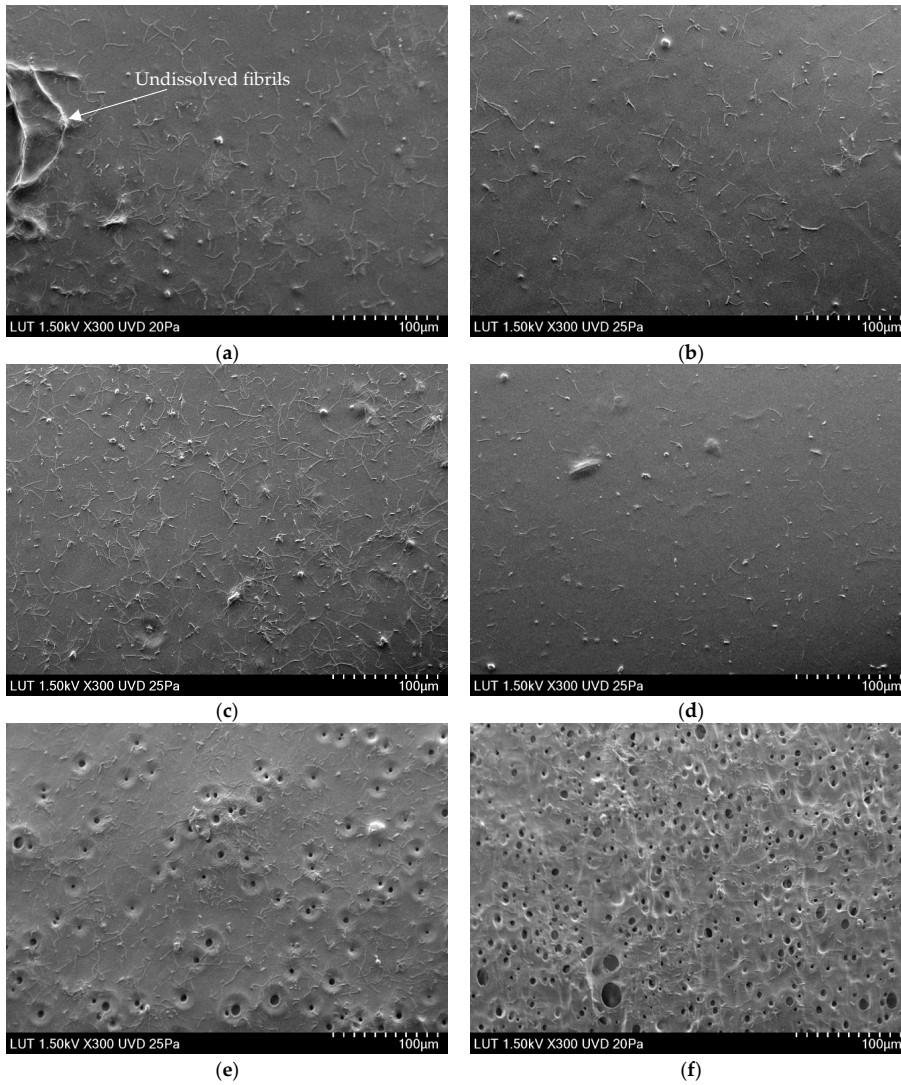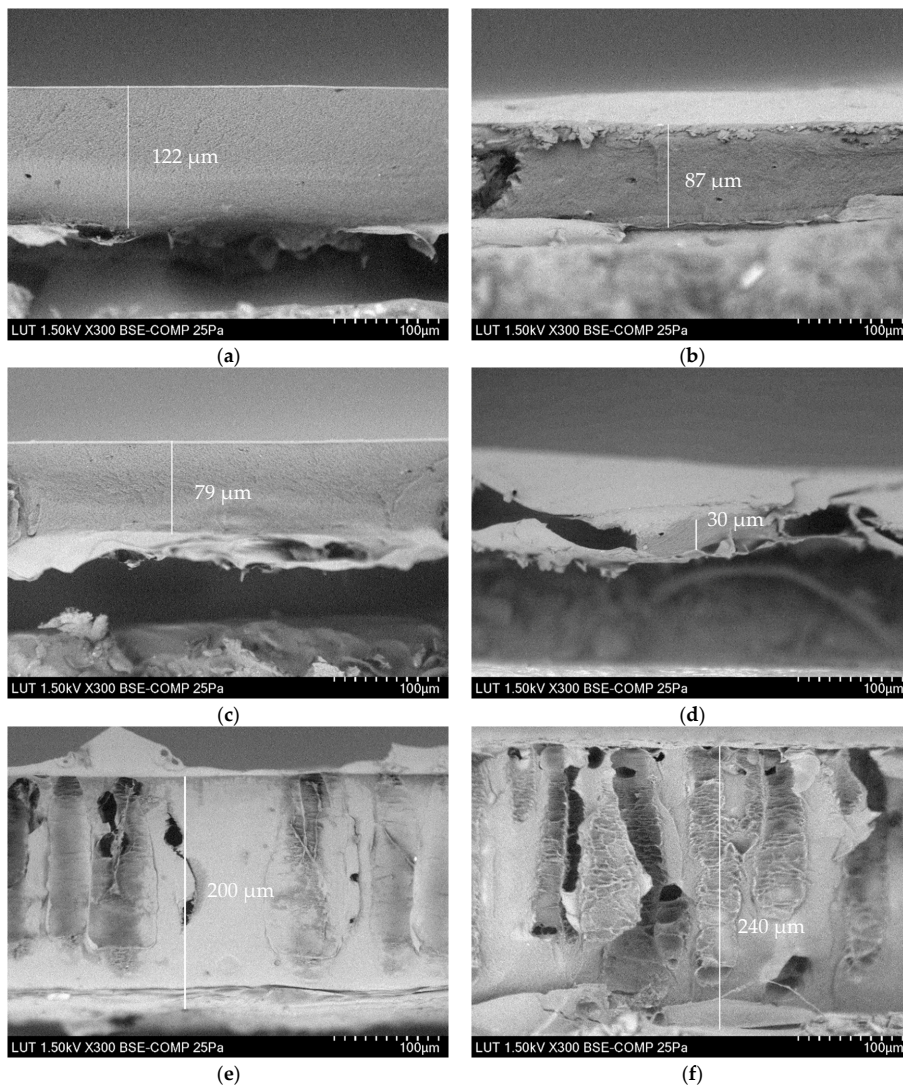
Figure 3. SEM images of membrane top surfaces taken via scanning electron microscope (Hitachi SU 3500, Japan) at an acceleration voltage of 1.5 kV in high vacuum conditions: (**a**) 0 wt.% LiCl, (**b**) 0.1 wt.% LiCl, (**c**) 0.3 wt.% LiCl, (**d**) 0.4 wt.% LiCl, (**e**) 0.5 wt.% LiCl, (**f**) 2 wt.% LiCl.
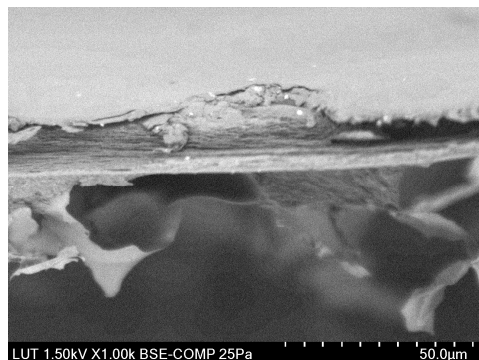
Figure 4. SEM images of membrane cross-sections taken via scanning electron microscope (Hitachi SU 3500, Japan) at an acceleration voltage of 1.5 kV in high vacuum conditions: (**a**) 0 wt.% LiCl, (**b**) 0.1 wt.% LiCl, (**c**) 0.3 wt.% LiCl, (**d**) 0.4 wt.% LiCl, (**e**) 0.5 wt.% LiCl, (**f**) 2 wt.% LiCl.

Figure 5. SEM image of 0.4 wt.% LiCl membrane's cross-section taken via scanning electron microscope (Hitachi SU 3500, Japan) at an acceleration voltage of 1.5 kV in high vacuum conditions.

3.2.2. Thickness of the Membranes

In phase-inversion processes, the viscosity of the polymer solution can affect membrane thickness and interdiffusion of solvent and non-solvent [55,56]. According to general consensus, instantaneous demixing accelerates the precipitation of polymer chains, thereby increasing the membrane thickness, while delayed demixing delays precipitation completion [55]. As the viscosity of the casting solution increased continuously, from 0 wt.% to 0.4 wt.% LiCl concentration, the resulting membranes demonstrate similar sponge-like structures without macrovoids, which is a common feature of cellulose membranes precipitated from ILs' solutions (Figure 4) [17]. It has also been reported that lithium-based additives positively affect the suppression of macrovoids formation [57]. As a result of the gradually increased casting solution's viscosity and delayed demixing, the precipitation process finalised over a longer time, and thereby the thickness of the membrane decreased by ~75.4% (compared to the unmodified membrane) when the LiCl content reached 0.4 wt.%. At LiCl dosage above 0.4 wt.% in dope solution, the viscosity of polymer solution is drastically decreased (see Figure 2). At higher than 0.4 wt.% LiCl dosage, the thermodynamic miscibility of casting solution reduces and consequently promotes the kinetics of solvent outflux and non-solvent influx, which in turn increases the overall thickness of the membrane. As shown from the cross-section micrographs of modified membranes with 0.5 and 2% LiCl presented in Figure 3, the sponge structure gradually changes towards finger-like pores. This alteration can be attributed to the role of lower viscosity, reduction of thermodynamic stability of polymer solution and potential release of LiCl to the coagulation bath, which all lead to a faster exchange rate of solvent and non-solvent and formation of more open membranes [26,49,58].

The magnified cross-section of 0.4 wt.% LiCl membrane is depicted in Figure 5 to highlight its different morphology. It can be seen that only 0.4 wt.% LiCl membrane demonstrates a multi-layered structure, whereas the membranes with lower concentrations of LiCl show sponge-like morphologies and membranes with higher LiCl concentrations developed finger-like pores (see Figure 4). Although this kind of morphology alteration has been previously reported for more significant differences in salt concentrations, it might be concluded that in this particular complex system, even a more minor change in LiCl concentration possesses immense effect over the formed membranes' morphology [59].

3.3. The Effect of LiCl Content on the Chemical Structure of the Membranes

FTIR spectra of unmodified membrane and modified with LiCl ones were recorded to evaluate the possible occurrence of chemical changes or interaction within the membrane structure (see Figure 6). Regardless of the added amount of LiCl, the spectra demonstrate

the presence of the typical cellulose membrane's peaks, the assignments of which can be found in the literature [37,60–64]. The peaks of practical interest are located at 1430 cm^{-1}, representing in-plane symmetric bending characteristic of cellulose I$_\beta$ crystal, and at 899 cm^{-1}, characteristic of amorphous cellulose regions' C-H deformation in β-glycosidic linkages. The absorbance values ratio at these peaks (A$_{1430}$/A$_{899}$) represents the amount of crystalline and amorphous cellulose in the membrane's matrix or the lateral order index (LOI). The lower the value of LOI, the less ordered the cellulose structure and hence the lower the crystallinity [39,40,65]. The calculation shows a distinctive difference between LOI values of 0.1, 0.3, 0.5, and 2% LiCl membranes (all showing the LOI values within 1.21–1.23 interval) and 0 and 0.4% LiCl membranes, showing LOI of 1.33 and 1.28, respectively, indicating higher content of crystalline cellulose in those membranes. Although previously it has been stated that LiCl addition does not affect the crystallinity of the polymers [57], it might work differently for the cellulose regenerated from solutions with higher viscosity due to delayed demixing and improved orientation of the regenerated crystals and amorphous regions along the fibre axis [9].
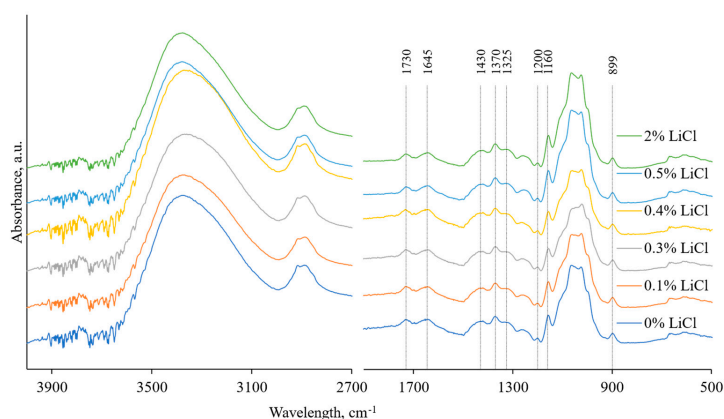

Figure 6. FTIR spectra of tested membranes were recorded using the Perkin Elmer Frontier spectrometer with a universal ATR module of diamond crystal at a resolution of 4 cm^{-1} in the absorbance mode.

3.4. The Effect of LiCl Content on Hydrophilicity and Zeta Potential of the Membranes

Several factors influence the contact angle value, such as roughness, hydrophobicity or hydrophilicity, pore size and porosity, and distribution of pores. Figure 7 depicts changes in the membranes' apparent contact angles and estimated porosities. All the tested membranes show the contact angle values typical for the regenerated cellulose membranes [5,52,66,67]. Generally, LiCl is reported to have a slight positive effect on the membranes' surface hydrophilicity when coupled with petroleum-based polymeric membranes [47]. However, considering that the 0 wt.% LiCl membrane was very hydrophilic already before the LiCl addition (see. Figure 7), the addition of LiCl seems not to be having a similar effect on the hydrophilicity. It is worth stressing that the measured contact angle values are highly dependent on the surface's morphology, which notably differs from one membrane sample to another and poses an effect over the measured values (see Figure 3).
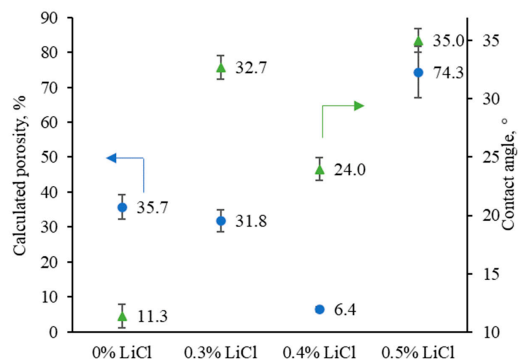
Figure 7. Variations in membranes' porosity and contact angle as a function of LiCl additive concentration in the casting solution; the contact angle values of the prepared membranes were recorded using the captive bubble method with KSV CAM 101 equipment connected to a CCD camera.

The zeta potential versus the pH of the reference and LiCl-modified membranes are presented in Figure 8. As can be seen, there is generally a negatively charged surface on the fabricated membranes over a wide pH range (4 to 7). Further confirmation of the speculation of changed interactions before and after 0.4 wt.% and induced solvent power by the addition of LiCl can also be noted in the isoelectric point shift of the modified membranes with 0.3 and 0.5 wt.% towards lower pH [68]. In general, with the increase in crystalline content in cellulose, the accessibility towards its charged group is more complicated compared to amorphous regions. As a result, it leads to cellulose with less negative surface charge [52]. Compared to the other membranes, 0 wt.% and 0.4wt.% LiCl ones showed a higher lateral order index, i.e., higher crystalline cellulose content, which can be considered a possible reason for their less negative surface charge. Another reason for increased zeta potential values can be found in the other membranes' considerably higher overall porosity, including surface porosity. For example, the overall porosity of modified membranes with 0.3 and 0.5 wt.% increased by ~4.9 and ~11.6 times compared to 0.4 wt.% modified membrane. According to previously published reports, the increase in the accessibility of functional groups results in more negative net ζ-potential, which inevitably follows the formation of multiple openings when 0.5 wt.% LiCl is added (see Figure 3e) [68–72].
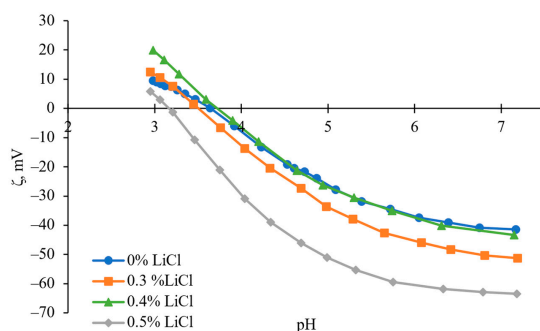

Figure 8. The zeta potential curves of prepared membranes were recorded using a SurPASS electrokinetic analyser with the adjustable gap cell method and using 0.001 M KCl solution as an electrolyte.

3.5. The Effect of LiCl Content on the Filtration Performance of the Membranes

The performance of the prepared membranes as a function of the addition of LiCl is reported in Figure 9. The performance of fabricated membranes, i.e., flux and retention behaviours, are in accordance with the membranes' morphology and the viscosity of the dope solutions. The pure water flux of the membrane was slightly increased with the increase in LiCl content up to 0.4 wt.%, which can be related to the reduction of membrane thickness (see Figure 4). Due to the dominant role of viscosity, particularly at the highest one (i.e., 0.4 % LiCl dosage, see Figure 2), the solvent/non-solvent mutual diffusion is hindered, and so-called delayed demixing takes place, resulting in the formation of denser structure (see Figure 7). Slow demixing results in nucleation after a specific time, which increases polymer concentration in the top layer. After that, nucleation occurs successively over a short period of time in the inferior layer. Hence, it can be said that slow demixing prevents the unrestrained growth of limited nuclei on the top layer, resulting in many small nuclei scattered throughout the film [73].
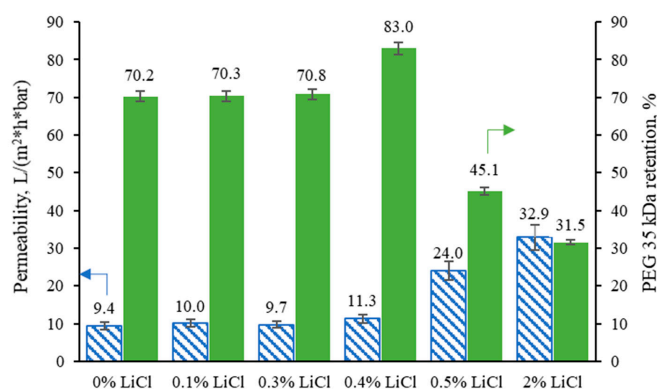

Figure 9. Pure water permeability values were measured at 1 bar, and PEG 35 kDa of the tested membranes was measured in an Amicon ultrafiltration cell at 25 °C and a mixing rate of approximately 300 rpm.

Consequently, the suppression of macrovoids and the formation of denser structure occurs, which can be considered a reason for the ~13% improvement of PEG 35 kDa retention for membrane fabricated at 0.4 wt.% LiCl content compared to the 0 wt.% membrane. At a concentration above 0.4 wt.%, the possible washing out of the salt from the membrane matrix and the viscosity reduction (see Figure 2) enhances the solvent/non-solvent exchange rate, i.e., instantaneous demixing. It thus leads to the formation of more open membranes (see Figure 3) with higher porosity (see Figure 7), which dominates a trade-off between higher permeability and worse selectivity.

4. Conclusions

In this work, cellulose-based ultrafiltration membranes were prepared from wood using a wet phase inversion casting method. Lithium chloride was chosen as a good pore-forming additive and added to the mixture of [Emim][OAc] and DMSO before adding DES-treated and bleached birch biomass. The concentration range for LiCl was kept low to study the effect of low concentrations and suggest the sustainable concentration of the additive. Based on the available literature, the expected outcome was an increase in membranes' permeability. However, the results showed that in the mixture with wood-based biomass of complex composition and chosen solvents, the effect of LiCl over the membrane morphology and performance did not repeat the same trends as it did with other polymers. Even small changes in the amount of added LiCl were found to have an immense effect

on the viscosity of casting solutions and the morphology of the formed membranes. The optimum concentration of the LiCl additive was found to be 0.4 wt.%, where an improvement of the separation efficiency by 13% is observed without the loss of permeability. In contrast, the further increase in LiCl dosage was impractical. The complexity of LiCl interactions with wood polymers chains, solvent, and co-solvent molecules might explain why LiCl shows different effects over the casting solution viscosity and consequently on the membrane's morphology and performance depending on the concentration, where even the tiny alteration changes the entire outcome of LiCl presence.

References

1. Goh, P.S.; Othman, M.H.D.; Matsuura, T. Waste Reutilization in Polymeric Membrane Fabrication: A New Direction in Membranes for Separation. *Membranes* **2021**, *11*, 782. [CrossRef] [PubMed]
2. Zou, D.; Nunes, S.P.; Vankelecom, I.F.J.; Figoli, A.; Lee, Y.M. Recent Advances in Polymer Membranes Employing Non-Toxic Solvents and Materials. *Green Chem.* **2021**, *23*, 9815–9843. [CrossRef]
3. Van der Bruggen, B.; Vandecasteele, C.; Van Gestel, T.; Doyenb, W.; Leysenb, R. Review of Pressure-Driven Membrane Processes. *Environ. Prog.* **2003**, *22*, 46–56. [CrossRef]
4. El Seoud, O.A.; Kostag, M.; Jedvert, K.; Malek, N.I. Cellulose Regeneration and Chemical Recycling: Closing the "Cellulose Gap" Using Environmentally Benign Solvents. *Macromol. Mater. Eng.* **2020**, *305*, 1900832. [CrossRef]
5. Livazovic, S.; Li, Z.; Behzad, A.R.; Peinemann, K.V.; Nunes, S.P. Cellulose Multilayer Membranes Manufacture with Ionic Liquid. *J. Memb. Sci.* **2015**, *490*, 282–293. [CrossRef]
6. Warsinger, D.M.; Chakraborty, S.; Tow, E.W.; Plumlee, M.H.; Bellona, C.; Loutatidou, S.; Karimi, L.; Mikelonis, A.M.; Achilli, A.; Ghassemi, A.; et al. A Review of Polymeric Membranes and Processes for Potable Water Reuse. *Prog. Polym. Sci.* **2018**, *81*, 209–237. [CrossRef] [PubMed]
7. Alves, L.; Medronho, B.; Antunes, F.E.; Topgaard, D.; Lindman, B. Dissolution State of Cellulose in Aqueous Systems. 1. Alkaline Solvents. *Cellulose* **2016**, *23*, 247–258. [CrossRef]
8. Medronho, B.; Lindman, B. Competing Forces during Cellulose Dissolution: From Solvents to Mechanisms. *Curr. Opin. Colloid Interface Sci.* **2014**, *19*, 32–40. [CrossRef]
9. Medronho, B.; Lindman, B. Brief Overview on Cellulose Dissolution/Regeneration Interactions and Mechanisms. *Adv. Colloid Interface Sci.* **2015**, *222*, 502–508. [CrossRef]
10. Hummel, M.; Michud, A.; Tanttu, M.; Asaadi, S.; Ma, Y.; Hauru, L.K.J.; Parviainen, A.; King, A.W.T.; Kilpeläinen, I.; Sixta, H. Ionic Liquids for the Production of Man-Made Cellulosic Fibers: Opportunities and Challenges. In *Cellulose Chemistry and Properties: Fibers, Nanocelluloses and Advanced Materials*; Springer: Berlin/Heidelberg, Germany, 2016; pp. 133–168.
11. Xia, Z.; Li, J.; Zhang, J.; Zhang, X.; Zheng, X.; Zhang, J. Processing and Valorization of Cellulose, Lignin and Lignocellulose Using Ionic Liquids. *J. Bioresour. Bioprod.* **2020**, *5*, 79–95. [CrossRef]
12. Amini, E.; Valls, C.; Roncero, M.B. Ionic Liquid-Assisted Bioconversion of Lignocellulosic Biomass for the Development of Value-Added Products. *J. Clean. Prod.* **2021**, *326*, 129275. [CrossRef]
13. Abushammala, H.; Mao, J. A Review on the Partial and Complete Dissolution and Fractionation of Wood and Lignocelluloses Using Imidazolium Ionic Liquids. *Polymers* **2020**, *12*, 195. [CrossRef]
14. Xu, A.; Wang, J.; Wang, H. Effects of Anionic Structure and Lithium Salts Addition on the Dissolution of Cellulose in 1-Butyl-3-Methylimidazolium-Based Ionic Liquid Solvent Systems. *Green Chem.* **2010**, *12*, 268–275. [CrossRef]

15. Isik, M.; Sardon, H.; Mecerreyes, D. Ionic Liquids and Cellulose: Dissolution, Chemical Modification and Preparation of New Cellulosic Materials. *Int. J. Mol. Sci.* **2014**, *15*, 11922–11940. [CrossRef] [PubMed]

16. Gericke, M.; Fardim, P.; Heinze, T. Ionic Liquids—Promising but Challenging Solvents for Homogeneous Derivatization of Cellulose. *Molecules* **2012**, *17*, 7458–7502. [CrossRef]

17. Durmaz, E.N.; Zeynep Çulfaz-Emecen, P. Cellulose-Based Membranes via Phase Inversion Using [EMIM]OAc-DMSO Mixtures as Solvent. *Chem. Eng. Sci.* **2018**, *178*, 93–103. [CrossRef]

18. Ma, B.; Qiao, X.; Hou, X.; He, C. Fabrication of Cellulose Membrane with "Imprinted Morphology" and Low Crystallinity from Spherulitic [Bmim]Cl. *J. Appl. Polym. Sci.* **2016**, *133*, 1–7. [CrossRef]

19. Kim, D.; Nunes, S.P. Green Solvents for Membrane Manufacture: Recent Trends and Perspectives. *Curr. Opin. Green Sustain. Chem.* **2021**, *28*, 100427. [CrossRef]

20. Colburn, A.; Vogler, R.J.; Patel, A.; Bezold, M.; Craven, J.; Liu, C.; Bhattacharyya, D. Composite Membranes Derived from Cellulose and Lignin Sulfonate for Selective Separations and Antifouling Aspects. *Nanomaterials* **2019**, *9*, 867. [CrossRef]

21. Hassan, M.L.; Fadel, S.M.; Abouzeid, R.E.; Abou Elseoud, W.S.; Hassan, E.A.; Berglund, L.; Oksman, K. Water Purification Ultrafiltration Membranes Using Nanofibers from Unbleached and Bleached Rice Straw. *Sci. Rep.* **2020**, *10*, 11278. [CrossRef]

22. Arthanareeswaran, G.; Sriyamuna Devi, T.K.; Mohan, D. Development, Characterization and Separation Performance of Organic-Inorganic Membranes. Part II. Effect of Additives. *Sep. Purif. Technol.* **2009**, *67*, 271–281. [CrossRef]

23. Arthanareeswaran, G.; Kumar, S.A. Effect of Additives Concentration on Performance of Cellulose Acetate and Polyethersulfone Blend Membranes. *J. Porous Mater.* **2010**, *17*, 515–522. [CrossRef]

24. Yang, Z.; Peng, H.; Wang, W.; Liu, T. Novel Method of Synthesizing Poly(Ether Sulfone) Membranes Containing Two Solvents and a Lithium Chloride Additive and Their Performance. *J. Appl. Polym. Sci.* **2010**, *116*, 2658–2667. [CrossRef]

25. Lee, J.; Park, B.; Kim, J.; Park, S. Bin Effect of PVP, Lithium Chloride, and Glycerol Additives on PVDF Dual-Layer Hollow Fiber Membranes Fabricated Using Simultaneous Spinning of TIPS and NIPS. *Macromol. Res.* **2015**, *23*, 291–299. [CrossRef]

26. Bottino, A.; Capannelli, G.; Munari, S.; Turturro, A. High Performance Ultrafiltration Membranes Cast from LiCl Doped Solutions. *Desalination* **1988**, *68*, 167–177. [CrossRef]

27. Lee, H.J.; Won, J.; Lee, H.; Kang, Y.S. Solution Properties of Poly(Amic Acid)-NMP Containing LiCl and Their Effects on Membrane Morphologies. *J. Memb. Sci.* **2002**, *196*, 267–277. [CrossRef]

28. Zheng, L.; Wu, Z.; Wei, Y.; Zhang, Y.; Yuan, Y.; Wang, J. Preparation of PVDF-CTFE Hydrophobic Membranes for MD Application: Effect of LiCl-Based Mixed Additives. *J. Memb. Sci.* **2016**, *506*, 71–85. [CrossRef]

29. Medina-Gonzalez, Y.; Aimar, P.; Lahitte, J.F.; Remigy, J.C. Towards Green Membranes: Preparation of Cellulose Acetate Ultrafiltration Membranes Using Methyl Lactate as a Biosolvent. *Int. J. Sustain. Eng.* **2011**, *4*, 75–83. [CrossRef]

30. Bansod, P.G.; Sapkal, V.S.; Sapkal, R.S. The Optimization and Production Polyethersulfone Ultra Filtration Flat Sheet Membranes Using Lithium Chloride as Additives. *Int. J. Eng. Res. Dev.* **2012**, *1*, 65–68.

31. Sayyed, A.J.; Deshmukh, N.A.; Pinjari, D.V. A Critical Review of Manufacturing Processes Used in Regenerated Cellulosic Fibres: Viscose, Cellulose Acetate, Cuprammonium, LiCl/DMAc, Ionic Liquids, and NMMO Based Lyocell. *Cellulose* **2019**, *26*, 2913–2940. [CrossRef]

32. Acharya, S.; Liyanage, S.; Abidi, N.; Parajuli, P.; Rumi, S.S.; Shamshina, J.L. Utilization of Cellulose to Its Full Potential: A Review on Cellulose Dissolution, Regeneration, and Applications. *Polymers* **2021**, *13*, 4344. [CrossRef] [PubMed]

33. Yang, Y.J.; Shin, J.M.; Kang, T.H.; Kimura, S.; Wada, M.; Kim, U.J. Cellulose Dissolution in Aqueous Lithium Bromide Solutions. *Cellulose* **2014**, *21*, 1175–1181. [CrossRef]

34. Pang, Z.; Dong, C.; Pan, X. Enhanced Deconstruction and Dissolution of Lignocellulosic Biomass in Ionic Liquid at High Water Content by Lithium Chloride. *Cellulose* **2016**, *23*, 323–338. [CrossRef]

35. Su, C.; Gan, T.; Liu, Z.; Chen, Y.; Zhou, Q.; Xia, J.; Cao, Y. Enhancement of the Antioxidant Abilities of Lignin and Lignin-Carbohydrate Complex from Wheat Straw by Moderate Depolymerization via LiCl/DMSO Solvent Catalysis. *Int. J. Biol. Macromol.* **2021**, *184*, 369–379. [CrossRef] [PubMed]

36. Sivakumar, M.; Mohan, D.R.; Rangarajan, R. Studies on Cellulose Acetate-Polysulfone Ultrafiltration Membranes: II. Effect of Additive Concentration. *J. Memb. Sci.* **2006**, *268*, 208–219. [CrossRef]

37. Lopatina, A.; Anugwom, I.; Esmaeili, M.; Puro, L.; Virtanen, T.; Mänttäri, M.; Kallioinen, M. Preparation of Cellulose-Rich Membranes from Wood: Effect of Wood Pretreatment Process on Membrane Performance. *Cellulose* **2020**, *27*, 9505–9523. [CrossRef]

38. Lopatina, A.; Liukkonen, A.; Bec, S.; Anugwom, I; Nieminen, J.; Mänttäri, M.; Kallioinen-mänttäri, M. Wood-Based Cellulose-Rich Ultrafiltration Membranes: Alkaline Coagulation Bath Introduction and Investigation of Its Effect over Membranes' Performance. *Membranes* **2022**, *12*, 581. [CrossRef]

39. Nelson, M.L.; O'Connor, R.T. Relation of Certain Infrared Bands to Cellulose Crystallinity and Crystal Lattice Type. Part II. A New Infrared Ratio for Estimation of Crystallinity in Celluloses I and II. *J. Appl. Polym. Sci.* **1964**, *8*, 1325–1341. [CrossRef]

40. Nelson, M.L.; O'Connor, R.T. Relation of Certain Infrared Bands to Cellulose Crystallinity and Crystal Latticed Type. Part I. Spectra of Lattice Types I, II, III and of Amorphous Cellulose. *J. Appl. Polym. Sci.* **1964**, *8*, 1311–1324. [CrossRef]

41. Zhang, W.; Hallström, B. Membrane Characterization Using the Contact Angle Technique I. Methodology of the Captive Bubble Technique. *Desalination* **1990**, *79*, 1–12. [CrossRef]

42. Ma, J.; Xiao, T.; Long, N.; Yang, X. The Role of Polyvinyl Butyral Additive in Forming Desirable Pore Structure for Thin Film Composite Forward Osmosis Membrane. *Sep. Purif. Technol.* **2020**, *242*, 116798. [CrossRef]

43. Le, K.A.; Rudaz, C.; Budtova, T. Phase Diagram, Solubility Limit and Hydrodynamic Properties of Cellulose in Binary Solvents with Ionic Liquid. *Carbohydr. Polym.* **2014**, *105*, 237–243. [CrossRef] [PubMed]
44. Wittmar, A.S.M.; Koch, D.; Prymak, O.; Ulbricht, M. Factors Affecting the Nonsolvent-Induced Phase Separation of Cellulose from Ionic Liquid-Based Solutions. *ACS Omega* **2020**, *5*, 27314–27322. [CrossRef]
45. Li, X.; Loh, C.H.; Wang, R.; Widjajanti, W.; Torres, J. Fabrication of a Robust High-Performance FO Membrane by Optimizing Substrate Structure and Incorporating Aquaporin into Selective Layer. *J. Memb. Sci.* **2017**, *525*, 257–268. [CrossRef]
46. Shi, L.; Wang, R.; Cao, Y.; Liang, D.T.; Tay, J.H. Effect of Additives on the Fabrication of Poly(Vinylidene Fluoride-Co-Hexafluropropylene) (PVDF-HFP) Asymmetric Microporous Hollow Fiber Membranes. *J. Memb. Sci.* **2008**, *315*, 195–204. [CrossRef]
47. Darwish, N.B.; Alkhudhiri, A.; AlRomaih, H.; Alalawi, A.; Leaper, M.C.; Hilal, N. Effect of Lithium Chloride Additive on Forward Osmosis Membranes Performance. *J. Water Process Eng.* **2020**, *33*, 101049. [CrossRef]
48. Mansourizadeh, A.; Ismail, A.F. Effect of LiCl Concentration in the Polymer Dope on the Structure and Performance of Hydrophobic PVDF Hollow Fiber Membranes for CO_2 Absorption. *Chem. Eng. J.* **2010**, *165*, 980–988. [CrossRef]
49. Fontananova, E.; Jansen, J.C.; Cristiano, A.; Curcio, E.; Drioli, E. Effect of Additives in the Casting Solution on the Formation of PVDF Membranes. *Desalination* **2006**, *192*, 190–197. [CrossRef]
50. Idris, A.; Ahmed, I. A Production of Polyethersulfone Asymmetric Membranes Using Mixture of Two Solvents and Lithium Chloride as Additive. *J. Teknol.* **2007**, *47*, 25–34. [CrossRef]
51. Agarwal, S.; Hossain, A.; Choi, Y.S.; Cheong, M.; Jang, H.G.; Lee, J.S. Imidazolium Chloride-Licl Melts as Efficient Solvents for Cellulose. *Bull. Korean Chem. Soc.* **2013**, *34*, 3771–3776. [CrossRef]
52. Lindman, B.; Medronho, B.; Alves, L.; Costa, C.; Edlund, H.; Norgren, M. The Relevance of Structural Features of Cellulose and Its Interactions to Dissolution, Regeneration, Gelation and Plasticization Phenomena. *Phys. Chem. Chem. Phys.* **2017**, *19*, 23704–23718. [CrossRef] [PubMed]
53. Chen, H.; Liang, Y.; Wang, C.G. Solubility of Highly Isotactic Polyacrylonitrile in Dimethyl Sulphoxide. *J. Polym. Res.* **2005**, *12*, 325–329. [CrossRef]
54. Nevstrueva, D.; Pihlajamäki, A.; Nikkola, J.; Mänttäri, M. Effect of Precipitation Temperature on the Properties of Cellulose Ultrafiltration Membranes Prepared via Immersion Precipitation with Ionic Liquid as Solvent. *Membranes* **2018**, *8*, 87. [CrossRef]
55. Esmaeili, M.; Lahti, J.; Virtanen, T.; Mänttäri, M.; Kallioinen, M. The Interplay Role of Vanillin, Water, and Coagulation Bath Temperature on Formation of Antifouling Polyethersulfone (PES) Membranes: Application in Wood Extract Treatment. *Sep. Purif. Technol.* **2020**, *235*, 116225. [CrossRef]
56. Azizi Namaghi, H.; Haghighi Asl, A.; Pourafshari Chenar, M. Identification and Optimization of Key Parameters in Preparation of Thin Film Composite Membrane for Water Desalination Using Multi-Step Statistical Method. *J. Ind. Eng. Chem.* **2015**, *31*, 61–73. [CrossRef]
57. Saputra, B.; Noor, E. High Performance Membranes Using Lithium Additives: A Review. *Int. J. Sci. Eng. Res.* **2015**, *6*, 407–410.
58. Hung, W.L.; Wang, D.M.; Lai, J.Y.; Chou, S.C. On the Initiation of Macrovoids in Polymeric Membranes—Effect of Polymer Chain Entanglement. *J. Memb. Sci.* **2016**, *505*, 70–81. [CrossRef]
59. Leipner, H.; Fischer, S.; Brendler, E.; Voigt, W. Structural Changes of Cellulose Dissolved in Molten Salt Hydrates. *Macromol. Chem. Phys.* **2000**, *201*, 2041–2049. [CrossRef]
60. Karatzos, S.K.; Edye, L.A.; Wellard, R.M. The Undesirable Acetylation of Cellulose by the Acetate Ion of 1-Ethyl-3-Methylimidazolium Acetate. *Cellulose* **2012**, *19*, 307–312. [CrossRef]
61. Široký, J.; Blackburn, R.S.; Bechtold, T.; Taylor, J.; White, P. Attenuated Total Reflectance Fourier-Transform Infrared Spectroscopy Analysis of Crystallinity Changes in Lyocell Following Continuous Treatment with Sodium Hydroxide. *Cellulose* **2010**, *17*, 103–115. [CrossRef]
62. Mohamed, M.A.; Salleh, W.N.W.; Jaafar, J.; Ismail, A.F.; Abd Mutalib, M.; Jamil, S.M. Feasibility of Recycled Newspaper as Cellulose Source for Regenerated Cellulose Membrane Fabrication. *J. Appl. Polym. Sci.* **2015**, *132*, 1–10. [CrossRef]
63. Li, X.L.; Zhu, L.P.; Zhu, B.K.; Xu, Y.Y. High-Flux and Anti-Fouling Cellulose Nanofiltration Membranes Prepared via Phase Inversion with Ionic Liquid as Solvent. *Sep. Purif. Technol.* **2011**, *83*, 66–73. [CrossRef]
64. Zhang, S.; Kai, C.; Liu, B.; Zhang, S.; Wei, W.; Xu, X.; Zhou, Z. Facile Fabrication of Cellulose Membrane Containing Polyiodides and Its Antibacterial Properties. *Appl. Surf. Sci.* **2020**, *500*, 144046. [CrossRef]
65. Gaur, R.; Agrawal, R.; Kumar, R.; Ramu, E.; Bansal, V.R.; Gupta, R.P.; Kumar, R.; Tuli, D.K.; Das, B. Evaluation of Recalcitrant Features Impacting Enzymatic Saccharification of Diverse Agricultural Residues Treated by Steam Explosion and Dilute Acid. *RSC Adv.* **2015**, *5*, 60754–60762. [CrossRef]
66. Al Manasrah, M.; Kallioinen, M.; Ilvesniemi, H.; Mänttäri, M. Recovery of Galactoglucomannan from Wood Hydrolysate Using Regenerated Cellulose Ultrafiltration Membranes. *Bioresour. Technol.* **2012**, *114*, 375–381. [CrossRef] [PubMed]
67. Wang, D.; Yuan, H.; Chen, Y.; Ni, Y.; Huang, L.; Mondal, A.K.; Lin, S.; Huang, F.; Zhang, H. A Cellulose-Based Nanofiltration Membrane with a Stable Three-Layer Structure for the Treatment of Drinking Water. *Cellulose* **2020**, *27*, 8237–8253. [CrossRef]
68. Reischl, M.; Stana-Kleinschek, K.; Ribitsch, V. Electrokinetic Investigations of Oriented Cellulose Polymers. *Macromol. Symp.* **2006**, *244*, 31–47. [CrossRef]
69. Shi, Q.; Su, Y.; Zhu, S.; Li, C.; Zhao, Y.; Jiang, Z. A Facile Method for Synthesis of Pegylated Polyethersulfone and Its Application in Fabrication of Antifouling Ultrafiltration Membrane. *J. Memb. Sci.* **2007**, *303*, 204–212. [CrossRef]

70. Esmaeili, M.; Anugwom, I.; Mänttäri, M.; Kallioinen, M. Utilization of DES-Lignin as a Bio-Based Hydrophilicity Promoter in the Fabrication of Antioxidant Polyethersulfone Membranes. *Membranes* **2018**, *8*, 80. [CrossRef] [PubMed]
71. Susanto, H.; Ulbricht, M. Influence of Ultrafiltration Membrane Characteristics on Adsorptive Fouling with Dextrans. *J. Memb. Sci.* **2005**, *266*, 132–142. [CrossRef]
72. Ribitsch, V.; Stana-Kleinschek, K.; Kreze, T.; Strnad, S. The Significance of Surface Charge and Structure on the Accessibility of Cellulose Fibres. *Macromol. Mater. Eng.* **2001**, *286*, 648–654. [CrossRef]
73. Saljoughi, E.; Amirilargani, M.; Mohammadi, T. Effect of PEG Additive and Coagulation Bath Temperature on the Morphology, Permeability and Thermal/Chemical Stability of Asymmetric CA Membranes. *Desalination* **2010**, *262*, 72–78. [CrossRef]

ACTA UNIVERSITATIS LAPPEENRANTAENSIS

1075. ESANOV, BAKHTIYOR. Adaptive user-controlled personalization for virtual journey applications. 2023. Diss.

1076. SILTANEN, JUKKA. Laser and hybrid welding of high-strength structural steels. 2023. Diss.

1077. NOUSIAINEN, JALO. Model-based reinforcement learning and inverse problems in extreme adaptive optics control. 2023. Diss.

1078. USTINOV, STANISLAV. Fast and accurate simulation of fluid power circuits in the presence of small volumes using advanced methods and models for numerical stiffness elimination. 2023. Diss.

1079. HUSSAIN, HAFIZ MAJID. Heuristic-based packetized energy management for residential electricity demand. 2023. Diss.

1080. HÄMÄLÄINEN, MINNA. Principals managing entrepreneurship education in schools. 2023. Diss.

1081. WANG, ZHAO. Photocatalytic degradation of pharmaceutical and person care products (PPCPs) by commercial and synthesized catalysts under UV irradiation. 2023. Diss.

1082. LOHRMANN, ALENA. The water footprint of the global power sector: Status quo, challenges, and opportunities for tackling the global water crisis. 2023. Diss.

1083. PONOMAREV, NIKOLAI. A salt and alkali synergy for synthesising active carbons from lignin: porosity development and techno-economic assessment. 2023. Diss.

1084. AFANASYEVA, SVETLANA. Wind farm layout optimization: project economics and risk. 2023. Diss.

1085. VOSTROV, KONSTANTIN. Reduction of non-circulating bearing currents by electrical machine design. 2023. Diss.

1086. CARILLO MELGAREJO, DICK. Improving the design of cellular networks beyond 5G for smart grids. 2023. Diss.

1087. MALACINA, IRYNA. Zooming in and out: The strategic management of innovation across multiple levels of complex supply networks. 2023. Diss.

1088. SORE, SARISEELIA. Impact of information system capabilities on business value creation: Aspects of IT-producing and IT-consuming companies. 2023. Diss.

1089. IMMONEN, EERO. Advances in optimal design of shapes and processes by computational fluid dynamics. 2023. Diss.

1090. LAVOYE, VIRGINIE. Augmented reality in consumer retail: a presence theory approach. 2023. Diss.

1091. HÄRKÖNEN, KALEVI. Smart buildings in the green energy transition. 2023. Diss.

1092. TSYTSYNA, EVGENIYA. Motives, uncertainties, and imbalances in the evolution of a sustainable business ecosystem. 2023. Diss.

1093. JÄÄSKELÄINEN, ATTE. Business model innovation opportunities when news has become a public good. 2023. Diss.

1094. ADEDIPE, TAIWO. Atmospheric boundary-layer characteristics and their significance in wind energy and urban air quality assessment. 2023. Diss.

1095. SOSUNOVA, INNA. Model and guidelines for designing Internet-of-Things-enabled smart waste management system in smart cities. 2023. Diss.

1096. VUORELA, JYRI. Operative business development through system model and changing business structures. 2023. Diss.

1097. TRIAPITCIN, ILIA. Knowledge injection method for real-time decision support. 2023. Diss.

1098. RÄISÄNEN, OTTO. Open data in distribution network asset management. 2023. Diss.

1099. MATELA, MIKA. Procurement improvement in the public agency. 2023. Diss.

1100. SHAH, DIPAL. Quantification of synchronization. 2023. Diss.

1101. GHAFOURI, MEHRAN. Thermomechanical finite element simulation of welding, and elevated-temperature mechanical behaviour of high and ultra-high strength steels. 2023. Diss.

1102. NEUVONEN, RIKU. Numerical ductile fracture assessment of weldments in direct-quenched, ultra-high-strength steel. 2023. Diss.

1103. HUPPONEN, MARI. Long-term evolution of greenhouse gas emissions from municipal solid waste management. 2023. Diss.

1104. WANG, QI. Dynamic analysis and parameter identification for robotic manipulators. 2023. Diss.

1105. KIMPIMÄKI, JAAN-PAULI. From observation to insight: Computational abduction and its applications in sustainable strategy research. 2023. Diss.

1106. YIN, RUOCHEN. Research on key technologies for lightweight maintenance operations of the remote handling system for a fusion reactor. 2023. Diss.

1107. MUNIR, QAISAR. Designing printing parameters for geopolymer concrete prepared from construction and demolition waste and industrial side streams. 2023. Diss.

1108. ROHANI RAFTAR, HAMIDREZA. Assessment of weld root fatigue strength of load-carrying fillet welded joints using notch stress approaches and finite element analysis. 2023. Diss.

1109. SADIQA, AYESHA. Sustainable energy transition for Pakistan: Assessing the role of energy, water supply, social and gender equity dimensions. 2023. Diss.

1110. GHOREISHI, MALAHAT. The role of artificial intelligence in circular value creation: A conceptual framework and evidence from case studies. 2023. Diss.

1111. SUURONEN, JARKKO. On numerical implementation of α-stable priors in Bayesian inversion. 2023. Diss.

1112. PIILI, HEIDI. A conceptual, holistic framework to overcome limitations and constraints of design in laser based powder bed fusion of metals: Case novel separation and purification units. 2023. Diss.